Etude de la signalisation contrôlant l'accommodation intracellulaire au cours de la symbiose Medicago/Sinorhizobium

Elhosseyn Aït-Salem

Thèse de doctorat

NNT : 2020UPASS096

université PARIS-SACLAY

Etude de la signalisation contrôlant l'accommodation intracellulaire au cours de la symbiose *Medicago/Sinorhizobium*

Thèse de doctorat de l'université Paris-Saclay

École doctorale n° 567, Sciences de végétal : du gène à l'écosystème (SdV)
Spécialité de doctorat: Biologie
Unité de recherche : Université Paris-Saclay, CNRS, INRAE, Univ Evry, Institute of Plant Sciences Paris-Saclay (IPS2), 91405, Orsay, France.
Référent : Faculté des sciences d'Orsay

Thèse présentée et soutenue à Orsay, le 26/05/2020, par

Elhosseyn AÏT-SALEM

Composition du Jury

Isabelle Fudal DR2, INRAE Bioger	Présidente
Marta MARCHETTI Chargée de recherche (HDR) INRAE, LIPM Toulouse	Rapporteur & Examinatrice
Pierre FRENDO Professeur, Université Côte d'Azur	Rapporteur & Examinateur
Anouck DIET Maitre de conférences, Université Paris Diderot	Examinatrice
Péter KALO Docteur, Department of Genetics, Agricultural Biotechnology Institute (NARIC), Gödöllő. Hongrie	Examinateur
Pascal RATET DR1 (CNRS), Université Paris Saclay	Directeur de thèse

SOMMAIRE

Résumé : Les légumineuses en milieu carencé en azote, établissent une relation symbiotique avec les bactéries du sol appelées rhizobia. Cette interaction conduit à la formation d'un nouvel organe racinaire, la nodosité. Au sein de celle-ci, les rhizobia se différencient en bactéroïdes fixant l'azote atmosphérique au profit de la plante. La colonisation massive et chronique des cellules symbiotiques de nodosités par les rhizobia ne déclenche aucune réaction de défense visible. Au laboratoire nous avons isolé deux mutants symbiotiques développant des réactions de défense dans les nodosités de *Medicago truncatula* indiquant qu'il existe un contrôle strict de l'immunité dans cet organe.

L'objectif de cette thèse est de comprendre comment l'immunité symbiotique contrôle les voies de signalisation hormonales de défense afin d'héberger le partenaire symbiotique et de trouver de nouveaux outils pour mieux comprendre les mécanismes de défense. Pour cela, des approches moléculaires, pharmacologiques et génétiques sont utilisées.

Les résultats obtenus dans cette thèse suggèrent que les mécanismes de défense adoptés par *M. truncatula* varient en fonction de l'écotype de la plante. L'écotype A17 exploite deux voies de résistance : la voie de la sénescence et la voie des réactions de défense. Cependant, l'écotype R108 n'exploite que la voie des réactions de défense.

Ce travail suggère également que chez *M. truncatula* A17, la protéine SymCRK réprime la voie de signalisation de l'acide jasmonique qui conduit au déclenchement de la sénescence, tandis que la protéine DNF2 réprime principalement la voie de signalisation de l'acide salicylique qui conduit au déclenchement des réactions de défense et aussi réprime secondairement la voie acide jasmonique. Chez *M. truncatula* R108, les deux protéines SymCRK et DNF2 contrôlent les voies de signalisation de l'acide salicylique et de l'éthylène, avec DNF2 contrôlant préférentiellement la voie acide salicylique et SymCRK contrôlant préférentiellement la voie éthylène.

Cette thèse suggère aussi l'implication des protéines R dans le contrôle de l'accommodation intracellulaire des rhizobia. Un gène *CNL*-5 semble être impliqué dans le contrôle de l'infection des cellules symbiotiques, et deux autres gènes *CNL*-4 et *TNL*-2 semblent être impliqués dans le contrôle de l'efficacité de l'infection.

Finalement, cette thèse a permis d'isoler une souche bactérienne *E. adhaerens*, capable se comporter comme un symbiote ou comme un pathogène pour plusieurs espèces de Medicago.

Abstract: When grown under limited nitrogen resources, legumes establish a symbiotic relationship with soil bacteria called rhizobia. This interaction leads to the formation of a new root organ, the nodules. Within nodules, rhizobia differentiate into bacteroids and fix atmospheric nitrogen for the plant. The massive and chronic colonization of nodule symbiotic cells by the rhizobia does not trigger any visible defense reactions. In the laboratory, we previously isolated two symbiotic mutants developing defense reactions in *Medicago truncatula* nodules, indicating a strict control of the nodule immunity.

The thesis project aimed first to understand the relationship between symbiotic genes and immunity mediated by defense hormones and second to find new tools to help to better understand nodules defense mechanisms. For this, molecular, pharmacological and genetic approaches were used.

The results obtained in this thesis suggest that the defense mechanisms adopted by *M. truncatula* vary depending on the plant ecotypes. The A17 ecotype uses two resistance pathways; senescence and defense reactions. While, the R108 ecotype uses defense reactions pathway to fight against rhizobia.

This work also suggests that in *M. truncatula* A17, the SymCRK protein represses the jasmonic acid signaling pathway involved in senescence triggering. In contrast, the DNF2 protein mainly represses the salicylic acid signaling pathway involved in defense reactions and also represses the JA pathway. In *M. truncatula* R108, the two proteins SymCRK and DNF2 control salicylic acid and ethylene signaling pathways involved in triggering defense reactions. DNF2 controls the salicylic acid pathway more than the ethylene signaling pathway, while, SymCRK controls more the ethylene pathway than the salicylic acid signaling pathway in nodules.

This thesis also suggests the involvement of R proteins in the control of intracellular accommodation of rhizobia. The intracellular receptor CNL-5 appears to be involved in controlling the infection of symbiotic cells and the receptors *CNL-4* and *TNL-2* genes appear to be involved in controlling the infection efficacy of the symbiotic cells.

Finally, this thesis allowed the identification of a new bacterial strain *E. adhaerens*, capable of behaving as a symbiont or as a pathogen for several Medicago species. This can be used as a tool to study the nodules defense induction and to understand the rhizobia intracellular accommodation in symbiotic cells.

Remerciement

Je tiens à exprimer ma profonde gratitude à mon directeur de thèse **Pascal RATET**, qui m'a accueilli à bras ouverts au sein de son équipe de recherche « Symbiose et immunité » et qui m'a guidé tout au long de ma thèse. Pascal m'a donné la chance et l'opportunité d'intégrer le monde de la recherche. Pascal, grâce à toi j'ai appris comment être un bon chercheur, un bon père et comment être utile aux gens qui nous entourent. Pascal sans toi ça thèse n'aurait jamais vu le jour. Pour cela je ne te remercierai jamais assez.

Je voudrai remercier tous les membres de l'équipe « Symbiose et immunité ». Je remercie **Marie GARMIER** pour sa gentillesse, ses conseils et les discutions qui nous avons échangé sur les voies de signalisation de SA et le crosstalk entre les autres hormones de défense. Je remercie **Véronique GRUBER** pour sa gentillesse, ses conseils et son dévouement à l'équipe ainsi que pour les discutions que nous avons eu sur la senescence et le rôle de *SymCRK* dans l'immunité des nodosités et aussi pour le reviewing du manuscrit de la thèse. Je tiens à remercier **Sophie MASSOT**, pour son soutien surtout dans les moments difficiles, sa disponibilité, son encouragement et son dévouement à l'équipe et à l'institut. Sophie sans toi on peut rien faire et ce n'est pas que moi qui dis ça tous les anciens et actuels doctorants en attestent. Je remercie **Gautier BERNAL** et **Shengbin LIU** pour leur aide, soutien, et encouragement. Je tiens aussi à remercier les anciens thésards **Fathi BERRABAH** et **Kevin MAGNE** qui m'ont guidé lorsque je faisais mes premiers pas hésitants au laboratoire.

Je remercie les membres de mon comité de thèse, **Alia DELLAGI**, **Peter MERGAERT** et **Mathias BRAUT** pour leur disponibilité, leurs idées pertinente et tous les conseils qu'ils m'ont prodigués pour mener à bien mes travaux de thèse.

Je remercie **Peter KALO, Pierre FRENDO, Isabelle FUDAL, Marta MARCHETI** et **Anouck DIET** d'avoir accepté de faire partie des membres du jury de ma thèse et **Pascal Ratet** pour avoir encadré cette thèse.

Je remercie l'université de Paris Saclay et le ministère de l'enseignement supérieur de la recherche et de l'innovation pour le financement de ma thèse.

Je remercie les différents collaborateurs qui ont participé à la réalisation de mes travaux, Je remercie **Heribert Hirt** pour le séquençage du génome de la bactérie *Ensifer adhaerens* T4. Je remercie **Eleonora Rolli** pour le marquage de de la bactérie *Ensifer adhaerens* T4. Et je remercie également **Julia Buitink** pour nous avoir fourni les graines des mutants *MYC2*.

J'adresse mes remerciements à tous mes collègues de l'IPS2, et je tiens à remercier le personnel des services communs qui veille sur nous au quotidien pour qu'on puisse réaliser nos recherches dans de meilleures conditions.

J'aimerai aussi remercier ma femme **Lina** et ma mère **Anifa** pour leur soutiens, leur compréhension et leur patience. Et mes remercîment iront aussi à mon fils **Anis** qui m'apporter beaucoup de joie et d'espoir à ma vie.

MERCI A VOUS TOUS

Liste des figures

List des tableaux

Liste des abréviations

AAMG : Automatic Annotation of Microbial Genomes

ABA : Abscisic Acid

ACC : 1-Amino-Cyclopropane-1-Carboxylate

ACD : ACC Deaminase

ACO : ACC Oxydase

ACS : ACC Synthase

ARA : Acetylene Reduction Assay

At : Arabidopsis thaliana

AVG : Aminoethoxyvinylglycine

Avr : avirulence

bHLH : basic Helix Loop Helix

BNM : Buffered Nodulation Medium

CC-NBS-LRR (CNL) : Coiled Coil-Nucleotide Binding Site- Leucine Rich Repeat

Chr : Chromosome

CK : Cytokinine

CP : Cysteine Protease

CRE : Cytokinin REspons

CTR1 : Constitutive Triple Response 1

DAMP : Damage Associated Molecular Pattern

DHF : DiHydroxyFlavone

*DMI :*Does not Make Infection

DNF2 : Does Not Fix nitrogen 2

DNF2^{A17} : *M. truncatula* Jemalong nodules *DNF2*

DNF2^{R108} : *M. truncatula* R108 nodules *DNF2*

E. : *Ensifer*

E./S. medicae : Ensifer/Sinorhizobium medicae

EBF : Ethylene Insensitive3 Binding F-Box

EIN : Ethylene Insensitive

ERF : Ethylene Responsive transcription Factor

ERN : ERF Required for Nodulation

CLE :CLAVATA3/Endosperm surrounding region-related

ETI : Effector Triggered Immunity

ETP : Ethylene insensitive 2 Targeting Protein

fig. : figure

fix- : do not fix nitrogen

fix+ : fix nitrogen

FS : Flavone Synthase

FST : Flanking Sequence Tags

G/RFP : Green/Red Fluorescence Protein

GC : Gas Chromatography

HGAP : Hierarchical Genome Assembly Process

HK : His Kinase

HR : Hypersensitive Reaction

IPD3 : Interacting Protein of DMI3

IRLC : Inverted Repeat-Lacking Clade

IT : infection Thread

JA : Jasmonic Acid

JAZ : Jasmonate Zim domain

Kana : kanamycin

KD : Kinase Domain

LAR : local acquired resistance

LB : Luria-Bertani broth

Lb : Leghemoglobin

LCO : Lipo-Chito-Oligosaccharides

LIN : Lumpy Infection

LOX : LIPOXYGENASE

LRR-RLK : Leucine-Rich Repeat Receptor-Like Kinase

LYK3 :LYsine motif Kinase 3

LysM-RLKs : Lysine Motif Receptor-Like Kinases

MAPK : Mitogen Activated Protein Kinase

Me-JA : Methyl Jasmonate

Ms : Medicago sativa

Mt :Medicago truncatula

MTA : 5'-MethylThioAdenosine

NAD1 : Nodules with Activated Defense 1

NBS-LRR : Nucleotide Binding Site- Leucine Rich Repeat

NCR : Nodule-specific Cysteine Rich

NF : Nod Factor

ET : C_2H_2 : Ethylene

NFP : Nod Factor Perception

NIN : Nodule INception

NLR : Nucleotide-binding domain Leucine-rich Repeat

NOOT : NOdule roOT

NPR : Non-expressor of Pathogenesis-Related genes

NSP : Nodulation Signaling Pathway

OD : Optical Density

P/MAMP : Pathogen/Microbe-Associated Molecular Patterns

PBM : Peri-Bacteroid Membrane

PBS : Peri-Bacteroid space

PCR : Polymerase Chain Reaction

PI-PLCXD : phosphatidylinositol phospholipase C with X domaine

Pls : Plasmid

PR : Pathogenesis-Related protein

PRR : Pattern Recognition Receptor

PTI : PAMP Triggered Immunity

R genes//proteins : Resistance genes//proteins

RAN1 : Responsive to ANtagonist1

RNAseq : RNA sequencing

ROS : Reactive Oxygen Species

RSD : Regulator of Symbiosome Differentiation

RT-qPCR : Reverse Transcription-Quantitative Polymerase Chain Reaction

SA : Salicylic Acid

SAR : Systemic acquired resistance

S-doMet : S-Adenosyl Methionine (SAM)

SICKLE/SKL/EIN2 : Ethylene Insensitive 2

SymCRK : Cysteine-rich Receptor-like Kinase

SymCRK^{A17} : M. truncatula Jemalong nodules *SymCRK*

SymCRK^{R108} : M. truncatula R108 nodules *SymCRK*

T. : Trifolium

T3SS : Type 3 Secretion System

TIR-NBS-LRR (TNL) : Toll/Interleukin Receptor -Nucleotide Binding Site- Leucine Rich Repeat

UV : Ultraviolet-Visible

VSP : Vegetative Storage Protein

Xaa : Xanthomonas alfalfae subsp alfalfa

Xcc : Xanthomona campestris subsp campestris

YEB : Yeast Extract Broth

Introduction générale

I. Interaction microorganismes - plantes

1. Interaction agents pathogènes – plantes

1.1. Introduction

Au cours de leur cycle de vie, les plantes et les microorganismes interagissent pour assurer leur survie. Cette interaction est tantôt bénéfique tantôt néfaste au moins pour l'un des deux partenaires. Pour se défendre contre les microorganismes pathogènes, les plantes ont mis en place deux mécanismes de défenses ; la défense passive et la défense active. Ces mécanismes de défense sont développés par les plantes grâce à leur adaptation temporelle à des conditions climatiques ou environnementales particulières.

La défense passive est à un processus constitutif constant dans le temps qui protège les plantes contre la plupart des agents pathogènes et des prédateurs auxquels elles sont confrontées en permanence. Elle existe donc chez toutes les plantes, mais à des degrés divers. Elle se divise en deux grandes catégories : les barrières structurales constitutives (paroi cellulaire, poils,…) et les substances chimiques préformées (les composés phénoliques, les alcaloïdes,…) qui empêchent l'invasion microbienne des tissus végétaux (Heath, 2000; Kamoun, 2001; Nürnberger *et al.*, 2004).

Lorsque la défense passive est insuffisante pour contrer une attaque par des agents biotiques particulièrement agressifs, une défense active se met en place pour détruire les agresseurs ou tenter de les confiner au site de pénétration et qui permet à la plante d'acquérir une résistance contre l'agresseur.

Ce type de défense est défini par l'incompatibilité génétique entre l'agent avirulent et la plante hôte. En effet, la plante reconnaît une protéine d'avirulence (Avr) de l'agent pathogène *via* les protéines de résistance (PR) (Flor, 1971; Keen, 1990). Ceci conduit à une réponse d'hypersensibilité (HR) et à la formation de nécroses sur le lieu d'infection qui se traduit par la mort rapide des cellules végétales et bactériennes (Pontier *et al.*, 1998; Agrios, 2005).

Cette réponse envoie des signaux de stress aux cellules adjacentes à la zone nécrotique puis aux autres cellules plus éloignées du site d'infection, ce qui permet à la plante de développer une résistance localisée (LAR) (Fritig *et al*., 1998) et une résistance systémique (SAR) aux différents agents pathogènes (Sticher *et al*., 1997 ; Van Loon, 1997, Fritig *et al*., 1998).

1.2. **Reconnaissance et induction des défenses**

Lorsque les moyens classiques de défense, constitués par les barrières de défense préformées n'arrivent pas à neutraliser l'agent pathogène virulent (Agrios, 2005), la plante fait appel à des mécanismes de défense induits par des éliciteurs de défense d'origine microbienne. Ces éliciteurs sont constitués soit par des motifs moléculaires conservés d'origine microbienne ou MAMP (Microbe-Associated Molecular Patterns) perçus par des récepteurs extra-membranaires type PRR (Pattern Recognition Receptor), soit par des effecteurs injectés par le pathogène dans le cytoplasme des cellules végétales qui sont reconnus par des protéines R (codées par la famille des gènes NBS-LRR). Des éliciteurs endogènes induits par l'hôte végétal peuvent également être produits en réponse à des pathogènes ou des stress abiotiques (Chuberre *et al.*, 2018). Ces motifs moléculaires conservés issus des cellules végétales endommagées sont appelés DAMP (Damage Associated Molecular Pattern) et sont perçus par des récepteurs extra-membranaires de type PRR. L'ensemble des mécanisme de défense induits a pour but de limiter et minimiser les maladies causées par les agents pathogènes (Montesano *et al.*, 2003; Garcia-Brugger *et al.*, 2006).

Ces types de défense sont le résultat et le produit évolutif et concurrentiel entre les microorganismes et les plantes. Les microorganismes cherchent à développer leurs mécanismes d'attaque pour infecter les plantes et ces dernières améliorent leurs mécanismes de défense pour se protéger contre les attaques des agresseurs. Ce duel d'attaques et de résistances entre les plantes et les microorganismes a été simplifié dans le modèle Zig-Zag proposé par Jones et Dangl en 2006. Ce modèle a été adapté et complété dans la revue de Zvereva et Pooggin (2012) et Abdul et al (2020. fig.1).

1.2.1. Modèle zig-zag

1.2.1.1. **Perception de l'agent pathogène**

Les mécanismes de défense sont activés après la perception directe ou indirecte des pathogènes. Principalement, on distingue deux niveaux de perception. Un premier niveau extracellulaire active les mécanismes de défense dès les premières secondes de contact avec les facteurs de stress tandis qu'un deuxième niveau intracellulaire les induit plus tardivement.

1.2.1.2. Immunité déclenchée par les pathogènes (PTI)

La perception extracellulaire se fait par des récepteurs membranaires de type PRR (Pattern Recognition Receptor) localisés dans la membrane plasmique et qui sont composés généralement d'un domaine extracellulaire impliqué dans la perception, d'un domaine transmembranaire impliqué dans l'encrage à la membrane plasmique, et d'un domaine intracellulaire impliqué dans la transduction du signal.

La partie extracellulaire des PRR reconnait des épitopes bien conservés chez les microorganismes et des motifs libérés par la plantes suite à l'infection par le pathogène appelés respectivement P/MAMPs (Pathogen /Microbe – Associated Molecular Patterns) et DAMPs (Damage – Associated Molecular Patterns).

Suite à la perception des molécules immunogènes, la partie intracellulaire des PRRs déclenche une cascade de signalisation telle que les flux ioniques et l'activation de phosphorylation par les MAPK (Mitogen Activated Protein Kinase) et les ROS qui induisent à leur tour des réactions de défense de type PTI (PAMP - Triggered Immunity) (fig.1. Macho et Zipfel, 2014; Zipfel, 2014; Böhm *et al.*, 2014 ; Kwak *et al.*, 2006).

1.2.1.3. Immunité déclenchée par des effecteurs (ETI)

Afin de diminuer l'immunité de la plante, certains pathogènes introduisent des protéines d'avirulance dans le cytosol de la plante hôte soit par internalisation pour le cas des champignons ou soit par injection pour les bactéries possédant le système de sécrétion de type 3 (T3SS) pour bloquer la cascade de signalisation de la PTI.

Pour faire face, la plante hôte recrute des récepteurs intracellulaires codés par des gènes (R) capables d'intercepter les effecteurs injectés par les pathogènes. Les protéines (R) sont composées généralement de trois domaines : un domaine de fixation aux nucléotides appelé NBS (Nucleotide Binding Site), un domaine LRR permettant la perception des effecteurs et un troisième domaine variable qui peut être un domaine TIR (Toll/Interleukin-like Receptor) ou un domaine super-hélice CC (Coiled Coil) dont la fonction est inconnue. Suite à la perception des effecteurs par les protéines (R), une réaction immunitaire de type ETI (Effector Triggered Immunity) est déclenchée (Fig.1 et 10. abdul *et al.* 2020 ; Zvereva et Pooggin 2012 ; Jones et Dangl 2006).

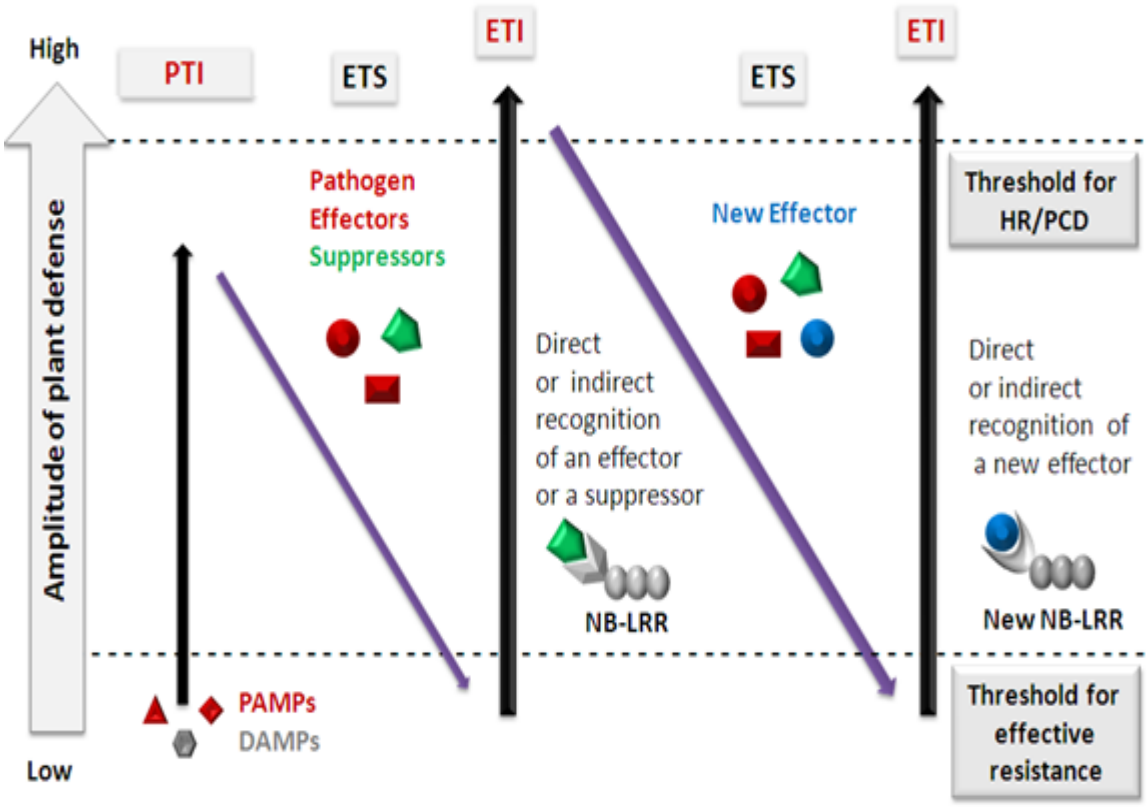

Figure 1. Le modèle zig-zag dans les interactions pathogènes – plantes. Les motifs moléculaires associés aux agents pathogènes (PAMP) et les motifs moléculaires associés aux cellules végétales endommagées (DAMP) déclenchent l'immunité PAMP (PTI), sénescence et l'hypersensibilité (HR). Les effecteurs secrétés par les pathogènes contribuent à la sensibilité déclenchée par effecteur (ETS). Les plantes recrutent les protéines de résistance (NB-LRR) qui détectent les effecteurs pathogènes et déclenchent l'immunité (ETI). L'amplitude de la défense est indiquée sur l'axe y, et le seuil d'activation de la sénescence est également indiqué. (Zvereva et Pooggin, 2012, adapté et complété à partir du modèle de Jones et Dangl 2006).

1.3.Mécanismes de résistance

Les plantes développent plusieurs réponses pour faire face aux pathogènes comme l'induction de gènes de résistance (PR protéines), ROS ou la production de métabolites secondaires (phénylpropanoïdes ; Fondevilla *et al.*, 2011 ; Kwak *et al.*, 2006). Ces réponses sont en général médiés par des hormones de défense. L'utilisation de l'une ou l'autre de ces réponses par la plante dépend de l'agent pathogène et du type d'infection (Kankanala *et al.*, 2019).

Le rôle des phytohormones ainsi que leurs voies de synthèse et de signalisation sont détaillés dans le chapitre phytohormones. Les deux chapitres ci-dessous décrivent brièvement le rôle des métabolites primaires et secondaires dans les mécanismes de défense.

1.3.1. Rôle des métabolites dans les réactions de défense

1.3.1.1. Rôle des métabolites primaires

Le besoin en nutriment et en énergie est le point commun qui associe les plantes et les microorganismes (Fagard *et al.*, 2014). L'activité métabolique primaire fourni à la plante les nutriments et l'énergie nécessaire pour son développement et pour le renforcement de son système de défense (Bolton, 2009). Les microorganismes pathogènes infectent la plante et utilisent ses nutriments comme source d'énergie (Snoeijers *et al.*, 2000). Cependant, la plante exploite son activité métabolique primaire comme un système de garde moléculaire capable de déclencher des réactions de défense en réponse aux infections par les pathogènes (Kachroo et Robin, 2013). L'activité métabolique primaire participe indirectement dans les réaction de défense en limitant la disponibilité des nutriments et en régulant les voies de biosynthèse des sucres, des protéines et des lipides (Rojas *et al.*, 2014).

Les métabolites primaires comme les sucres, sont impliqués dans la régulation positive des gènes *PR* connus comme acteurs majeurs dans les réactions de défense contre les pathogènes (Rojas *et al.*, 2014 ; Park *et al.*, 2004 ; Patkar et Chattoo, 2006).

1.3.1.2. Rôles des métabolites secondaires

Les phenylpropanoïdes sont des produits dérivés de la L-phenylalanine. Les dérivés phenylpropanoïdes sont présents sous deux formes : une forme simple composée d'un squelette phenylpropane C_6C_3 comme les acides hydroxycinnamique et les monolignols, et une forme plus complexe composée d'un squelette formée d'une unité phenylpropane couplée à une unité dérivée d'acétate. Cette forme complexe regroupe les flavonoïdes et les isoflavonoïdes. La famille C_6C_1 des acides benzoïques qui comprend l'acide salicylique, est composée d'un squelette correspondant à une forme simplifiée des acides hydroxycinnamiques. Ces composés ne sont pas présents chez toutes les espèces végétales. Cependant, les classes d'acide hydroxycinnamiques et de flavonoïdes sont omniprésentes chez les plantes supérieures (Dixon, 2002).

Les flavonoïdes et les composés phénoliques sont parmi les métabolites secondaires les plus importants produits par la plante. Ils sont impliqués dans plusieurs processus biologiques comme la protection contre les stress abiotiques et biotiques (UVs, infections microbiennes, etc… ; Fait *et al.,* 2008 ; Hassan and Mathesius 2012), la nodulation, la germination de pollens et de nombreux autres processus (Treutter, 2005 ; Kobayashi *et al.,* 2004 ; Mahajan *et al.*, 2011). En raison de leurs rôles de défense, ils sont aussi appelés phytoalexines.

Chez les légumineuses les flavonoïdes en particulier les isoflavones et les isoflavanones sont impliqués dans la défense contre les attaques des bactéries, champignons et oomycètes pathogènes et dans la signalisation cellulaire (fig.2 ; Dixon, 2002 ; He and Dixon, 2000, O'Neill et Sanders, 1994).

1.3.2. Rôle des protéines liées à la pathogénèse (PR proteins)

Les gènes *PR*s sont parmi les gènes les plus induits chez les plantes infectées par les bactéries, les virus, les oomycètes ou les champignons pathogènes (Van Loon *et al.,* 2006). Dans les racines des légumineuses, l'expression de *PR10* est contrôlée par le SA (Salicylic Acid), le JA (Jasmonic Acid) et par l'ABA (Abscisic Acid) (Srivastava *et al.,* 2006). Chez plusieurs espèces et y compris les légumineuses, les PR protéines comme PR10 (Ribonuclease-like proteins), PR12 (defensins), PR13 (thionins) et PR14 (Lipid-transfer protein) sont connues pour leurs effets antibactériens (Kaur *et al.,* 2017 ; Robert et Martha, 2010 ; Park *et al.,* 2004). Il a été rapporté que la surexpression de *PR14* confère à la plante une meilleure résistance aux bactéries pathogènes et que *PR10* a un pouvoir antibactérien

contre les pathogènes tels que *Agrobacterium tumefaciens*, *Pseudomonas syringae*, *P. aureofaciens*, *Serratia marcescens* et *A. radiobacter*. (Jiang *et al.*, 2015 : Xie *et al*., 2010).

Les PR protéines interviennent dans les réactions de défense au cours de l'ETI. Suite à l'infection du tissu végétal par les pathogènes bactériens, une accumulation d'espèces réactives d'oxygène conduit à la synthèse des composés phénoliques sur le site d'infection en même temps que l'activation de l'expression des gènes PRs et le déclenchement de la réponse HR (Hypersensitive Reaction). Ceci entraine la mort ou l'inhibition de la croissance bactérienne dans les tissus infectés (fig.2. Jones *et al.*, 2016; Agrios 2005).

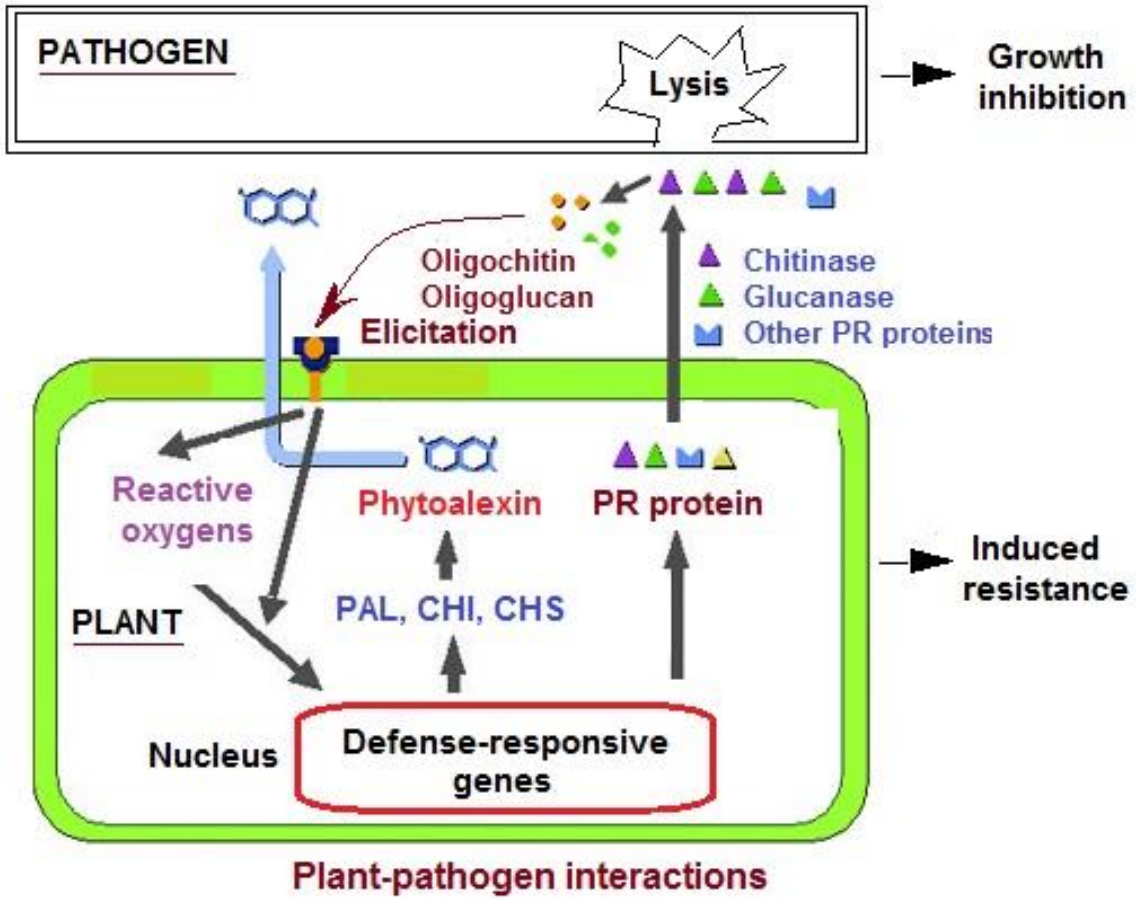

Figure 2. Mobilisation des métabolites contre les pathogènes. La perception des P/MAMP par des récepteurs membranaires de la cellule végétale induit les réactions de défense *via* l'activation des espèces réactives oxygénées (ROS) qui induit la biosynthèse des composés flavonoïdes (phytoalexine) et des PR protéines (Chitinase, Glucanase et les PRs) capables de tuer ou ralentir la croissances des agents pathogènes. (http://www.biotech-ecolo.net/plant-resistance/active-defenses-plants.html).

2. Interaction symbiotique rhizobium-légumineuse

2.1.Phase précoce de la nodulation

2.1.1. Reconnaissance symbionte – plante

Les plantes communiquent avec leur entourage au niveau de la rhizosphère par la sécrétion de molécules organiques de type flavonoïdes comme la lutéoline (5,7,3',4'-tetrahydroxyflavone) et la 7,4'-dihydroxyflavone (DHF ; Kobayashi *et al.,* 2004 ; Peters *et al.,* 1986; Redmond *et al.,* 1986). Cette sécrétion a pour objectif d'attirer des microorganismes bénéfiques comme les rhizobia et les champignons mycorhiziens vers les racines et leur fournir les oligoéléments nécessaires à leur survie. Parmi ces organismes symbiotiques, les rhizobia sont des bactéries de la famille des *Alphaproteobacteria* (*Rhizobium*, *Ensifer*, *Bradyrhizobium*) et des *Betaproteobacteria* (*Burkholderia* et *Cupriavidus*). Elles sont capables de produire des molécules lipochito-oligosaccharidiques (LCOs) appelées facteurs Nod (NFs) suite à la perception de métabolites secondaires de type flavonoïdes. La perception de ces NFs par la plante va induire la formation de nodosités au sein desquelles, les rhizobia réduisent l'azote atmosphérique en ammonium au profit de la plante hôte (fig.3 ; Gyaneshwar eta l., 2011; Remigi *et al.,* 2016).

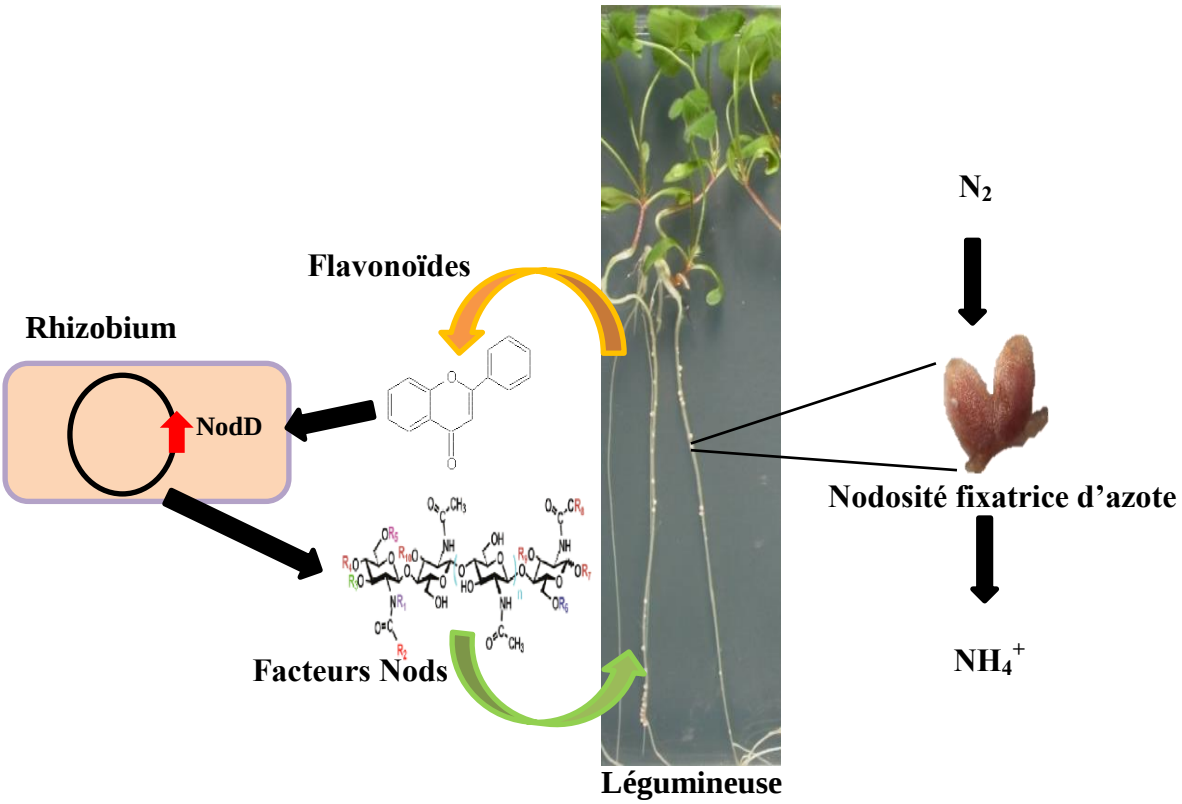

Figure 3. Diagramme simplifié du dialogue moléculaire entre les partenaires symbiotiques et la formation des nodosités. Le dialogue commence par la sécrétion de molécules de flavonoïdes par la racine. Les rhizobia sont attirées vers les racines et synthétisent des NFs suite à la perception des flavonoïdes par la protéine régulatrice NodD qui déclenche l'expression des gènes *nod*. Sous l'influence des NFs, l'extrémité des poils absorbants se courbe sous forme d'une « crosse de berger ». Le cordon d'infection qui se forme facilite l'infection des cellules racinaires corticales et la formation des nodosités fixatrices d'azote.

2.1.1.1. Facteurs Nod

2.1.1.1.1. Structure et biosynthèse des facteurs Nod (NFs)

La production des NFs est assurée par un groupe des gènes appelés gènes de nodulation. Ces gènes de nodulation sont classés en trois familles ; la famille des gènes ***nod***, la famille des gènes ***nol*** et la famille des gènes ***noe.*** Souvent chez les rhizobia symbiotiques fixatrices d'azote, les gènes de nodulation et les gènes de fixation sont colocalisés sur un grand plasmide (pSym). Cependant, chez certaines souches du genre *Azorhizobium*, *Bradyrhizobium* et la souche *Rhizobium loti*, les gènes de nodulation sont chromosomaux (Freiberg *et al.*, 1997).

Le gène *NodD* de la famille des gènes ***nod***, est hautement conservé chez les rhizobia. Il joue un rôle très important dans la perception des flavonoïdes et dans la spécificité hôte/rhizobia (Horvath *et al.*, 1987). L'interaction directe entre le facteur de transcription codé par le gène *NodD* et les flavonoïdes n'est pas encore montré *in vitro* (Kelly *et al.*, 2018) mais grâce à la génétique cette hypothèse reste solide. Il a été montré que la mutation du gène *NodD* bloque la synthèse des NFs, et la spécificité rhizobia/plante hôte peut être modifiée en transférant le gène *NodD* d'une souche spécifique à une souche non spécifique de la plante hôte (Horvath *et al.*, 1987; Spaink *et al.*, 1987).

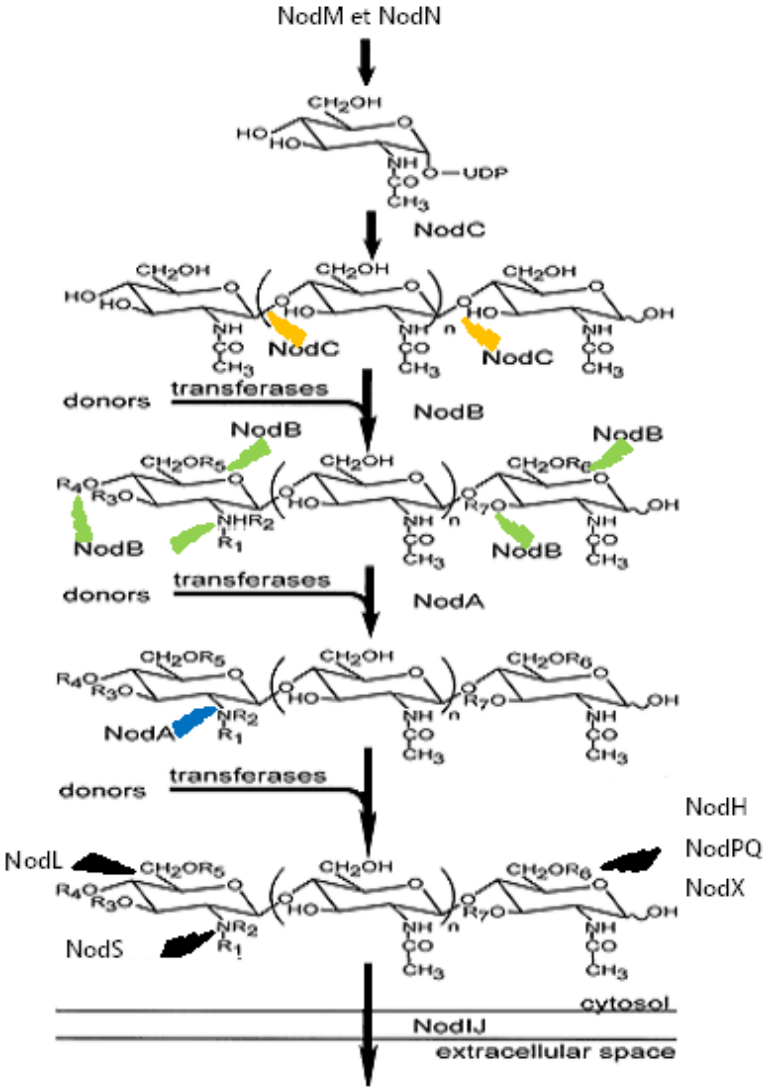

Figure 4. Structure et biosynthèse des facteurs Nod. La biosynthèse de la structure de base des NFs est assurée chez tous les rhizobia par les gènes *NodABC*. La structure de base subit des modifications souche-dépendante par des gènes comme *NodS, NodL, NoDH* et *NodPQ.* Les NFs synthétisés sont secrétés par les protéines NodJ et NodI. Donor : donneur du substrat LCO, n : nombre de résidus GLcNAc. n : prend les valeurs de 1 à 3 (Mergaert *et al.*, 1997 ; modifié).

Suite à l'activation des gènes ***NodD*** par l'inducteur végétal, les gènes de nodulation sont induits en cascade pour la synthèse des NFs (fig.4). Le gène ***NodM***, codant une enzyme glucosamine synthase est le premier intervenant dans ce processus. Cette enzyme catalyse, au niveau de l'interface cytoplasme / membrane plasmique, les 6-P-fructose et glutamine en 6-P-glucosamine (UDP-GNAc) qui est le précurseur des NFs (Marie *et al.*, 1992). Par la suite, la chitine-oligomère synthase codée par le gène ***NodC*** intervient pour transformer l'UDP-GNAc en oligomères de chitine acétylés (UDP-N-acétyl-glucosamine ; Geremia *et al.*, 1994;

Anderson *et al.*, 2018). L'enzyme chitine déacétylase codée par le gène ***NodB***, déacétyle la terminaison non réductrice de l'UDP-N-acétyl-glucosamine (John *et al.*, 1993). Par la suite, l'enzyme *N*-acyltransférase codée par ***NodA***, substitut le groupement *N*-acétyl par un groupement *N*-acyle sur le résidu non-réducteur de l'oligosaccharide (Atkinson *et al.*, 1994). Les trois gènes *NodABC* sont requis pour la synthèse du squelette de base des NFs chez tous les rhizobia. Toutefois, la structure des NFs diffère suite à l'action de gènes *Nod* hôte-spécifique (*hsn*) ou génotype-spécifique (*gsn*) impliqués dans la modification de la structure de base des facteurs Nod comme : *NodH (*sulfotransférase), *NodP* (ATP sulfurylase), *NodQ* (ATP sulfurylase, APS kinase), *NodL* / *NodX* (6-O-acétyltransférase / acétyltransférase), *NodS* (S-adénosyl méthionine méthyltransferase), *NodZ* (fucosyltransférase), *NoeL et NolK* (sucre épimerase), *NolA* (régulateur de type MER), *NodE* (β-kétoacyl synthase) et *NodF* (transporteur de groupements acyl) (Denarié *et al.*, 1996 ; Heidstra et Bisseling, 1996 ; Mergaert *et al.*, 1997).

2.1.1.1.2. Régulation des gènes de nodulation

La biosynthèse des NFs est contrôlée par deux types de gènes régulateurs, les régulateurs positifs comme les gènes *NodD* et *SyrM*. Ces deux gènes codent pour un récepteur type Lys-R. Les deux récepteurs NodD et SyrM régulent positivement l'opéron ***nodABC*** en présence d'inducteurs végétaux comme les flavonoïdes (Demont *et al.*, 1994 ; Loh and Stacey, 2003). Les gènes ***NodV*** et ***NodW*** contribuent aussi à réguler positivement l'expression des gènes *Nod* chez *Bradyrhizobium japonicum*, en formant un réseau complexe de régulation qui module l'expression des locus de nodulation de manière spécifique à l'hôte (Göttfert *et al.*, 1990). Le gène *NolR*, quant à lui, régule négativement l'expression des gènes *Nod* de base mais pas des gènes *hsn* ou *gsn* (Cren *et al.*, 1994 ; Kondorosi *et al.*, 1991 ; Kondorosi *et al.*, 1989).

2.1.1.1.3. Effets des facteurs Nod

En plus de leur effet sur la racines et l'induction de la formation des nodosités chez les légumineuses (voir chapitre suivant), les NFs ont un effet positif et direct sur la croissance, le développement et la germination des plantes, qu'elles soient légumineuses ou non. Cet effet est de type hormonal.

Ainsi selon les travaux menés par Röhrig *et al.* (1995) et Schell *et al.* (1999), les NFs ont un rôle positif sur la croissance cellulaire. Ils ont montré que le traitement des cellules de tabac par les lipochito-oligosaccharides (LCOs) peut remplacer les phytohormones

nécessaires pour la croissance cellulaire (l'auxine et les cytokinines). Cet effet positif sur le développement des plantes est observé aussi chez d'autres espèces telles que le colza, le maïs et la tomate (Röhrig *et al.*1995 ; Schell *et al.* 1999). En outre, les NFs peuvent également améliorer la germination des graines et l'établissement de jeunes plants de maïs, riz, colza, pommier et vigne, et peuvent augmenter les taux de photosynthèse (Dakora, 2003).

2.1.1.2.Perception et transduction du signal des NFs par la plante hôte

Chez *Medicago truncatula*, les NFs produits par les partenaires symbiotiques compatibles, sont perçus par des récepteurs membranaires extracellulaires de la famille Lysine Motif Receptor-Like Kinases (LysM-RLKs) comme Nod Factor Perception (NFP), LYsine motif Kinase 3 (LYK3/HCL) (Gough *et al.*, 2018 ; Oldroyd. 2013 ; Limpens *et al.*, 2003) et LysM-RLK 3 (LYR3) (Fliegmann *et al.*, 2013) (fig.5 et 6). Au niveau intracellulaire, la transduction du signal des NFs débute par l'activation d'un gène codant pour une Leucine-Rich Repeat Receptor-Like Kinase (LRR-RLK), appelée Does not Make Infection 2 (DMI2. Oldroyd. 2013 ; Endre *et al.*, 2002). Suite à l'activation de DMI2 une oscillation calcique est déclenchée dans le cytoplasme. L'oscillation calcique entre le noyau et le cytoplasme est assurée par un canal cationique situé sur la membrane nucléaire codé par le gène *DMI1* (Oldroyd. 2013 ; Ané *et al.*, 2004). Dans le noyau, la protéine calmoduline kinase DMI3 interagit avec le calcium internalisé (Oldroyd. 2013 ; Mitra *et al.*, 2004 ; Lévy *et al.*, 2004) et phosphoryle une protéine avec un domaine coiled-coil Interacting Protein of DMI3 (IPD3) (Oldroyd. 2013 ; Messinese *et al.*, 2007). L'activation de l'IPD3 induit deux facteurs de transcription de la famille GRAS (NSP1 et NSP2) (Oldroyd. 2013 ; Kaló *et al.*, 2005 ; Smit *et al.*, 2005) impliqués dans la régulation des gènes de nodulation *ENOD* (*Early noduline*) comme : *Nodule INception* (*NIN*. Hirsch *et al.*, 2009 ; Marsh *et al.*, 2007) et *Ethylene Responsive factor required for Nodulation 1* (*ERN1*) (Cerri *et al.*, 2012) indispensables pour la nodulation (fig.5 et 6).

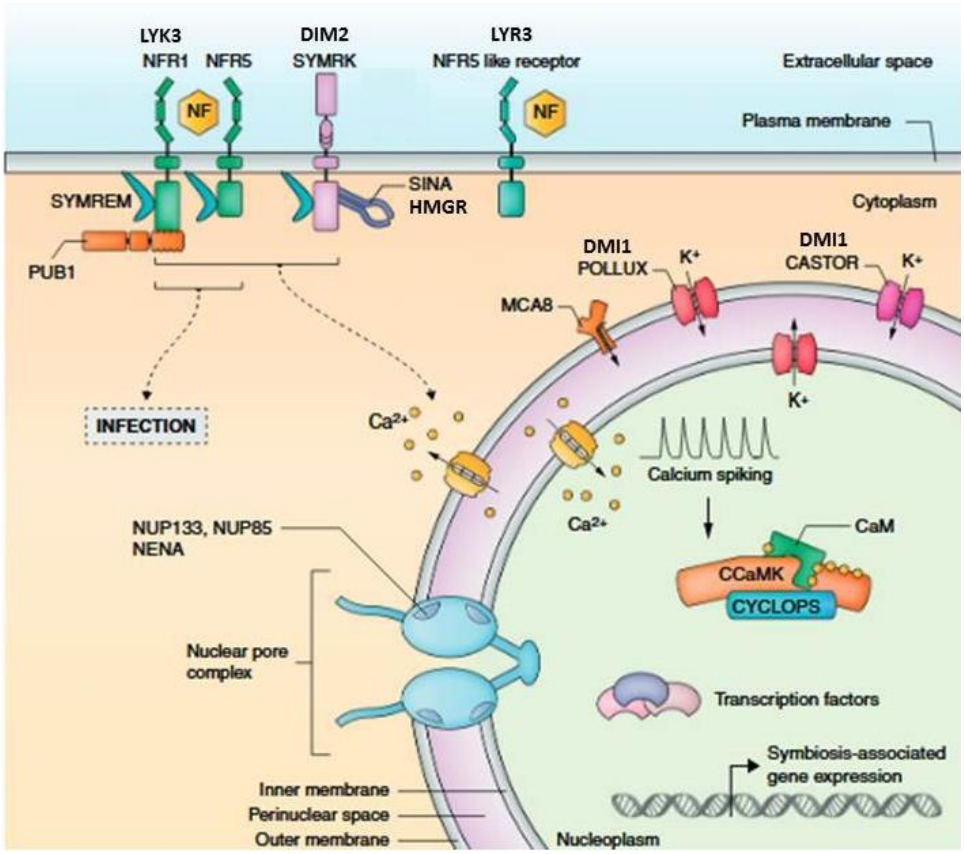

Figure 5: Schéma de synthèse de la transduction du signal NF chez *M. truncatula et Lotus japonicus.* Modifiée. Les facteurs nod sont perçus au niveau de la membrane plasmique par des récepteurs type LysM kinase (LYK), représentés par NFR1 et NFR5 chez *Lotus japonicus* et LYK3 et NFP *chez Medicago truncatula*. Plant U-Box protein 1 (PUB1) interagit avec le domain kinase de LYK3 alors que SINA, l'homologue de SEVEN IN ABSENTIA SINA4, interagit avec (DOES NOT MAKE INFECTIONS 2). La perception des facteurs Nod conduit par la suite à une oscilation calcique dans le noyau médiée par des pompes situées dans la membrane nucléaire (CASTOR/POLLUX/DMI1, NUP85, NUP133, NENA). Les complexes CCaMK/DMI3, CYCLOPS/IPD3 interagissent avec les facteurs de transcription comme NSP1/2 et NIN pour induire l'expression des gènes de nodulation (Singh and Parniske, 2012).

2.1.1.3. Formation des cordons d'infection

Les rhizobia infectent le cortex racinaire et induisent la formation des nodosités à travers les cordons d'infection (ITs, Oldroyd. 2013). Chez *M. truncatula,* les gènes comme *Required for Infection Thread* (*RIT*) de la famille *SCAR/WAVE* (Miyahara *et al.*, 2010) et *Lumpy INfection* (*LIN*) interviennent dans la formation des ITs. En effet, l'interruption de ces gènes codant respectivement pour un suppresseur du récepteur WASP et une E3 ubiquitine ligase avec un domaine U-box/WD40, inhibe le développement des ITs au niveau de l'épiderme racinaire (Miyahara *et al.*, 2010 ; Kiss *et al.*, 2009). Les gènes en aval du gène *NIN* comme le gène *ERN1* et son régulateur *MtNF-YA* (*HAP2-1*) ainsi que les gènes *FLOT2*, *FLOT4*, *LYK3*, *LYK4* et *NFP* sont impliqués dans la pénétration des ITs dans le cortex racinaire. L'interruption de l'expression d'un de ces gènes bloque la progression des ITs vers le cortex (fig.6. Laloum *et al.*, 2014 ; Laporte *et al.*, 2014 ; Soyano *et al.*, 2013 ; Popp et Ott, 2011 ; Haney et Long, 2010 ; Middleton *et al.*, 2007 ; Limpens *et al.*, 2003). En plus, la phytohormone éthylène connue pour son rôle dans les réactions de défense contre les infections par les pathogènes, régule négativement l'infection des racines par les rhizobia. En effet, la mutation du gène *sickle* orthologue du gène *AtEIN2* impliqué dans la voie de signalisation de l'éthylène, cause un phénotype hyper-nodulateur chez la plante modèle *M. truncatula* (Penmetsa *et al.*, 2003).

2.1.1.4. Infection des cellules symbiotiques

Les rhizobia colonisent les ITs pour arriver aux cellules du cortex avant de se différentier en bactéroïdes. Un dialogue moléculaire est établi entre les rhizobia et les cellules symbiotiques pour réussir l'internalisation des rhizobia dans les cellules symbiotiques. Les rhizobia émettent des NFs qui sont perçus chez Medicago par les récepteurs *NFP* et *LYK3* situés sur la membrane plasmique des cellules symbiotiques (Gavrin *et al.*, 2017 ; Moling *et al.*, 2014 ; Limpens *et al.*, 2003). Les NFs activent l'expression du gène *DMI2* qui participe à l'activation les protéines membranaires MtSyt1/3 ou MtSyt2/3 responsables de l'endocytose des rhizobia dans les cellules symbiotiques (Gavrin *et al.*, 2017 ; Moling *et al.*, 2014 ; Limpens *et al.*, 2003). Dans la cellule symbiotique, les rhizobia matures (bactéroïdes) sont enveloppées par une membrane péri-bactéroïdienne (PBM) issue de la membrane cellulaire de la cellule hôte formant les symbiosomes (fig.7).

2.1.1.5. Organogénèse des nodosités

L'organogénèse et la formation des nodosités fonctionnelles requièrent l'implication de plusieurs facteurs des deux partenaires symbiotique. Le déclenchement de l'organogénèse des nodosités nécessite principalement l'implication de deux facteurs moléculaire d'origine microbienne et végétale : Les facteurs Nods (NFs) et la phytohormone cytokinine (CK ; Suzaki *et al.*, 2015). Il a été démontré que le traitement des racines non-inoculées par des NFs ou la surexpression du gène *DMI3*, gène impliqué dans la voie de signalisation des NFs, induisent la dédifférenciation et la profération des cellules corticales conduisant à l'apparition des structures nodosités-like ou primordia de nodosités (Oldroyd *et al.*, 2011 ; Stacey *et al.*, 2006a ; Tirichine *et al.*, 2006). Il a aussi été rapporté que l'application de FNs sur des racines non-inoculées déclenche une accumulation racinaire de CK, une phytohormone impliquée dans le développement des plantes (Van Zeijl *et al.*, 2015). Chez *M. truncatula*, la perception des CKs dans les racines par des récepteurs *Cytokinin REspons 1* (*MtCRE1*) induit l'expression de gènes impliqués dans la nodulation comme *Nodule INception* (*NIN*), *ERF Required for Nodulation 1* (*ERN1*), et *Nodule Signal Pathways 2* (*NSP2*). Ceci suggère un rôle des CKs en aval des NFs dans le déclenchement de l'organogénèse des nodosités racinaire (Gamas *et al.*, 2017; Ariel *et al.*, 2012 ; Gonzalez-Rizzo *et al.*, 2006). Cependant, ces deux facteurs seuls sont incapables d'induire les gènes *Lumpy infection-4* (*LIN-4*) et *basic Helix Loop Helix* (*MtbHLH1)* responsables de la formation et du développement de faisceaux vasculaires importants pour l'échange métabolique et le fonctionnement des nodosités matures. Or, l'expression de ces gènes responsable de la formation de nodosités fonctionnelles requiert l'infection des cellules symbiotiques par des rhizobia (Guan *et al.*, 2013 ; Godiard *et al.*, 2011).

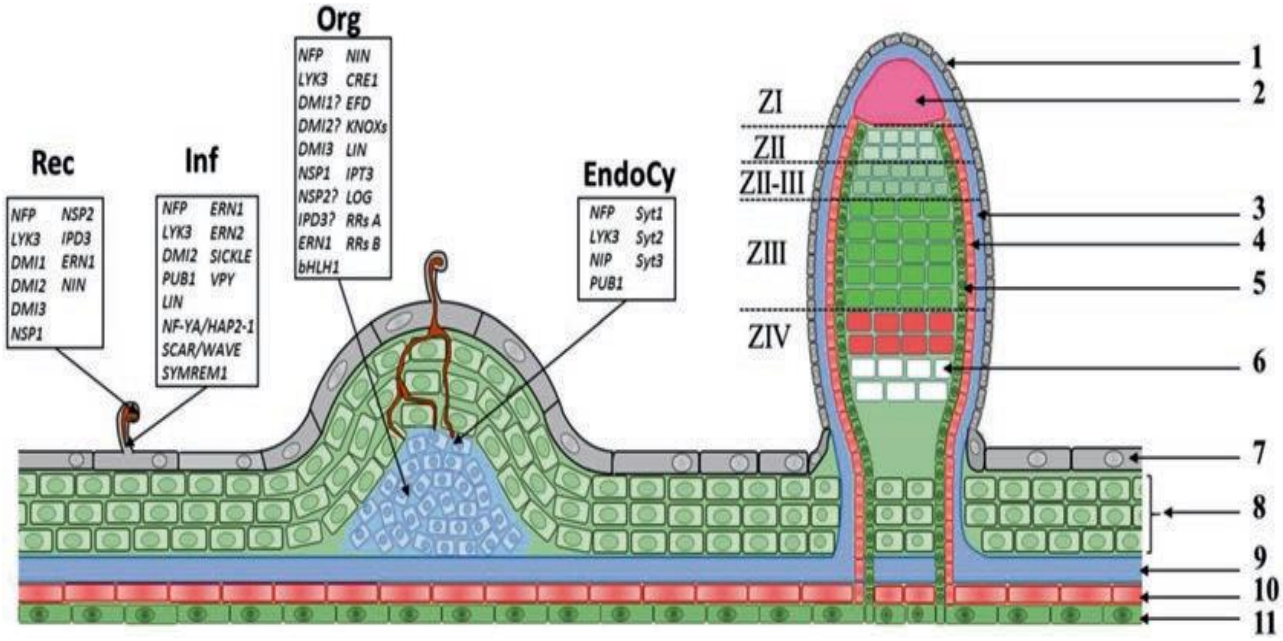

Figure 6. Processus de formation et structure de nodosités. La formation d'une nodosité fixatrice d'azote passe par plusieurs étapes développementales. La nodulation démarre par la reconnaissance (Rec) entre la plante et son partenaire bactérien. Ensuite se déroulent simultanément deux étapes ; l'infection (Inf) et l'organogénèse (org). Les rhizobia atteignent les cellules corticales *via* des cordons d'infection générés suite à leur pénétration par les poils absorbants. Les cellules corticales subissent des divisons cellulaires pour former des primordia nodulaires qui intègrent par endocytose les bactéries libérées des cordons d'infection. (EndoCy). Cette interaction donne naissance à une nodosité mature composée des zones : zone méristématique (ZI), zone d'infection (ZII), zone de fixation (ZIII) séparée de la zone d'infection par une interzone (ZII-III) et zone de sénescence (ZIV). Rectangles noirs: gènes associés à chaque étape développementale. 1: épiderme nodulaire ; 2: méristème nodulaire; 3: cortex nodulaire (endoderme) ; 4: xylème ; 5: phloème ; 6: cellules vide ; 7: épiderme racinaire ; 8: cortex racinaire ; 9: endoderme racinaire ; 10: xylème ; 11: phloème. (Berrabah *et al.*, 2018a).

2.2. Phase tardive de la nodulation

2.2.1. Formation des nodosités matures

Les nodosités de *M. truncatula* sont caractérisées par une forme indéterminée. Cette forme est due à la présence d'un tissu méristématique à forte activité mitotique dans la région apicale de la nodosité (fig.6). L'activité mitotique de la région méristématique de la nodosité mature est contrôlée par un groupe de gènes : *MtHAP2-1, CLAVATA* (*SUNN*) et *NOOT1*. Le facteur de transcription *MtHAP2-1* est exprimé dans le méristème des nodosités matures et son inactivation conduit à la formation de petites nodosités parfois de forme anormale (Combier *et al.*, 2006). Les gènes CLAVATA/embryo-surrounding region codent pour des récepteurs des peptides mobiles comme *CLE3, CLE12* et *CLE13* exprimés dans la zone 1 des nodosités (Roux *et al.*, 2014). Il a été rapporté que la famille *CLAVATA* est impliquée dans la régulation de l'activité méristématique des bourgeons d'*Arabidopsis thaliana* (Williams et Fletcher 2005 ; Mayer *et al.*, 1998). Ceci suggère que les gènes *CLE* jouent un rôle dans la régulation de l'activité méristématique des nodosités. Le gène NOdule roOT (NOOT) est exprimé dans les nodosités et est impliqué dans la détermination de leur identité. En effet, le phénotype du mutant *noot* se caractérise par des racines qui émergent de la région méristématique des nodosités (Couzigou *et al.*, 2012).

La configuration du tissu méristématique dans la nodosité chez les différentes espèces de légumineuses permet aussi de distinguer deux types de nodosités matures : les nodosités déterminées caractérisées par une forme sphérique due à un tissu méristématique diffus et les nodosités indéterminées caractérisées par une forme allongée due à la présence du méristème en position apicale de la nodosité (Vasse *et al.*, 1990).

Chez *Medicago truncatula*, les nodosités indéterminées (Gubry *et al.*, 2010) sont formées sur le plan développemental et physiologique par quatre zones nodulaires qui se différencient successivement de l'apex vers la base (Ogden *et al.*, 2017 ; Xiao *et al.*, 2014 ; Fig 6). La zone I correspondant au méristème apical persistant assure la croissance de la nodosité. Elle est suivie de la zone II dite d'infection qui contient des cordons d'infection et des cellules symbiotiques nouvellement infectées par les rhizobia. Les rhizobia intracellulaires sont entourées d'une membrane d'origine végétale et forment une structure de type organite appelé symbiosome. Ensuite, se trouve l'interzone II-III dans laquelle les rhizobia commencent à se différencier en bactéroïdes. Dans la zone III dite de fixation, les bactéroïdes colonisent massivement les cellules symbiotiques et utilisent des molécules

carbonées à leur profit. En contrepartie, elles fixent l'azote atmosphérique au profit de la plante. Dans les nodosités âgées, stressées ou traitées par le nitrate, une zone de sénescence appelée zone IV apparait en aval de la zone III. Dans cette zone, les cellules symbiotiques et les bactéroïdes en fin de vie sont dégradées et recyclées. Cette zone est aussi colonisée par des rhizobia saprophytiques (Saeki, 2011).

2.2.2. Différenciation des bactéroïdes

Les bactéroïdes différenciés capables de réduire l'azote atmosphérique au profit de la plante hôte sont incapables de survivre à l'extérieur de la cellule symbiotique (Alunni et Gourion, 2016 ; Mergaert *et al.*, 2006). La différenciation des bactéroïdes ne se produit que dans les cellules symbiotiques de certaines légumineuses de la branche des « Legume Inverted Repeat-Lacking Clade » (IRLC) (Czernic *et al.*, 2015). La différenciation est déclenchée suite à l'action de petits peptides antimicrobiens riches en cystéines spécifiques du nodule (Nodule-specific Cysteine Rich (NCR)) qui sont localisés dans l'espace péribactéroïdien des symbiosomes (Haag *et al.*, 2011 ; Kereszt *et al.*, 2011 ; Maunoury *et al.*, 2010 ; Van de Velde *et al.*, 2010 ; Mergaert *et al.*, 2006). Dans le symbiosome, des NCRs interagissent avec des médiateurs cellulaires pour favoriser la duplication du génome et l'augmentation de la taille cellulaire du bactéroïde ; par exemple le NCR247 bloque la division cellulaire du bactéroïde en inhibant la protéine FtsZ (Farkas *et al.*, 2014 ; Kereszt *et al.*, 2011). Il a aussi été montré que la différenciation des bactéroïdes est contrôlée par le symbiosome à travers son transporteur membranaire BacA responsable de la détoxification des NCRs avant qu'ils soient internalisés dans le symbiosome (fig.7. Haag *et al.*, 2011 ; Kereszt *et al.*, 2011).

2.2.3. Fixation de l'azote et régulation négative du système immunitaire des nodosités

Grâce à leur activité nitrogénase, les bactéroïdes différenciés sont capables de réduire l'azote atmosphérique en ammonium assimilable par la plante hôte (Udvardi et Poole 2013). Afin de protéger la nitrogénase bactérienne vis-à-vis de l'oxygène, la plante hôte régule la diffusion de l'oxygène dans les nodosités par la production de leghémoglobine (Lb), une protéine capable de fixer l'oxygène atmosphérique et de réduire son taux dans la nodosité. La leghémoglobine confère aux nodosités une pigmentation rose qui est un indicateur d'un état fixateur d'azote des nodosités (Ott *et al.*, 2005).

Le maintien de la viabilité des bactéroïdes et le bon fonctionnement des nodosités requiert des gènes capables de réprimer le système immunitaire des nodosités (Wang *et al.*, 2016 ; Gourion *et al.*, 2015 ; Berrabah *et al.* ; 2014a ; Bourcy *et al.*, 2013 ; Veereshlingam *et al.*, 2004). Plusieurs gènes symbiotiques sont impliqués dans ce processus comme par exemple, les gènes *Does Not Fix nitrogen 2* (*DNF2*), *Symbiotic Cysteine-rich Receptor-like Kinase* (*SymCRK*), *Nodules Activated Defense 1* (*NAD1*) et *Regulator of Symbiosome Differentiation* (*RSD*) codant respectivement pour une protéine phospholipase C phosphatidyl-inositol-dependant putative, un récepteur RLK doté d'un domaine dont la fonction est inconnue (DUF26), une protéine transmembranaire avec deux domaines et un facteur de transcription de la famille Cysteine-2/Histidine-2. Ces gènes sont capables de réprimer le système immunitaire des nodosités. En effet, la mutation d'un de ces gènes perturbe le mécanisme de protection des bactéroïdes du système immunitaire de la plante hôte. Les nodosités des mutants *dnf2*, *symCRK*, *nad1* et *rsd* réactivent le système immunitaire des nodosités comme par exemple l'activation de gènes de défense, tels que les gènes codant les PR protéines et l'accumulation des composés phénoliques. L'activation des défenses conduit à la mort des bactéroïdes et à la perte de la capacité fixatrice d'azote atmosphérique qui se traduit par la perte de la pigmentation rose et l'apparition des taches brunes sur les nodosités (Berrabah *et al.*, 2015 ; Berrabah *et al.*, 2014a ; Bourcy *et al.*, 2013 ; Wang *et al.*, 2016 ; Sinharoy *et al.*, 2013). Chacun de ces gènes symbiotiques contrôle le système immunitaire dans un stade particulier du processus symbiotique. Le phénotype fixateur est restauré chez le mutant *dnf2* lorsqu'il est cultivé dans un milieu dépourvu d'agents capables d'induire des réactions de défense (Berrabah *et al.* 2014b), indiquant que *DNF2* réprime les réactions de défense d'une manière dépendante de l'environnement. En revanche, le phénotype fix^- du mutant *symCRK* est indépendant des conditions environnementales (Berrabah *et al.*, 2014a). Cependant, les nodosités des mutants *symCRK* et *rsd* ne montrent aucune réaction de défense lorsqu'elles sont induites par le mutant bactérien *bacA* incapable de se différencier. Cela suggère que l'activation des gènes *SymCRK*, et *RSD* ou l'activation de leur protéine correspondante requiert la différenciation des bactéroïdes (Berrabah *et al.*, 2015). En outre, les gènes *NAD1*, *NCR211* et *NCR169* sont impliqués dans la régulation du système immunitaire et la viabilité intracellulaire des bactéroïdes. Le gène *NAD1* code pour une petite protéine membranaire dont la fonction est inconnue (Wang *et al.*, 2016). Les réactions de défense dans les nodosités du mutant *nad1* sont activées, et l'expression des gènes *DNF2*, *SymCRK*, et *RSD* est réprimée ce qui suggère que ce gène *NAD1* inhibe les réactions de défense très tôt, peut-être même avant *DNF2* (Wang *et al.*, 2016). Les gènes *NCR211 et NCR169* sont

impliqués dans la maintenance de la survie des bactéroïdes indifférenciés et différenciés, respectivement (fig.7 ; Horváth *et al.*, 2015 ; Kim *et al.*, 2015).

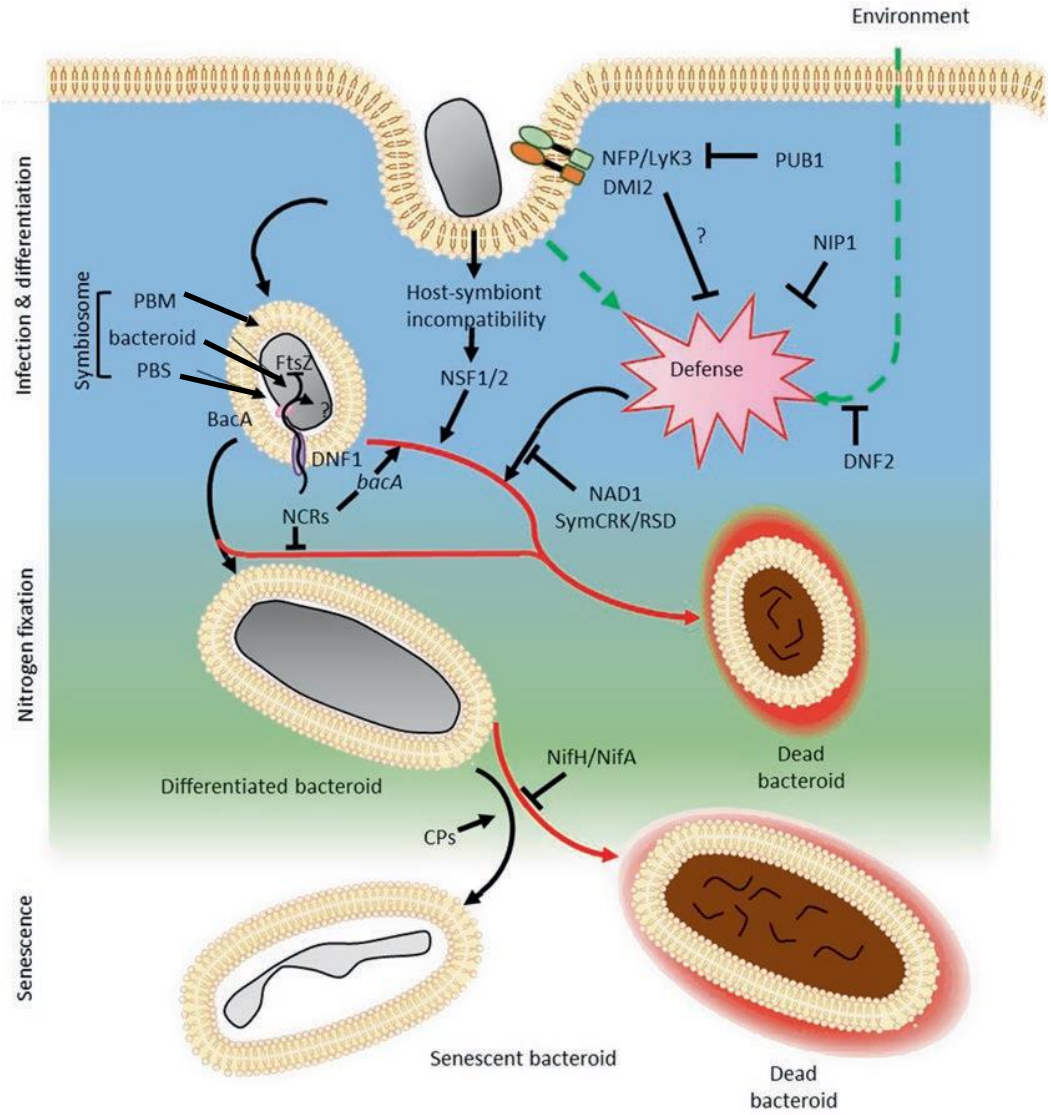

Figure 7. Processus endosymbiotique dans une nodosité mature. Le rhizobium du cordon d'infection entre en contact avec la cellule corticale. Grâce aux gènes *NFP/LYK3*, *DMI2* et *NIP1*, le rhizobium pénètre la cellule corticale par endocytose sans déclencher des réactions de défense. Dans le cas d'infection incompatible, l'endocytose est bloquée par PUB1. Dans la zone II, le bactéroïde requiert une membrane d'origine végétale formant un symbiosome constitué d'une membrane péribactéroïdienne (PBM) et du bactéroïde séparés par un espace péribactéroïdien (PBS). Dans la zone III, grâce à DNF1 (une petite sous-unité endopeptidase située dans PBM) et BacA (un transporteur de la membrane plasmique bactérienne), les NCRs pénètrent dans le cytosol et bloquent la division des bactéries en inhibant la protéine FtsZ. Les NCRs, NFS1 et NFS2 participent à la lyse des bactéroïdes incompatibles. Les réactions de défense sont contrôlées négativement durant tout le processus symbiotique par NAD1, DNF2, SymCRK et RSD. La plante déclenche des réactions précoces de sénescence pour éliminer les bactéroïdes non fixateurs d'azote, ce qui a été observé chez les mutants bactériens *nifH/nifA* incapables de fixer l'azote atmosphérique et les bactéroïdes en fin de cycle dans la zone IV (Berrabah *et al.*, 2018a).

II. Les hormones de défense

1. Ethylène (ET)

1.1. **Introduction**

L'éthylène (ET : $H_2C=CH_2$) est un gaz de la famille des alcènes composé de deux atomes de carbones et quatre atomes d'hydrogène. Cette molécule est importante pour la croissance et le développement des plantes (Ecker, 1995). Elle intervient dans la germination des graines, la senescence des fleurs, l'abscission, la maturation des fruits, le développement des poils absorbants et la nodulation (Johnson et Ecker, 1998), et aussi dans le gravitropisme et la réponse à différents stress (Abeles *et al.* 1992).

1.2.Voies de la biosynthèse de l'ET

La synthèse de l'éthylène est fortement régulée par des facteurs internes et environnementaux (stress biotiques et abiotiques) (fig.8 ; Wang *et al.* 2002).

Dans le cytoplasme, la biosynthèse de l'ET se fait en deux étapes. La première étape débute par la catalyse de la méthionine en Adenosyl-$_L$-Methionine (S-adoMet) grâce à la S-Adenosyl-Methionine synthetase (SAM synthetase). Puis cette S-adoMet est convertie en 1-Amino-Cyclopropane-1-Carboxylate (ACC) et en 5'-MethylThioAdenosine (MTA) par l'ACC synthase (ACS). Le MTA, est recyclé en méthionine par le cycle de Yang (fig.8) pour rétablir la concentration cellulaire de méthionine au cours de la synthèse de l'ET. La deuxième étape est l'oxydation de l'ACC en ET par l'ACC oxydase (ACO ; Gupta et Pandey., 2019).

Il a été rapporté que la voie ACC n'est pas la voie unique pour la production de l'éthylène. En effet, certaines plantes supérieures et aquatiques sont capables de produire l'éthylène indépendamment de la voie ACC. Par exemple, la fougère aquatique *Regnellidium* et l'angiosperme aquatique *Spirodela oligorrhiza* sont capables de produire l'éthylène sans utiliser l'ACC. Par ailleurs, l'ACC ne participe pas à la production d'éthylène dans les racines d'I*pomoea batatas* (Patate douce) infectées par l'ascomycète *Ceratocystis* et dans les épines de *Picea abies.* Cette production ACC indépendante de l'ET implique l'acide linolénique et / ou la méthionine comme précurseurs dans une voie médiée par les radicaux libres *(*Épicéa commun : Mattoo et Suttle, 2018).

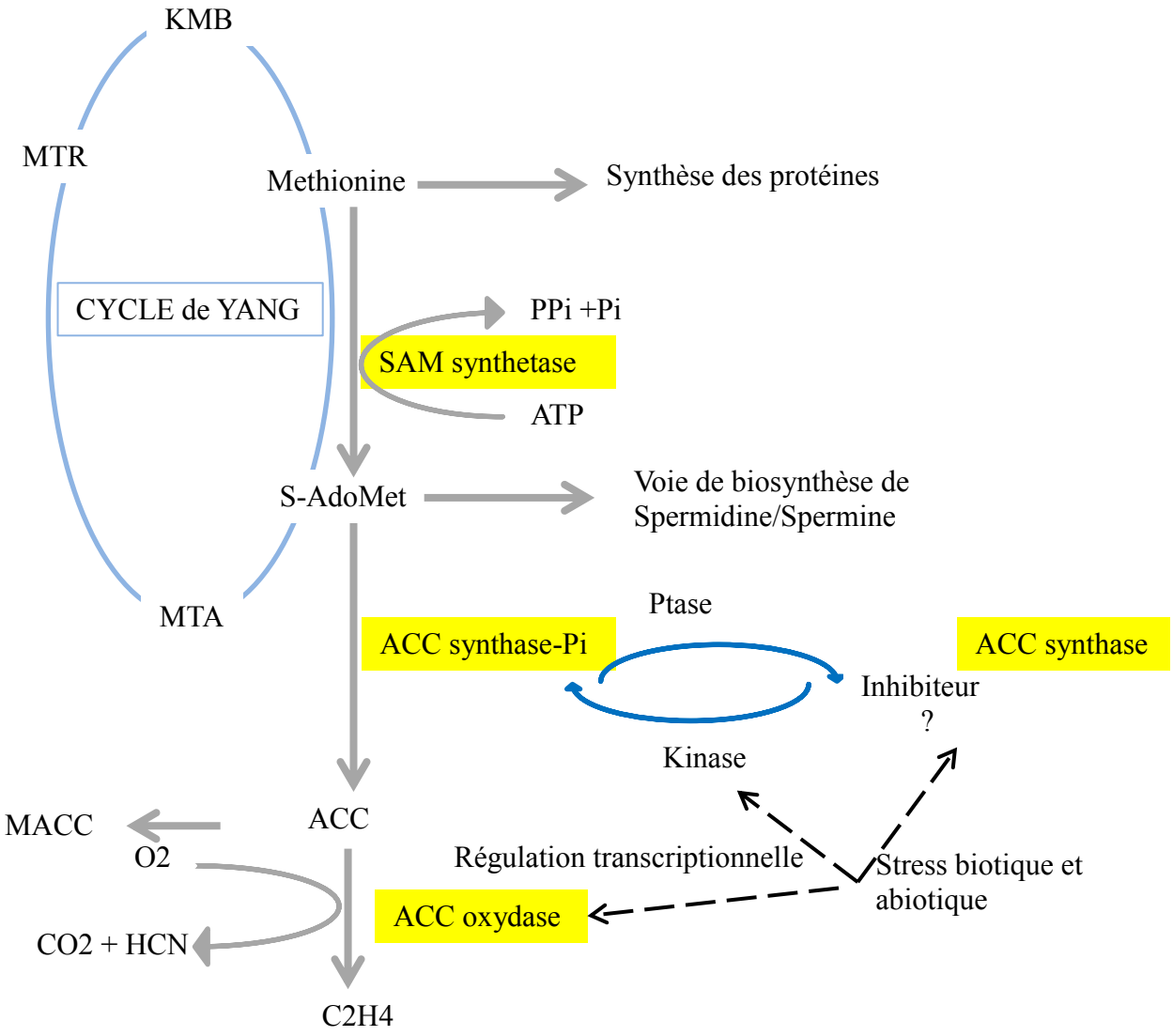

Figure 8. Biosynthèse et régulation de l'ET. La SAM synthetase transforme la méthionine en S-AdoMet en présence d'une molécule d'ATP. Par la suite, S-AdoMet est transformé en ACC et en MTA par l'action de l'ACC synthase. Dans le cycle de Yang, le MTA est recyclé en méthionine en passant par plusieurs intermédiaires comme le MethylThioRibose (MTR) et le 2-Keto-4-MethylthioButyrate (KMB). En outre, le MTA est impliqué dans la voie de biosynthèse des polyamines (précurseur de la voie de biosynthèse de Spermidine/Spermine). L'ACC oxydase catalyse l'ACC en éthylène et génère du dioxyde de carbone et du cyanure d'hydrogène. La conjugaison du N-Malonyl à l'ACC quant à elle va donner du N-Malonyl ACC (MACC) non volatile qui génère une réserve métabolique. La régulation transcriptionnelle de l'ACC synthase et de l'ACC oxydase est indiquée par des flèches en pointillés. La phosphorylation réversible de l'ACC synthase serait induite par des phosphatases inconnues (Ptase) et des kinases. Les kinases sont probablement activées par des stress biotiques et abiotiques. Les deux formes de l'ACC synthase (native et phosphorylée ; ACC synthase-Pi) sont fonctionnelles. Un inhibiteur hypothétique est associé à l'ACC synthase à l'extrémité carboxyle et serait dissocié si l'état de phosphorylation de l'enzyme est modifié à sa proximité. (Arc et al., 2013 ; Wang et al., 2002).

1.3.Voies de signalisation de l'ET

L'ET synthétisé est perçu au niveau du réticulum endoplasmique (RE) par une famille de récepteurs nécessitant du cuivre comme cofacteur qui est fourni par le transporteur de cuivre Responsive to ANtagonist1 (RAN1). Chez *Arabidopsis*, cette famille est composée de cinq membres (ETR1, ETR2, ERS1, ERS2 et EIN4 ; Hall et al. 2000). Ces récepteurs sont en général dimériques transmembranaires et constitués de deux domaines. Le domaine extracellulaire cuivre-dépendant forme un ligand avec l'ET et le domaine intracellulaire de type histidine kinase s'active en réponse aux facteurs environnementaux (fig.9. Gupta et Pandey., 2019 ; Wang et al., 2002).

Cette perception, déclenche une cascade de signalisation induisant des réponses spécifiques à l'ET telles que la triple réponse, qui est caractérisée par l'épaississement et la diminution de la longueur de l'hypocotyle et la modification du crochet terminal des plantules germées dans l'obscurité (Bleecker et al. 1988; Guzman et Ecker 1990; Kieber *et al.* 1993).

En absence de l'ET, les récepteurs membranaires de l'ET sont fonctionnels et activent le domaine kinase (KD) du répresseur CTR1 (Constitutive Triple Response 1) qui est une protéine kinase homologue aux protéines de la famille Raf-like kinase (MAPK3). CTR1 activé va phosphoryler le domaine C-terminal de EIN2 (ou SICKLE). La phosphorylation empêche EIN2 (SICKLE) de transduire le signal, et par conséquence il est ciblé par les protéines F-box ETHYLENE INSENSITIVE 2 TARGETING PROTEIN1/2 (ETP1/2) pour une dégradation par le protéasome 26S. Parallèlement à cela, dans le noyau, les protéines F-box ETHYLENE INSENSITIVE3 BINDING F-BOX1/2 (EBF1/2) ciblent les facteurs de transcription EIN3 / EIL1 pour une dégradation par le protéasome 26S et empêche l'induction de l'expression des gènes en réponse à l'éthylène (fig.9. Ju et Chang, 2015 ; Kieber *et al.*, 1993).

En revanche, en présence d'ET, les récepteurs de l'ET inactivent *CTR1* et libèrent la région C-terminale de EIN2 (SICKLE) qui est alors clivée et envoyée dans le noyau. Son interaction avec le facteur de transcription EIN3 permet l'activation de gènes *ERFs* (ou *EREBPs* ; Solano *et al.* 1998) qui sont alors capables d'interagir avec la boite **GCC** des gènes de réponse à l'éthylène et activent la transcription des gènes ET-dépendant (fig.9. Wang *et al.*, 2002, Wang *et al.*, 2013). En outre, il existe une voie secondaire d'activation de la signalisation ET qui est basée sur l'autophosphorylation d'un résidu His par le domaine His kinase (HK) des récepteurs (Ju et Chang, 2015).

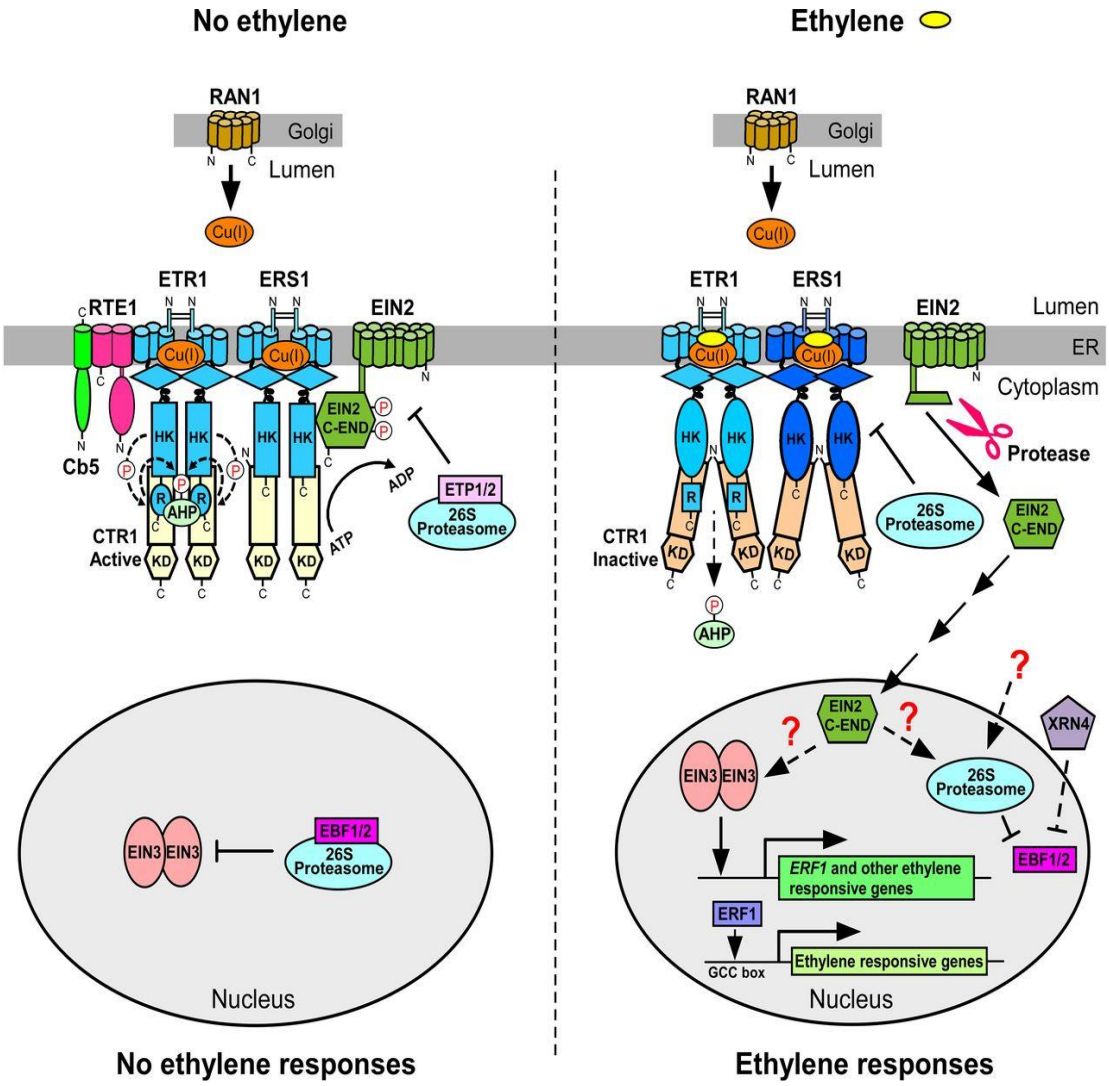

Figure 9. Schéma du model de la voie de signalisation d'ET. L'ET est perçu par les récepteurs de la membrane du RE (ETR1 et ERS1) en présence du RTE1 et du cuivre fourni par RAN1. La perception d'ET désactive la signalisation des récepteurs. Par conséquence, les récepteurs d'éthylène n'activent plus CTR1, et donc EIN2 (SKL) n'est plus phosphorylé. Une partie cytoplasmique d'EIN2 est libérée suite au clivage de la partie C-terminale de l'EIN2 (C-END) par une protéase inconnue. La partie libérée d'EIN2 se déplace dans le noyau et entraîne la dégradation des protéines F-box EBF1/2 par le protéasome 26S dépendant d'EIN2, provoquant ainsi la stabilisation et l'accumulation de facteurs de transcription EIN3 / EIL1. EIN3 / EIL1 activent la cascade transcriptionnelle du facteur de transcription ERF1 et des gènes ET-dépendant **(**Ju et Chang, 2015).

1.4. L'ET au cours de la symbiose

L'ET intervient dans différents stades de la symbiose : réponse aux facteurs Nod (NFs), développement et sénescence des nodosités (Lynch et Brown, 1997; Csukasi *et al.*, 2009; Ding et Oldroyd, 2009) et détermination du phénotype des nodosités chez *Sesbania rostrata*, (Fernandez-Lopez *et al.*, 1998).

1.4.1. Rôle de l'éthylène dans les phases précoces de la nodulation

Le traitement exogène de l'éthylène peut avoir un effet négatif sur la nodulation en inhibant localement la formation des nodules. Cependant, l'application de l'aminoethoxyvinylglycine (AVG) inhibiteur de la voie de synthèse d'éthylène augment le nombre de nodosités (Larrainzar *et al.*, 2015 ; Oldroyd *et al.*, 2001 ; Nukui *et al.*, 2000 ; Penmetsa et Cook 1997 ; Lee et LaRue 1992 ; Grobbelaar *et al.*, 1971). En outre, elle peut avoir un effet positif sur l'infection à certaines étapes de la nodulation en assurant une infection adéquate des cellules symbiotiques par les rhizobia (Guinel, 2015). De manière surprenante, le traitement exogène des racines du soja par l'éthylène ne perturbe pas la nodulation (Lee et LaRue 1992; Schmidt *et al.*, 1999; Nukui *et al.*, 2000).

Au cours des phases précoces de la nodulation, l'oscillation calcique est contrôlée par la concentration intracellulaire d'éthylène. La faible concentration intracellulaire d'éthylène ralentit l'oscillation calcique, ce qui favorise l'induction des gènes codant pour les nodulines et facilite l'invasion des poils absorbants par les rhizobia (Reid *et al.*, 2018 ; Capoen *et al.*, 2009 ; Oldroyd *et al.* 2001). En revanche, en présence de forte concentration d'éthylène, l'oscillation calcique est bloquée dans les cellules des poils absorbants, inhibant ainsi la nodulation (Wood, 2001).

1.4.2. Rôle de l'éthylène dans les phases tardives de la nodulation

Les travaux de Lee et LaRue (1992) ont montré que l'ET a un effet négatif sur la fixation de l'azote atmosphérique par les nodosités. Pour contrer cet effet négatif de l'ET sur la fixation, *Medicago truncatula* recrute un gène symbiotique *SymCRK* capable de protéger les bactéroïdes différenciés fixateurs d'azote hébergés dans les nodosités et d'assurer un apport stable en azote assimilable (Berrabah et al 2018b).

1.5. ET et réponses immunitaires

Les plantes sont en challenge perpétuel par différents stress biotiques et abiotiques. Pour s'adapter, elles mettent en place un système de défense adapté aux dangers menaçant leur survie.

1.5.1. Rôles de l'ET dans les réponses immunitaires de type PTI

La réponse directe commence par la perception par des récepteurs membranaires ou PRRs (Pattern Recognition Receptors) (Cook *et al.*, 2015 ; Zipfel, 2014), des éliciteurs de défense tels que les épitopes des pathogènes PAMP/MAMP (Pathogene-Associeted Molecular Patterns/Microbe-Associeted Molecular) ou/et par des débris des cellules végétales endommagées par les pathogènes ou DAMP (Damage-Associated Molecular Patterns) (Ferrari *et al.*, 2013; Savatin *et al.*, 2014; Acevedo *et al.*, 2015). Par la suite, le complexe ligand-récepteur active le premier niveau de résistance ou PTI (Pattern-Triggered Immunity). Cette activation se traduit par la biosynthèse de l'ET (fig.10) et d'autres composés comme des dérivés réactifs de l'oxygène ou ROS (Reactive Oxygen Species) et l'activation de la voie de signalisation MAPK (Mitogen-Activated Protein Kinase) qui régulent la production des protéines de défense (PR) et des métabolites secondaires (fig.10. Boller et Felix, 2009; Wu et Baldwin, 2010).

Au cours de la PTI, on distingue deux voies de signalisation intracellulaires. La première voie est basée sur l'activation de la voie ROS et l'oscillation calcique et la seconde est basée sur la phosphorylation par des MAPK. Les voies conduisent à la transmission de signaux de détresses dans le noyau qui induisent les gènes de biosynthèse de l'ET (fig.10 ; Couto et Zipfel 2016 ; Liu et Zhang 2004).

1.5.2. Rôles de l'ET dans les réponses immunitaires de type ETI

La réponse indirecte débute lorsque les pathogènes contournent la réponse directe impliquant des effecteurs qui bloquent le PTI (Pel et Pieterse, 2013). Selon le type d'effecteurs, les plantes font appel à des récepteurs intracellulaires de type NLRs (Intracellular Nucleotide-binding domain Leucine-rich Repeat), qui reconnaissent le(s) effecteur(s) et déclenchent l'ETI (Effector-Triggered Immunity) (Jones et Dangl, 2006; Cui *et al.*, 2015). Cette interaction conduit à l'activation immédiate de la biosynthèse de l'ET (fig.10) et à la mort cellulaire programmée sur le site d'infection (Broekgaarden *et al.*, 2011).

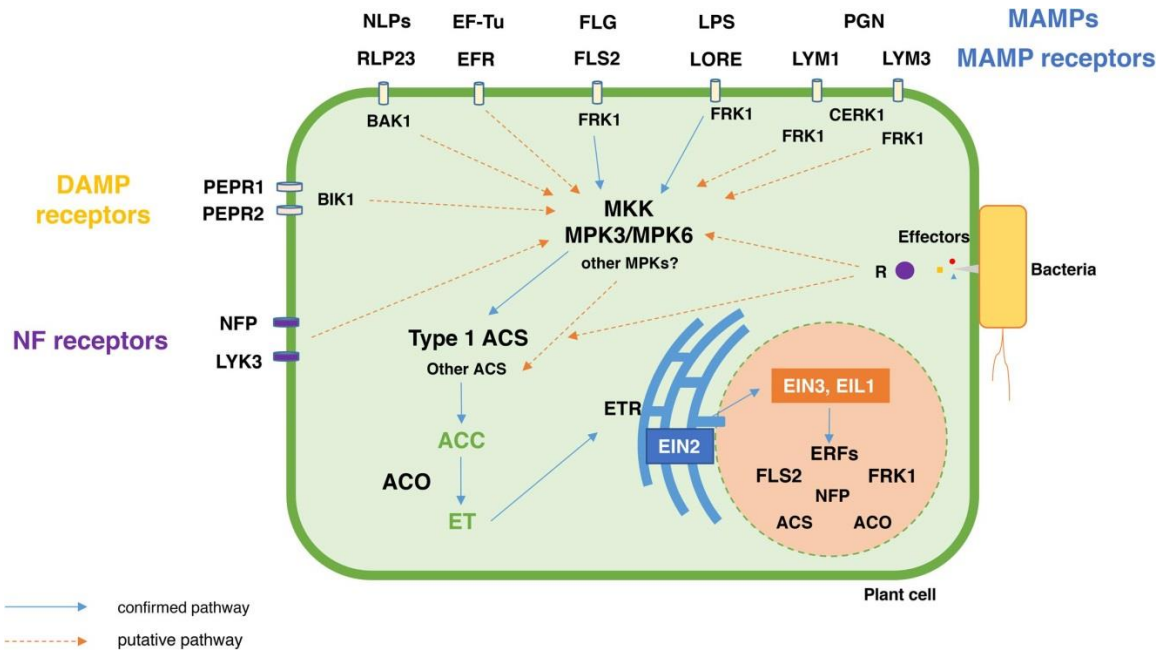

Figure 10. Dialogue moléculaire entre bactérie et cellule végétale. Les différents motifs bactériens sont perçus par leurs récepteurs membranaires appropriés présents dans la membrane externe des cellules végétales et activent des cascades de signalisation MAPKinase qui induisent la production d'ACC et d'ET par l'activation de l'ACS type 1. Néanmoins, l'activation de la voie ET par les protéines R reste inconnue.

MAMP : Microbe Associated Molecular Pattern; DAMP : Damage Associated Molecularpattern; FLG : Flagelline; EF-Tu : facteur d'élongation-Tu; LPS : lipopolysaccharide; PGN : Peptidoglycane; PNL : nécrose et peptides inducteurs d'éthylène; NF : Facteurs de nodulation; FLS2 : récepteur de la flagelline; EFR : récepteur du facteur d'élongation-Tu; RLP23 : récepteur de peptides inducteurs de nécrose et d'éthylène; LORE : récepteur des lipopolysaccharides; LYM1 et LYM3 : récepteurs des peptidoglycanes; NFP et LYK3 : récepteurs du facteur de nodulation; PEPR1-2 : récepteur Pep1. R : protéine de résistance impliquée dans la reconnaissance effectrice; CERK1 : kinase du récepteur LysM; FRK1-Kinase1 : receptor-like kinase1 induit par FLG22; BAK1 : kinase associée à la brassinostéroïde insensible 1 (BRI1); BIK1 : kinase 1 induite par le botrytis; MKK : protéine kinase kinase activée par un mitogène; MPK : protéine kinase activée par un mitogène. ACS : ACC synthase; ACO : ACC oxydase; ERF : Facteur de réponse à l'éthylène (Nascimento *et al.*, 2018).

1.5.3. Des microorganismes dégradent l'ET grâce à des ACC déaminases.

Les bactéries, les levures et les champignons peuvent produire et sécréter une 1 aminocyclopropane-1-carboxylate déaminase (ACD) (Jia *et al.* 2000; Shah *et al.* 1998; Minami *et al.* 1998). Cette enzyme est capable de réduire l'ACC produit par les plantes en ammoniac et en acide alpha-cétobutyrique (fig.11) ce qui limite la disponibilité de l'ACC et ralentit la biosynthèse d'ET chez les plantes (Penrose *et al.*, 2001). Cette réduction de la disponibilité du précurseur de l'ET, confère à la plante la capacité de maintenir une croissance stable dans des conditions de stress biotiques et abiotiques et permet aux microorganismes de mieux résister aux défenses de la plante induites par l'ET (Burd *et al.* 2000 ; Wang *et al.* 2000 ; Grichko et Glick 2001).

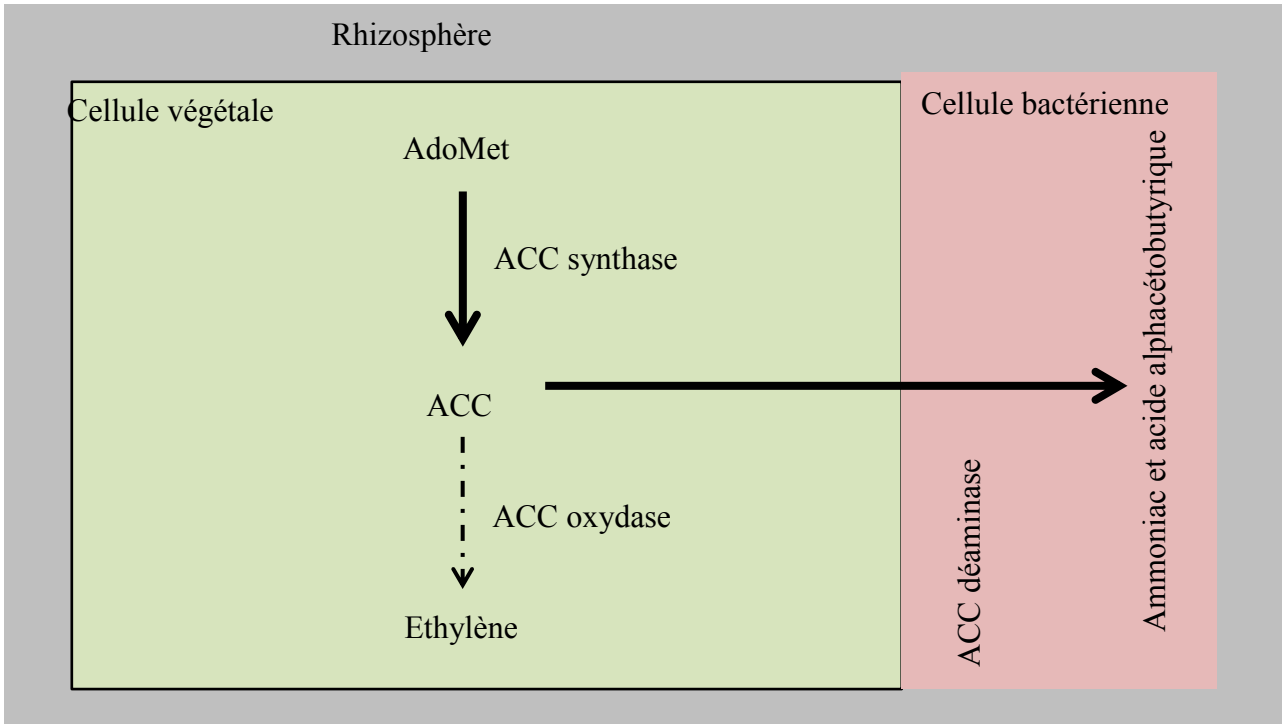

Figure 11. Inhibition de la biosynthèse de l'ET par l'ACC déaminase. L'ACC déaminase des bactéries abaisse le niveau d'éthylène dans les plantes en dégradant l'ACC exsudé en ammoniac et en acide alphacétobutyrique. Flèche en pointillé : production réduite d'éthylene (Glick et Pasternak, 2003 modifié).

1.5.4. Microorganismes producteurs de l'ET

Certaines microorganismes sont capables de synthétiser de l'ET. Fukuda *et al.* (1989) a rapporté que l'éthylène est produit par 7 souches de bactéries sur 34, 13 souches de levures sur 45, 27 souches de champignons sur 52 et 2 actinomycètes sur 35. Globalement, le taux des microorganismes capables de synthétiser l'ET, selon cette étude, est d'environ 30% (49 souches sur un total de 166 souches testées), mais cette biosynthèse est conditionnée par la disponibilité en méthionine, précurseur de l'ET, peu disponible dans l'environnement naturel (Mattoo et Suttle, 2018 ; Lieberman, 1979 ; Wilkes *et al.*, 1989 ; Primrose, 1976 ; Shipston et Bunch,1989).

Parmi ces microorganismes, on trouve des bactéries du sol comme *Escherichia coli* (Mattoo et Suttle, 2018; Primrose 1976 ; Primrose et Dilworth, 1976) *Pseudomonas solanacearum,* (Mattoo et Suttle, 2018 ; Freebairn et Buddenhagen, 1964), *Pseudomonas syringae* pv. *phaseolicola* (Mattoo et Suttle, 2018 ; Goto *et al.*, 1985) et *P. syringae* pv. *Glycinea* (Mattoo et Suttle, 2018 ; Sato *et al.*, 1987), des levures *Saccharomyces cerevisiae* (Mattoo et Suttle, 2018 ; Thomas et Spencer, 1977) et *Cryptococcus albidus* (Mattoo et Suttle, 2018 ; Fukuda *et al.*, 1989), des champignons *Penicillium digitatum* (Mattoo et Suttle, 2018 ; Biale,1940 ; Miller, 1940), *Blastomyces dermatitidis* (Mattoo et Suttle, 2018; Nickerson,1948) et certaines actinomyces (Mattoo et Suttle, 2018; Ilag et Curtis, 1968).

Le rôle de l'ET produit par ces microorganismes dans l'interaction plante-microorganisme est peu connu. Goto *et al.* (1985) ont rapporté que l'ET présent dans les tissus de *Pueraria* (le kudzu) infectés par *Pseudomonas syringae* est essentiellement produit par la bactérie, et pourrait conduire à une amélioration concomitante de l'apport en nutriments pour les bactéries et à une élimination des molécules antimicrobiennes comme la tulipaline (Mattoo et Suttle, 2018 ; Freebairn et Buddenhagen, 1964 ; Beijersbergen et Bergman, 1973).

2. Acide salicylique (SA)

L'acide salicylique (SA), est une phytohormone impliquée dans l'activation des voies de défense contre les pathogènes en particulier les biotrophes (Li *et al.*, 2019). Elle induit la résistance systémique acquise (SAR) et la résistance locale acquise (LAR) active l'expression des gènes PR (Li *et al.*, 2019 ; Kumar, 2014).

La biosynthèse du SA se fait via deux voies ; la voie isochorismate et la voie phenolpropanoïde en utilisant un dérivé de la voie chikimate, le chorismate (Li *et al.*, 2019). Chez la plante modèle *A. thaliana*, le SA est perçu par trois protéines de la famille **NPR (**Non-expressor of Pathogenesis-Related genes), **NPR1, NPR3 et NPR4** qui sont des régulateurs de l'induction des gènes de défense. Ces régulateurs interagissent avec des facteurs de transcription spécifiques (TGA) qui sont des régulateurs positifs de l'expression des gènes de défense, tels que les gènes PR (fig.12). Parmi ces trois protéines NPR, la protéine NPR1 est le régulateur principal de la signalisation du SA chez *Arabidopsis*. Elle interagit directement avec les facteurs de transcription TGA, alors que les deux autres protéines, NPR3 et NPR4, régulent l'accumulation de NPR1 dans le noyau en fonction de la concentration intranucléaire du SA (fig.13). NPR1 joue aussi un rôle dans la perception du SA dans le cytosol et la régulation de la diaphonie entre la reprogrammation transcriptionnelle médiée par le SA et le JA (acide jasmonique. Ding *et al.*, 2018 ; Seyfferth et Tsuda 2014).

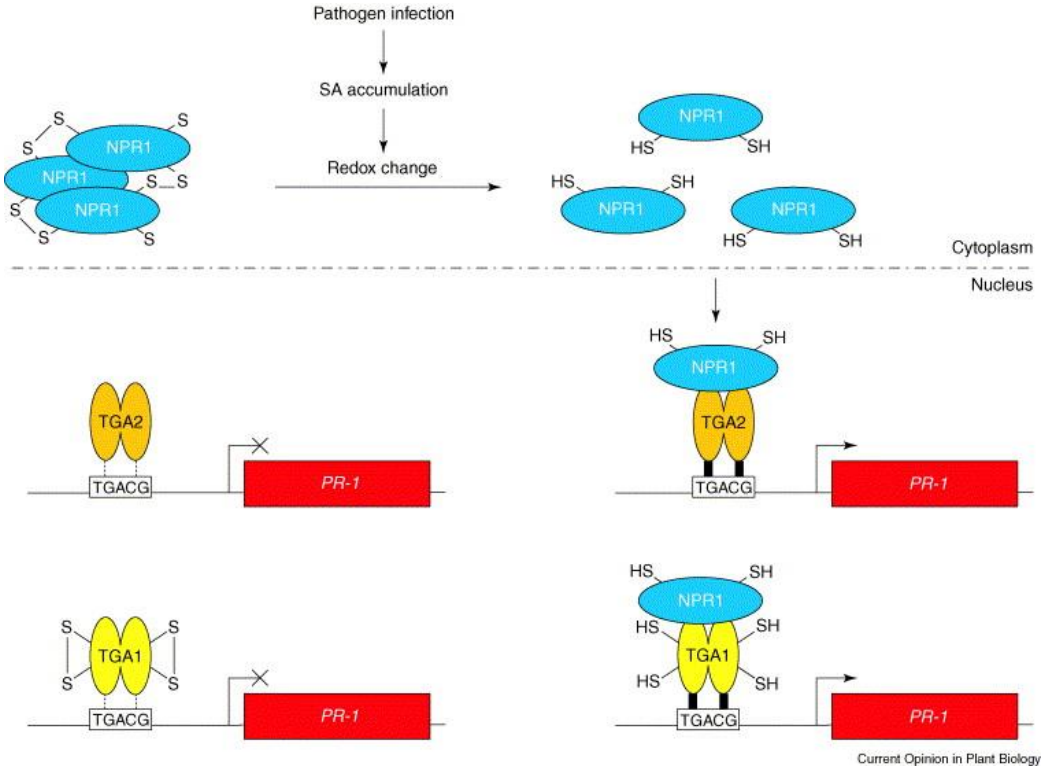

Figure 12. Modèle de réponse du SA chez Arabidopsis. Dans les cellules non stressées. NPR1 oxydé forme des oligomères inactifs dans le cytosol. Par conséquence, les TGAs restent liés à la région promotrice (TGACG) des gènes sensibles au SA comme le gène *PR-1*. Lors d'un stress biotique, le SA s'accumule dans le cytosol et change le statut redox. Ce changement réduit les liaisons disulfures des TGAs et NPR1 passe à un état de monomères actifs. NPR1 sous sa forme monomérique est ensuite transloqué dans le noyau où il interagit avec les TGAs, tels que le TGA2. Le complexe NPR1/TGA stimule l'expression du gène PR-1. (Pieterse et Van Loon, 2004).

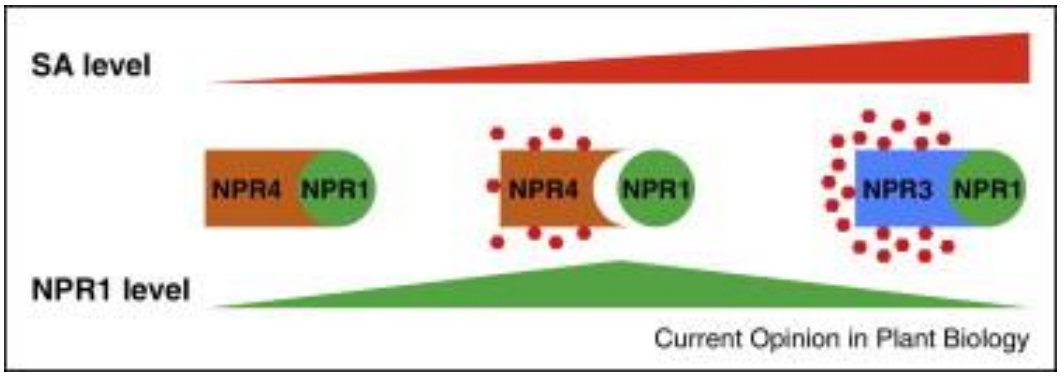

Figure 13. Modèle de la régulation de NPR1 par NPR3 et NPR4. NPR1 est un régulateur positif des réponses médiées par le SA. NPR3 est un récepteur du SA à faible affinité et NPR4 est un récepteur du SA à haute affinité. Les protéines NPR3 et NPR4 régulent la dégradation de NPR1. Le SA bloque l'interaction NPR4-NPR1 et facilite l'interaction NPR3-NPR1. Lorsque le niveau de SA est très bas, le niveau NPR1 est faible car NPR4 facilite sa dégradation. Lorsque le niveau SA est très élevé, le niveau de NPR1 est également faible car NPR3 facilite sa dégradation. Au niveau de SA moyen, le niveau de NPR1 est le plus élevé parce que le SA est suffisant pour perturber l'interaction NPR4-NPR1, mais pas assez pour faciliter l'interaction NPR3-NPR1 **(**Yan et Dong, 2014).

Le SA est aussi impliqué dans la nodulation. Il inhibe en effet la formation et le développement des nodosités indéterminées et pourrait réduire le nombre de nodosités déterminées à forte concentration (Lian *et al.*, 2000). En revanche, le SA n'a aucun effet sur la formation des nodosités déterminées à faible concentration (Van Spronsen *et al.*, 2003). De plus, l'expression de l'enzyme salicylate hydroxylase (*NahG*) dans les racines réduit le taux de SA dans ces racines et conduit à une augmentation du nombre d'infection et de nodosités (Stacey *et al.*, 2006b).

Il est noté également que la synthèse du SA est dépendante du partenaire bactérien et plus précisément des facteurs Nod (NFs) émis pas ce dernier. En effet, en inoculant les plantes avec son partenaire symbiotique, la concentration du SA reste stable à un niveau bas. Cependant, l'accumulation du SA atteint à niveau élevé lors de l'inoculation par un partenaire incompatible ou par son partenaire compatible déficient dans la synthèse de facteurs Nod (NFs, Martínez-Abarca *et al.*, 1998) ou encore en inoculant des plantes déficientes dans la perception des facteurs Nod (NFs) par son partenaire symbiotique (Blilou *et al.*, 1999).

3. Acide jasmonique (JA)

L'acide jasmonique (JA) est une phytohormone qui joue un rôle primordial dans la signalisation végétale. Elle intervient dans la régulation de nombreux processus physiologiques comme les réponses aux blessures, la synthèse des métabolites secondaires, la défense contre les stress biotiques et abiotiques (Li *et al.*, 2019 ; De Vleesschauwer *et al.*, 2014)**.** La biosynthèse du JA se fait en deux étapes. La première étape se déroule au niveau chloroplastique, elle commence par l'oxygenation de l'acide linolenique. Le produit de l'oxydation de l'acide linolénique soubit ensuite une série de catalyses par la 13-lipoxygénase (LOX), l'allene oxide synthase (AOS) et l'allene oxide cyclase (AOC) appelé aussi 12-oxophytodienoic (OPDA). La deuxième étape se déroule au niveau du peroxisome, dans lequel l'OPDA chloroplastique est converti en JA suite aux actions de l'OPDA réductase 3 (OPR3) et l'acyl-CoA-oxidase 1(ACX1). Le JA ainsi formé est transféré dans le cytosol (LOX. Li *et al.*, 2019 ; Robert *et al.*, 1997). Le JA cytosolique est perçu dans le noyau sous sa forme conjuguée à l'isoleucine (JA-Ile) par le récepteur SCFCOI1. Ce complexe (JA-Ile-SCFCOI1) interagit par la suite avec les protéines JASMONATE ZIM DOMAIN (JAZ) qui sont des régulateurs négatifs des gènes JA- dépendant. En effet, les JAZ répriment les facteurs de transcription du sous-groupe IIIe des basic-helix-loop-helix (bHLH), tels que les gènes *MYC2* (Wasternack et Strnad, 2017)**.** Le complexe (JA-Ile-SCFCOI1-JAZ) est, par la suite, reconnu par la machinerie de dégradation ubiquitine-protéasome afin de libérer le facteur de transcription MYC2 et activer la transcription des gènes de défense (fig.14) (Wasternack et Strnad, 2017 ; Santner et Estelle, 2007).

Dans les étapes précoces des réactions symbiotiques rhizobium/legumineuse, le JA régule la formation des cordons d'infection en influençant l'oscillation calcique dans les cellules corticales et la production des facteurs Nod (NFs) par les rhizobia ; l'application modéré du JA (0,1 µM) stimule l'expression des gènes Nod et la production des NFs et augmente le nombre de cordons d'infection et de nodosités chez *Lotus japonicus* (Basso et Veneault-Fourrey, 2020 ; Suzuki *et al.*, 2011 ; Mabood et Smith 2005). De plus, le traitement des racines de *M. truncatula* pendant une heure par les NFs augmente la concentration de l'oxylipine précurseur du JA. Cependant, l'application du JA à des doses plus élevées inhibe la formation de cordons d'infection et la nodulation (Basso et Veneault-Fourrey, 2020 ; Nakagawa et Kawaguchi, 2006) et réduit la sensibilité de la plante aux facteurs Nod chez *M. truncatula* et *L. japonicus* (NFs) (Sun et al, 2006). En outre**,** L'expression des gènes de biosynthèse ou de perception du JA est inhibée dans les feuilles après inoculation par les

rhizobia chez *G. max* (Kinkema et Gresshoff, 2008)**.** En revanche, la concentration du JA est très élevée dans les feuilles du mutant hyper-nodulateur *nts* de *G. max* en comparé à la plante sauvage. L'application du n-propyl gallate, un inhibiteur de la biosynthèse du JA, sur des feuilles de *G. max* réduit aussi le nombre de nodosités surtout chez le mutant *nts* (Kinkema et Gresshoff, 2008 ; Seo *et al.,* 2006)**.** En revanche, l'augmentation locale et systémique des niveaux d'acide jasmonique causée par les blesseurs répétées des feuilles n'affecte par l'interaction entre rhizobia et *M. truncatula* (Landgraf *et al.* 2012 ; Basso et Veneault-Fourrey, 2020).

Dans les étapes tardives de la nodulation, le JA semble avoir un effet négatif sur la différenciation des bactéroïdes et la fixation d'azote dans les nodosités matures bien que, le gène de biosynthèse de l'oxylipine, précurseur du JA, ne soit pas exprimé dans les nodosités fixatrices d'azote et que l'altération ou l'augmentation de la biosynthèse du JA n'a aucun effet sur la nodulation chez *M. truncatula*. L'activation de la voie JA dans les nodosités de *Astragalus sinicus* par silencing du régulateur negatif JAZ1 de la voie de signalisation du JA, réduit la différenciation des bactéroïdes et la capacité fixatrice d'azote, suggèrant que d'autres types d'oxylipine sont impliquées dans la biosynthèse du JA dans les nodosités. En plus, le JA module la capacité fixatrice d'azote en agissant sur l'activité de la Leghemoglobine (Basso et Veneault-Fourrey, 2020). Ceci, suggère que la signalisation JA active le pré-contact entre les deux partenaires symbiotiques en activant le dialogue moléculaire symbiotique et permet une infection efficace des cellules corticale. En revanche, la signalisation JA affecte négativement la différenciation des bactéroïdes et la capacité fixatrice des nodosités dans les étapes tardives de la nodulation.

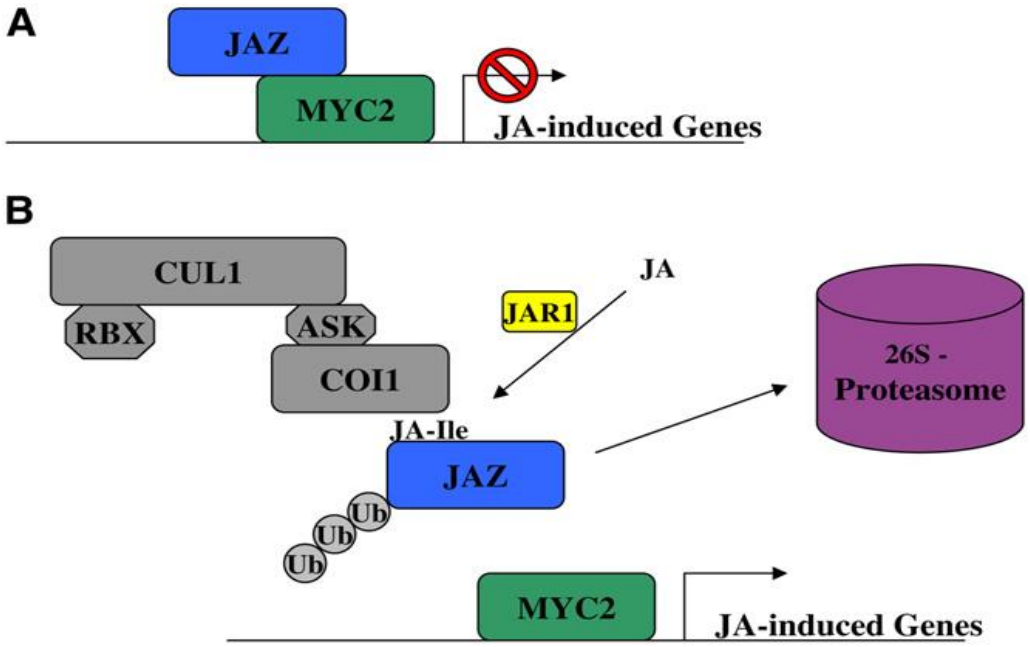

Figure 14. Modèle de réponse de Jasmonate chez Arabidopsis. (A) MYC2 (en vert) se lie aux motifs de la boîte G adjacents aux gènes régulés par le JA. La protéine JAZ (en bleu) réprime l'activité de MYC2 par une interaction directe entre son extrémité C terminale avec l'extrémité N terminale de MYC2. (B) Le JA est conjugué à Ile par JAR1 (en jaune). Le JA-Ile favorise l'interaction des protéines JAZ avec SCFCOI1 (en gris), conduisant à la poly-ubiquitination (Ub) et à la dégradation du complexe par le protéasome 26S (en rose) (Santner et Estelle, 2007).

En plus des homones dite de défense (l'éthylène, l'acide salicylique et l'acide jasmonique), les hormones de développement comme l'auxine, les cytokinines, les strigolactones et les gibbérellines peuvent aussi participer dans la mise en place de la nodulation en jouant généralement un rôle moins important. Dans cette étude les hormones de développement ne seront pas traitées

4. Crosstalk entre ET, SA et JA

En réponse aux différents stress biotiques et abiotique, la plante optimise ses stratégies de défense en favorisant les voies les moins coûteuses énergiquement. Parmi les stratégies moins coûteuses figure la potentialisation entre les voies de signalisation. Cette stratégie est le bon exemple de la coopération entre les hormones en réponse aux stress biotiques et abiotiques (Beckers et Conrath, 2007). Ce phénomène de potentialisation a été décrit dans la partie aérienne de plusieurs espèces végétales comme le tabac et *Arabidopsis thaliana* en réponse aux stress biotiques et abiotiques (Beckers et Conrath, 2007 ; Lawton *et al.*, 1994 ; Xu *et al.*, 1994).

Au cours de la croissance, des hormones ont peu de gènes cibles en commun (Nemhauser et al., 2006). Cependant, certains gènes hormone-spécifique sont régulés par d'autres hormones, ce qui explique l'effet antagoniste ou synergique entre les voies hormonales (Koorneef et Pieterse, 2008). Dans la littérature existe plusieurs exemples qui témoignent de ce phénomène. Par exemple chez *A. thaliana*, y a une synergie entre l'ET et le SA dans l'induction du gène *PR1* et tous les deux sont requis lors de l'activation des réactions de défense contre les pathogènes nécrotrophes. Donc ce gène est induit à la fois par le SA et l'ET (Li *et al.*, 2019 ; Lawton et al., 1994). En outre, ce gène *PR1* est induit aussi par le JA et l'ET chez les jeunes plantules de tabac (Xu et al., 1994). Ce phénomène synergique entre les hormones est observé chez d'autres espèces végétales. Par exemple, le traitement combiné de SA et JA sur des jeunes plantules de pois ou le traitement par le JA induisent l'activation du gène *PAL*. En outre, le SA est capable aussi d'induire l'expression du gène *PAL* chez les jeunes plantules de pois après inhibition de la voie de biosynthèse du JA par l'acide nordihydroguaiaretique (NDGA). A cet effet, SA et JA agissent en synergie sur le métabolisme phénolique induit par PAL (Li *et al.*, 2019 ; Yang *et al.*, 2011 ; Campos-Vargas et Saltveit, 2002). En plus, Schenk et al., (2000) montrent une synergie entre le JA et l'ET dans la régulation d'un nombre de gènes impliqués dans les réactions de défense contre plusieurs pathogènes (fig.15).

Cependant, des effets antagonistes sont aussi cités dans plusieurs travaux (Doares et al., (1995) ; Gu et al., (2000) ; Gupta et al., (2000)) qui montrent que le SA est capable de contrôler négativement l'expression des gènes ET-dépendant et JA-dépendant, ainsi que la voie de biosynthèse de JA chez la tomate. Le mutant *coil1* chez *A. thaliana*, altéré dans la voie de de signalisation de JA, favorise la voie SA pour contrer l'agression par *Pseudomonas*

syringae (fig.15 ; Feys et al., 1994). En outre, il a été montré que les régulateurs positifs de la voie JA et ET comme le facteur de transcription Ethylene Insensitive 3 (EIN3), ANAC019 et leurs homologues répressent l'expression du gène *ICS1* impliqué dans la biosynthèse du SA

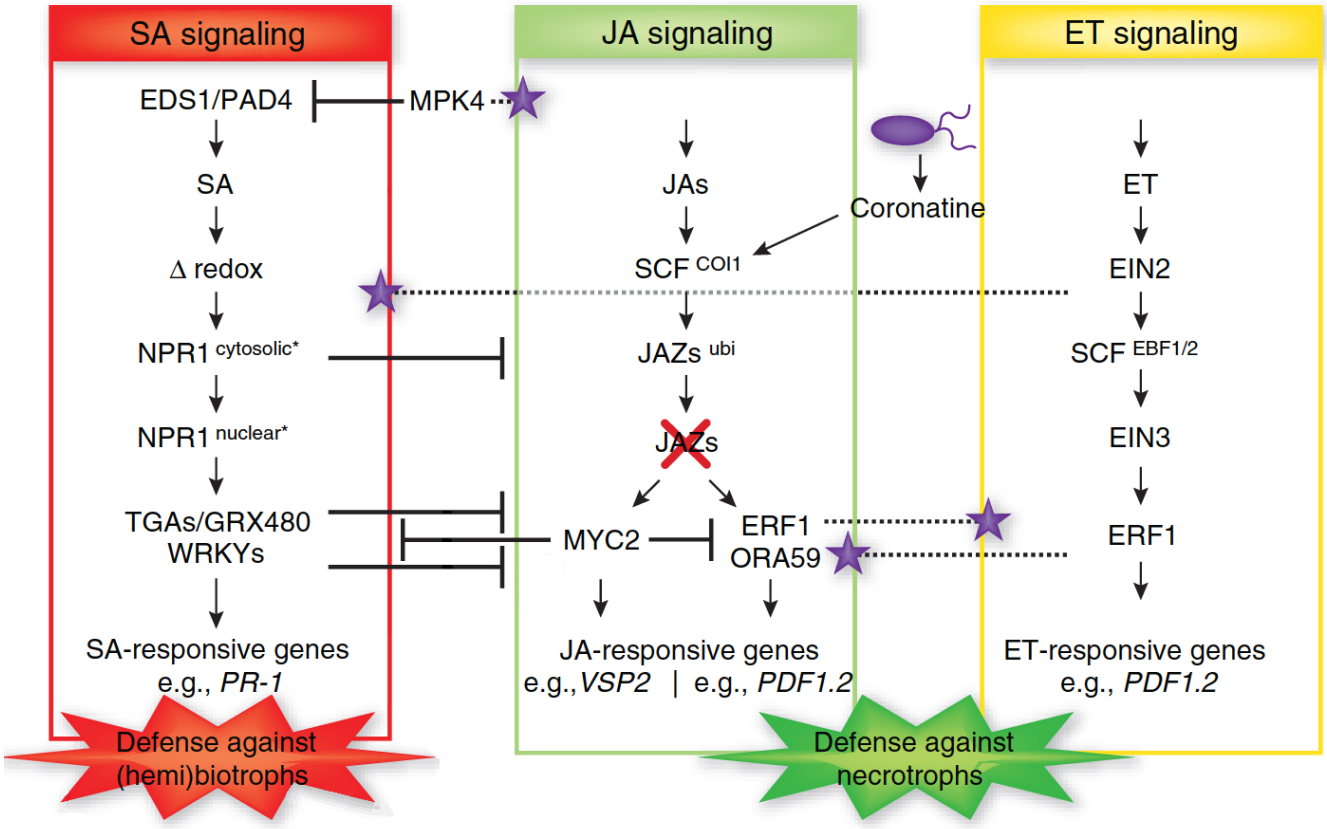

Figure 15. Cross talk entre les phytohormones en réponse aux pathogènes. L'intercommunication entre les hormones défense SA, JA et ET confère à la plante une plasticité de défense contre les pathogènes. Certaines bactéries pathogènes émettent dans les cellules de la plante hôte des molécules effectrices comme la coronatine pour interférer la signalisation hormonale et le déclenchement des réactions de défense. Ligne barrée: effet négatif (répression); étoiles violettes: effet positif (induction. Pieterse *et al.* 2009, modifié).

Contexte et objectifs du projet de la thèse

Le laboratoire a identifié chez *Medicago truncatula* R108, deux gènes symbiotiques, *DNF2* et *SymCRK*, impliqués dans les phases tardives de la nodulation. Ces deux gènes codent pour une phosphatidylinositol phospholipase C à domaine X (PI-PLCXD) et une cysteine-rich receptor-like kinase, respectivement, et sont importants pour la mise en place des nodosités fixatrice. Les nodosités mutées pour un de ces deux gènes (*dnf2* ou *symCRK*) sont incapables de fixer l'azote atmosphérique et déclenchent des réactions de défense dans les nodosités. Ceci se traduit par l'induction des gènes de défense comme les gènes *PR* et l'accumulation de composés phénoliques (Bourcy *et al.*, 2014 ; Berrabah *et al.*, 2014a).

Le laboratoire dispose des lignées *M. truncatula* R108 mutées dans les gènes symbiotiques *dnf2* (MS240, NF2496, NF0217, NF1526) et *symCRK* (NF0737, NF16231, NF21165) et des lignées mutées dans le gène *myc2* impliqué dans la voie de signalisation de l'acide jasmonique (NF18028, NF18829, NF13601). Dans le fond génétique A17 le laboratoire dispose des lignées mutées dans les mêmes gènes symbiotiques *symCRK* (dnf5-2) et *dnf2* (dnf2) et une lignée mutée dans le gène *sickle* (*skl*) analogue du gène *AtEIN2* impliqué dans la voie de signalisation de l'éthylène.

Les travaux de Berrabah *et al.*, (2008b), ont montré que l'éthylène joue un rôle majeur dans les réactions de défense des nodosités du mutant *symCRK* fond R108. Cette étude a montré que l'ajout d'un inhibiteur de la voie de synthèse de l'éthylène (AVG) dans le milieu de culture des mutants *symCRK* réduit la surface des nécroses des nodosités. De plus, le traitement exogène des nodules sauvages de *M. truncatula* R108 par l'éthylène entraîne un arrêt de l'activité fixatrice de l'azote et une accumulation des composés phénoliques dans les nodosités ce qui phénocopie le mutant *symCRK*.

L'objectif de mon projet de thèse a été d'étudier les mécanismes responsables de l'accommodation intracellulaire des rhizobia dans les cellules symbiotiques afin de contribuer à une meilleure compréhension du processus symbiotique *M. truncatula* / rhizobium.

Pour cela, je me suis intéressé : (1) à l'étude du rôle des hormones de défense (éthylène, acide salicylique et acide jasmonique) dans les réactions de défense des nodosités dans le but de comprendre le lien entre les gènes symbiotiques et la régulation des voies hormonales ; (2) à l'identification de gènes marqueurs spécifiques de chaque hormone exprimés dans les nodosités afin de révéler l'implication des hormones de défense dans les mécanismes de

défense des nodosités ; (3) au décryptage du rôle de gènes NBS-LRR et révéler leur implication dans l'accommodation de la survie intracellulaire des rhizobia ; (4) à la recherche de nouveaux gènes symbiotiques pour mieux comprendre le processus de la mise en place de la nodulation fixatrice d'azote ; (5) à la recherche et la création d'outils génétique capables de simplifier la recherche des gènes impliqués dans la symbiose et la recherche des bactéries capables d'induire la formation des nodosités non-fonctionnelles et d'y déclencher des réaction de défense pour mieux comprendre les mécanismes de défense dans les nodosités matures.

Chacun des objectifs se décline comme suit :

Objectif 1 : Pour étudier le rôle des hormones de défense dans les réactions de défense dans les nodosités, j'ai eu recours à quatre approches:

- Approche microbiologique : dans cette approche j'ai créé des souches de *S. Medicae* WSM419 capables de réduire les taux d'éthylène et d'acide salicylique dans les nodosités par la surexpression des gènes *ACD* (1-aminocyclopropane-1-carboxylate déaminase**)** et *NahG* (*naphthalene* hydroxylase G) codant pour une ACC déaminase et une salicylate hydroxylase, respectivement.
- Approche génétique : dans cette approche j'ai construit des doubles mutants symbiotiques et hormonaux : *dnf2/skl et symCRK/skl* fond A17 et *myc2b/symCRK* fond R108.
- Approche pharmacologique : dans cette approche j'ai traité les racines de jeunes plantules soit par l'ACC qui est le précurseur de synthèse l'éthylène, soit par un inhibiteur de la voie de biosynthèse d'éthylène (AVG), ou par l'acide jasmonique (MeJA), ou par l'acide salicylique (salicylate de sodium).
- Approche moléculaire : consiste à étudier l'expression de différents gènes marqueurs (symbiotiques, hormonaux, de senescence et de défense) dans des nodosités provenant de plantes de *M. truncatula* issues des approches génétique et pharmacologique.

Objectif 2 : Pour identifier des gènes marqueurs spécifiques de chaque hormone exprimés dans les nodosités, j'ai utilisé des données ARNseq personnelle et publiques (prévenant des sites mtgea.noble.org et de papiers scientifique), et j'ai validé les gènes sélectionnés par RT-qPCR.

Objectif 3 : L'étude du rôle de gènes NBS-LRR a été réalisée en utilisant la stratégie décrite pour le point précédent.

Objectif 4 : La recherche de nouveaux gènes symbiotiques a été effectuée en criblant et caractérisant deux nouveaux mutants symbiotiques (NF2071 et NF343) incapables de fixer l'azote atmosphérique (mutants fix-) et en développant une nouvelle approche pour identifier les gènes mutants.

Objectif 5 : Pour mieux comprendre le déclenchement des réactions de défense dans les nodosités, nous avons identifié et étudié une nouvelle souche bactérienne capable d'induire des nodosités non-fonctionnelles et d'y déclencher des réactions de défense.

Chapter I: New tools development

Introduction

This chapter summarizes the different approaches used to understand the role of defense hormones during symbiosis and describes a new tool that can facilitate the identification of new genes involved in the formation of functional nodules. These approaches are briefly presented below, because they did not yielded useful results.

Production of a *sickle* mutant using the CRISPR-Cas9 technology

Because we could not obtain a *sickle* (*skl*) *Tnt1* mutant in the R108 background (see below) we aimed at constructing it using the CRISPR-CAS9 technology. To obtain the *skl* mutant in *Medicago truncatula* R108 background, three RNA guides targeting the *SKL* gene and two RNA guides targeting the *SymCRK* gene were designed by blasting the R108 *SymCRK* and *SKL* genes sequences against the crispor-tefor web site (wwww.crispor.tefor.fr). The selected RNA guides presented the least possible off-targets and the best specificity score (Table 1). The *SymCRK* gene was used as a positive control in this experiment because we thought that the fix- would be easy to test in the transgenic plants if the technology worked.

Table 1. Description of the RNA guides.

Targeted gene	RNA guide	Position from start codon	off-targets	specificity score
SICKLE	*SKL guide 1*	53 bp	00013	96%,
SICKLE	*SKL guide 2*	160 bp	00007	99%
SICKLE	*SKL guide 3*	3012 bp	00001	100%
SymCRK	*SymCRK guide 1*	410 bp	00016	99%
SymCRK	*SymCRK guide 2*	693 bp	00002	100%

Code to understand the off target score: each digit in the number indicates the number of mismatch. 00013 (0 off-targets with 0 mismatch, 0 off-targets with 1 mismatch, 0 off-targets with 2 mismatches, 1 off-targets with 3 mismatches and 3 off-targets with 4 mismatches,

The selected ARN guides were inserted into the pCambia 1300 vector upstream of the CRISPR-Cas9 construction (fig.1). CRISPR-Cas9 vectors were electroporated into

Agrobacterium rhizogenes AR1193 to be used for the transformation of R108 (*M. truncatula* wild type), *symCRK* mutant (NF16231), and *dnf2* mutant (MS240) plants (table 2).

Table 2. The realized transformations

	Cas9/gRNASKL1	Cas9/gRNASKL2	Cas9/gRNA SKL3	Cas9	Cas9/gRNA SYMCRK1	Cas9/gRNA SYMCRK2
R108	+	+	+	+	+	+
NF16231	+	+	+	+	-	-
MS-240	+	+	+	+	-	-

+ : realized transformation; - : not realized transformation

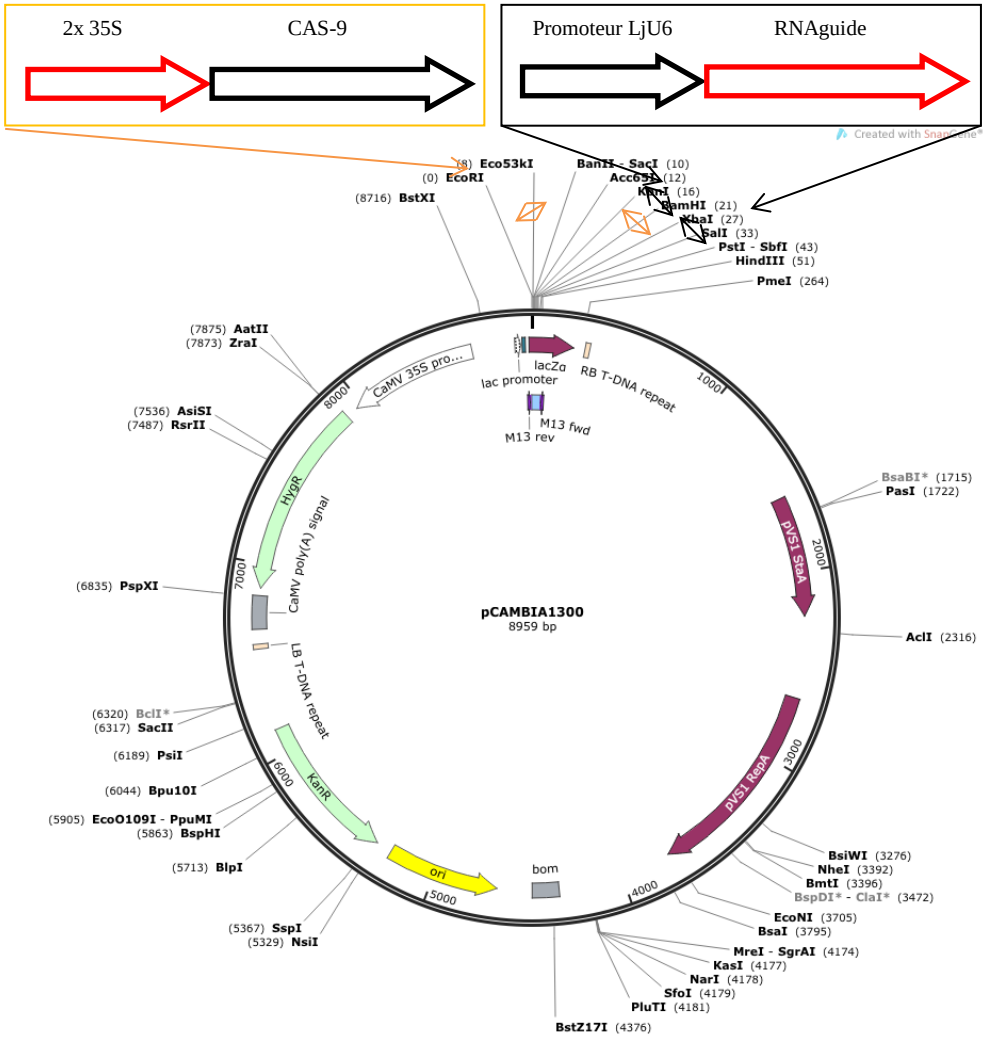

Figure 1. Structure of the CRIPSPR-Cas9 constructs. The fusions *2*35S-CAS9* and *LjU6-ARNguide* were cloned into pCAMBIA1300 vector into *EcoRI* / *KpnI* and *KpnI* / *XbaI*, sites respectively (Wang *et al.*, 2016). RNA guides were inserted individually in a pCambia1300 vector downstream of the promoter LjU6 and downstream of the 35S::*Cas9* gene. One vector without RNA guide was constructed as a negative control

Among the 14 realized transformations, I obtained 2 transformed plants able to grow in the greenhouse. The first transformed plant corresponds to a *dnf2* mutant (MS240) transformed with the nonfunctional vector carrying the CRISPR-Cas9 construction without RNA-guide and the second transformed plant corresponds to a *symCRK* mutant (NF16231) transformed with the functional vector carrying the RNA guide *skl*-2 and the CRISPR-Cas9 construction. These plants were grown in the greenhouse and analyzed in details. The presence of the mutation in the *SKL* gene and the expression of the different parts of the constructs were checked in the transformed plants using molecular approaches (PCR and sequencing). Unfortunately, no mutation was created in the *SKL* gene targeted zone (Table 3). To investigate the reason of the nonfunctioning of the CRISPR-Cas9 in this transformed plant, the expression of *M. truncatula* housekeeping gene (*actine*), bacterial resistance gene (*Hygromycine*), *SKL* gene and *CAS9* gene were checked in nodules from R108 wildtype, *symCRK* transformed mutant and *dnf2* transformed mutant using RT-qPCR. The molecular approach indicates that the CRISPR-Cas9 construction is entirely integrated the plant genome and is correctly expressed, except for the RNA guide that is not detected probably because the cNDA was generated with polyA primers (Table 3).

Table 3. Molecular characterization of the CRISPR-Cas9 plants

Material	**construction**	***Actine***	***Hygromycine***	***Sickle***	**Cas9**	**RNA guide**
R108 wildtype ADNg	absent	present	absent	present	absent	absent
Transformed NF21165 ADNg	Cas9-*skl* guide*2*	present	present	present	present	present
Transformed MS240 ADNg	Cas9	present	present	present	present	absent
Transformed NF21165 cDNA	Cas9-*skl* guide*2*	expressed	expressed	expressed	expressed	Not expressed
Transformed MS240 cDNA	Cas9	expressed	expressed	expressed	expressed	Not expressed

Absent: the target genes are not inserted in the plant genome; Present: the target genes are inserted in the plant genome; not expressed: the target genes are not expressed; expressed: the target genes are expressed.

Suppression of ethylene and salicylic acid effect in fix⁻ mutants

To To investigate whether ethylene and salicylic acid are involved in the fix⁻ phenotypes of the *dnf2* and *symCRK* mutants, a physiological approach was used to reduce the salicylic acid and ethylene effects in nodules. This approach consists in reducing the SA and ET amounts in symbiotic cells by using rhizobia overexpressing the *NahG* salicylate hydroxylase and the 1-aminocyclopropane-1-carboxylate deaminase (*ACD*) genes from *Sinorhizobium medicae* and *Pseudomonas putida* respectively. The constructions of rhizobia overexpressing *NahG* and *ACD* were performed by transforming *S. medicae* WSM419 strains with pBIN19 carrying the *SmACD* coding sequence under the control of the NifH promoter or with pBIN19 carrying Pp*NahG* coding sequence under the control of the NifH promoter promotor (fig.2).

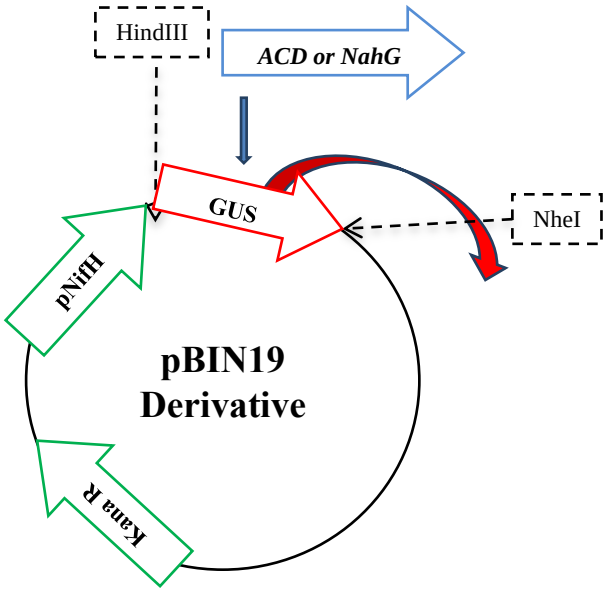

Figure 2. Structure of the plasmid overexpressing ACC deaminase (ACD) or NahG enzymes. The ACD or NahG coding sequences were exchanged with the GUS sequence using the HindIII and NheI restriction enzymes.

The transformed *S. medicae* WSM419::*NahG* (WSM419::*NahG)* and *S. medicae* WSM419::*ACD* (WSM419::*ACD*) were used separately to inoculate *M. truncatula* A17 and R108 wild-types and their corresponding symbiotic mutants (*dnf2* and *symCRK*) and the hormonal mutant (*skl*) in the A17 or R108 genetic backgrounds.

The results show (fig.3) that these strains, putatively reducing the salicylic acid and ethylene levels in symbiotic cells, are unable to restore the fix+ phenotype in nodules from *symCRK* and *dnf2* mutants in both *M. trancatula* A17 and R108 genetic backgrounds. However, the reduction of SA production in the R108 wild-type nodules (Fig.3b) leads to a better nitrogen fixation capacity.

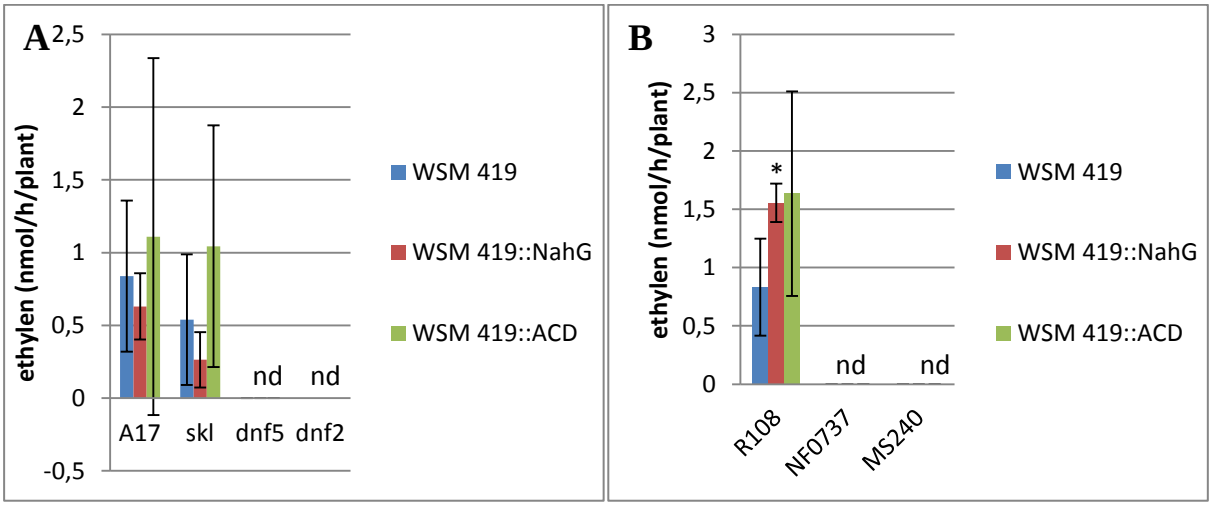

Figure 3. *S. medicae* WSM419 over expressing ACC deaminase and NahG enzymes do not restore fix$^+$ phenotype. *Skl*, *symCRK*^{A17}, dnf2^{A17}, *symCRK*^{R108} (NF0737) and *dnf* ^{R108} (MS240) mutants and their respective wild-types A17 and R108, cultivated on BNM medium solidified with bacto-agar and inoculated with *S. medicae* WSM419 overexpressing ACC deaminase and NahG enzymes, were subjected to ARA at 21 dpi. (a) In comparison to the A17 wild-type, the symbiotic mutants do not show a reduction of the acetylene activity even after transformation with bacteria expressing ACC deaminase and NahG enzymes. (b) Inoculation with *S. medicae* ACC deaminase or NahG over-expressors do not restore the fix$^+$ phenotype in *symCRK*^{R108} mutants. Error bars, ± SE from three independent experiments with one technical replicate for each experiment. nd : not detectable**.** Asterisks indicate significant induction ($P<0.05$) compared to the non-treated samples.

These results suggest that ethylene and salicylic acid are not the unique players in triggering nodule defense reactions or that the use of the transformed bacteria did not reduce enough the hormone contents in nodules. On the other hand, reduction of SA seemed to promote the nitrogen-fixing efficiency in R108 nodules.

Rapid identification of causative *Tnt1* insertion

The *M. truncatula R108 Tnt1* mutant collection represents a valuable tool in functional genomic studies. Thanks to this collection many genes involved in nodulation and nitrogen fixation were identified. However, the PCR based classical identification technique used to determine the causative-*Tnt1* insertion in *M. truncatula* are not very efficient and are time consuming. To make the identification of the causative *Tnt1*-insertion easier and more efficient we decided to use a new identification strategy based on RNA sequencing. The principle of this strategy is based on the observation that gene loci corresponding to *Tnt1*-tagged genes produce chimeric transcripts containing part of the tagged gene and part of the *Tnt1* sequence. These chimeric transcripts are easily identified by RT-qPCR experiments using one primer on the tagged gene and one primer on the LTR region of *Tnt1*. The strategy of this approach is than based on the comparison between the transcriptomes of a small mutant population and a small sibling population exhibiting a wild-type phenotype. By comparing the chimeric transcript(s) which is (are) chimeric homozygote in the mutant population and are chimeric heterozygote or wild-type in the wild-type sibling population, the tagged gene should be easily identified (Fig. 4).

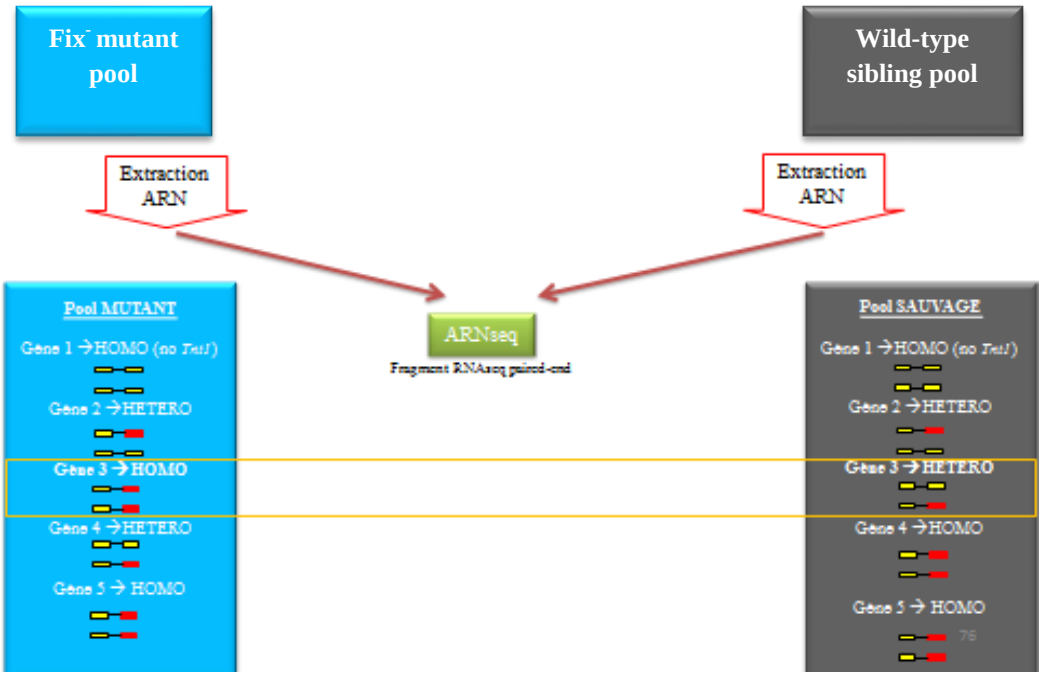

Figure 4. Scheme of the strategy for the rapid identification of causative *Tnt1* insertion. The *Tnt1* insertion homozygote in the mutant pool and heterozygote in the WT pool is a candidate insertion for the mutant phenotype

To confirm this strategy and to identify the causative *Tnt1* insertion in the NF2071 Fix- mutant line, RNAs pool extracted from NF2071 fix^+ nodules and RNA of one NF2071 fix^- were subjected to RNA sequencing at the POPS platform (http://ips2.u-psud.fr/fr/plateformes/spomics-interatome-metabolome-transcriptome/pops-plateforme-transcriptomique.html). The RNAseq was performed using a TruSeq RNA Sample Preparation Kit (Illumina, San Diego, CA) and sequenced on 29100 bp paired-end flow cells using HiSeq2000 device (Illumina), generating ~30 million reads per sample. In addition, to check the efficiency of this new strategy, RNAs from two known *Tnt1* mutant lines and one *MERE1* mutant line were sequenced at the same time with NF2071.

Nodules RNAs from a pool of eight *symCRK Tnt1* mutant (NF0737) and leaves RNAs from a pool of *npr2 Tnt1* mutants were used as positive controls. In addition a pool of nodules RNAs from eight *dnf2 MERE1* mutants (MS240) was used as negative control.

Chimeric sequences were obtained by mapping the RNAseq sequences against the wild-type annotated genome *of Medicago truncatula*. After that, the homozygote chimeric sequences were assembled with their corresponding gene. To confirm that this technology works, I aligned *SymCRK* wild-type sequence gene with the obtained *symCRK* chimeric sequence using (http://biosrv.cab.unina.it/webcap3/). As shown in the figure 5, there is an interruption of the gene sequences upstream and downstream of the *Tnt1* insertion point (5 bp duplication) represented here by letters in the black box. In addition the sequences spanning this insertion point are chimearic and contain *Tnt1* LTR sequences (in grey) following the SymCRK sequence. With this approach, it is thus possible to determine exactly the insertion site, represented in fig.5 by a black rectangle.

Figure 5. Localization of *symCRK* mutation using the rapid identification technology. Nodule RNAs were obtained from eight *M. truncatula* wild-type sibling and eight *symCRK* mutant (NF0737) plants inoculated with *S. medicae* WSM419 and harvested at 21 dpi. RNAs extracted from these WT and mutant nodule pools were sequenced using the paired-end sequencing strategy.

Unluckly, I did not find the causative *Tnt1* insertion in the mutant line NF2071 as four potential candidate genes were detected using the rapid identification strategy. Among them, the gene Medtr2g090050 coding for an unknown protein with a DUF566 domain was nodule specific according to the *Mt*GEA (*M. truncatula* Gene Expression Atlas, https://mtgea.noble.org/v3/) database and represented a good candidate. Unfortunately, PCR and sequencing analyses revealed that the mutation of this gene is not responsible for the observed fix$^-$ phenotype, because this mutation is heterozygous in the mutant line. The failure to find the good gene by the rapid identification of causative *Tnt1* insertion technique can be explained by the fact that we used the nodule RNA sample from a unique mutant fix$^-$ plant and that this was a limitation to identify the mutated locus in NF2071. We planned to start again this work in the appropriate experimental conditions.

However, it should be noted that the technology works with the control lines and allowed to confirm the mutated gene identified in the previous studies.

Chapter II: Screening of symbiotic and hormonal mutants

Introduction

In order to characterize news fix$^-$ mutants as well as *skl* and *MYC2* mutants, eight lines were selected from our team collection as known or putative fix- lines (NF0217, NF343, NF1526, NF2071, unpublished) or ordered from other laboratories (NF18028, NF18829, NF13601 and NF3119).

We used different approaches to screen the mutant lines such as a physiological approach by performing acetylene reduction assay (ARA) to measure the nitrogen fixation activity or a molecular approach like PCR to identify the affected genes.

Material and methods

Bacterial strain and inoculation

The *Sinorhizobium medicae* strain WSM419 (Howieson et Ewing, 1986), was cultivated at 30°C in yeast extract broth (YEB) medium (Krall *et al.*, 2002) supplemented with 12.5 µg.mL^{-1} of chloramphenicol. The bacterial inoculum was prepared by washing twice a fresh overnight liquid culture of *S. medicae* WSM419 with sterile distilled water. The OD 600nm of the bacterial culture was adjusted to 0.15 with sterile distilled water and used for plant inoculation.

Plants material and growth conditions

Seeds of the *Medicago truncatula* R108 and Jemalong A17 genotypes, their corresponding mutants (*dnf2, symCRK/dnf5, myc2* and *skl)* or putative new mutant alleles were scarified with sulfuric acid for 10 minutes, washed three times in sterile water, then sterilized in sodium hypochlorite for 30 min, washed three times in sterile water and incubated 1 hour in sterile water. The sterilized seeds were transferred onto water-agarose 1% medium (50mL plates) and vernalized for at least 48 h at 4°C in the dark. Seeds were then germinated at 24°C for 36h.

For screening and seed production of new *symCRK, myc2* and *skl* alleles, the seedlings were transferred onto pots containing soil in the greenhouse under long day conditions (photoperiod 16h light/8h dark) at 24°C, 50% humidity. Plants were watered with tap water and a nutrient solution containing nitrogen is applied every 2 weeks.

For RNAs extraction and acetylene reduction assay, the seedlings were transferred onto square plates (8 plants per plate) filled with buffered nodulation BNM medium (Ehrhardt *et al.*, 1992) solidified by bacto-agar (1.5%). The seedling roots were inoculated with 1mL of bacterial suspension per plate. The plates were then incubated in growth chamber under long day condition (16h light/8h dark) at 24°C. All experiments were conducted on nodules harvested at 21 days post-inoculation (dpi).

***In silico* screening**

The new mutant lines were screened *in silico* using the public databases as *Mt*GEA (mtgea.noble.org) and phytozome (phytozome.jgi.doe.gov) or RNAseq data (not published yet).

Microscopy

To obtain the pictures of necrotic nodules for the three *symCRK* mutant alleles, and the new symbiotic mutants, the nodules of eight plants for each alleles and R108 wild-type were harvested at 21 dpi and cut by surgical blades. The dissected nodules were immediately imaged with a Stemi 305 ZEISS stereomicroscope.

DNA extraction and PCR analysis

Genomic DNA was extracted from mutant plant leaves as described by D'Erfurth *et al.* (2003) and subjected to a polymerase chain reaction analysis as described by Tadege *et al.* (2008) and Cheng *et al.* (2011).

For the *Tnt1* mutant plants, the PCR analysis was performed with three primers per reaction, two primers corresponding to the target gene and one primer corresponding to the external part of the retrotransposon *Tnt1*. The primers are listed below in Table 1.

Table 1. List of primers for the genotypin.

GENE	NUMERO D'ACCESSION	FORWARD	REVERSE
NAD1	Medtr7g022640.1	CTCATTCAAGTCTAGTTAGTGCCAAG	CTTGGATAGTTGCTCACCTTGTACA
RSD	Medtr7g063220.1	GTGGTAGCTAACCTTTTGACCCC	GAAGTGGAAGAAGAGGTAGGTACG
dnf2-1	Medtr4g085800.1	GTCGGAATAGGACATCAAGAAGGC	CCCCAATCTGTTATGAATTGTTGCTC
dnf2-2	Medtr4g085800.1	GGCATCATGACTCTAGACATTTCAC	CCATTCATAGGCAATGCGTTCAG
dnf2-3	Medtr4g085800.1	CCATTACAGATCAGCTGCGTGTA	CCATTCTGCAGCAGAAAATGGC
dnf2-4	Medtr4g085800.1	GCCAAAGAATGGTAGTGATTGGC	CAAAACCGGTGAATAATTCGGACC
SYMCRK(DNF5)-1	Medtr3g079850.1	CATTCTGACGCGGAATCAAAGAT	GAGGTAGTCTAAGATGAACCAAC
SYMCRK(DNF5)-2	Medtr3g079850.1	GCTGGATCTTGTAACTCAAGCA	TTGCAGAGAGTTCACTTCTGATGT
SYMCRK(DNF5)-3	Medtr3g079850.1	GCACTCTATGAGATAGTTGTTTCA	GATTTCTGTGTTGAAGCTTGGCT
SYMCRK(DNF5)-4	Medtr3g079850.1	GTTTGTGATGTAGGGAATGTTTCC	AAAACTGGCCGAGCATTGCATATT
SYMCRK(DNF5)-5	Medtr3g079850.1	TCACCAATGATGAGCTTTTTCCCC	ACTAGTACTACCACTAAAAGAGGG
SUNN-1	Medtr4g070970.1	GTCTACTCGTGGACTTAACTAGTGG	ATCAGGCTAACGATTTCCTCTGG
SUNN-2	Medtr4g070970.1	CTTCCCCGGCAACATCACTTTCGG	CTCCGGTGGGATCAATCCGGTGAG
SUNN-3	Medtr4g070970.1	CCAGCTTTCATCGGCGATCTT	GCGTCGTTAGACTCGTCATGAAT
SUNN-4	Medtr4g070970.1	GACTGCAGTTGACTTCAGCCGA	GCACCATGAAGCCACTCACCTAAA
SUNN-5	Medtr4g070970.1	GCGTTTAGTTGGACAAGGAAGTGG	GCACTTTCTACCGCTAAGCCAAG
SUNN-6	Medtr4g070970.1	CCACCATAAGGCATAGTGTGGCTG	CTCATGGTAGGCCTTGCAGGTC
SUNN-7	Medtr4g070970.1	GGAGATGGAGTAGACATCGTTGG	CACTTCTGCCAATCTGATACAAGTAC
SICKLE A17	Medtr0041s0030.1	TGATTCTGGTGAGAGGCGCTATT	AGCTGCAGCTCCAGGGGAGCTA
SICKLE-1	Medtr0041s0030.1	GCATTGAGTTCTGAACAGACGAAG	CTGATACGTGACGATTTCTTCTC
SICKLE-2	Medtr0041s0030.1	CACCAATCTCTTGATCAATGTGG	GGAGAACTGAAAACAAGACAGAC
SICKLE-3	Medtr0041s0030.1	CTGGTGATAGGATGCTGGTATAG	CTGAGCAAGATCTCGTCCAGTGATTACA
MYC2A-1	Medtr5g030430.1	AGGCAAGGTCAAGAACATGGTAT	GGAACCTCAGTTAAAGTACTCGA
MYC2A-2	Medtr5g030430.1	CTTCAGTAATGGAGGCTTTCATG	GGAACCTCAGTTAAAGTACTCGA
MYC2A-3	Medtr5g030430.1	AACGTTTGTTGAAGCCGGAATC	AACCGCTCGAAGTGCATAGAAT
MYC2A-4	Medtr5g030430.1	TATGGATTCCTGGTAGCTATCTC	TGATAGATCAGACAACCTGCATG
MYC2B	Medtr5g030420.5	TCGAAAGGCGAATTGGAGATACAAT	GCTAGTACTAGTACTTTCTGTTAGC
LOX	Medtr8g018430.1	GCAAGGTTTGCCTAATGATCTAC	TCAATCAACTCTGTGCGAGTTTG
EFD	Medtr4g008860.1	TCATCATCATGGCAAGACCACAA	TCTTGCTGCTTCATCATATGCTC
LTR4	*Tnt1*	TACCGTATCTCGGTGCTACA	
LTR6	*Tnt1*	GCTACCAACCAAACCAAGTCAA	

Acetylene reduction assay ARA

Measurement of the nitrogen fixation efficiency of nodules was performed using a modified ARA protocol from Koch et Evans (1966). Whole 21 dpi-aged nodulated plants were placed individually into 20 mL glass vials sealed with rubber septa. 500 µL of acetylene was injected into each vial and incubated for 2 hours in a growth chamber under long day condition (16h light/8h dark) at 24°C. The vials were moved to gas chromatograph (GC 7820A, Agilent) to measure the produced ethylene by injecting 200 µL of gas from the incubated vial. The amount of ethylene produced was calculated as following:

$$[C2H4] = \frac{Pic\ area\ \times 99}{incubation\ time\ \times 495} \times 60$$

$[C_2H_4]$: nmol C_2H_4 $.h^{-1}.plant^{-1}$; Pic area: $pA.s^{-1}$; 99: gas volume for an entire vial 1/99 of vial was injected in GC; Incubation time: min; 495: slope of the relation between pic area values and C_2H_4 concentration values; 60: min

Three biological repetitions were used for each experiment. n = 16 plants per lineage

Results

Screening for new symbiotic and hormonal mutants

Screening for hormone signaling mutants:

In the literature, there is little information concerning immunity and its activation by defense hormones on the root part and even less in nodules. In fact, most existing knowledge comes mainly from the aerial parts of the Arabidopsis model plant. In order to study the role of hormonal signaling in controlling intracellular accommodation during symbiosis, *M. truncatula* mutants affected in hormonal signaling pathway were searched and used in a genetic approach by crossing them with symbiotic mutants.

Search for a *MYC2* mutant in R108

The basic helix-loop-helix (bHLH) MYC2 transcription factor is known as a primary player in the JA signaling cascade in *Arabidobsis thaliana* (Kazan and Manners, 2013). BLAST alignment of the *AtMYC2* gene sequence using the plant genomics ressource phytozome (phytozome.jgi.doe.gov) led to three *MYC2* homologs in *Medicago truncatula* named *MYC2a*, *MYC2b* and *MYC2c*.

The putative *MYC2* mutant seeds were kindly provided by Dr. Julia Buitink from INRA-Angers. The lines NF18829, NF13601 and NF3119 correspond to *myc2a* alleles and the NF18028 line fits with the *myc2b* mutant (Table 2). Genomic DNAs of these lines were extracted and amplified for *MYC2* genes by PCR using two primer pairs corresponding to the target genes and one primer corresponding to the external part of the retrotransposon *Tnt1* (Table 1). The PCR products were sequenced to confirm and locate the *Tnt1* transposon insertion sites. The sequencing results showed that the lines NF18829 and NF13601 are affected in the *MYC2*a gene (Medtr5g030430.1), 436 bp and 1026 bp downstream of the predicted ATG respectively. For the line NF3119, the *Tnt1* insertion is located in the non-coding sequence of the *MYC2a* gene, 302 bp downstream the stop codon. For the line NF18028 the *Tnt1* retrotransposon is inserted in the *MYC2b* gene (Medtr8g067280.1), 1796 bp downstream of the ATG.

Table 2. List of the identified *myc2* mutants

	SYMCRK	*DNF2*	*RSD*	*NAD1*	*SUNN*	*LOX*	*SKL*	*MYC2*	fixation
NF18028								*myc2*b	Fix +
NF18829								*myc2*a	Fix +
NF13601								*myc2*a	Fix +
NF3119								*myc2*a	Fix +

Search for a *sickle* mutant in R108

The initial objective was to study the role of ethylene signaling in the symbiotic mutants generated in the R108 genetic background that were previously described in the laboratory. For this, our strategy was to create a double mutant between symbiotic mutants (*symCRK* and *dnf2*) and *sickle* mutant affected in ethylene signaling pathway.

To find the *skl* (*sickle*) *Tnt1* mutant, the *SICKLE* coding sequence of *M. truncatula* (Medtr0041s0030.1) was blasted against the *Tnt1* mutant database (Noble Research Institute, https://medicago-mutant.noble.org/mutant/index.php). Three lines NF6978, NF6998 and NF9166 exhibiting FSTs with the best identity score for the *SKL* gene were selected and ordered. The genomic DNAs from leaves of the three lines were extracted and the genotyping was performed using PCR with primer pairs covering the whole *SKL* gene (Table 1). The sequencing of the PCR products indicated that no *Tnt1* insertion was present in the *SKL* gene in these lines and thus that they correspond to false positives. The Nobel Research Institute checked also these three lines and confirmed the result. In addition, they tested more lines of the *Tnt1* mutant collection and confirmed the absence of *skl* mutant in this collection. All together, these data indicate that no *Tnt1 skl* mutant in the R108 genetic background is currently available.

Screening for new defense symbiotic mutants:

To promote the housing of nitrogen-fixing rhizobia in symbiotic cells, legumes are able to inhibit the nodule immune system by the activation of nodule specific genes. Thanks to *M. truncatula Tnt1* mutant characterization, a few nodule specific genes as *DNF2*, *SymCRK*, *NAD1* and *RSD*, were identified but we could explain only a limited number of the steps involved in the symbiosis regulation. To access to a global understanding of the symbiosis regulation mechanism explaining more steps controlling the intracellular accommodation during symbiosis, a screen for more mutants affected in nitrogen fixing activity was initiated.

We selected two new *Tnt1* lines, NF0343 and NF2071 with a R108 genetic background that are available at the Noble Research Institute. Based on ARA assay and microscopy analyses, we demonstrated that these two lines NF0343 and NF2071 are unable to fix atmospheric nitrogen (Fig.1B) and exhibit defense-like reactions as indicated by accumulation of phenolic compounds (Fig. 1A). In addition, these two mutant lines are not totally the same as they show different infection and/or bacteroides differentiation phenotypes (Fig.1A).

All the previously described symbiotic genes inhibiting nodule defense-like reactions (*RSD, NAD1, DNF2* and *SymCRK*) were amplified in the two lines NF0343 and NF2071 by PCR and the PCR products were sequenced (Table 1). The results indicate that the lines NF0343 and NF2071 are not affected in the tested symbiotic genes. Furthermore, the *Tnt1* flanking sequence tags (FST) of the two lines corresponding to symbiotic genes were checked by PCR and the PCR products were entirely sequenced. The sequencing results indicate that the genes tagged by *Tnt1* are not responsible for the observed fix^- phenotype. This indicates that the lines NF2071 and NF0343 are affected in new genes.

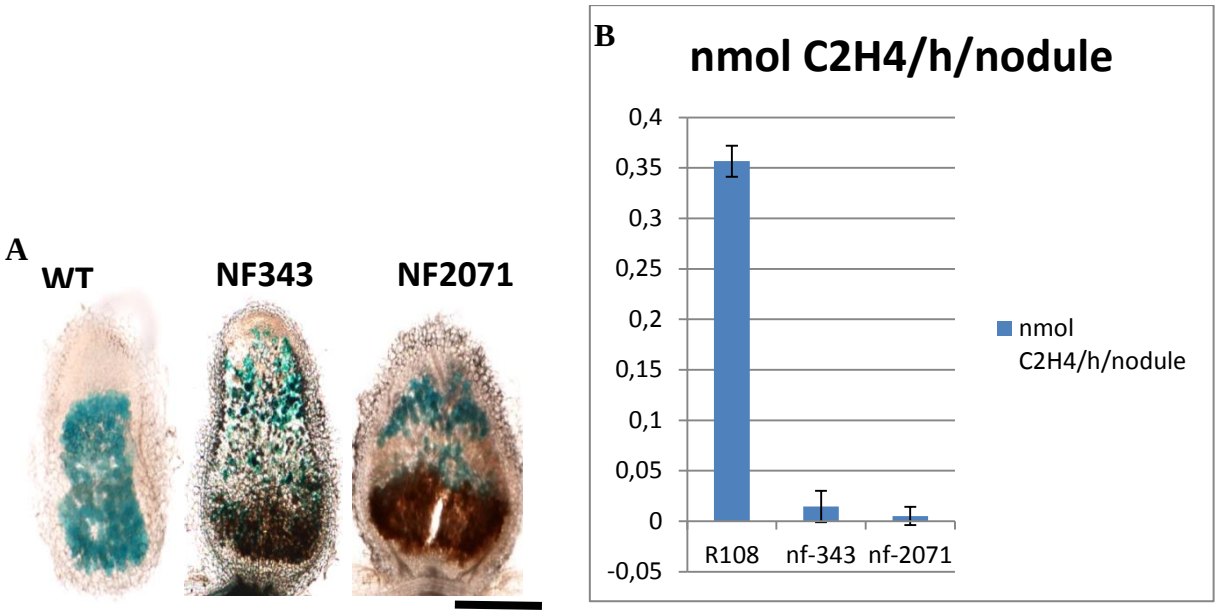

Figure 1. NF343 and NF2071 new mutant lines exhibit defense-like reactions. (a) *Medicago truncatula* nodule sections of the *new* mutants NF343 and NF2071 inoculated by *Sinorhizobium medicae* WSM419::lacZ and harvested at 14 days after inoculation (dpi). They exhibit accumulation of phenol compound compared to the *M. truncatula* wild-type. Scale bar 500µm. (b) The acetylene reduction assay (ARA) was performed with at least eight nodulated plants from each mutant, NF343 and NF2071, and the wild-type genotype R108 (control). The plants were cultivated on BNM solidified with bacto-agar 1.5% and harvested at 14 dpi. They do not display acetylene reduction activity compared to the wild-type. Error bars, ± SE from two independent experiments with one technical replicate for each experiment.

Screening for new *dnf2* and *symCRK* alleles

The *Tnt1* technology has enabled the creation of a large collection of *M. truncatula* R108 mutants. This technology contributes to the discovery and understanding of the role and functions of many genes. The disadvantage of this technology is that it is difficult to define exactly how many genes are affected in a mutated plant. To avoid this problem and to eliminate parasitic effect of mutations in other genes in future transcriptomics experiments, a screen of new alleles for the *symCRK* and *dnf2* symbiotic mutants was realized.

***dnf2* mutant screening**

The *dnf2* putative mutants from the team's collection have been selected for genotyping. The line NF1526 presents a supernodulating and fix$^-$ phenotype. The line NF0217 exhibits a fix$^-$ phenotype due to *dnf2* gene disruption (Bourcy *et al.*; 2013) and to a mutation of a *LOX* gene.

First to identify and confirm the genes that are responsible for the fix$^-$ phenotype in these two lines, the symbiotic genes like *DNF2, SymCRK, RDS* and *NAD1* known to exhibit a fix$^-$ phenotype were amplified by PCR and the PCR products were sequenced. The *LIPOXYGENASE (LOX9)* gene reported as being able to induce a fix$^-$ phenotype was also included in this analysis. In addition, we considered also the two genes, *SUNN* and *SKL* whose disruption is responsible for a supernodulating phenotype (Schnabel *et al.* 2005; Penmetsa and Cook,1997).

The sequencing results indicate that the line NF1526 is affected in *DNF2* and in *SUNN* (Medtr4g070970.1), while the NF0217 line is affected in *DNF2* and *LOX9* (Medtr8g018430) (Table 3). In the NF1526 line, a *Tnt1* retrotransposon is inserted in the *DNF2* gene in the sixth exon at 1855 bp downstream of the predicted start codon, and, in the *SUNN* gene at 398 bp downstream of the ATG. In the NF0217 line, a *Tnt1* retrotransposon is located in sixth exon of the *DNF2* gene at 1487 bp downstream of the predicted translation start and in the eight exon of the *LOX* gene at 3794 bp downstream of the predicted translation start.

Table 3. List of the new selected symbiotic *dnf2* mutant alleles

	SYMCRK	*DNF2*	*RSD*	*NAD*	*SUNN*	*LOX*	*SKL*	*MYC2*	**fixation**
NF1526		*dnf2*			*sunn*				Fix -
NF0217		*dnf2*				*lox*			Fix -

The NF0217 line was back-crossed with the R108 wild-type to separate the two mutations. The PCR and sequencing results confirm the success of the back-cross, but unfortunately the simple *dnf2* and *lox9* mutants were not obtained in the F2 generation from the homozygote double mutant.

***symCRK* mutant screening**

To identify new *symCRK* mutant alleles within the R108 genetic background, the *symCRK* coding sequence of *M. truncatula* Medtr3g079850.1) was used to screen the *Tnt1* mutant database (Noble Research Institute, https://medicago-mutant.noble.org/mutant/index.php. Three lines NF21175, NF16231 and NF21165 containing putative insertions in the *symCRK* gene were ordered at the Noble Research Institute. Thirteen seeds for each line were grown in the greenhouse and genotyped for *Tnt1* insertion in the *SymCRK* gene. Among them, only the NF16231 and NF21165 lines (Table 4) exhibit a *Tnt1* retrotransposon disrupting the *SymCRK*; in the first exon at 196 bp for NF16231, and, at 426 bp downstream the ATG for the NF21165 (fig. 2).

Table 4. List of the new selected symbiotic mutant alleles

	SYMCRK	*DNF2*	*RSD*	*NAD*	*SUNN*	*LOX*	*SKL*	*MYC2*	**fixation**
NF21165	*symCRK*								Fix -
NF16231	*symCRK*								Fix -
NF21175	*SymCRK*								Fix +

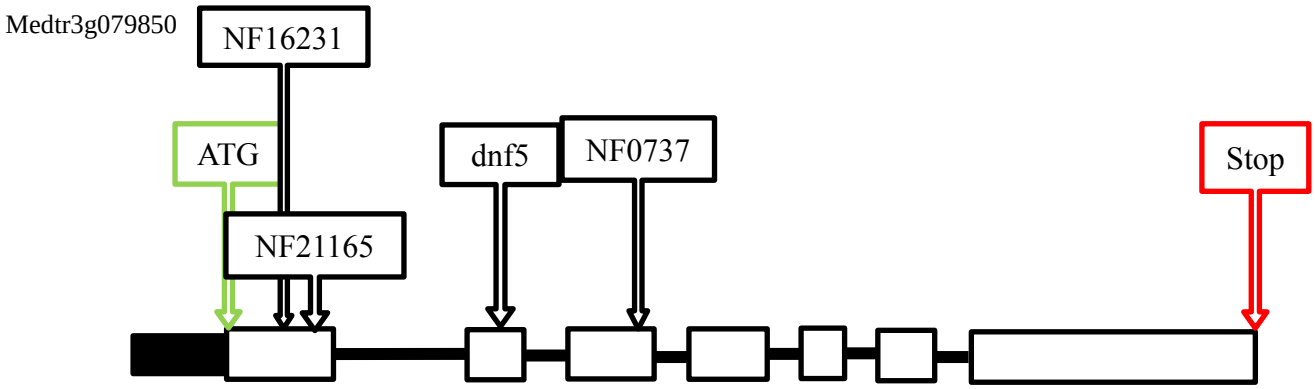

Figure 2. Mutation positions in the *SymCRK* gene. The *SymCRK* gene (Medtr3g079850) contains seven exons represented by white boxes. The predicted translation start is represented by a green arrow and the stop codon is represented by a red arrow. The mutation positions and the name of the mutant lines are represented by black arrows. In the R108 background, there are three mutant lines with *Tnt1* insertions located in the first exon for the two mutant lines NF16231 and NF21165 and, in the third exon for the NF0737 mutant line. In the Jemalong background, one nucleotide deletion mutation (*dnf5*) is located in the second exon.

Berrabah *et al.* (2014a) showed that the nodules of the *symCRK* mutant (NF0737) in the R108 background accumulate phenolic compounds and are unable to fix atmospheric nitrogen. To check whether the two new *symCRK* mutant lines NF16231 and NF21165 accumulate phenolic compound and are unable to fix atmospheric nitrogen, nodules sections were observed by microscopy and the nodule fixing capacity was also measured using the acetylene reduction assay (ARA). The nodules of the two new *SymCRK* mutants also accumulate phenolic compounds (fig.3A). The proportion of phenolic inside the nodules was estimated by measuring the necrotic aera in the nodule sections using ImageJ (fig.3B). The three mutant lines have 20 to 50 % of the surface area containing phenolic (data not shown). This shows that the phenolic accumulation in the new lines is similar to the one observed in line NF0737. The nitrogen fixation capacity of the three *SymCRK* alleles measured using the ARA test shows that NF16231 and NF21165 lines are unable to fix atmospheric nitrogen as NF0737 (fig.3C). The results are consistent with the previous data obtained by Berrabah *et al.* (2014a).

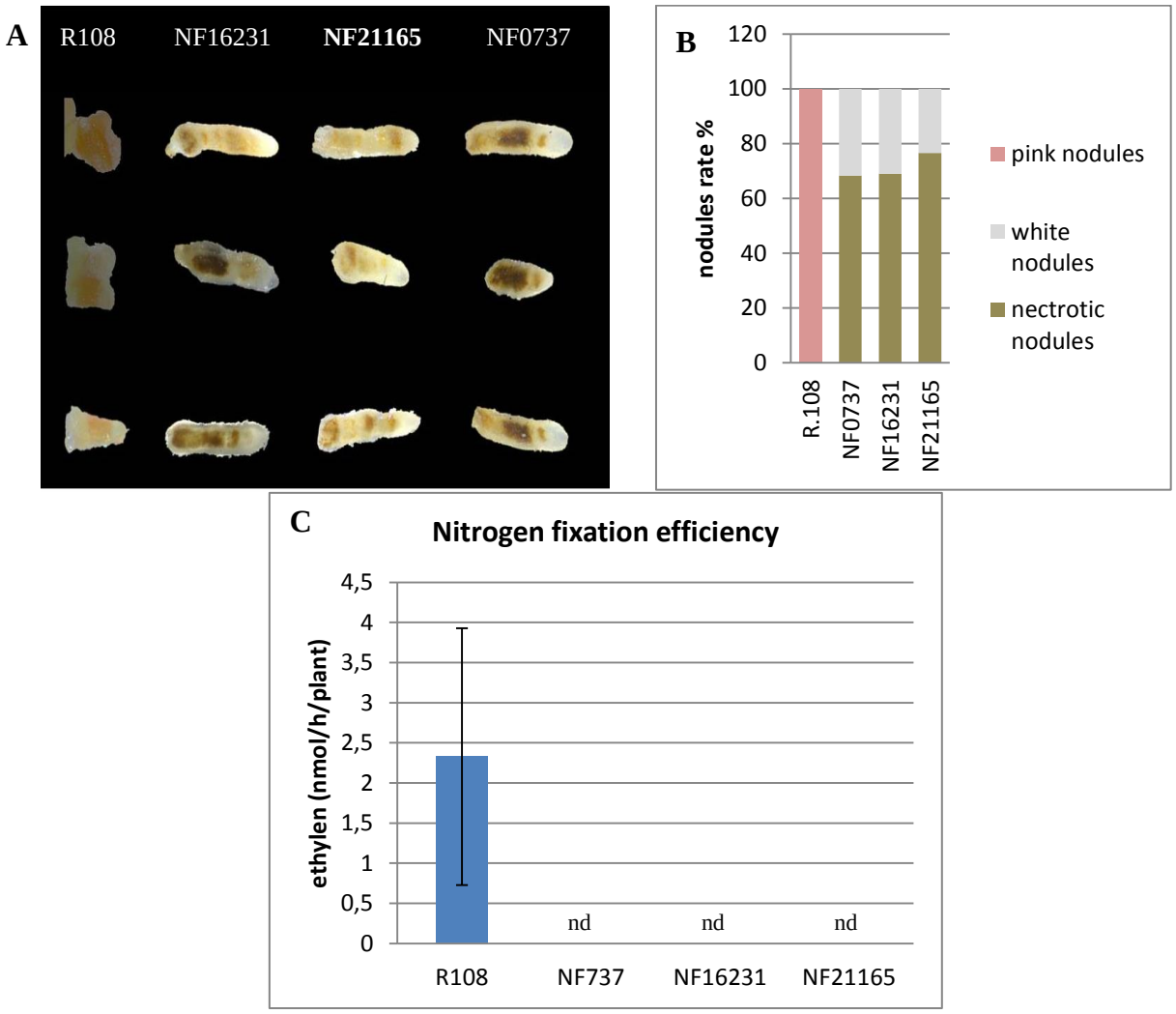

Figure 3. New *symCRK* mutants exhibit necrosis and fix⁻ nodules. (a) *Medicago truncatula symCRK* mutant nodules induced by *S. medicae* WSM419 harvested at 21 days after inoculation (dpi) accumulate phenolic compounds as compared to the *M. truncatula* wildtype. (b) The nodules were classified according to their color. The rate of pink nodules is represented by pink bars, white nodules represented by white bars, and necrotic nodules accumulating phenolic compounds are represented by brownish bars. (c) The acetylene reduction assay ARA was performed in twenty-four nodulated plants from mutants NF0737, NF16231, NF21165 and wildtype R108. The plants were cultivated on BNM solidified with bacto-agar and harvested at 21 dpi. Mutants do not show any acetylene reduction activity. Error bars, ± SE from three independent experiments with one technical replicate for each experiment. nd: not detectable.

All together the data indicate that the two new mutant lines, NF16231 and NF21165, correspond to two *symCRK* mutant alleles. They are fix⁻ and exhibit defense-like reactions.

Conclusions

In this genetic work we have characterized *myc2* mutants and new allels for the *dnf2* and *symCRK* mutants. This material will be used in further studies.

Chapter III: Comparison of *symCRK* mutant phenotypes in *M. truncatula* A17 and R108 backgrounds

Introduction

Legume plants are able to obtain reduced nitrogen from rhizobia hosted in a dedicated symbiotic organ, the nodule. This feature allows legume plants to develop in nitrogen-poor soil. To obtain a sufficient amount of nitrogen for their growth, the plants host hundreds of rhizobia per symbiotic cells. To establish this chronic infection, legume plants like *M. truncatula* recruit symbiotic genes like *DNF2* and *SymCRK* to protect the nitrogen-fixing rhizobial partner from their own immune system.

The *DNF2* gene (Medtr4g085800) encodes a phosphatidylinositol-specific phospholipase C with X domain (PI-PLCXD) protein required for the establishment of a successful nodulation. The gene sequence is 2084 bp long from the predicted start to the stop codon and it is composed of eight exons (Bourcy *et al.*, 2013). According to the Medicago *Tnt1* mutant-database and to the literature, several putative *Medicago DNF*2 mutant lines exist (medicago-mutant.noble.org; Starker *et al.*, 2006; Bourcy *et al.*, 2013; Berrabah *et al.*, 2014b; Lang et long, 2015). For this study we use four *DNF2* mutant lines, one in Jemalong A17 background and three in R108 background (lines MS240, NF2496 and NF0217). In the *MS240* mutant line, the *DNF2* gene is interrupted by the *Medicago* retrotransposon *MERE1* inserted in the sixth exon, 1481 bp downstream of the start codon. In the NF2496 and NF0217 lines, a *Tnt1* retrotransposon is inserted in the third exon, 544 bp downstream of the start codon for line NF2496 and in the sixth exon, 1487 bp downstream of the start codon for the line NF0217. Nodules of *dnf2* mutants are fix^- and exhibit defense-like reactions (Bourcy et al, 2013). However, this phenotype is conditional, because in certain conditions the *dnf2* mutant behaves like wild-type (Bourcy et al, 2013; Berrabah et al, 2014b).

The *SymCRK* gene (Medtr3g079850) encodes a cysteine-rich receptor-like kinase required for bacteroids differentiation and for rhizobia maintenance within the nodules symbiotic cells. The gene is 2845 bp long from the predicted start to the stop codon and it is composed of seven exons and six introns. There are two *symCRK* lines described in the Jemalong A17 background named *dnf5-1* (Pislariu and Dickstein, 2007) and *dnf5-2* (Domonkos *et al.* 2013) and one line (NF0737) described in the R108 background. In the NF0737 line, the *SymCRK* gene is interrupted by a *Tnt1* insertion at the end of the third exon, 1065 bp downstream the ATG. The *symCRK* mutant nodules are unable to fix nitrogen and exhibit defense-like reactions (Berrabah *et al.*, 2014a). In the Jemalong background, *dnf5-2* is altered in the *SymCRK* gene by a deletion of one nucleotide in the second exon at 895 bp downstream of the start codon, creating a frame shift. The *dnf5* mutant does not fix nitrogen

but contrary to the R108 mutant alleles does not seem to exhibit defense reactions and does not accumulate phenolic compounds in nodules.

The *Medicago Sickle (SKL)* gene (Medtr0041s0030) is an ortholog of the *Arabidopsis thaliana EIN2* and codes for an ethylene co-receptor essential for ethylene signaling. According to the sequence available in the public databases (phytozome.jgi.doe.gov), the *SKL* genomic sequence is 6247 bp long from the predicted start to the stop codon and the coding sequence is distributed over six exons. In the *skl* mutant, the *SKL* gene sequence is interrupted in the sixth exon by a stop codon, 2680 bp downstream of the start codon. The *skl* mutant is super nodulator and is characterized by the formation of a string of small pink nodules along the plant roots (Penmetsa and Cook, 1997).

Ethylene is a phytohormone important in many plant life aspects (Bleecker and Kende, 2000). Many studies link ethylene to defense reactions and especially against necrotrophic pathogens (Pieterse *et al.*, 2012; Zipfel, 2014). The work by Berrabah *et al.* (2018b) indicates that ethylene appears as a major actor in defense-like reactions elicited in *symCRK* nodules. This study shows that the treatment of functional R108 wild-type nodules with ethylene stops the nitrogen fixation contrary to the same treatment of the *sickle* mutant. In addition, wild-type nodules treated with ethylene mimics different aspects of the *SymCRK* phenotype. By opposition, the treatment of *symCRK* mutant nodules with an inhibitor of ethylene biosynthesis reduces the nodule necrosis surface.

To confirm the role of ethylene in nodules defense-like reactions observed in the two mutants and with the aim to restore at least partially a fix^+ phenotype to *symCRK* and *dnf2* mutants, a genetic approach was chosen. For this the *dnf2* and *symCRK*, mutants were crossed separately to the *skl* mutant. In this study, we used the Jemalong A17 background to create the double mutants because it was not possible to obtain or create a *skl* mutant in the R108 background. Our efforts to obtain the *Tnt1 skl* mutant or CRISPR-Cas9 *skl* mutant failed (Chapter I). We also used *myc2* mutants to initiate crosses with the symbiotic mutants with the long term aim to also study the role of jasmonate in the defense reactions elicited in the symbiotic mutant backgrounds.

In the other hand, we compared defense mecansims and hormonal effects in *M. truncatula* A17, R108 and their symbiotic mutants using biochemical and genetic approaches.

Material and methods

Bacterial strain and inoculation

The *Sinorhizobium medicae* strain WSM419 (Howieson & Ewing, 1986), was cultivated at 30°C in yeast extract broth (YEB) medium (Krall *et al.*, 2002) supplemented with 12.5 µg.mL^{-1} of chloramphenicol. The bacterial inoculum was prepared by washing twice a fresh overnight liquid culture of *S. medicae* WSM419 with sterile distilled water and then the culture was suspended and adjusted to optical density 0.15 at 600nm in sterile distilled water.

Plants material and growth conditions

Seeds of the *Medicago truncatula* genotype R108 and Jemalong A17, their corresponding mutants (*dnf2, symCRK/dnf5* and *skl)* or their putative new mutant alleles were scarified by sulfuric acid for 10 minutes, washed three times in sterile water, then sterilized in sodium hypochlorite for 30 min, washed three times in sterile water and incubated 1 hour in sterile water. The sterilized seeds were transferred onto 50mL water agarose 1% plates and vernalized for at least 48 h at 4° C in the dark. Seeds were germinated by incubating them at 24°C for 36 h.

For screening new *symCRK* alleles, back-crossing, crossing or seed production, the seedlings were transferred onto pots containing soil in the greenhouse under long day conditions (16h light: 8h dark cycle) at 24°C, 50% humidity, watered alternately with tap water or nutrient solution containing nitrogen each two weeks.

Acetylene reduction assay ARA

Measurement of the nitrogen fixation efficiency of nodules was done using a modified ARA protocol from Koch et Evans (1966). Whole nodulated plants at 21 dpi were placed individually into 20 ml glass vials sealed with rubber septa. 500 µL of acetylene was injected into each vial and incubated for 2 hours in a growth chamber under long day condition (16h light / 8h dark) at 24°C. The vials were moved to gas chromatograph (GC 7820A, Agilent) to measure the produced ethylene by injecting 200 µL of gas from the incubated vial. The amount of ethylene produced was calculated following this calculation:

$$[C2H4] = \frac{Pic\ area\ \times 99}{incubation\ time\ \times 495} \times 60$$

[C_2H_4]: nmol C_2H_4 .h^{-1}.$plant^{-1}$; Pic area: pA.s^{-1}; 99: gas volume for an entire vial 1/99 of vial was injected in GC; Incubation time: min; 495: slope of the relation between pic area values and C_2H_4 concentration values; 60: min

Three biological repetitions were used for each experiment.

***In silico* screening**

The identification of genes involved in hormonal or defense signaling pathway was done by *in silico* screening using the public databases mtgea (mtgea.noble.org) and phytozome (phytozome.jgi.doe.gov) or personal RNAseq data (not published).

RNA extraction and RT-qPCR

Nodules from different mutants were harvested at 21 dpi and were frozen in liquid nitrogen in 2ml Eppendorf tubes in presence of one 3 mm diameter bead and two 5 mm diameter beads and crushed with TissueLyserII (Qiagen). At 4°C, the material was resuspended in 500 µL cold TRIzol reagent (ref# 15596026, AMBION) and incubated for 5 min. 100 µL cold chloroform was added to the mix and incubated for 10 min. after that the mix was centrifuged 5 min at 16000g and up to 500 µL of the aqueous phase was collected. RNAs were precipitated overnight at -20°C with 250 µL of isopropanol and 100 µL of sodium acetate 3 M pH5.2 and collected after 60 min at 16000g centrifugation. The precipitated pellet was washed with 1 mL of 70 % ethanol and centrifuged two times as above. The obtained RNAs were resuspended in RNase-free water.

The reverse transcription of the free-DNA RNAs was performed using SuperScript™ II Reverse Transcriptase kit (ref. 18064-014, Invitrogen). In a 200 µL micro-centrifuge tube, 1 µL of oligo dT primer (500ng/µL; ref. #SO132, Thermoscientific) 1 µl of dNTPs 10 mM, 1µg of DNA-free RNA and sterile RNase-free water were added in a 13µL finale volume. The mix was heated 5 min at 65 °C, quickly chilled on ice and briefly centrifuged. 4µL of 5X First-Strand Buffer [Tris-HCl pH: 8,3 250 mM, KCl 375 mM, $MgCl_2$ 15 mM], 2µL of dithiothréitol 0,1 M were added to the previous mix. The mix was gently homogenized and incubated 2 min at 42°C. Then, 1 µL of SuperScript™ II Reverse Transcriptase 200 units was added, the 20µL finale mix was gently homogenized and incubated 50 min at 42°C for the reaction. The reaction was stopped by inactivating the enzyme during 15 min at 70 °C. The obtained cDNA was diluted 1/20 with DNase-free water.

The Relative qPCRs were performed on cDNAs using 2X LightCycler 480 SYBR Green I Master (ref. 04 887 352 001, Roche), 2 µL of each primers (2,5 µM each) and 1µL of

cDNA, in a final volume of 10 µL. qPCR were launched on a LightCycler (480 II Roche). The SYBR Green fluorescence was detected between 465 and 510 nm. Cycle threshold and primer specificities were performed with the LightCycler 480 software release 1.5.0 SP4. Primer efficiencies were calculated with LinReg PCR: Analysis of Real-Time PCR Data, version 11.1. Actin Medtr2g008050 was used as reference in relative qPCR experiments. Primers used for this study are listed in table 1.

Table 1. List of tested genes and corresponding primers.

Gene	ID	Forward	Reverse
ACTINE	Medtr2g008050.2	TGGCATCACTCAGTACCTTTCAACAG	ACCCAAAGCATCAAATAATAAGTCAACC
PR10-like	Medtr2g035190.1	AGGCAAACTATGGATACAACTACA	AATTGGCTAGTAATTAGGGTTTGCC
Chitinase	Medtr7g115220.1	CACAGGAAACAGTGAGAATTGTAGA	TAAATGATGGAGAACAAAGGGTTGG
EIN3-1	Medtr4g114650.1	AGTTTGGTTGCAGTTGAAGACA	CAACGCCTGGCCTAATTTCATA
EIN3-2	Medtr4g114640.1	CCTAATCGCGATGGAACTGC	ACAACCGAGTCAACAAACCG
EIN3-3	Medtr1g012520.1	GCCAGATGAGTGCCTCTTTG	CAAGCTGCGGGAAAGGTATC
EIN3-4	Medtr3g078770.1	ACTGGGAAGGAAGAGTGGTG	ATTGACGATTGCAAGCCAGG
EIN3-5	Medtr3g107280.1	GACACTTGAATCGCTAGCTGTT	AGCCCGATATCTGTTACTCCAG
EIN3-6	Medtr5g087790.1	AATGACAGCCAAGGAAAGCG	TTCTCGGGTTTTCGGTCCTC
ACS-1	Medtr8g098930.1	GGCACAGTTATGGACAGAAACA	CGAGGTTACGGTCACATTCA
ACS-2	Medtr4g097540.1	CCACCGGCAATGTTAATGGT	CACACACACACACACTACGA
ACO-1	Medtr3g083370.1	ACCCTGGTAGTGATGCTGTT	AAACGGTTGCTATTGGACCC
ACO-2	Medtr5g085330.1	TGGACACATTGGAGAGGTTGA	TTCAGGGAGGTGACGAACAT
ACO-3	Medtr2g025120.1	CCCTCCAATGCCTCACTCTA	GCGTCTCAAGTGTATCTGCA
ACO-4	Medtr6g092620.1	TGAGGGGAAGTTGATGGAGA	CGGACGATGCCAAATGAAGAA
ACO-5	Medtr8g028435.1	GCTCCTGATACTCCCAAACC	CATGGTGTCGTGTTGGTGTC
SKL	Medtr0041s0030	GCATTGAGTTCTGAACAGACGAAG	GCAAGATCTCGTCCAGTGATTACA
ACO-6	Medtr1g032250.1	ATCCCCACAATCGACCTCTC	ACACCTTCTTCCTCTCCTCC
PR1	Medtr2g435490.1	TTCGGGTTGGATGTGCTAAG	GGTTGAAGCTCAATGGCACT
CP2	Medtr5g022560.1	CTTACCCTACTGCTTAAATGC	AACTAGAAACCATGATGAATGTAG
CP3	Medtr4g107930.1	GTGGATGCCGCTGAAGG	TCAATCACAGTTTTGCTCAAATTAC
CP4	Medtr4g079770.1	TATTGTTCGTTCTTCTCCTTC	TAAACACCTGAAATCCCTTTG

Statistical analysis

The means of all observations were calculated and ranked using Excel software (Microsoft 2010). And then the ranks were subjected to analysis of variation and to test the frequency distribution of the values of genes relative expression using Mann–Whitney U-test (Walpole and Myers, 1978).

Results

Characterization of the *symCRK* mutant (*dnf5-2*) in A17 background

In the previous study (Berrabah *et al.*, 2014), it was shown that the *symCRK* mutant in R108 background (*symCRK*^{R108}) does not fix atmospheric nitrogen and exhibit defense-like reaction reflected by the accumulation of phenolic compounds. To examine whether the phenotype of the *symCRK* mutant in the Jemalong A17 background (*dnf5-2*) is similar to the one observed in the R108 background, we measured the nitrogen fixation activity using the ARA test as well as the development of necrotic lesions in the nodules. The results show that *dnf5-2* (dnf5) and *symCRK*^{R108} (NF0737) mutants are unable to fix nitrogen (Fig. 1A), but in contrast to the R108 mutants, *dnf5-2* does not accumulate phenolic compounds in the nodules (Fig. 1B) as only 2% of the mutant nodules show necrosis.

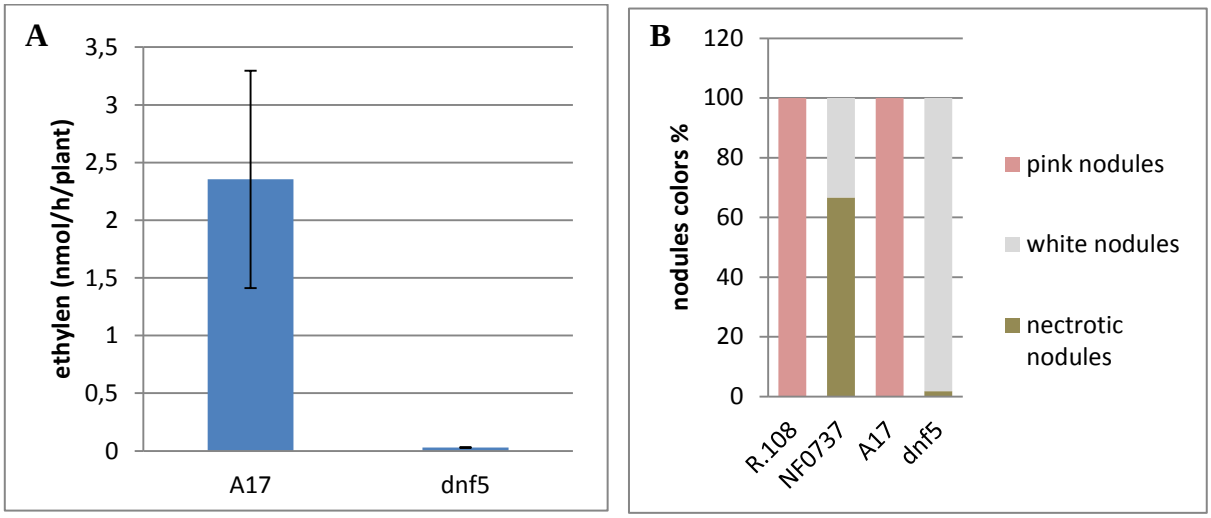

Figure 1. *symCRK* A17 mutants (*dnf5-2*) exhibit fix$^-$ but not necrotic nodules. (A) *dnf5* line cultivated on BNM solidified with bacto-agar harvested at 21 dpi does not show acetylene reduction activity when compared to wild-type A17. (B) *dnf5* and wild-type nodules classified by their color. The proportion of pink nodules is represented by pink bars, white nodules are represented by white bars, and necrotic nodules accumulating phenolic compounds are represented by brownish bars. Error bars, ± SE from three independent experiments with one technical replicate for each experiment.

This comparative analysis shows that *symCRK*^{A17} and *symCRK*^{R108} mutants have different phenotypes.

Comparison of defense and senescence genes expression in fix$^-$ mutants

To investigate the origin of the difference observed between the fix$^-$ mutants, the relative expression of three defense-related genes and three senescence-related genes were checked. Three defense markers were used, the two genes markers *PR10* and *Chitinase* were taken from Berrabah *et al.* (2014a) and *PR10*-like (Medtr2g035150.1) was chosen based on the NF0737 RNAseq data (not published). The three senescence-related cysteine protease 2, 3 and 4 genes (*CP2, CP3, CP4*) were taken from Pérez Guerra *et al.*, (2010). The relative expression of the six marker genes was checked by RT-qPCR using nodule cDNAs from fix$^-$ mutants and WT plants generated into the two genetic backgrounds A17 and R108. The results indicate that the *PR10, PR10-like* and *chitinase* defense genes are induced with similar patterns in the two R108 mutant alleles (fig.2A). In contrast they are induced in the d*nf2*^{A17} mutant but not in the *symCRK*^{A17}mutant (fig.2B). This shows a clear difference between the *symCRK* mutants in the two genetic backgrounds. In addition the CP senescence-related genes are activated in *symCRK*^{A17} but not in d*nf2*^{A17} (fig.2D) nor in R108 fix$^-$ mutants (fig.2C).

This experiment confirms the phenotypic difference observed between the *symCRK* alleles in the two genetic backgrounds and shows that defense genes are not induced in the A17 background contrary to the senescence genes. In contrast defense genes are induced albeit at lower level in the d*nf2*^{A17} mutant suggesting that the *symCRK* mutant behavior in A17 is specific.

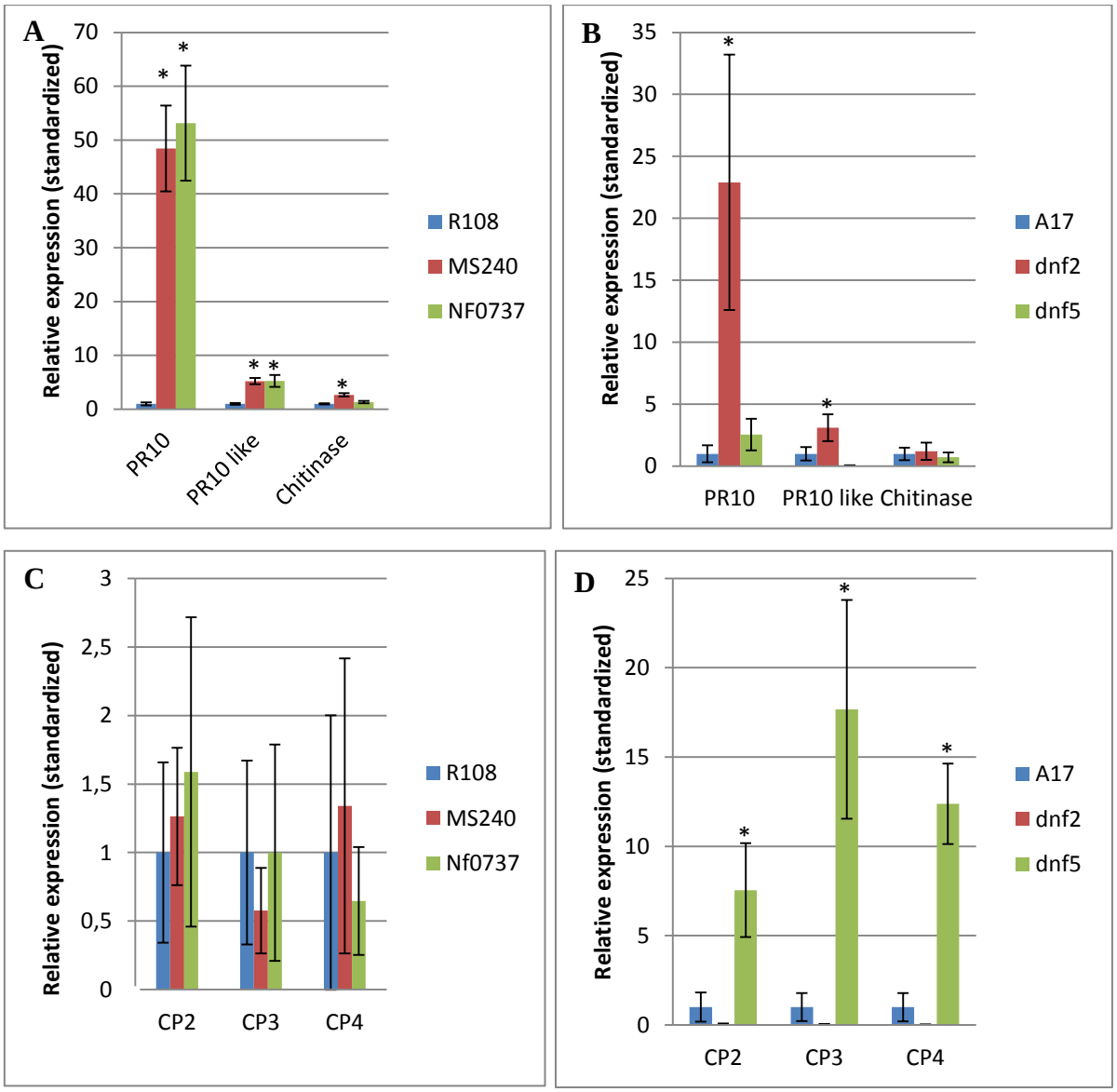

Figure 2. Relative expression of defense and senescence genes in different fix⁻ mutants. The expression of defense and senescence-related genes was evaluated by RT-qPCR using RNAs extracted from nodules of R108 and A17 wild-type as well as *dnf2*^{R108} (MS240), *dnf2*^{A17} (dnf2), and *symCRK*^{R108} (NF0737) and *symCRK*^{A17} (dnf5) mutants. Nodules were produced *in vitro* after inoculation with *S. medicae* WSM419 strain and harvested at 21 dpi. Fold change versus wild-type is presented after normalization with an actin gene as an internal control. Error bars, ± SE from three independent experiments with one technical replicate for each experiment. Asterisks indicate significant induction ($P<0.05$) compared to the non-treated samples.

Activation of the ethylene signaling and biosynthetic genes in the symbiotic mutants

In a previous study Berrabah et al, (2018b), showed that ethylene (ET) could play a role in the defense process observed in the R108 fix$^-$ mutants, particularly in the *symCRK* mutant. In order to determine whether ethylene participate to the defense-like reactions in the nodules of the different mutants backgrounds, genes involved in ET biosynthesis and ET signaling pathway (table 1) were tested by RT-qPCR in *M. truncatula* wildtype and *symCRK*^{R108} (NF0737), *dnf2*^{R108} (MS240), *symCRK*^{A17} (*dnf5*), *dnf2*^{A17} (*dnf2*) mutant nodules.

For the ethylene biosynthesis genes, two 1-aminocyclopropane-1-carboxylate synthase genes (*ACS*-1 and *ACS*-2) and six 1-aminocyclopropane-1-carboxylate oxydase genes (*ACO*-1, *ACO*-2, *ACO*-3, *ACO*-4, *ACO*-5 and *ACO*-6) were tested. For the ethylene signal transduction genes, the relative expression of the gene *sickle* and six Ethylene insensitive 3 genes (*EIN3*-1, *EIN3*-2, *EIN3*-3, *EIN3*-4, *EIN3*-5 and *EIN3*-6) were checked. Similarly, the expression of pathogen-related protein-1 gene (*PR1)* was checked as an ethylene related gene marker (cf Chapter IV).

The results presented in Fig. 3A indicate that the ethylene biosynthesis genes (*ACS*-1 and *ACO*-1) are strongly induced in *symCRK*^{R108} mutant contrary to *symCRK*^{A17} mutant, in which these ethylene biosynthesis genes are not induced, except (*ACO*-5) which is slightly induced. For the ethylene signal transduction genes, *symCRK*^{R108} mutant shows induction of the signaling genes *EIN3*-1, *EIN3*-2, *EIN3*-6 and *SKL*. In contrast *symCRK*^{A17} shows no activation of the ethylene signaling genes. In addition, there is activation of *PR1* gene in *symCRK*^{R108} and not in *symCRK*^{A17}.

The results in fig. 3B show that the ethylene biosynthesis genes (*ACS*-1 and *ACO*-2) are strongly induced in *dnf2*^{R108} mutant and show that the *ACO*-5 gene is slightly induced in *dnf2*^{A17}. Moreover, the signaling genes *EIN3*-3 and *SKL* are induced in the two *dnf2* mutant alleles, but the induction of these genes (*EIN3*-3 and *SKL)* is reduced in the d*nf2*^{A17} mutant. The fairly strong stimulation of the expression of the ethylene biosynthetic pathway in *dnf2*^{R108} correlates with the expression of the *PR1* gene. In contrast, in *dnf2*^{A17}, the level of activation of the ethylene pathway is not sufficient to induce *PR1* gene.

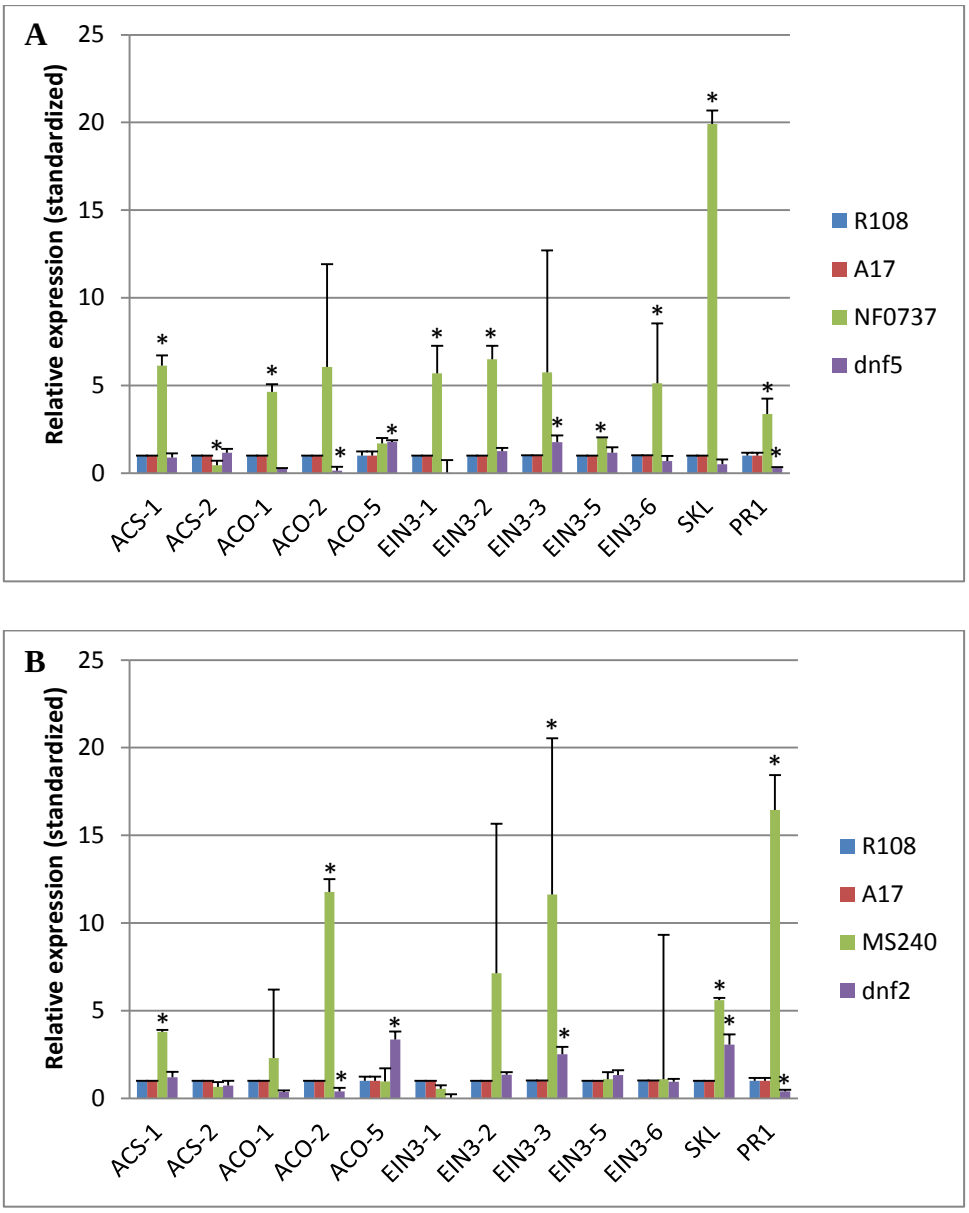

Figure 3. Expression of the ethylene signaling and biosynthesis genes in nodule defense-like reactions. The expression of ethylene biosynthesis and ethylene signaling genes was evaluated by RT-qPCR using cDNAs prepared from RNAs extracted from R108, A17 wildtype, *dnf2*^{R108}, *dnf2*^{A17}, and *symCRK*^{R108} and *symCRK*^{A17} mutants. Nodules were produced *in vitro* after inoculation with *S. medicae* WSM419 strain and harvested at 21 dpi. Fold change versus wildtype is presented after normalization with an actin gene as an internal control. Error bars, ± SE from three independent experiments with one technical replicate for each experiment. Asterisks indicate significant induction ($P<0.05$) compared to the non-treated samples.

Conclusion:

These results indicate, first that the control of the immune system in nodules is different between the two *M. truncatula* background A17 and R108 and secondly that the symbiotic genes *SymCRK* and *DNF2* control strictly the ethylene biosynthesis and signaling in R108 background. Finally, ethylene seems important for intracellular accommodation of bacteroids during symbiosis in R108 background and less in A17 background. These results are in agreement with the results published previously (Berrabah *et al.*, 2018b) suggesting the implication of ethylene in defense reactions induced in *Medicago truncatula* R108 nodules.

These results lead us to validate the hormone molecular markers and to study the hormonal response in nodules of these two plants and their corresponding mutants.

Chapter IV: Hormonal related genes screening

Introduction

To determine the role of hormones in nodule defense reactions, we started by looking for marker genes whose expression is hormone-dependent. For this the expression of a set of genes was checked in roots treated with defense hormones (Jasmonic acid ethylene precursor or salicylic acid) or mock treated. The hormones more related to development (auxines, cytokynines, giberrelines, strigolactones and abscisic acid) were not tested in this work.

To test ET-responsive genes, we evaluated the expression of ET biosynthesis and signaling genes. The ethylene biosynthesis genes include six 1-aminocyclopropane-1-carboxylate oxidase genes (*ACO*-1, *ACO*-2, *ACO*-3, *ACO*-4, *ACO*-5 and *ACO*-6). For the ethylene signaling genes, the relative expression of the *sickle* gene and six Ethylene INsensitive 3 genes (*EIN3*-1, *EIN3*-2, *EIN3*-3, *EIN3*-4, *EIN3*-5 and *EIN3*-6) were checked. In addition, JA related genes: Vegetative Storage Protein (*VSP*; Sinharoy *et al.* 2013; Pré *et al.* 2008). *MYC2a MYC2b* and *MYC2c* (Ribeiro *et al.*, 2020) were also tested. Similarly the defense related-genes; *PR10* and *PR10*-like (Berrabah *et al.* 2018b) and pathogen-related protein-1 gene (*PR1*), Quinone Methide (*QM)* gene (Pucciariello *et al.*, 2009), flavone synthase-1 (*FS1*) genes induced in *symCRK*^{R108} nodules (data not shown) were also studied.

Material and methods

Bacterial strain and inoculation

The *Sinorhizobium medicae* strain WSM419 (Howieson & Ewing, 1986), was cultivated at 30°C in yeast extract broth (YEB) medium (Krall *et al.*, 2002) supplemented with 12.5 µg.mL^{-1} of chloramphenicol. The bacterial inoculum was prepared by washing twice a fresh overnight liquid culture of *S. medicae* WSM419 with sterile distilled water and then the culture was suspended and adjusted to 0.15 for OD600 nm in sterile distilled water.

Plants material and growth conditions

Seeds of the *Medicago truncatula* R108 and Jemalong A17 genotypes were scarified by sulfuric acid for 10 minutes, washed three times in sterile water, sterilized then in sodium hypochlorite for 30 min, washed three times in sterile water and incubated 1 hour in sterile water. The sterilized seeds were transferred onto 50mL water agarose 1% plates and vernalized for at least 48 h at 4° C in the dark. Seeds were germinated by incubating them at 24°C for 36 h.

Hormonal treatment

In order to correlate gene induction with hormone responses, 2 day-old R108 and A17 wild-type seedlings were transferred into magenta pots filled with 100 mL liquid BNM and incubated with gentle shaking in a growth chamber, under long day condition (16h light/8h dark) at 24°C for 1 week. Seeds were maintained over the liquid medium by a metal grid so that roots can grow in the medium. The seedlings were then transfered to new pots and incubated in 100 µM methyl jasmonate (Me-JA, Zhang *et al.*, 2012) or 10 µM 1-aminocyclopropane-1-carboxylic acid (ACC, Prayitno *et al.*, 2006) or medium without hormone. In order to determine the incubation time required for the marker gene induction, a kinetic was performed on treated roots at five time points (0, 2, 4, 6 and 8 hours). Two further biological replicates were then performed and, the treated roots were harvested at the two selected time points of 4 and at 6 hours post treatments. The collected roots were immediately frozen in liquid nitrogen for RNA extraction.

In silico screening

The screening of new genes involved in hormonal or defense signaling pathways was performed *in silico* using the public databases *Mt*GEA (Noble Research Institute,

mtgea.noble.org) and phytozome (phytozome.jgi.doe.gov) or personal RNAseq data (not published).

RNA extraction and RT-qPCR

Roots were harvested and frozen in liquid nitrogen in 2mL Eppendorf tubes in presence of one 3 mm diameter bead and two 5 mm diameter beads and crushed with TissueLyserII (Qiagen)**.** . At 4°C, the material was resuspended in 500 µL cold TRIzol reagent (ref# 15596026, AMBION) and incubated for 5 min. 100 µL cold chloroform was added to the mix and incubated for 10 min. The mix was then centrifuged 5 min at 16000g and up to 500 µL of the aqueous phase was collected. RNAs were precipitated overnight at -20°C with 250 µL of isopropanol and 100 µL of sodium acetate 3 M pH5.2 and were collected after 60 min at 16000g centrifugation. The precipitated pellet was washed with 1 mL of 70% ethanol and centrifuged two times as above. The obtained RNAs were resuspended in RNase-free water.

The reverse transcription of the free-DNA RNAs was performed using SuperScript™ II Reverse Transcriptase kit (ref. 18064-022, Invitrogen). In a 200 µL micro-centrifuge tube, 1 µL of oligo dT primer (500ng/µL; ref. #SO132, Thermoscientific), 1 µl of dNTPs 10 mM, 1µg of DNA-free RNA and sterile RNase-free water were added to a 13µL final volume. The mix was heated 5 min at 65 °C, quickly chilled on ice and briefly centrifuged. 4µL of 5X First-Strand Buffer [Tris-HCl pH: 8,3 250 mM, KCl 375 mM, $MgCl_2$ 15 mM], 2µL of dithiothreitol 0.1 M were added to the previous mix. The mix was gently homogenized and incubated 2 min at 42°C. Then, 1 µL of SuperScript™ II Reverse Transcriptase 200 units was added, the 20µL final mix was gently homogenized and incubated 50 min at 42°C for the reaction. The reaction was stopped by inactivating the enzyme during 15 min at 70 °C. The obtained cDNA was diluted 1/20 with DNAse-free water.

The Relative qPCRs were performed on cDNAs using 2X LightCycler 480 SYBR Green I Master (ref. 04 887 352 001, Roche), 2 µL of each primers (2,5 µM each) and 1µL of cDNA, in a final volume of 10µL. qPCR were carried out on a LightCycler (480 II Roche). The SYBR Green fluorescence was detected between 465 and 510 nm. Cycle threshold and primer specificities were performed with the LightCycler 480 software release 1.5.0 SP4. Primer efficiencies were calculated with LinReg PCR: Analysis of Real-Time PCR Data, version 11.1. *Actin* (Medtr2g008050) was used as a reference gene for the relative qPCR experiments. Primers used in this study are listed in Table 1.

Table 1. List of RT-qPCR primers

Gene	ID	Forward	Reverse
ACTINE	Medtr2g008050.2	TGGCATCACTCAGTACCTTTCAACAG	ACCCAAAGCATCAAATAATAAGTCAACC
QM	Medtr3g062600.1	GTTGAGTCATGCTGAGTACTTG	GCAAGAAAGCTCTTCCAGGC
FS1	Medtr4g088160.1	CCCATGAAGCTACTTCCTTTAACAC	CAGCACTATTAGCCATGACCTTAAG
FS2	Medtr7g014570.1	CCATGTCTCTTAAATGGGCTGTTG	CCTCTAACAAGAAGCTCTGAAGC
VSP	Medtr8g014650.1	GTAGAGACCTTTGGGTGTTTGAC	CCTTCTGTTTGAGTGGTCTTCCT
MYC2c	Medtr5g030420	CGCTATCTTCTGGCAACCTTCTTA	GAAATAAGCTTGTCCAGGAAGTCC
MYB2b	Medtr8g067280.1	TCCTCCACCACAACAGTCTCTATT	GAGAATCTTTCTACGATGAGCCTG
MYC2a	Medtr5g030430.1	CTTGAAGCTCGAGATTCTGTTGAT	GGGAACCTCAGTTAAAGTACTCGA
PR10	Medtr2g035150.1	CATTGTTGGAGGTGTTGGCCTT	AGTAACCCTCTATAGCCTTGAA
PR10-like	Medtr2g035190.1	AGGCAAACTATGGATACAACTACA	AATTGGCTAGTAATTAGGGTTTGCC
Chitinase	Medtr7g115220.1	CACAGGAAACAGTGAGAATTGTAGA	TAAATGATGGAGAACAAAGGGTTGG
EIN3-1	Medtr4g114650.1	AGTTTGGTTGCAGTTGAAGACA	CAACGCCTGGCCTAATTTCATA
EIN3-2	Medtr4g114640.1	CCTAATCGCGATGGAACTGC	ACAACCGAGTCAACAAACCG
EIN3-3	Medtr1g012520.1	GCCAGATGAGTGCCTCTTTG	CAAGCTGCGGGAAAGGTATC
EIN3-4	Medtr3g078770.1	ACTGGGAAGGAAGAGTGGTG	ATTGACGATTGCAAGCCAGG
EIN3-5	Medtr3g107280.1	GACACTTGAATCGCTAGCTGTT	AGCCCGATATCTGTTACTCCAG
EIN3-6	Medtr5g087790.1	AATGACAGCCAAGGAAAGCG	TTCTCGGGTTTTCGGTCCTC
ACS-1	Medtr8g098930.1	GGCACAGTTATGGACAGAAACA	CGAGGTTACGGTCACATTCA
ACS-2	Medtr4g097540.1	CCACCGGCAATGTTAATGGT	CACACACACACACACTACGA
ACO-1	Medtr3g083370.1	ACCCTGGTAGTGATGCTGTT	AAACGGTTGCTATTGGACCC
ACO-2	Medtr5g085330.1	TGGACACATTGGAGAGGTTGA	TTCAGGGAGGTGACGAACAT
ACO-3	Medtr2g025120.1	CCCTCCAATGCCTCACTCTA	GCGTCTCAAGTGTATCTGCA
ACO-4	Medtr6g092620.1	TGAGGGGAAGTTGATGGAGA	CGGACGATGCCAAATGAAGAA
ACO-5 (ACO LIKE)	Medtr8g028435.1	GCTCCTGATACTCCCAAACC	CATGGTGTCGTGTTGGTGTC
SKL	Medtr0041s0030	GCATTGAGTTCTGAACAGACGAAG	GCAAGATCTCGTCCAGTGATTACA
ACO-6	Medtr1g032250.1	ATCCCCACAATCGACCTCTC	ACACCTTCTTCCTCTCCTCC
PR1	Medtr2g435490.1	TTCGGGTTGGATGTGCTAAG	GGTTGAAGCTCAATGGCACT

Statistical analysis

The means of all observations were calculated and ranked using Excel software (Microsoft 2010). The ranks were subjected to variation analysis and the frequency distribution of the values of genes relative expression was evaluated using Mann–Whitney U test (Walpole and Myers, 1978).

Results

Search for hormone induced marker genes in *M. truncatula* roots.

To determine the role of hormones in nodule defense reactions and to find gene markers whose expression is hormone-dependent, young R108 and A17 wild-type seedlings roots were mock-treated or treated with sodium salicylate (SA; only for R108), methyl jasmonate (Me-JA) or 1-aminocyclopropane-1-carboxylic acid (ACC). We first performed a temporal kinetic (0, 2, 4, 6 and 8 hours) with 100µM Me-JA and 10 µM ACC. This allowed us to select the 4 and 6 hours time points for the two further biological replicates. RNAs from treated and non-treated roots were subjected to RT-qPCR to assess the expression of marker genes. To complete the obtained results, I used the biological material from a SA kinetic performed on R108 roots at five times points (0, 3, 6, 9 and 24 hours). We used from this material previously prepared in the laboratory the 6 hours time point treatment to complete the results of the Me-JA and ACC treatments.

Genes expressions following ACC treatment

The expression of tested genes in *M. truncatula* R108 background in response to ACC treatment was studied. The results presented in fig.1 (right panels) show a strong induction of the *ACO1*, *ACO3* and *PR1* gene expression in *M. truncatula* R108 roots treated with ACC (right panels). In addition, the expression of *ACO2, EIN3-2, QM, FS1, PR10-like* and *PR10* genes (left panels), is also induced by the ACC treatment at 4 and 6 hours post-treatment. In contrast, the expression of the *VSP* gene is repressed at 4 and 6 hours post ACC treatment. The expression of the genes *EIN3-1, EIN3-5, Myc2b, Myc2c* and *SKL* is not induced by ACC treatment. In the other hand, the genes *ACO5* and *EIN3-3* are slightly induced at 4 hours ACC post treatment.

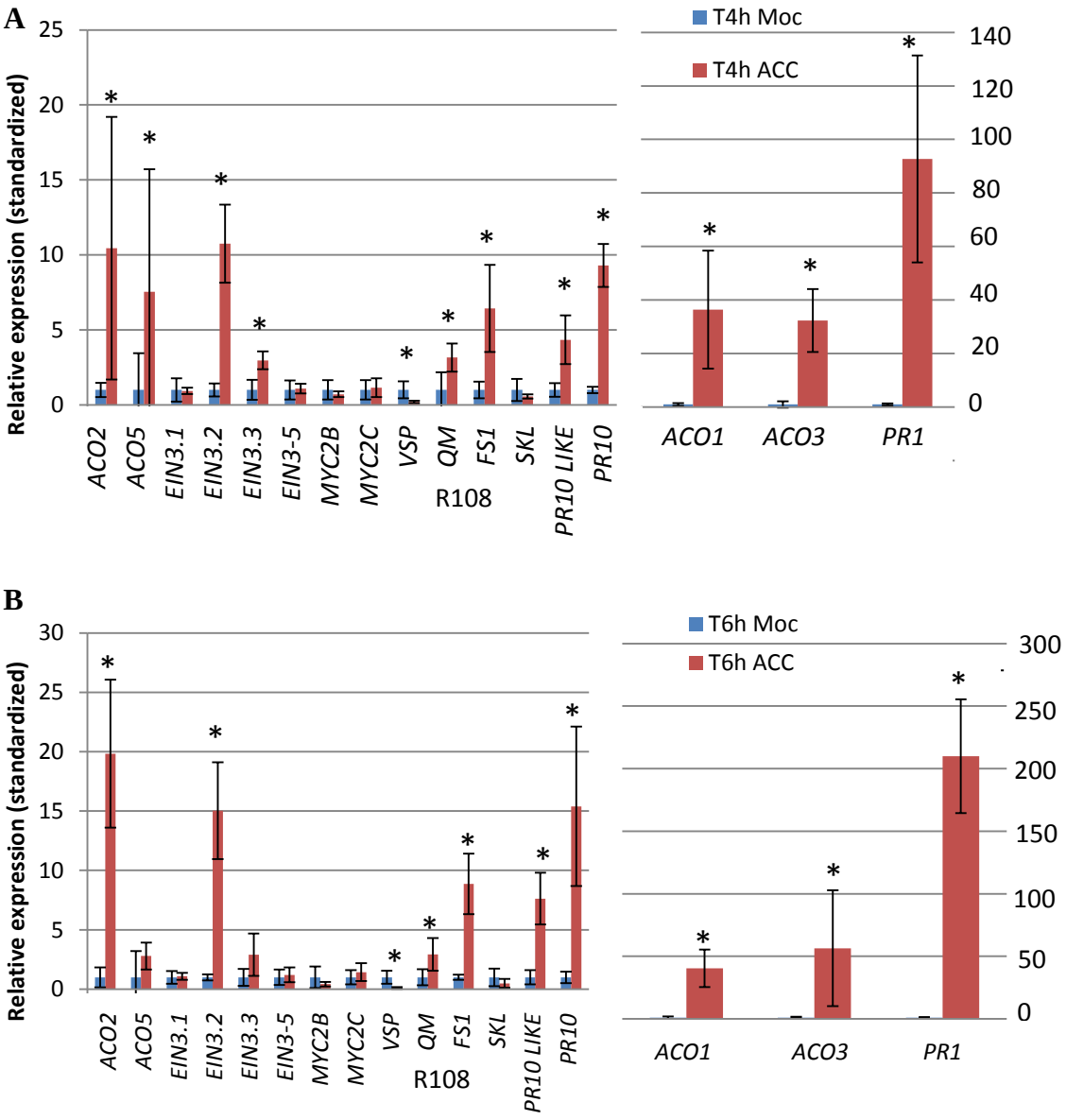

Figure 1. Relative expression of genes markers in R108 roots treated with ACC. The expression of the marker genes was evaluated by RT-qPCR using cDNAs prepared from R108 root RNAs. Roots were treated with ACC *in vitro* and harvested at 4 hours (panel A) and 6 hours (panel B) post-treatment. Fold change versus non treated roots is presented after normalization with an actin gene as an internal control. Error bars, ± SE from three independent experiments with two technical replicate for each experiment. Asterisks indicate significant induction (P<0.05) compared to the non-treated samples.

These results show that the expression of the *ACO1*, *ACO3*, and *PR1* genes is strongly activated by the ET treatment, suggesting that they are probably direct targets of the ethylene signaling pathway. In addition the biosynthetic and signaling ET genes *ACO2*, *ACO5*, *EIN3-2* and *EIN3-3*, together with the *QM*, *FS1*, *PR10* and *PR10-like* gene expressions are moderately

activated by the ET signaling pathway. In addition, the results suggest that the *VSP* gene expression is repressed by ethylene in R108 roots.

The expression of tested genes in *M. truncatula* A17 background in response to ACC treatment was studied. The results presented in fig.2 show a strong induction of the *ACO3* and *PR1* genes expression in *M. truncatula* A17 roots treated with ACC (right panels). In addition, the expression of *ACO1, ACO2, EIN3-2, PR10* and *PR10-like* genes is also induced by the ACC treatment. In contrast, the *VSP* and *MYC2b* genes are repressed by ACC treatment (left panels). In addition the expression of *FS1* gene is slightly induced at 6 hours post ACC treatment.

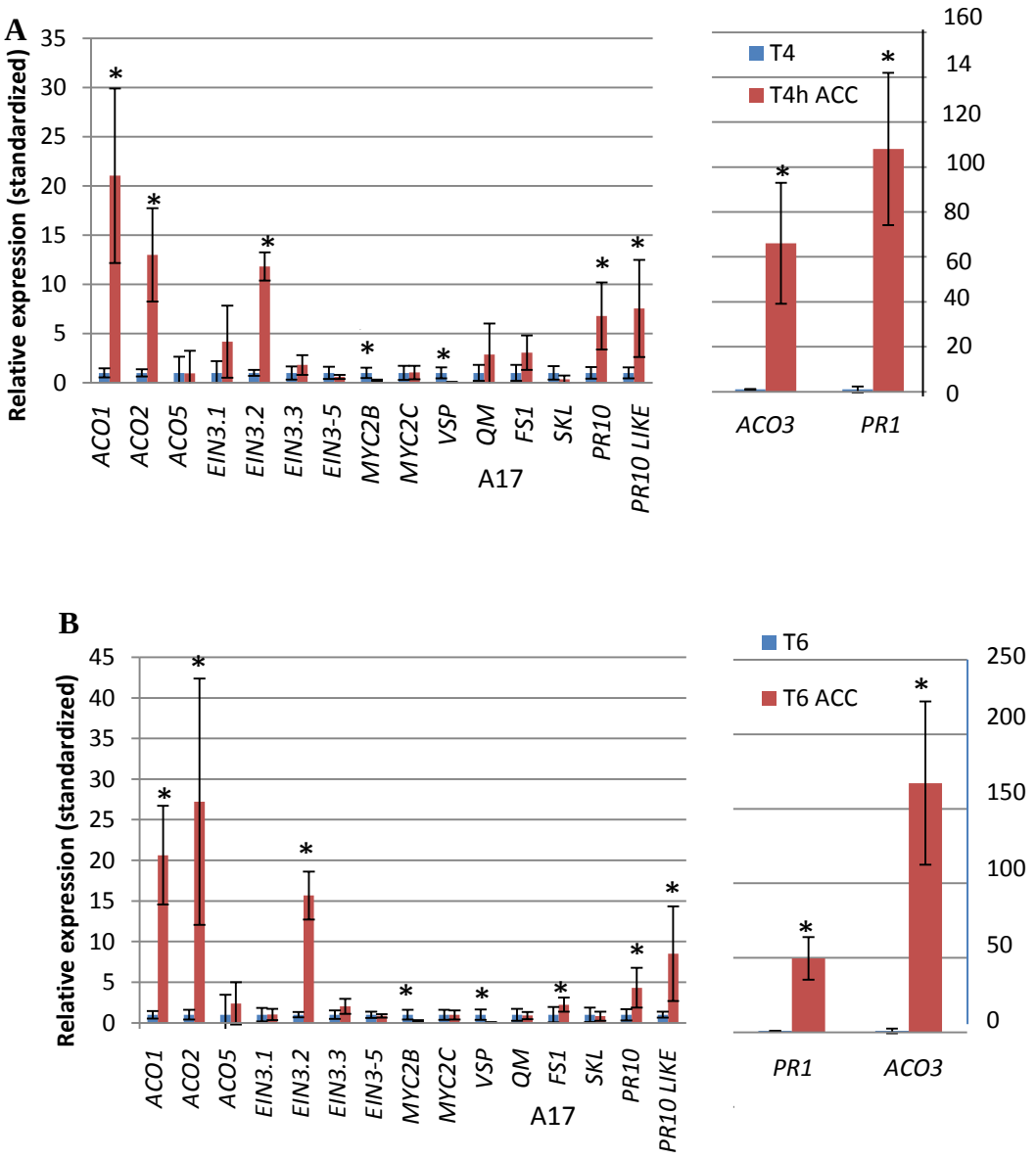

Figure 2. Relative expression of gene markers in A17 roots treated with ACC. The expression of the marker genes was evaluated by RT-qPCR using cDNAs prepared from A17 root RNAs. Roots were treated with ACC *in vitro* and harvested 4 hours (panel A) and 6 hours (panel B) post-treatment. Fold changes relative to those of non-treated roots are presented after normalization with an actin gene as an internal control. Error bars, ± SE from three independent biological replicates with two technical replicate for each replicate. Asterisks indicate significant induction (P<0.05) compared to the non-treated samples.

These results show that the expression of the *ACO3* and *PR1* genes is strongly activated by the ET treatment, suggesting that these genes are probably direct targets of the ethylene signaling pathway in *M. truncatula* A17 background. The *ACO1*, *ACO2*, *EIN3-2*, *PR10* and

PR10-like genes are moderately induced by ET signaling pathway. In addition, the results suggest that *VSP* and *MYC2b* genes are repressed by ethylene in A17 background.

All together the results indicate that the ET (ACC) effect in *M. truncatula* A17 and R108 backgrounds are not totally the same. For example, during the first 4 hours of treatment, ET induces the expression of *ACO5* and *EIN3-3* in R108 but not in the A17 background. After 6 hours of ET treatment, ET induces *QM* gene expression and more than twice *ACO1* expression in R108 compared to the A17 background. However, in both genetic backgrounds, at 4 and 6 hours post ET treatment, *ACO3* and *PR1* gene expressions are strongly induced. In addition, the expression of *ACO2*, *EIN3-2*, *FS1*, *PR10* and *PR10-like* genes is moderately induced by this treatment. In contrast, ET inhibits the expression of the *VSP* gene in the R108 roots and *VSP* and *MYC2b* genes in A17 roots. Herein, we conclude that expression of the *PR1* and *ACO3* and repression of the *VSP* genes are markers for ET signaling in both A17 and R108 roots.

Genes expressions following MeJA treatment

The expression of tested genes in *M. truncatula* R108 background in response to JA treatment was studied. The results presented fig.3 show a strong induction of the *MYC2b*, *VSP* and *QM* genes induction in *M. truncatula* R108 roots treated with MeJA. In addition, the expression of the *ACO2*, *ACO3*, *MYC2c* and *PR10-like* genes are also induced 4 and 6 hours post MeJA treatment. However, the expression of *EIN3-2*, *EIN3-3* and *PR10* are induced 6 hours post MeJA treatment. In contrast, *PR1* gene expression is repressed 6 houts post MeJA treatment in R108 roots (left panel).

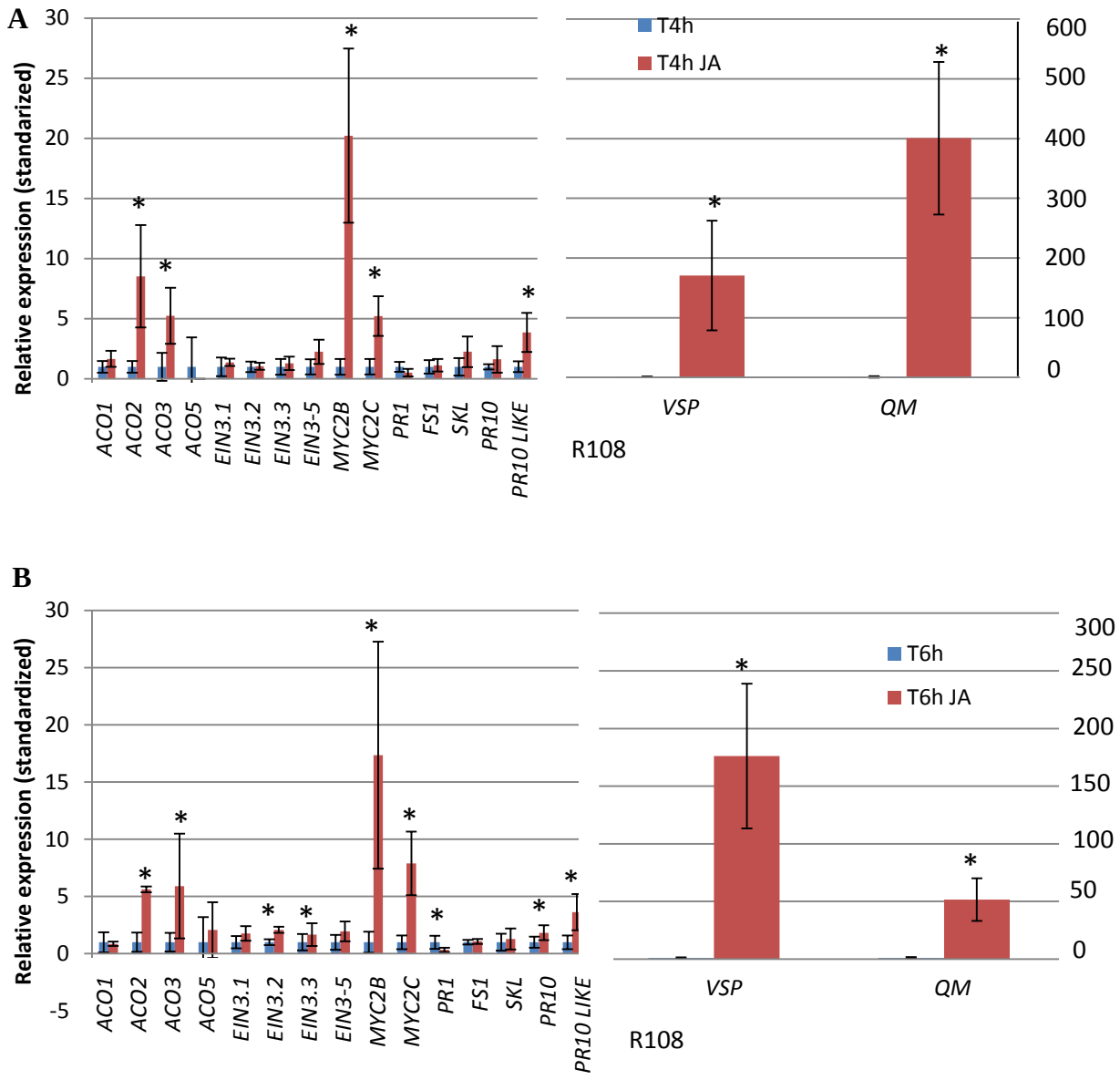

Figure 3. Relative expression of gene markers in R108 roots treated with MeJA. The expression of the marker genes was evaluated by RT-qPCR using cDNAs prepared from R108 root RNAs. Roots were treated with MeJA *in vitro* and harvested 4 hours (panel A) and 6 hours (panel B) post-treatment. Fold changes versus non treated roots is presented after normalization with an actin gene as an internal control. Error bars, ± SE from three independent biological replicates with two technical replicate for each replicate. Asterisks indicate significant induction ($P<0.05$) compared to the non-treated samples.

These results suggest that *VSP* and *QM* genes are strongly correlated to JA signaling pathway; in addition the *ACO2, ACO3, MYC2b, MYC2c* and *PR10-like* genes are also correlated to JA signaling pathway in R108 roots. By opposition, *PR1* gene expression is inversely correlated to JA signaling pathway at 6 hours JA post-treatment in R108 roots.

The expression of tested genes in *M. truncatula* A17 background in response to JA treatment was studied. The results present fig.4 show a strong induction of the *MYC2b, VSP* and *QM* genes in *M. truncatula* A17 roots treated with MeJA compared to non-treated roots. In addition, the expression of *ACO2, MYC2c, EIN3-5, EIN3-2* and *PR10-like* genes are also induced by MeJA treatment. However, the expression *PR1* gene is repressed by the MeJA at 4 and 6 hours post-treatment in A17 roots (left panel). On the other hand, the expression of *PR10, SKL and FS1* genes are slightly induced at 4 hours post MeJA treatment.

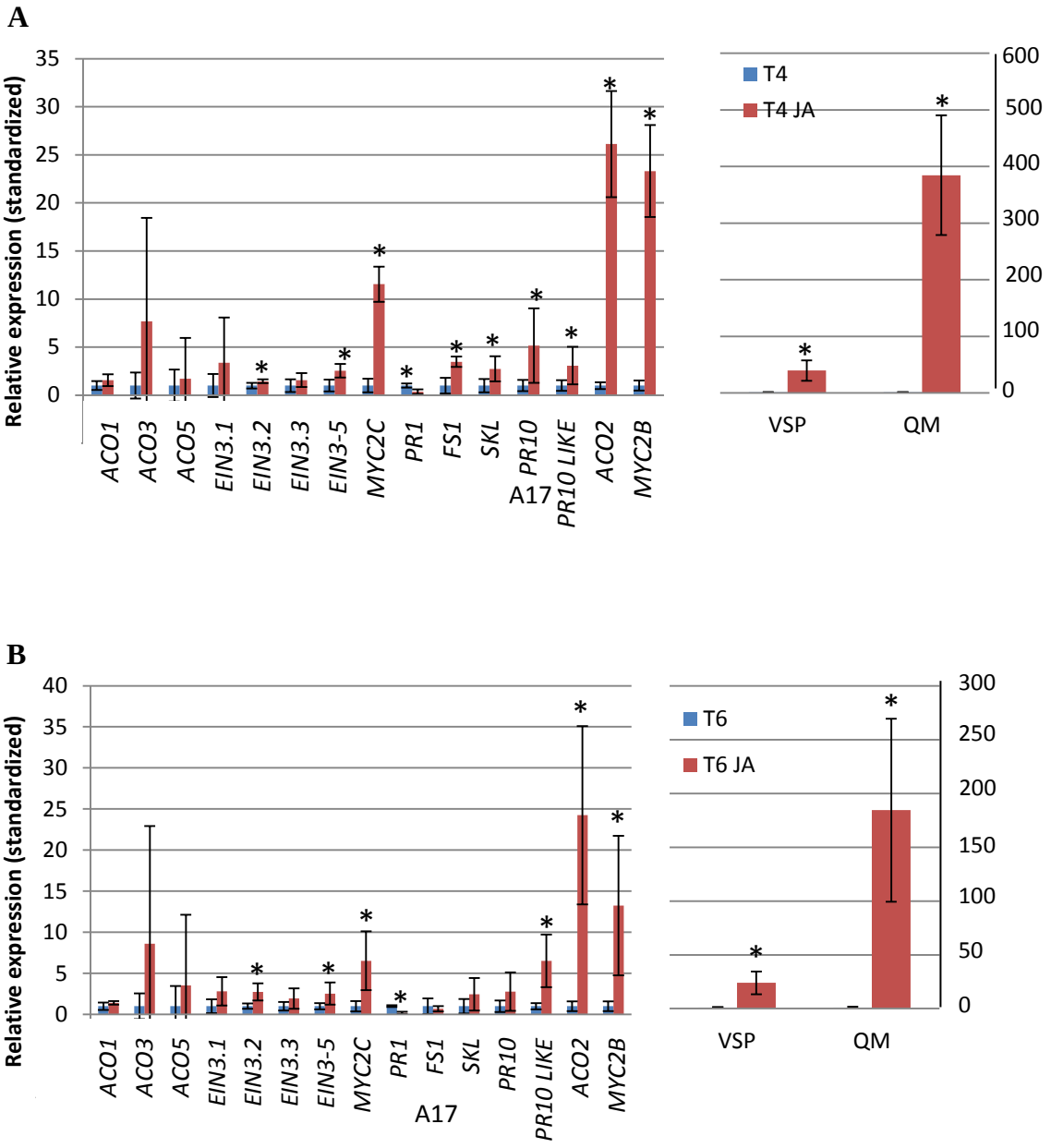

Figure 4. Relative expression of gene markers in A17 roots treated with MeJA. The expression of the marker genes was evaluated by RT-qPCR using cDNAs prepared from A17 root RNAs. Roots were treated with MeJA *in vitro* and harvested at 4 hours (panel A) and 6 hours (panel B) post-treatment. Fold change versus non treated roots is presented after normalization with an actin gene as an internal control. Error bars, ± SE from three independent experiments with two technical replicates for each experiment. Asterisks indicate significant induction ($P<0.05$) compared to the non-treated samples.

These results suggest that the MYC2b, *VSP* and *QM* gene expressions are strongly induced by JA treatment; in addition the *ACO2, MYC2c, EIN3-5, EIN3-2* and *PR10-like* genes are also correlated to JA signaling pathway on A17 roots. In contrast the *PR1* gene expression is inversely correlated to JA signaling pathway at 4 hours post treatment in A17 roots.

All together the results of the MeJA treatments in *M. truncatula* A17 and in R108 roots suggest that the JA effect is different between the two *M. truncatula* backgrounds. The first observed differences are that at 4 hours post JA treatment the *PR10, SKL, EIN3-5, EIN3-2* and *FS1* genes are induced in A17 background. In contrast the *PR1* gene is repressed in A17 roots and in R108 at 6 hours post MeJA treatment. We also noted the induction of the *ACO3* gene in R108 but not in A17 roots. Secondly, small differences were observed 6 hours post JA treatment: the expression of the *ACO3, EIN3-3* and *PR10* genes is lowly induced in R108 but not in A17 roots. By contrast, the *EIN3-5* gene is lowly induced only in A17 roots. We can conclude that the expression of the *VSP, QM, ACO2, MYC2b, MYC2c* and *PR10*-like genes is induced in both genetic backgrounds following the JA treatment. The *ACO2*, *PR10*-like and *QM* genes are also induced by ACC in the R108 background. So the genes *VSP, MYC2b, MYC2c* seem to correlate positively to JA. However, *PR1* gene is negatively correlated to JA.

Genes expressions following SA treatment

The expression of tested genes in *M. truncatula* R108 background in response to SA treatment was studied. The results present in fig.5 (right panel) show a strong induction of the *ACO5, PR10, ACO6* and *QM* genes expression in *M. truncatula* R108 roots treated for 6 hours with sodium salicylate. In addition, the expression of *ACO1, ACO2, EIN3-1, EIN3-2, EIN3-6,* MYC2b, MYC2c, *PR1, FS1* and *PR10-like* (left panel) is also induced by SA treatment. However, the expression of the *VSP* gene is repressed 6 hours post sodium salicylate treatment. The expression of the genes *ACO3, ACO4, myc2A* and *SKL* is not induced by this SA treatment.

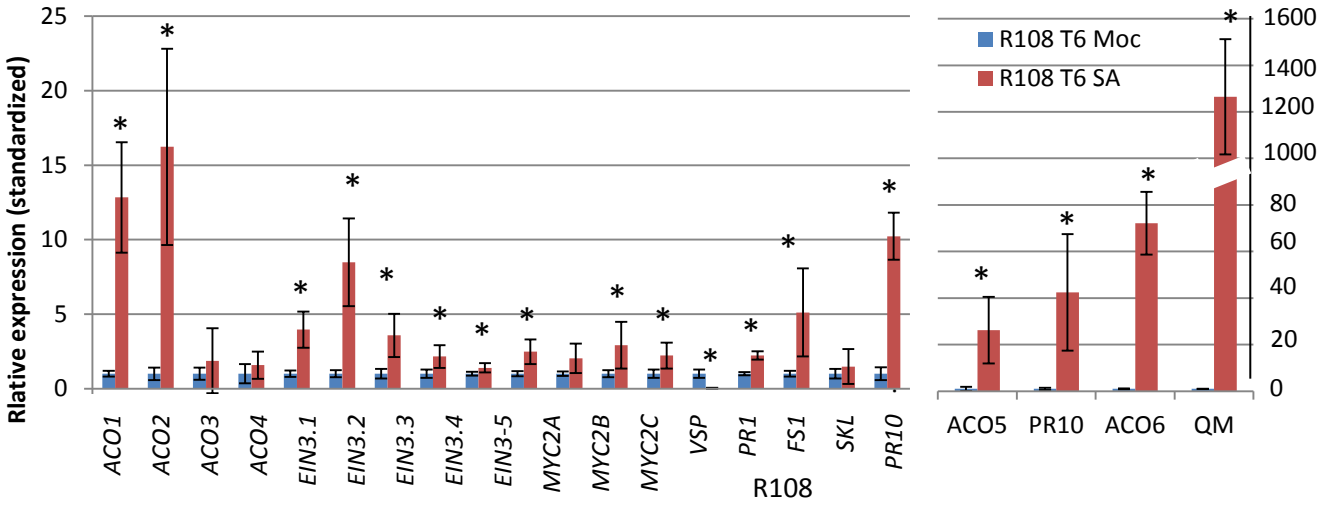

Figure 5. Relative expression of gene markers in R108 roots treated 6h with sodium salicylate. The expression of the marker genes was evaluated by RT-qPCR using cDNAs prepared from R108 root RNAs. Roots were treated with SA *in vitro* and harvested at 6 hours post treatment. Fold change versus non treated roots is presented after normalization with an actin gene as an internal control. Error bars, ± SE from three independent experiments with two technical replicate for each experiment. Asterisks indicate significant induction ($P<0.05$) compared to the non-treated samples.

These results suggest that the the *VSP* gene *is* repressed by the SA signaling pathway. However, the *ACO5, PR10, ACO6* and *QM* genes are strongly correlated to the SA signaling pathway in R108 roots. In addition, *ACO1*, *ACO2*, *EIN3-1*, *EIN3-2*, *EIN3-6*, MYC2b, MYC2c, *PR1*, *FS1* and *PR10-like* genes are correlated to the SA signaling pathway 6 hours post SA treatment in R108 roots.

Taken together the results of ACC, MeJA and SA treatment in *M. truncatula* A17 and in R108 roots suggest that the *VSP* gene is induced by JA and repressed by SA and ET. *ACO6* and *ACO5* genes are strongly correlated to SA and the *PR1* gene normally used as an SA induced gene is more correlated to ET then JA and SA.

Conclusion

In summary, these results suggest (fig.6); (1) Differences between R108 and A17 background in term of hormones effects. (2) JA is able to induce the expression of some ET biosynthetic genes (*ACO2*) and to repress ET induced genes (*PR1*). (3) ET represses the expression of some JA induced genes (*VSP*) and induces flavone synthase genes (*FS1*) in R108 background. (4) *ACO2* and *PR10-like* gene expression require SA, JA and ET signaling. (5) *PR1* is more correlated to ET signaling pathway and *VSP* is the best JA markers in both *M. truncatula* backgrounds A17 and R108.

This difference between these two *M. truncatula* ecotypes might reflect real ecotype differences but also the fact that R108 has been selected for an altered hormone response (see discussion of chapter 5).

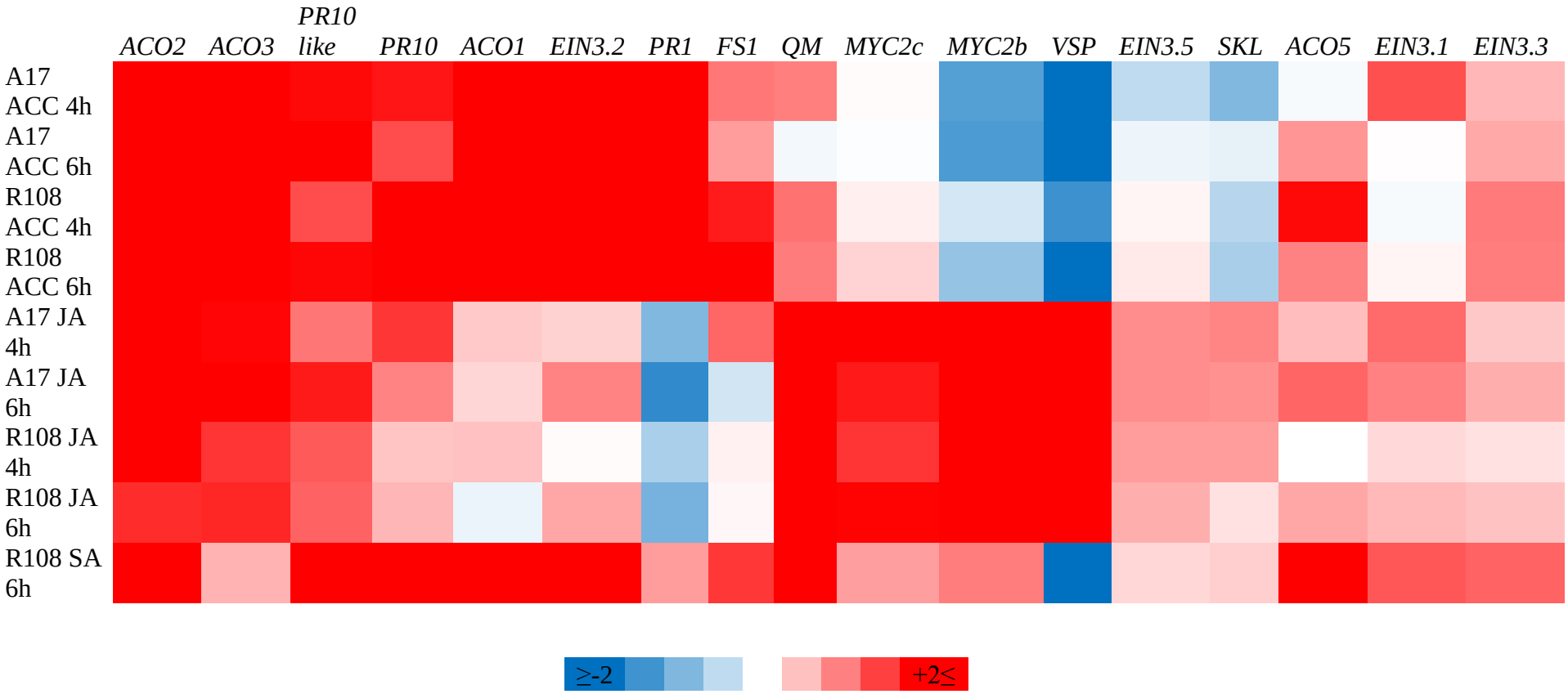

Figure 6. Heatmap showing the expression patterns of putative hormone correlated genes. *M. truncatula* A17 and R108 roots treated with SA, ACC and MeJA. The different colors correspond to the log (2) values of the gene expression changes shown in the bar row under the figure. The bleu color represents repressed expression level, **shade of blue to red** colors represents unchanged expression, and red color represents induction of the genes expression level.

Chapter V: Study of the inter-connection between symbiotic genes and defense hormone signaling pathway in the intracellular accomodation of rhizobia in the symbiotic cells

Introduction

The roles of defense hormone in the early nodulation steps are widely studied (see general introduction). Herein, we have studied the role of the defense hormones in the late steps of *M. truncatula* nodulation. This role is still not well known. We have evidence of the role of defense hormones in the induction of defense reactions and senescence in nodules. As previously shown (Chapter III), ET- dependent genes were strongly induced in nodules of the R108 *dnf2* and *symCRK* mutants. By contrast, the ET- dependent genes were not or slightly induced in the A17 fix^{-} mutant nodules. This shows that the expression of the ET- dependent genes participating in the ET-triggered defense vary according to the mutated symbiotic gene and to the background of the plants. There is limited information concerning the genes involved in the ET signaling in the A17 background. In order to better understand the ET signaling in the A17 mutants *dnf2* and *symCRK*, RT-qPCR experiments were performed using RNA isolated from nodules of *M. truncatula* wild-type and single and double mutants, *symCRK*^{A17} (*dnf5*), *dnf2*^{A17} (*dnf2*), *symCRK /skl* (*dnf5/skl*) and *dnf2/skl* (*dnf2/skl*).

In this part, we analyzed the expression of several ethylene biosynthesis genes as well as the expression of ethylene signal transduction genes, together with the expression of the pathogen-related protein-1 gene (*PR1)* as an ethylene responsive gene marker.

Material and methods

Bacterial strain and inoculation

The *Sinorhizobium medicae* strain WSM419 (Howieson & Ewing, 1986), was cultivated at 30°C in yeast extract broth (YEB) medium (Krall *et al.*, 2002) supplemented with 12.5 µg.mL^{-1} of chloramphenicol. The bacterial inoculum was prepared by washing twice a fresh overnight liquid culture of *S. medicae* WSM419 with sterile distilled water and then the culture was suspended and adjusted to an optical density (OD600 nm) of 0.15 in sterile distilled water.

Plants material an growth conditions

Seeds of the *Medicago truncatula* genotype R108 and Jemalong A17, their corresponding mutants (*dnf2*, *symCRK*, *dnf5* and *skl/dnf2* and *skl/dnf5*) were scarified by sulfuric acid for 10 minutes, washed three times in sterile water, then sterilized in sodium hypochlorite for 30 min, washed three times in sterile water and incubated 1 hour in sterile water. The sterilized seeds were transferred onto 50mL water agarose 1% plates and vernalized for at least 48 h at 4° C in the dark. Seeds were germinated by incubating them at 24°C for 36 h.

For nodulation tests, RNAs extraction and acetylene reduction assay, the seedlings were transferred onto square plates (8 plants per plate) filled with buffered nodulation medium BNM (Ehrhardt *et al.*, 1992) solidified by bacto-agar 1.5% or phytagel 1.5% and supplemented or not with 0.1µM 2-aminoethoxyvinyl glycine (AVG). The seedling roots were inoculated with 1mL of bacterial suspension per plate. The plates were then incubated in growth chamber under long day condition (16h light/8h) at 24°C. All experiments were conducted on nodules harvested at 21 days post-inoculation (dpi).

Geetic crosses

To backcross the *dnf2* mutant line NF0217 and to construct the double mutants *dnf2/myc2b, dnf2/skl* and *dnf5/skl*, an artificial crossing was performed as described by Pathipanawat et al. (1994). NF0217 and R108 wild-type or *skl*, *myc2b*, *dnf2* and *dnf5* mutant plants were used as male and female parents. Using a binocular loupe and extra fine forceps, anthers containing mature pollens obtained from young flowers were applied to the stigma of emasculated flowers. The fertilized flowers are covered by a 50 mL tube to prevent them from drying. The F1 plants were grown and genotyped by sequencing amplified PCR fragments

containing the mutations. The double heterozygote mutants were selected and planted to produce the F2 generation (Table 1). The F2 generation plants were screened by sequencing as above to select the homozygote mutants. These double homozygote mutants were reproduced and used for further experiments.

Table 1. List of the realized crosses: the name of the alleles is given first line and the corresponding line name is given second line.

	***dnf2*^{R108}** **MS240**	***dnf2*^{A17}** **dnf2**	***symCRK*** **dnf5**	***dnf2*^{R108}** **NF0217**
R108				*dnf2/DNF2-lox/LOX*
skl		*dnf2/skl*	*symCRK/skl*	
myc2b	*dnf2/myc2b*			

DNA extraction and PCR screening

Polymerase chain reaction screening was performed as described in Tadege *et al.* (2008) and Cheng *et al.* (2011), on genomic DNA extracted from mutant plant leaves as described by D'Erfurth *et al.* (2003). For the *Tnt1* mutant plants, the PCR screening was done with three primers per reaction, two primers corresponding to the target gene and one primer corresponding to the external part of the retrotransposon *Tnt1*. The primers are listed in the Table 2.

Table 2. List of the genotyping primers

GENE	NUMERO D'ACCESSION		Primers
DNF2	Medtr4g085800.1	FORWARD	CAAAACCGGTGAATAATTCGGACC
		REVERSE	GCCAAAGAATGGTAGTGATTGGC
SymCRK (DNF5)	Medtr3g079850	FORWARD	GAGGTAGTCTAAGATGAACCAAC
		REVERSE	CATTCTGACGCGGAATCAAAGAT
SICKLE A17	Medtr0041s0030.1	FORWARD	AGCTGCAGCTCCAGGGGAGCTA
		REVERSE	TGATTCTGGTGAGAGGCGCTATT
MYC2B-1	Medtr5g030420.5	FORWARD	GCTAGTACTAGTACTTTCTGTTAGC
		REVERSE	TCGAAAGGCGAATTGGAGATACAAT
LTR4	*Tnt1*		TACCGTATCTCGGTGCTACA
LTR6	*Tnt1*		GCTACCAACCAAACCAAGTCAA

Acetylene reduction assay ARA

Measurement of the nitrogen fixation efficiency of nodules was performed using a modified ARA protocol from Koch and Evans (1966). Whole nodulated plants at 21 dpi were placed individually into 20 mL glass vials sealed with rubber septa. 500 µL of acetylene was injected into each vial and incubated for 2 hours in a growth chamber under long day condition (16h light/8h dark) at 24°C. The vials were moved to gas chromatograph (GC 7820A, Agilent) to measure the produced ethylene by injecting 200 µL of gas from the incubated vial. The amount of ethylene produced was calculated following this calculation:

$$[C2H4] = \frac{Pic\ area\ \times 99}{incubation\ time\ \times 495} \times 60$$

$[C_2H_4]$: nmol C_2H_4 $.h^{-1}.plant^{-1}$; Pic area: $pA.s^{-1}$; 99: gas volume for an entire vial 1/99 of vial was injected in GC; Incubation time: min; 495: slope of the relation between pic area values and C_2H_4 concentration values; 60: min

Three biological replicates were used for each experiment.

RNA extraction and RT-qPCR

Nodules from different mutants were harvested at 21 dpi and were frozen in liquid nitrogen in 2mL Eppendorf tubes in presence of one 3 mm diameter bead and two 5 mm diameter beads and crushed with TissueLyserII (Qiagen). . At 4°C, the material was resuspended in 500 µL cold TRIzol reagent (ref# 15596026, AMBION) and incubated for 5 min. 100 µL cold chloroform was added to the mix and incubated for 10 min. The mix was then centrifuged 5 min at 16000g and up to 500 µL of the aqueous phase was collected. RNAs were precipitated overnight at -20°C with 250 µL of isopropanol and 100 µL of sodium acetate 3 M pH5.2 and were collected after 60 min 16000g centrifugation. The precipitated pellet was washed with 1 mL of 70% ethanol and centrifuged twice as above. The obtained RNAs were resuspended in RNase-free water.

The reverse transcription of the free-DNA RNAs was performed using SuperScript™ II Reverse Transcriptase kit (ref. 18064-022, Invitrogen). In a 200µL micro-centrifuge tube, 1 µL of oligo dT primer (500ng/µL; ref. #SO132, Thermoscientific) 1 µl of dNTPs 10 mM, 1µg of DNA-free RNA and sterile RNase-free water were added in a 13µL finale volume. The mix was heated 5 min at 65°C, quickly chilled on ice and briefly centrifuged. 4µL of 5X First-Strand Buffer [Tris-HCl pH8.3 250 mM, KCl 375 mM, $MgCl_2$ 15 mM], 2µL of dithiothreitol 0,1 M were added to the previous mix. The mix was gently homogenized and incubated 2 min at 42°C. Then, 1 µL of SuperScript™ II Reverse Transcriptase 200 units was added, the 20µL finale mix was gently homogenized and incubated 50 min at 42°C for the reaction. The reaction was stopped by inactivating the enzyme during 15 min at 70 °C. The obtained cDNA was diluted 1/20 with DNAse-free water.

The Relative qPCRs were performed on cDNAs using 2X LightCycler 480 SYBR Green I Master (ref. 04 887 352 001, Roche), 2 µL of each primers (2,5 µM each) and 1µL of cDNA, in a final volume of 10µL. qPCR were realized on a LightCycler (480 II Roche). The SYBR Green fluorescence was detected between 465 and 510 nm. Cycle threshold and primer specificities were performed with the LightCycler 480 software release 1.5.0 SP4. Primer efficiencies were calculated with LinReg PCR: Analysis of Real-Time PCR Data, version 11.1. *Actin* (Medtr2g008050) was used as reference in relative qPCR experiments.

Results

Role of Ethylene in bacteroids intracellular accommodation during symbiosis

Construction of *dnf2/skl* and *dnf5/skl* mutants

Because of the absence of a *skl* mutant in the R108 background, we have constructed double *dnf2/skl* and *dnf5/skl* mutants in the A17 background. Plants were crossed as described in the Material and Method sections and the confirmation of the cross was performed using a PCR approach and sequencing. Double heterozygotes (F1) were propagated and their progeny screened for the presence of double mutants using the same approach (PCR and sequencing). The sequencing of the PCR products from the F2 generation confirmed the success of the crossings between *skl* with $dnf2^{A17}$ and *skl* with $symCRK^{A17}$ mutants and the production of the double mutants.

Symbiotic phenotype of the double mutants

The *dnf2/skl* and *dnf5/skl* double mutants were nodulated using *S. medicae* WSM419. The double mutants showed additive phenotypes because they inherited the size and the number of nodules from their *skl* mutant parent, while keeping the fix^- phenotype of their symbiotic mutant parents.

Results presented fig.1 show that the A17 wildtype plant and the *skl* mutant reduce acetylene to ethylene indicating that the rhizobia inside nodules are fixing nitrogen. However, the mutant *dnf5* and the double mutant *dnf5/skl* are not able to reduce acetylene into ethylene indicating that the hosted rhizobia in nodules are unable to fix nitrogen which can be explain by the death of the bacteria (fig.1A). A17 wildtype, simple mutants *dnf2* and *skl* and double mutant *dnf2/skl* are able to fix atmospheric nitrogen when they are cultivated in BNM medium solidified with phytagel. In contrast, *dnf2* and *dnf2/skl* mutants are unable to reduce atmospheric nitrogen into ammonium when they are cultivated in BMN medium solidified with bacto-agar comparing to A17 wild-type and *skl* mutant (fig.1B).

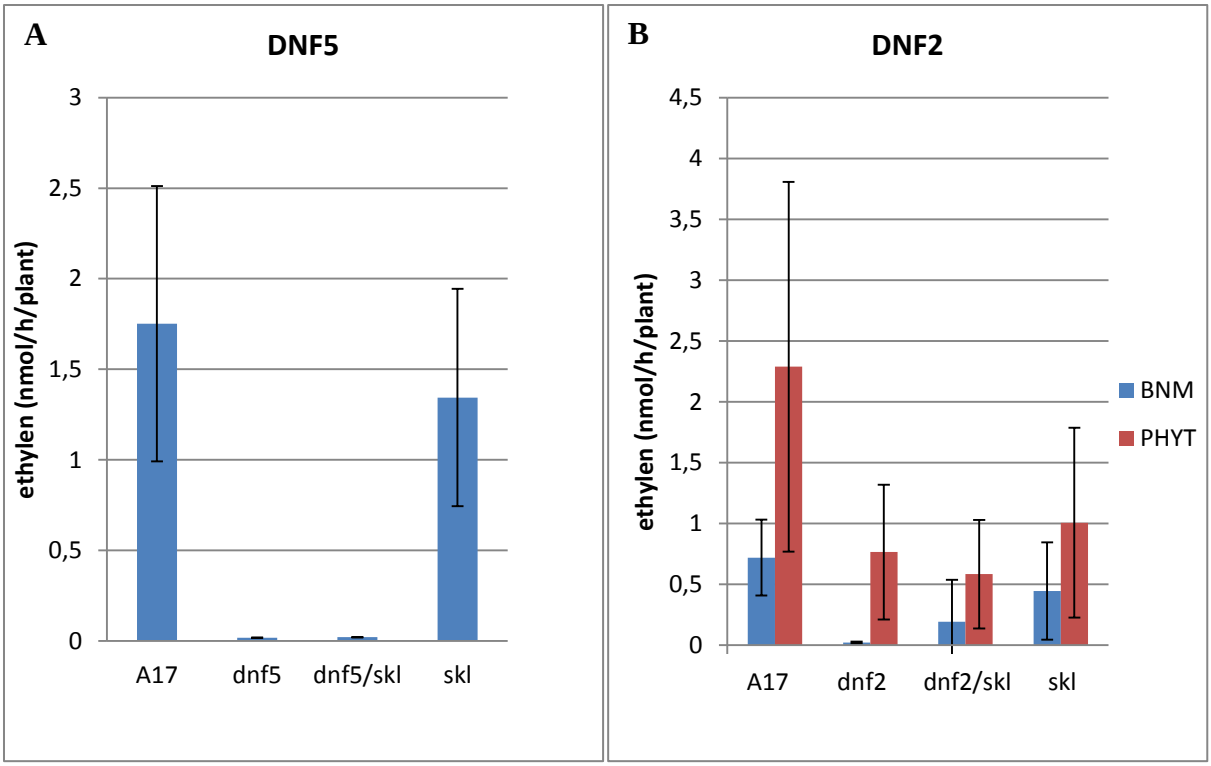

Figure 1. The double mutants retain their symbiotic phenotypes. The acetylene reduction assay (ARA) was performed with sixteen nodulated plants from A17, skl (*sickle*), dnf5 (*symCRK*^{A17}) and double mutant dnf5/skl cultivated on BNM solidified with bacto-agar (panel A). And from A17, skl (*sickle*), dnf2 (*dnf2*^{A17}) and double mutants dnf2/skl cultivated on BNM solidified with bacto-agar or with phytagel (panel B). Samples were harvested at 21 dpi. The double mutants are fix-. Error bars, ± SE from three independent experiments with one technical replicate for each experiment.

These results suggest that the fixation efficiency in A17 background is independent from ethylene. In fact, the ethylene signaling suppression does not affect the fixation capacity in *skl* mutant compared to wild-type, has no effect on the conditional phenotype of the *dnf2* mutant and does not restore the fix^{+} phenotype to *symCRK*^{A17} and *dnf2*^{A17} mutants.

Defense hormones and symbiotic genes relationship

Relationship between ethylene related genes and symbiotic genes *SymCRK* in *M. truncatula* A17

As previously shown (Chapter III), ET-dependent genes were strongly induced in nodules of the R108 *dnf2* and *symCRK* mutants. By contrast, the ET-dependent genes were not or slightly induced in the A17 fix$^-$ mutant nodules. This shows that the expression of the ET-dependent genes participating in the ET defense vary according to the mutated gene and to the background of the plants. There is limited information concerning the genes involved in the ET signaling in the A17 background. In order to better understand the ET signaling in the A17 mutants *dnf2* and *symCRK*, RT-qPCR experiments were performed using RNA isolated from nodules of *M. truncatula* wildtype and single and double mutants, *symCRK* ^{A17} (*dnf5*), *dnf2*^{A17} (*dnf2*), *symCRK* ^{A17}*/skl* (*dnf5/skl*) and *dnf2*^{A17}*/skl* (*dnf2/skl*).

In this part, I analyzed the expression of several ethylene biosynthesis genes corresponding to two 1-aminocyclopropane-1-carboxylate synthase genes (*ACS*-1 and *ACS*-2) and six1-aminocyclopropane-1-carboxylate oxydase genes (*ACO*-1, *ACO*-2, *ACO*-3, *ACO*-4, *ACO*-5 and *ACO*-6) as well as the expression of ethylene signal transduction genes corresponding to the gene *sickle* and six Ethylene insensitive 3 genes (*EIN3*-1, *EIN3*-2, *EIN3*-3, *EIN3*-4, *EIN3*-5 and *EIN3*-6) together with the expression of the pathogen-related protein-1 gene (*PR1)* as an ethylene responsive gene marker.

The results presented in fig.2, show that the expression of *ACO5* and *EIN3-3* genes are slightly induced in *SymCRK*^{A17} mutant. However, the expression of these genes is changed in double mutant *dnf5/skl*, where the expression of *ACO*5 gene is more induced and the expression of *EIN3*-3 gene is unchanged comparing to wild type. In addition, the expression of *ACO4* is repressed in *SymCRK*^{A17} nodules. In contrast, the *ACS2* gene is induced in *skl* and *dnf5/skl* and *SKL* gene is induced in double mutant *dnf5/skl*.

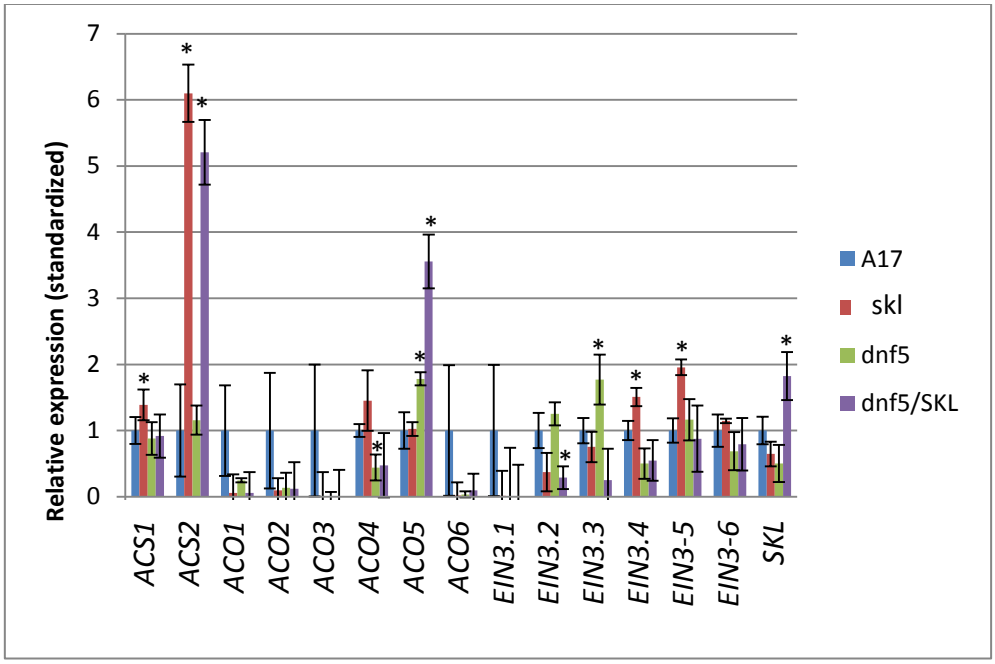

Figure 2. Relative expression of ET biosynthetic and signaling genes in the simple and double mutants. The expression of ethylene biosynthesis and ethylene signaling pathway genes was evaluated by RT-qPCR performed on RNAs extracted from A17 wild-type, *symCRK*^{A17} (*dnf5*) and the double mutant *symCRK*^{A17}*/skl* (*dnf5/skl*). Nodules were induced *in vitro* by inoculation with *S. medicae* WSM419 strain and harvested at 21 dpi. Fold change versus wild-type is presented after normalization with an *Actin* gene as an internal control. Error bars, ± SE from three independent experiments with one technical replicate for each experiment. Asterisks indicate significant induction ($P<0.05$) compared to the non-treated samples.

These results suggest that SymCRK^{A17} controls slightly the expression of *ACO5* gene and controls positively the expression of *ACO4* gene independently of ET. It also suggests that ET is not important in the control of the nodule defense reactions in *symCRK*^{A17} mutant, because in Chapter IV, I reported that the *ACO5* gene is strongly induced with SA treatment in roots. This suggests that defense reactions in the *SymCRK*^{A17} mutant are independent of ET and slightly depending to SA signaling pathway.

Relationship between defense genes and symbiotic *SymCRK* genes in *M. truncatula* A17

The results presented in fig.3 indicate that in the *symCRK*^{A17} mutant, the defense genes *PR10, PR10*-like and *Chitinase* were not activated. On the other hand, the mutation of the *SKL* gene in *symCRK*^{A17} mutant induces the expression of the *PR10* gene.

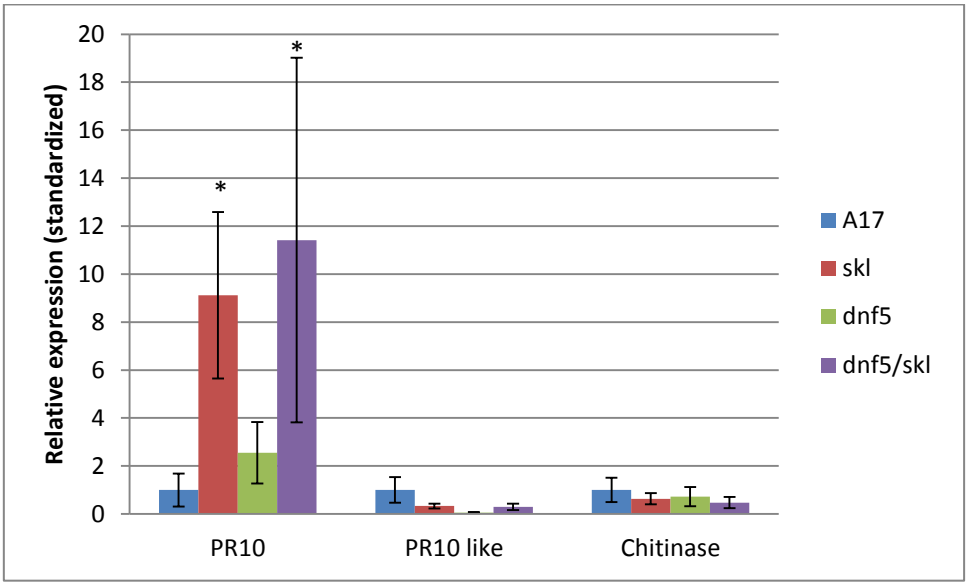

Figure 3. ET effects on defense-related genes expression. The expression of the *PR10, PR10*-Like and *Chitinase* defense genes was evaluated by RT-qPCR performed on RNAs extracted from A17 wild-type, skl (*skl),* dnf5 (*symCRK*^{A17}) and double mutant dnf5/skl (*symCRK*^{A17}*/skl*). Nodules were induced *in vitro* by *S. medicae* WSM419 strain and harvested at 21 dpi. Fold change versus wildtype is presented after normalization with an *Actin* gene as an internal control. Error bars, ± SE from three independent experiments with one technical replicate for each experiment. Asterisks indicate significant induction ($P<0.05$) compared to the non-treated samples.

These results suggest that the expression of the defense genes *PR10* and *Chitinase* are independent of the control of SymCRK^{A17}. In contrast, the expression of *PR10*-like is repressed by SymCRK^{A17}. On the other hand, the expression of PR10 is negatively controlled by ET.

Relationship between JA-related genes and symbiotic *SymCRK* genes in *M. truncatula* A17

The results presented fig.4 show that the expression of MYC2b is induced in *skl* and *symCRK*^{A17} mutants, and we observed a slight induction of *MYC2c* in *symCRK*^{A17} mutants. The induction of *MYC2b* and *MYC2c* are repressed in the double mutant *dnf5/skl*. However, the expression of *VSP* is unchanged in nodules of all mutant lines.

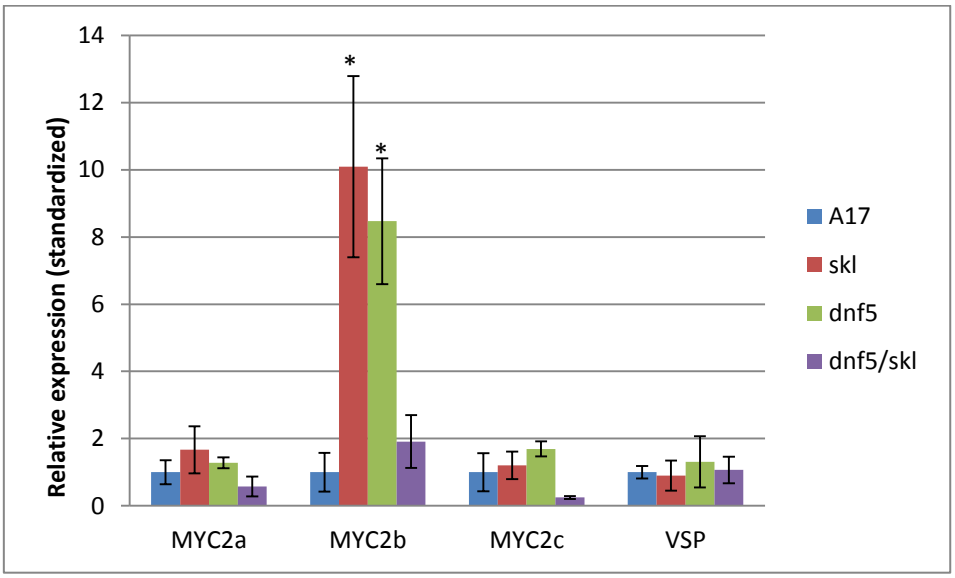

Figure 4. ET and *SymCRK* gene effects on JA-depending gene expression. The expression of JA-related genes was evaluated by RT-qPCR performed on RNAs extracted from A17 wild-type, skl (*skl)*, dnf5 (*symCRK*^{A17}) and double mutant dnf5/skl (*symCRK*^{A17}*/skl*). Nodules were induced *in vitro* by *S. medicae* WSM419 strain and harvested at 21 dpi. Fold change versus wild-type is presented after normalization with an actin gene as an internal control. Error bars, ± SE from three independent experiments with one technical replicate for each experiment. Asterisks indicate significant induction ($P<0.05$) compared to the non-treated samples.

These results suggest that *MYC2b* is negatively regulated by ET and *SymCRK*^{A17}. However, the control of *MYC2b* gene expression in the absence of ET and SymCRK^{A17} is not clear. In the previous Chapter IV, I suggest that the expression of *MYC2b* and *SKL* genes is correlated to JA signaling pathway. This suggests that the JA signaling pathway is controlled by SymCRK^{A17} and SKL^{A17}. In addition the expression of *MYC2c* gene is slightly controlled by SymCRK^{A17}via SKL in A17 background.

Relationship between other genes and symbiotic *SymCRK* genes in *M. truncatula* A17

The results presented in fig. 5 show that the *PR1* gene expression is repressed in the *symCRK*^{A17} and *skl* simple mutants. The expression of *QM* gene is induced in the *symCRK*^{A17} and *skl* simple mutants but this expression is eight times more induced in double mutant. However, the expression of the *FS1* gene is slightly induced in *skl* and *dnf5/skl* lines.

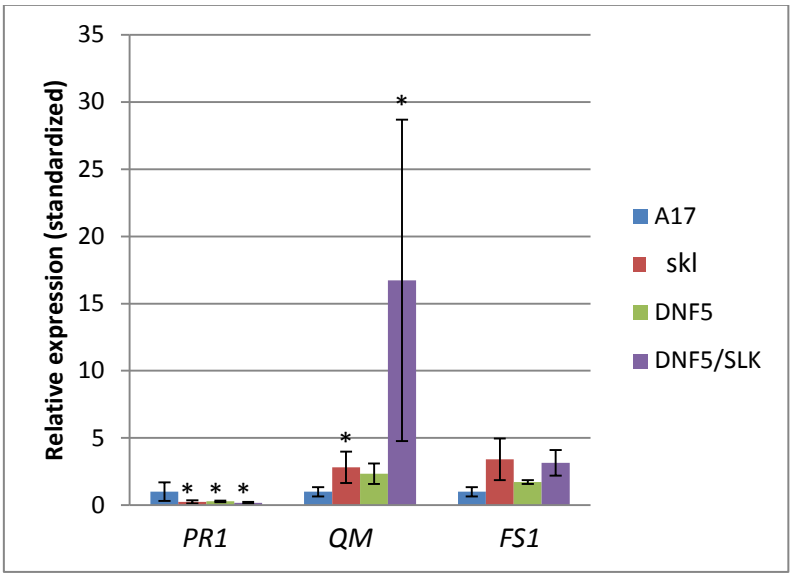

Figure 5. ET and *SymCRK* gene effects on SA-depending gene expression. The expression of SA-related genes was evaluated by RT-qPCR performed on RNAs extracted from A17 wild-type, skl (*skl)*, dnf5 (*symCRK*^{A17}) and double mutant dnf5/skl (*symCRK*^{A17}*/skl*). Nodules were induced *in vitro* by *S. medicae* WSM419 strain and harvested at 21 dpi. Fold change versus wild-type is presented after normalization with an *Actin* gene as an internal control. Error bars, ± SE from three independent experiments with one technical replicate for each experiment. Asterisks indicate significant induction ($P<0.05$) compared to the non-treated samples.

These results suggest that *PR1* gene expression is positively controlled by SymCRK^{A17} and SKL. The expression of *QM* gene is negatively regulated by ET and SymCRK^{A17}. However, the expression of *FS1* is negatively regulated by ET. On the other hand, in Chapter IV, I suggested that the expression of *PR1* gene is repressed by JA and induced by SA and ET. On the other hand, I suggested an induction of the *QM* gene expression by JA and SA. These results indicate that the *QM* induction is due to JA accumulation and ET is antagonist of JA in A17 nodules

Putting these results and data presented in chapters III and IV together, this work indicates that SymCRK^{A17} controls the induction of defense reactions in A17 nodules by repressing the JA signaling pathway which triggers cell death by cysteine protease activation.

Relationship between defense genes and symbiotic *SymCRK* genes in *M. truncatula* R108

The results presented fig.6 show that the *PR10* and *PR10*-like defense genes were induced in s*ymCRK*^{R108} mutant whereas *Chitinase* expression was not affected in s*ymCRK*^{R108}. Furthermore, the interruption of ethylene biosynthesis by AVG reduces the expression of *PR10* and *PR10*-like. .

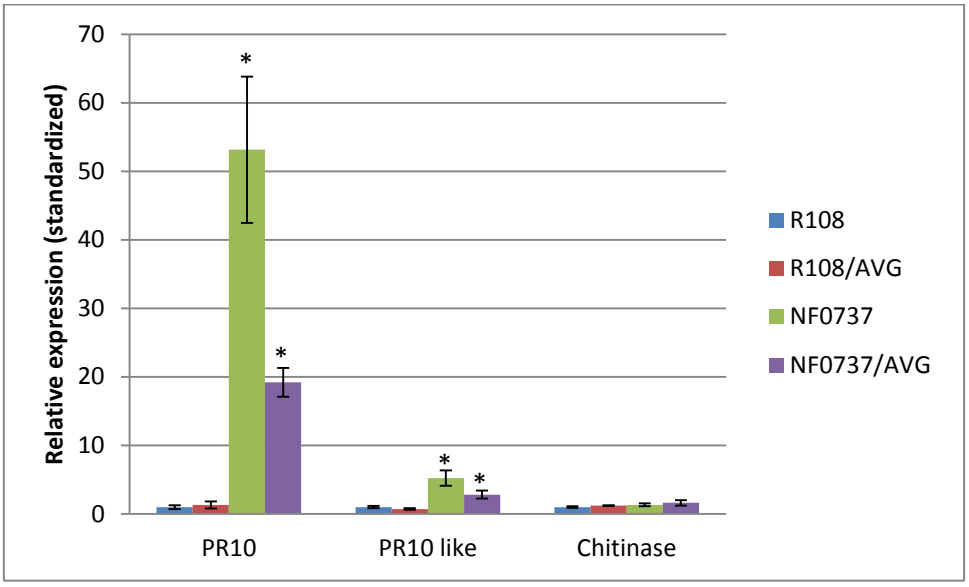

Figure 6. ET effects on defense-related genes expression. The expression of the *PR10, PR10*-Like and *Chitinase* defense genes was evaluated by RT-qPCR performed on RNAs extracted from R108, wild-type and NF0737 (*symCRK*^{R108}) treated or not with AVG. Nodules were induced *in vitro* by *S. medicae* WSM419 strain and harvested at 21 dpi. Fold change versus wild-type is presented after normalization with an *Actin* gene as an internal control. Error bars, ± SE from three independent experiments with one technical replicate for each experiment. Asterisks indicate significant induction ($P<0.05$) compared to the non-treated samples.

The results indicate that the *PR10* and *PR10*-like defense genes expression are controlled by SymCRK^{R108} and ET. In contrast, the expression of *Chitinase* gene is not correlated to SymCRK^{R108} or ET in R108 background nodules. In Chapter IV, the expression of *PR10* gene is strongly correlated to SA signaling pathway in R108 roots treated with SA.

Relationship between JA-related genes and symbiotic *SymCRK* genes in *M. truncatula* R108

The results presented fig.7 show that the expression of *MYC2a*, *MYC2b* and *VSP* are not induced in *symCRK*^{R108} mutant nodules treated or not with AVG. However, a slight induction of MYC2c gene expression was observed in *symCRK*^{R108} mutant.

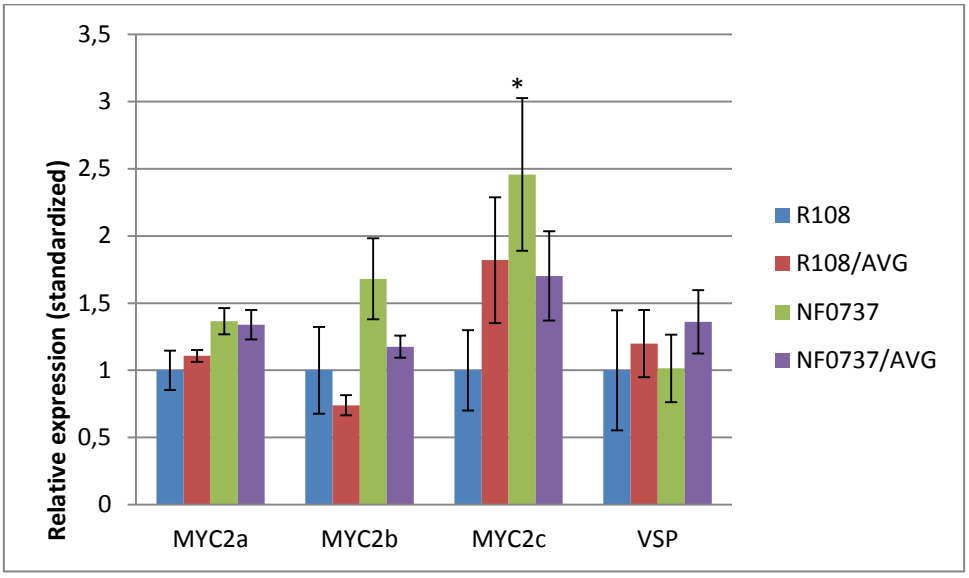

Figure 7. ET and *SymCRK* effects on JA-depending gene expression. The expression of JA-related genes was evaluated by RT-qPCR performed on RNAs extracted from R108 wild-type and NF0737 (*symCRK*^{R108}) mutant treated or not with AVG. Nodules were induced *in vitro* by *S. medicae* WSM419 strain and harvested at 21 dpi. Fold change versus wild-type is presented after normalization with an *Actin* gene as an internal control. Error bars, ± SE from three independent experiments with one technical replicate for each experiment. Asterisks indicate significant induction (P<0.05) compared to the non-treated samples.

These results indicate that *MYC2*b is negatively regulated by SymCRK under the control of ethylene and indicate that *MYC2*c is regulated negatively by SymCRK and ethylene. In Chapter IV, the expression of MYC2b and MYC2c are correlated to JA signaling treatment. According to Chapter IV, the *MYC2b* and *MYC2c* gene expression is similar to those obtained in R108 roots treated with SA.

.

Relationship between other genes and symbiotic *SymCRK* genes in *M. truncatula* R108

The results presented in fig.8 show that the expression of the *PR1* gene is induced in *symCRK*^{R108} mutant and downregulated after treatment with AVG. The expression of the *QM* gene is induced in *symCRK*^{R108} mutant nodules and this level of induction is not affected by the AVG treatment. However, the *FS1* gene is induced in wild-type nodules treated with AVG, and strongly induced in *symCRK*^{R108} mutant nodules. The AVG treatment of *symCRK*^{R108} nodules reduced the expression of the *FS1* gene.

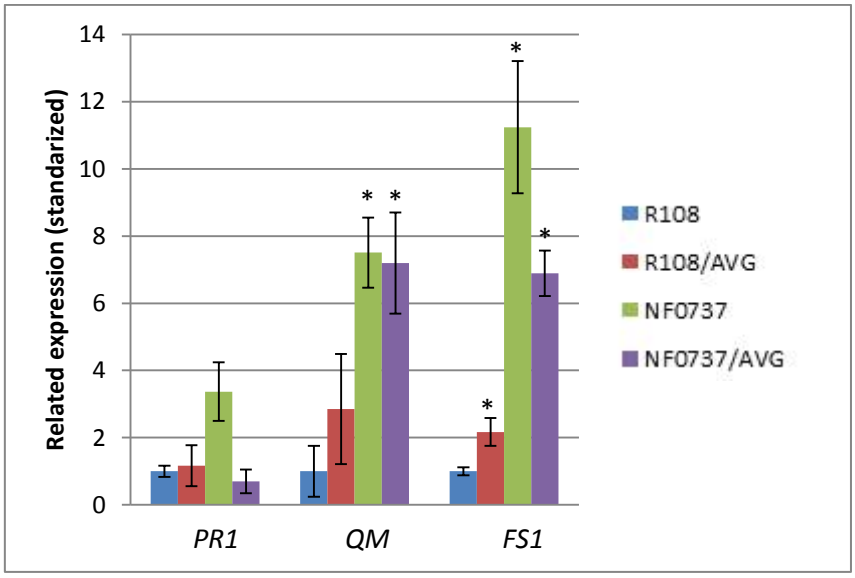

Figure 8. **ET and *SymCRK* effects on SA-depending gene expression**. The expression of SA-related genes was evaluated by RT-qPCR performed on RNAs extracted from R108 wild-type and NF0737 (*symCRK*^{R108}) mutant treated or not with AVG. Nodules were induced *in vitro* by *S. medicae* WSM419 strain and harvested at 21 dpi. Fold change versus wild-type is presented after normalization with an *Actin* gene as an internal control. Error bars, ± SE from three independent experiments with one technical replicate for each experiment. Asterisks indicate significant induction ($P<0.05$) compared to the non-treated samples.

These results suggest that *PR1* gene expression is correlated to ET signaling in agreement with the results of the Chapter IV. The induction of *FS1* expression is partially correlated to ET. According to chapter IV, the salicylic acid treatment induces the expression of *FS1* gene. The expression of the *QM* gene seems independent of ET, and induced by SA treatment as indicated in the previous Chapter IV.

Putting these results and the results presented in Chapter III and IV suggest that SymCRK controls the nodules defense reactions in the R108 background by repressing the ET and SA signaling pathways. Furthermore, SA and ET seem to act in synergy in R108 nodules.

Relationship between ET related genes and symbiotic *DNF2* genes in *M. truncatula* A17

The results presented in fig. 9, shows that the expression of *ACO5*, *EIN3*-3 and *SKL* genes is induced in *dnf2*^{A17} mutant. Nevertheless, the expression of *ASC2*, *ACO5*, *EIN3*-5 genes is induced in the double mutant *dnf2/skl*. In contrast, the expression of *EIN3*-3 and *SKL* genes is downregulated in this double mutant.

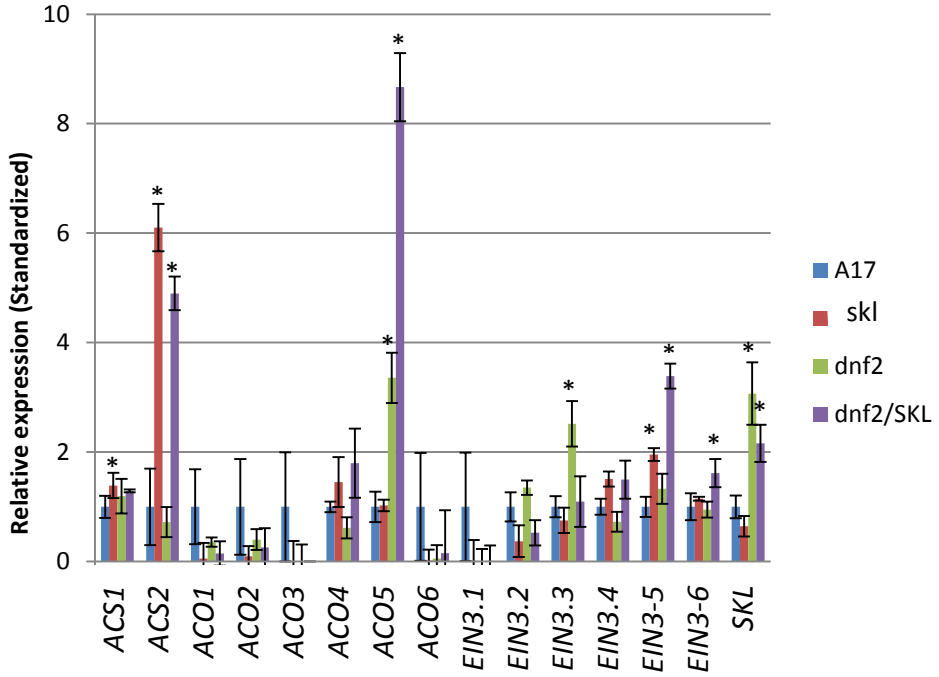

Figure 9. Relative expression of ET-biosynthetic and signaling genes in the simple and double mutants. The expression of ethylene biosynthesis and ethylene signaling pathway genes was evaluated by RT-qPCR performed on RNAs extracted from the A17 wild-type, dnf2 (*dnf2*^{A17}) and skl (*skl*) simple mutants, and the dnf2/skl (*dnf2*^{A17}*/skl*) double mutant. Nodules were induced *in vitro* by inoculation with *S. medicae* WSM419 strain and harvested at 21 dpi. Fold change versus wild-type is presented after normalization with an *Actin* gene as an internal control. Error bars, ± SE from three independent experiments with one technical replicate for each experiment Asterisks indicate significant induction ($P<0.05$) compared to the non-treated samples.

These results indicate that DNF2 regulates negatively the expression of *ACO5*, *EIN3*-3 gene *SKL* genes, while, the expression of *ACO5* is positively controlled by ET. In contrast *EIN3*-3 is negatively controlled by ET. The *ACS2* and *EIN3*-5 genes are negatively controlled by ET and DNF2. This suggests that defense reactions in *dnf2*^{A17} nodules are independent of the ET signaling pathway.

Relationship between defense genes and symbiotic *DNF2* genes in *M. truncatula* A17

The results presented in fig.10 indicate that the expression of the *PR10* gene is induced in the *skl* mutant. This induction is more than two times stronger in the *dnf2*^{A17} mutant and downregulated in the double mutant *dnf2/skl* nodules. The expression of *PR10*-like is induced in *dnf2*^{A17} mutant and repressed in *skl* and *dnf2/skl* double mutant. Furthermore, the expression of *Chitinase* gene is repressed in the double mutant dnf2/skl.

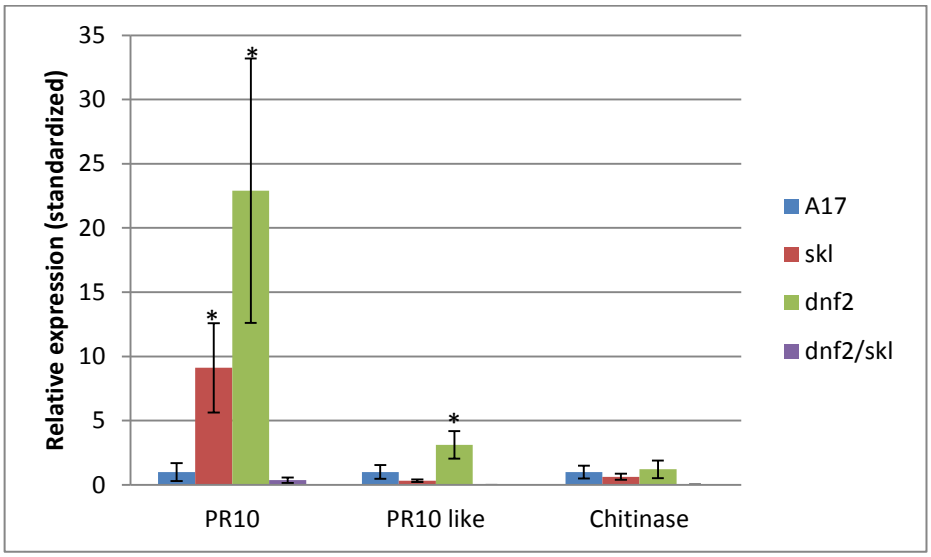

Figure 10. ET effects on defense-related genes expression. The expression of the *PR10*, *PR10*-like and *Chitinase* defense genes was evaluated by RT-qPCR performed on RNAs extracted from A17 wild-type, skl (*skl)*, dnf2 (*dnf2*^{A17}), and the double mutant dnf2/skl (*dnf2*^{A17}*/skl*). Nodules were induced *in vitro* by *S. medicae* WSM419 strain and harvested at 21 dpi. Fold change wild-type is presented after normalization with an *Actin* gene as an internal control. Error bars, ± SE from three independent experiments with one technical replicate for each experiment. Asterisks indicate significant induction ($P<0.05$) compared to the non-treated samples.

These results suggest that *PR10* gene expression is negatively controlled by ET and DNF2^{A17}. The repression of the *PR10* gene in nodules from the double mutant line *dnf2/skl* is probably controlled by an unknown pathway in the absence of ET signaling and DNF2^{A17}. *PR10*-like gene expression is repressed in the *skl* mutant and in the double mutant *dnf2/skl*. However, in *dnf2* mutant nodules, the expression of *PR10*-like gene is induced suggesting that this gene is positively controlled by ethylene and negative controlled by DNF2^{A17}.

All together these results indicate that DNF2^{A17} controls defense-related genes independently of ET.

Relationship between JA-related genes and symbiotic *DNF2* genes in *M. truncatula* A17

The results presented in fig.11 show that the expression of *MYC2b* gene is induced in the *skl* mutant nodules and the level of the expression of this gene is doubled in *dnf2* mutant. In nodules from the double mutant *dnf2/skl*, the expression of the *MYC2b* gene is reduced compared to *dnf2* mutant. In addition the expression of *MYC2c* is induced in the *dnf2* mutant and this expression is not affected by the *skl* mutation. The expression of *VSP* gene is not changed in *skl*, *dnf2* and *dnf2//skl* mutants

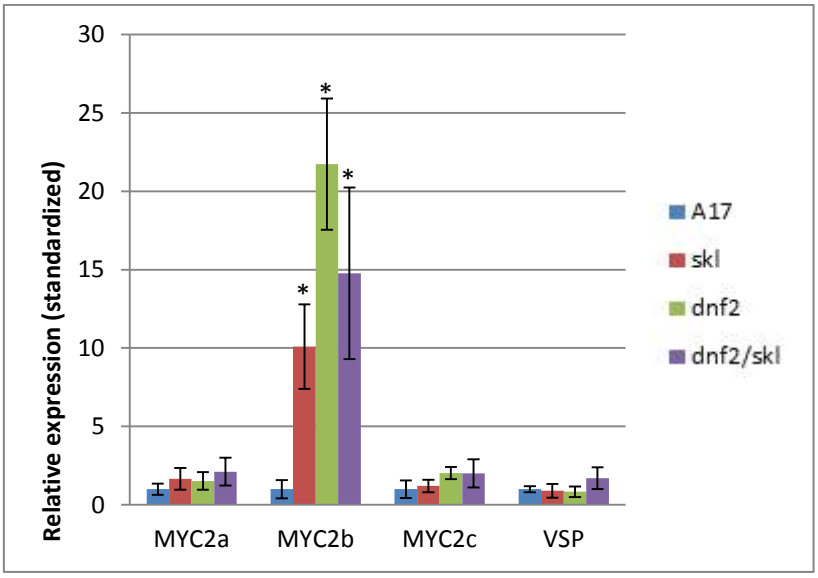

Figure 11. ET and *DNF2* gene effects on JA-depending gene expression. The expression of JA-related genes was evaluated by RT-qPCR performed on RNAs extracted from A17 wild-type, skl (*skl*) and dnf2 ($dnf2^{A17}$) simple mutants and dnf2/skl ($dnf2^{A17}$/*skl*) double mutant. Nodules were induced *in vitro* by *S. medicae* WSM419 strain and harvested at 21 dpi. Fold change wild-type is presented after normalization with an *Actin* gene as an internal control. Error bars, ± SE from three independent experiments with one technical replicate for each experiment. Asterisks indicate significant induction ($P<0.05$) compared to the non-treated samples.

The expression of *MYC2b* gene is negatively regulated by ET and $DNF2^{A17}$. In contrast the expression of *MYC2c* gene expression is negatively controlled by $DNF2^{A17}$ independently of ET. Putting together these results and the results presented in the Chapter IV, it indicates that $DNF2^{A17}$ controls the induction of defense reactions in nodules by controlling the expression of the JA pathway with the ET participation.

Relationship between other genes and symbiotic *DNF2* genes in *M. truncatula* A17

The results presented in fig.12 show that *PR1* gene expression is repressed in *skl*, *dnf2* and *dnf2/skl* mutants. However the expression of *QM* and *FS1* genes are induced in all tested mutants.

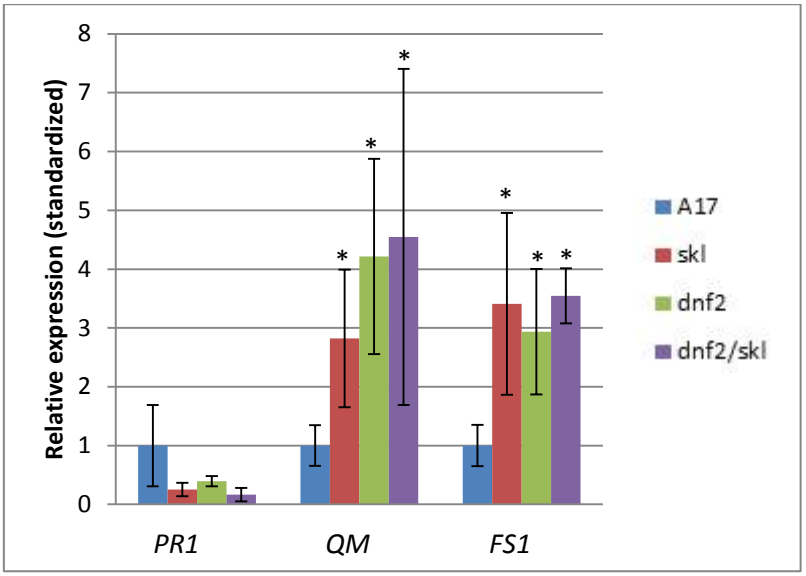

Figure 12. ET and *DNF2* gene effects on SA-depending gene expression. The expression of SA-related genes was evaluated by RT-qPCR performed on RNAs extracted A17 wild-type, skl (*skl*) and dnf2 (*dnf2*^{A17}) simple mutants and dnf2/skl (*dnf2*^{A17}*/skl*) double mutant. Nodules were induced *in vitro* by *S. medicae* WSM419 strain and harvested at 21 dpi. Error bars, ± SE from three independent experiments with one technical replicate for each experiment. Asterisks indicate significant induction ($P<0.05$) compared to the non-treated samples.

The results presented in Chapters III and IV, and these results suggest that DNF2 blocks the induction of the nodule defense reactions by controlling JA and SA signaling pathways.

Relationship between defense genes and symbiotic *DNF2* genes in *M. truncatula* R108

Results presented in fig.13 show a strong induction of *PR10* and *PR10*-like genes, a slight induction of *Chitinase* in *dnf2*^{R108} nodules, and the ethylene biosynthesis inhibitor does not affect the *PR10* induction.

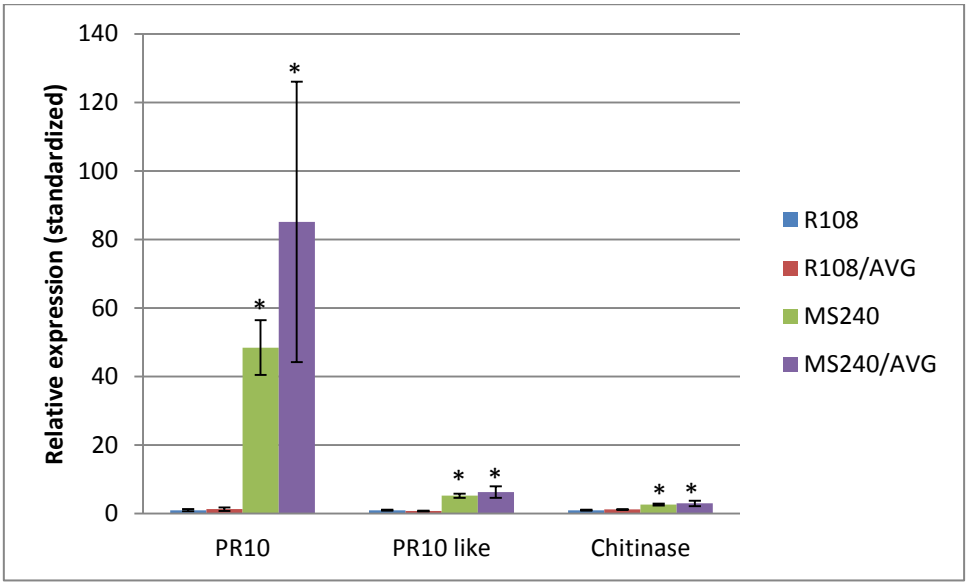

Figure 13. ET effects on defense-related gene expression. The expression of the *PR10, PR10*-Like and *Chitinase* defense genes was evaluated by RT-qPCR performed on RNAs extracted from R108 wild-type and MS240 (*dnf2*^{R108}) treated or not with AVG. Nodules were induced *in vitro* by *S. medicae* WSM419 strain and harvested at 21 dpi. Fold change versus wild-type is presented after normalization with an *Actin* gene as an internal control. Error bars, ± SE from three independent experiments with one technical replicate for each experiment. Asterisks indicate significant induction ($P<0.05$) compared to the non-treated samples.

These results indicate that the expression of *PR10*, *PR10-like* and *Chitinase* are negatively controlled by DNF2^{R108} independently of ET.

Relationship between JA-related genes and symbiotic genes *DNF2* in *M. truncatula* R108

The results presented fig.14 show that the *MYC2b* gene expression is induced in *dnf2*^{R108} nodules treated with AVG. However, the *MYC2c* is induced in wild-type nodules treated with AVG and in *dnf2*^{R108} nodules treated or not with the ethylene inhibitor. Furthermore, the VSP gene is induced in *dnf2*^{R108} nodules and its expression is doubled with the AVG treatment.

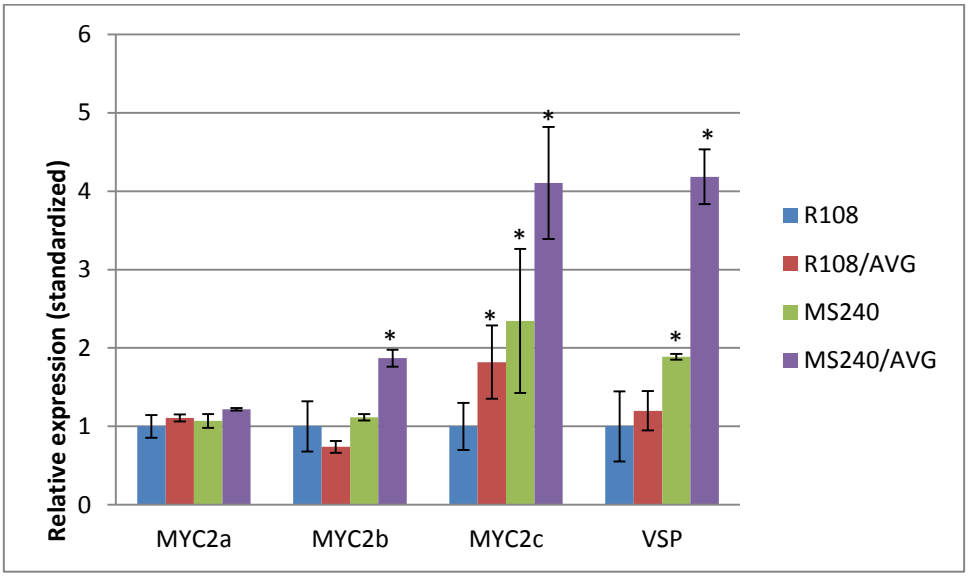

Figure 14. ET and *DNF2* gene effects on JA-depending gene expression. The expression of JA-related genes was evaluated by RT-qPCR performed on RNAs extracted from R108 wild-type and MS240 (*dnf2*^{R108}) mutant treated or not with AVG. Nodules were induced *in vitro* by *S. medicae* WSM419 strain and harvested at 21 dpi. Fold change versus wild-type is presented after normalization with an *Actin* gene as an internal control. Error bars, ± SE from three independent experiments with one technical replicate for each experiment. Asterisks indicate significant induction ($P<0.05$) compared to the non-treated samples.

These results suggest that the JA-related genes *MYC2c* and *VSP* are induced in *dnf2*^{R108} nodules and their expression are repressed by ET signaling pathway. This suggests that JA and ET have antagonist effects in nodules and participate in the induction of defense reactions.

Relationship between SA genes and symbiotic *DNF2* genes in *M. truncatula* R108

The results presented in fig.15 show a strong induction of *PR1* and *QM* and *FS1* genes in *dnf2*^{R108} nodules. However, the expression of *PR1* and *QM* gene are affected by the inhibition of ET signaling pathway contrary to *FS1* gene which is not affected by ET inhibition treatment. The expression of *PR1* gene is repressed by AVG. In contrast the expression of *QM* gene is more induced when the ethylene signaling pathway is disrupted.

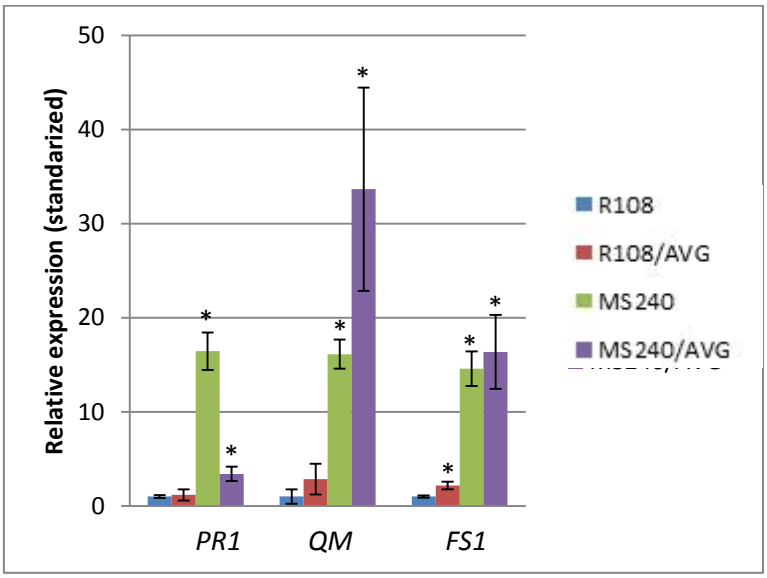

Figure 15. ET and *DNF2* gene effects on SA-depending gene expression. The expression of SA-related genes was evaluated by RT-qPCR performed on RNAs extracted from R108 wild-type and MS240 (*dnf2*^{R108}) mutant treated or not with AVG. Nodules were induced *in vitro* by *S. medicae* WSM419 strain and harvested at 21 dpi. Fold change versus wild-type is presented after normalization with an *Actin* gene as an internal control. Error bars, ± SE from three independent experiments with one technical replicate for each experiment. Asterisks indicate significant induction ($P<0.05$) compared to the non-treated samples.

Putting all these results together and according to the results presented in Chapter III and IV, it suggests that SA, with the participation of ET, plays an important role in controlling nodules defense reactions in R108 background.

Discussion

This study indicates that there is a strong relation between the symbiotic genes and defense hormones (ET, JA and SA) in *M. truncatula* A17 nodules. The control of the defense hormones by the symbiotic genes induced two different immune responses: defense reactions and senescence. In *M. truncatula* A17 background, the lack of control of the JA signaling pathway by the symbiotic symCRK^{A17} protein leads to induction of senescence. The induction of this senescence process results in the formation of white nodules and the induction of the expression of cysteine protease. Basso et Veneault-Fourrey (2020) reported that the activation of JA pathway by silencing the *JAZ1* gene in *Astragalus sinicus* nodules leads to stopping the bacteroids differenciation and the legumoglobin expression resulting in the formation of white non fixing nodules, which is similar to the phenotype observed in nodules showing activation of the JA pathway in this study (Basso et Veneault-Fourrey, 2020). In addition, the obtained result is in agreement with the results of Zhuo *et al.* (2019) and Zhang *et al.* (2018), showing that the JA treatment leads to the activation of the *MYC2* genes and the induction of leaf senescence in *A. thaliana* (Zhuo *et al.*, 2019 ; Zhang *et al.* 2018). In addition, JA up-regulates the expression of several lipoxygenase genes involved in nodule senescence (Guinel, 2015).

SA with the participation of JA can also induce defense reactions in *M. truncatula* A17 nodules. The *DNF2^{A17}* loss of function removes the control over SA and JA signaling and results in the formation of white nodules accumulating phenolic compounds and inducing defense genes expression. However, this induction of defense reactions is less strong as compared to the defense reactions observed in the *M. truncatula* R108 background. The synergic interaction between SA and JA was previously described. For example Yang *et al.*, (2011) and Campos-Vargas and Saltveit, (2002) reported that SA and JA act synergistically on the PAL-induced phenolic metabolism in lettuce and pea plants.

In addition, this study reveals that in *M. truncatula* R108 nodules only defense reactions are induced and this could be explained by the repression of the JA signaling pathway responsible for senescence activation by ET. This hypothesis is supported by Breakspear *et al.* (2014) work demonstrating that in the *Mtskl* mutant accumulating ET, the JA biosynthesis genes and the JA receptor JAZ2 are repressed by the bacterial inoculation. The symbiotic genes in this background control ET- and SA-mediated defense responses. The mutation of the DNF2^{R108} protein releases the ET and SA signaling pathway which activate defense genes expression and accumulation of phenolic compounds in nodules. The mutation of the

SymCRK^{R108} protein results in the same phenotype as the one observed in *dnf2*^{R108} mutant. However, in *symCRK*^{R108} nodules the necrosis surface is larger than the necrosis surface observed in *dnf2*^{R108} nodules (data not shown). This synergic interaction between SA and ET in plant defense against pathogens was widely documented in the literature (Lawton et al., 1994; Pieterse *et al.*, 1998).

So, the defense system in *M. truncatula* A17 nodules is mediated by JA and SA hormones instead of SA and ET hormones which mediated defense system in *M. truncatula* R108 nodules. On the other hand, it seems that JA orients the immune response to use senescence and SA and ET orients defense system to use defense reactions to fight against the symbiotic cells colonization.

This difference can be explained by the natural physiological differences between the two backgrounds or is due to the fact that *M. truncatula* R108 used in this study is a mutated line with increased response to auxine and cytokinin hormones. In fact, the R108 line used in our laboratory is a R108 derivative. It was generated by successive somatic embryogenesis which activates the *MERE1* retrotransposon in R108 genome and this created unkown mutations (Trinh *et al.*, 1998; Rakocevic *et al.*, 2009). To verify the obtained results it will be very interesting if this study is further developed using original 108-1 and A17 wild-type lines with *E. adhereans* T4 strain which can induce nonfunctional nodules in the two genetic backgrounds. Comparison of these genotypes with others Medicago genotypes or other legumes species which are compatible with *E. adhereans* T4 would also allow us to reinforce our observations.

Chapter VI: *Ensifer adhaerens*, a pathogenic and symbiotic partner of *Medicago truncatula*

Ensifer adhaerens, a pathogenic and symbiotic partner of *Medicago truncatula*.

El Hossein Ait Salem[1,2], Gautier Bernal[1,2], Sophie Massot[1,2], Nathalie Rézé[1,2], Antoine Maginier[1,2], Eleonora Rolli[1,2], Maged M. Saad[3], Heribert Hirt[3], Véronique Gruber[1,2], Benjamin Gourion[4] Pascal Ratet[1,2],

[1] Université Paris-Saclay, CNRS, INRAE, Univ Evry, Institute of Plant Sciences Paris-Saclay (IPS2), 91405 Orsay, France.

[2] Université de Paris, CNRS, INRAE, Institute of Plant Sciences Paris-Saclay (IPS2), 91405, Orsay, France.

[3] Center for Desert Agriculture, Division of Biological and Environmental Sciences and Engineering, King Abdullah University of Science and Technology, Thuwal, Saudi Arabia.

[4]LIPM, Université de Toulouse, INRA, CNRS, 31326 Castanet-Tolosan, France

Abstract:

Legume plants can grow without nitrogen fertilizers because they establish symbiosis with Rhizobia. This interaction results in the formation of root nodules in which rhizobia fix atmospheric nitrogen for the benefit of the plant. This interaction is not always successful as non-fixing rhizobia can also elicit nodules and symbiotic organs can host non-rhizobial bacteria. These non-rhizobial nodule endophytes can represent an important part of the nodule inhabitants. The molecular determinants (recognition specificity and immunity) governing the output of these interactions are not fully understood.

From *Medicago truncatula* nodules, we have isolated an atypical bacterium (*Ensifer adhaerens* T4) that behaves as a pathogen or as a nodulating rhizobium on the same plant species. The output of the interaction (death or symbiosis) depends on the plant age. *E. adhaerens* T4 can also co-colonize *M. truncatula* nodules induced by a classical rhizobium. The genome of this strain was sequenced. This bacterium should help understanding the complex interaction between legume plants and symbiotic and pathogenic partners.

Introduction

Legume plants are important for agricultural sustainability because they are rich in proteins even when grown without nitrogen fertilizer input. This high protein content of the legume plants or seeds is the main reason for their wide use in non-industrial countries as they represent the main source of protein for human and animal consumption. Legume plants are also considered as important factors for developing a more sustainable agriculture because they can grow without the addition of expensive and polluting nitrogen fertilizers. This capacity is based on their ability to establish symbiosis with bacteria (Rhizobia). This symbiotic interaction is initiated by specific flavonoids excreted by plant roots and by the production of the Nod factor (NFs) by the bacteria, and results in the formation of a dedicated root organ called the root nodule where rhizobia fix atmospheric nitrogen and thus allow the plant to overcome nitrogen limitation. Nodules represent thus new root organs ensuring optimal conditions for the rhizobia to fix atmospheric nitrogen and to provide plants with ammonia essential for their growth during this mutualistic interaction (Poole *et al.*, 2018). Efficient symbiosis results in nodule symbiotic cells that house spectacular densities of nitrogen fixing bacteria, however despite this high colonization, nodules do not develop defense reactions. The model legume *Medicago truncatula* establishes an efficient symbiosis with *Ensifer medicae* (syn. *Sinorhizobium*).

Ecological studies suggest that rhizobia can behave as cheaters and this behavior may explain the existence of tight genetic controls all along establishment of the symbiotic organ including in the symbiotic cells the chronic infection stage (Berrabah *et al.*, 2018a). Symbiotic cheaters are generally rhizobia or closely related species that fix poorly (or not at all) nitrogen in the nodule and it is known that these situations exist *in natura* (Schumpp et Deakin, 2010; Regus *et al.* 2017). In addition, in fields, other non rhizobial bacteria are present inside nodules (Martinez-Hidalgo *et al.*, 2017). Their roles as endophytes, Plant Growth Promoting Bacteria (PGPB) or parasites, are unknown but it is generally accepted that they are representing a specific microbiome of the nodule (Zgadzaj *et al.* 2015 ; De Meyer *et al.* 2015 ; Leite *et al.* 2016). These examples define a continuum of associations from parasitism to highly beneficial symbioses. In addition these studies indicate that interactions may be more complexes than generally described, involving multiple bacterial partners for the plant (Martinez-Hidalgo *et al.*, 2017)

With the aim to isolate non rhizobial, or cheater bacteria from nodules to study these complex interactions, we have isolated from *M. truncatula* R108 nodules grown in a non-sterile soil collected in a garden lawn different bacteria with nodulating and non nodulating capacities. Amongst them we identified an atypical bacterium that can behave as a pathogen or as a symbiotic-like partner. To our knowledge, bacteria with pathogenic and symbiotic behaviors on the same plant species were never described and are of particular interest since it is generally admitted that mutualistic symbiosis evolved from pathogenic relationships. This bacterium is an *Ensifer adhaerens* (gram-negative *Alphaproteobacteria*) previously described as capable of adhering to and to lyse gram-negative and gram-positive soil bacteria. *E. adhaerens* is not mandatory bactericide, and becomes a bacteria predator only under nutrient limitation conditions (Casida, 1982). *Ensifer adhaerens* belongs to a non-symbiotic rhizobial group (Casida, 1982), is able to induce nodules formation by acquiring *in vitro* symbiotic plasmids but do not fix atmospheric-nitrogen (Pandya *et al.*, 2013; Rogel *et al.*, 2001).

To better understand the interaction between this strain and *M. truncatula*, physiology and genetic approaches were used to study its nodulation capacity, its intracellular accommodation and its pathogenic behavior.

Material and Method

Ensifer adhaerens T4 DNA extraction and sequencing

Bacterial growth and genomic DNA isolate

The *E. adhaerens T4* strain was grown in Luria-Bertani (LB) broth (Lennox L Broth Base, Invitrogen) or on LB agar (Sigma Aldrich, Germany) plates at 28°C. Fresh, pure bacterial cultures were used for total genomic DNA extraction using Sigma's GenElute bacterial genomic DNA kit (Sigma Aldrich, Germany) following the manufacturer's protocol. DNA quality and quantity were assessed by using the NanoDrop 2000 (Thermo Fisher Scientific, USA) and Qubit dsDNA BR assay kit (Thermo Fisher Scientific, USA).

PacBio library preparation and genome sequencing

DNA was size selected to 10 kb using the BluePippin™ Size-Selection System (Sage Science, USA), following the "High-Pass™ DNA Size Selection of ~20kb SMRTbell™ Templates" manual. The SMRTbell™ template library was prepared according to the instructions from Pacific Biosciences's "Procedure & Checklist - 20 kb Template Preparation using BluePippin™ Size-Selection System" guide. The SMRT cells were run at the KAUST Bioscience Core Labs on the PacBio *RSII* (Pacific Biosciences, USA) sequencing platform using P6-C4 chemistry.

Genome assembly and annotation

PacBio reads were assembled into 6 contigs by using the *de novo* Hierarchical Genome Assembly Process (HGAP.2) algorithm with default parameters. Genome annotation was conducted by using the in-house Automatic Annotation of Microbial Genomes (AAMG) pipeline (Alam *et al.*, 2013)

Plasmids extraction and electroporation

Plasmids constructively expressing red fluorescent protein (pDG71 heamA::RFP) and green fluorescent protein (pDG71 heamA::GFP) were extracted from *E. coli* (Gage. 2002) using the miniprep kit NucleoSpin® Plasmid according to the manufacturer's instructions (MACHERY-NAGEL, https://www.mn-net.com). Plasmids (pDG71 heamA::RFP) and (pDG71 heamA::GFP) were electroporated into *S. medicae* WSM419 and plasmid pDG71 heamA::RFP in E. *adhaerens*.

The E. *adhaerens* T4 strain was also tagged on the chromosome using the miniTn7 (Gm) P:rrnB P1GFP-A construct described by Lambertsen *et al.* (2004). The GFP tagged stain is called *E. adhaerens* T4::GFP in the rest of the manuscript.

Bacterial strain and inoculation

Ensifer adhaerens T4, *Sinorhizobium medicae* strain WSM419 (Howieson & Ewing, 1986), *Sinorhizobium medicae* Rm*1021* (Burton, 1984), *Xanthomonas alfalfae* subsp *alfalfae* (Riker *et al.*, 1935; Esnault *et al.*, 1993) and *Xanthomona campestris* subsp *campestris* (Assis *et al.*, 1996), were cultivated at 30°C in liquid yeast extract broth (YEB) medium (Krall *et al.*, 2002). *S. medicae* strain WSM419 was cultured in presence of 12.5 µg.mL^{-1} chloramphenicol. The bacterial inoculums were prepared by washing twice a fresh overnight liquid culture with sterile distilled water and the bacterial suspension was adjusted to optical density of 1.5 at OD600 nm. *E. coli* strains containing the pDG71 plasmids were cultivated on liquid YEB medium with 5µg.mL^{-1} tetracyclin at 37 °C for 24 h. Next, the seedlings were inoculated by imbibing them in bacterial suspension for 1 hour in sterile square plates before transfer to BNM plates.

Plants materials an growth conditions

Five *Medicago truncatula genotypes* (*M. t* R108, *M. t* A17, *M. t Parragio*, *M. t* F83, *M. t Gore*) and *M. t* A17 (promEnod11::GUS), five *Medicago sativa* genotypes (*M. s* WL903, *M.s* G968, *M. s Salina*, *M. s Oleron* and *M. s Super* GRI8), one *M. polymorpha Ciliaris*, three Trifolium (*T. pratense pratense*, *T. repens White Clover* and *T. subterraneum*) and *Vicia hirsuta* were surface sterilized by sulfuric acid for 3 minutes, washed three times in sterile water then re-sterilized in sodium hypochlorite for 30 min and then washed three times in sterile water. Seeds were then incubated 1 hour in sterile water. The sterilized seeds were transferred on 50mL water agarose (1%) plates and vernalized for at least 48 h at 4° C in dark. Seeds were then germinated by incubating them at 24°C for 36 h.

The seedlings were transferred onto square plates filled with buffered nodulation medium (BNM) solidified by bacto-agar and inoculated with 1mL of bacterial suspension and incubated in growth chamber under long day condition (16h light: 8h dark cycle at 24°C) for 21 days.

GUS staining

One week inoculated *Medicago truncatula* A17 and *M. truncatula* A17 (promEnod11::GUS) roots inoculated with *S. medicae* WSM419, *Agrobacterium rhizogenes* A4TC24 and *Ensifer adhaerens* T4, were prefixed in cold acetone 90% during 1h at -20°C. Plants were rinsed twice with phosphate buffer (50mM) vacuum infiltrated 30min (≈500mm Hg) in freshly prepared X-gluc staining buffer [phosphate buffer pH7.2 (50mM), potassium ferri-cyanide (1mM), potassium ferro-cyanide (1mM), sodium dodecyl sulfate (SDS) 0.1%, EDTA (1mM), 5-bromo-4-chloro-3-indolyl-beta-D-glucuronic acid (X-gluc)] containing cyclohexylammonium (CHA) salt (1.25mM) and plants were incubated overnight at 37°C in the same X-gluc staining buffer. The stained samples were rinsed twice with phosphate buffer (50mM) and imaged with a stereomicroscopy Stemi 305 (ZEISS).

LIVE/DEAD staining

M. truncatula R108 seedlings were co-inoculated with S. *medicae* WSM419 and *E. adhaerens* T4, *S. medicae* WSM419Δ*NodABC* and *E. adhaerens* T4 or *S. medicae* WSM419Δ*NifH* and *E. adhaerens* T4 on BNM medium square plates. The induced nodules were collected at 21 dpi separately and subjected to a Live/Dead staining. The nodule preparation, section, staining and observation were performed as previously described in Haag *et al.*, (2011) and Bourcy *et al.*, (2013)**.**

Acetylene reduction assay (ARA)

Measurement of the fixation efficiency of nodules was done using the ARA protocol modified from Koch & Evans (1966). Whole nodulated plants at 21 dpi were placed individually into 20 mL glass vials sealed with rubber septa. 500 µL of acetylene was injected into each vial and incubated for 2 hours in growth chamber. The vials were moved to gas chromatography machine (GC) (7820A, Agilent) to measure produced ethylene by injecting 200 µL of gas from the incubated vial. The amount of ethylene produced was calculated following this calculation:

$$[C2H4] = \frac{Pic\ area\ \times 99}{incubation\ time\ \times 495} \times 60$$

[C_2H_4]: nmol C_2H_4 .h^{-1}.$plant^{-1}$. Three biological repetitions were used in this experiment.

Pic area: $pA.s^{-1}$

99 : gas volume for an entire vial (1/99 of vial was injected in GC)

Incubation time: min

495: slope of the relation between pic area values and C_2H_4 concentration values.

60: min.

Comparison between *E. adhaerens* T4 and **Pathogens**

M. truncatula R108 and A17 wild-type seedlings were inoculated with *E. adhaerens* T4, *S. medicae* WSM419, *Xanthomonas alfalfae* subsp *alfalfae* or *Xanthomona campestris* subsp *campestris* separately. The plants (16 per test) were cultivated in square plates containing BNM medium in growth chamber under long day condition (16h light: 8h dark cycle at 24°C) for 21 days. Image of the plants were taken by Panasonic Lumix DMC-FZ200 camera.

RNA extraction and RT-qPCR

Nodules induced by *E. adhaerens* T4 and *S. medicae* WSM419 were harvested at 21 dpi and frozen in presence of one bead (3 mm of diameter) and 2 beads (5 mm of diameter). Samples were crushed in a 1.5 mL falcon tube by vortexing. At 4°C, the material was re-suspended in 500 µL cold TRIzol reagent (ref# 15596026, AMBION) and incubated for 5 min. 100 µL cold chloroform was added to the mix and incubated for 10 min, the mix was centrifuged 5 min at 16000g and up to 500 µL of the aqueous phase was collected. RNAs were precipitated overnight at -20°C with 250 µL of isopropanol and 100 µL of sodium acetate (3 M) pH5.2 and collected after a centrifugation of 60 min at 16000g and washed with 1 mL of ethanol 70 % and centrifuged two times. The obtained RNAs were re-suspended in RNase-free water.

The reverse transcription of the obtained RNAs was performed using SuperScript™ II Reverse Transcriptase kit (ref. 18064-022, Invitrogen). In a 200 µL micro-centrifuge tube, 1 µL of oligo $(dT)_{18}$ primer (500ng/µL) (ref. #SO132, Thermoscientific), 1 µl of dNTPs (10 mM), 1µg of DNA-free RNA and sterile RNase-free water were added in a 13µL final

volume. The mix was heated 5 min at 65 °C, quickly chilled on ice and briefly centrifuged. 4µL of 5X First-Strand Buffer [(Tris-HCl pH8.3 (250 mM), KCl (375 mM), $MgCl_2$ (15 mM)], 2µL of dithiothreitol (0,1 M) were added to the previous mix. The mix was gently homogenized and incubated 2 min at 42°C. Then, 1 µL of SuperScript™ II Reverse Transcriptase (200 units) was added, the 20µL finale mix was gently homogenized and incubated 50 min at 42°C for the reaction. The reaction was stopped by inactivating the enzyme during 15 min at 70°C. The obtained cDNA was diluted 1/20 with DNAse-free water.

The Relative qPCR were performed on DNA-free cDNA using 2X LightCycler 480 SYBR Green I Master (ref. 04 887 352 001, Roche), 2 µL of each primers (2.5 µM) and 1µL of cDNA, in a final volume of 10 µL. qPCR were launched on a LightCycler 480 II (Roche) The SYBR Green fluorescence was detected between 465 and 510 nm. Cycle threshold and primer specificities were performed with the LightCycler 480 software release 1.5.0 SP4. Primer efficiencies were calculated with LinReg PCR: Analysis of Real-Time PCR Data, version 11.1. *Actin* (Medtr2g008050) was used as reference in relative qPCR experiments.

Results

Ensifer adhaerens T4 isolation and identification

Medicago truncatula R108 plants were grown in 1,5 liter pots containing a mixture of backyard soil (50 ml) and sterile sand-perlite mixture (33%/66%) in a growth chamber under long-day conditions (16h light: 8h dark cycle) at 24°C, 50% humidity, watered with water and nitrogen-free nutrient solution alternately twice a week. The nodulated roots (30 days post germination) were gently washed under running tap water to remove adhering soil particles, and then transferred into 50 ml tubes where they were sterilized with sodium hypochlorite (6° Cl) for 5 min. Under sterile conditions, the nodulated roots were washed three times with sterile distilled water and then the nodules were collected using sterile forceps and surgical blades in 1.5 ml Eppendorf tubes containing 200µL yeast extract broth (YEB) medium. Using sterile sticks the nodules were crushed in the bottom of the tube and the suspension was plated on solid YEM medium and incubated 48 hours at 30°C. The bacterial colonies were purified according to their appearance (color, shape, brilliance and presence of exopolysaccharides) or for resistance to chloramphenicol and gentamycin and phenotypically compared to *E. medicae* WSM419 a symbiotic partner of *M. truncatula*. 19 clones with phenotypes different from WSM419 were then tested individually for their symbiotic capacity. To facilitate inoculation, bacterial cultures of the different clones were inoculated on germinating seedlings (1 cm long root) in liquid cultures for 1 hour and the seedlings were then placed on BNM plates. When doing this with rhizobia, the plants develop normally and root nodules appear 1 week to 10 days post-inoculation. Following this inoculation procedure, 5 clones could form nodules and were considered as rhizobia. For ten clones plants grew but never develop nodules suggesting that they are non-rhizobia or putative endophytes. Surprisingly, for three clones the seedlings stop to grow few days post-inoculation and die after a week. We then concluded that these bacteria were pathogen for *M. truncatula* R108. However in other experiments using inoculation on 48h old seedlings the plants develop normally and nonfunctional fix- nodules were formed.

PCR fragments of the 16S ribosomal RNA were sequenced from 8 clones including three pathogens, three putatitive endophytes and two putative rhizobia. These sequences indicate that the symbiotically efficient bacteria are *S. medicae* strains, the three putative endophytes Microbacterium bacteria and the three putative pathogens *Ensifer adhaerens* strain. The Gyrase and RPO genes partial sequences from these three strains indicated that they are probably three times the same *E. adhaerens* strain. *E. adhaerens* was first described

as a soil bacteria predator of other bacteria and is closely related to *E. medicae*, one symbiont of *M. truncatula*.

Ensifer adhaerens T4 molecular characterization

The literature and database search indicates that two *E. adhaerens* genomes were already fully sequenced but they contain no symbiotic genes. We thus sequenced the whole genome of the *Ensifer adhaerens* T4 strain isolated from *M. truncatula* nodules using the PacBio technology. The genome sequence of the *E. adhaerens* T4 strain was assembled and this shows (Table 1) that it is composed of one large chromosome (5.975 Mb) and 5 plasmids. The total genome size is 8.451824 Mb, around 60% GC and codes for 8142 ORFs. There are also 62 tRNAs and 15 rRNAs genes in this strain. The largest plasmid is 1 Mb and codes for 3 rRNAs and 3 tRNAs genes. Plasmid PLS2 also codes for 1 tRNA gene. The smallest plasmid is 0.18 Mb large.

The T4 genome is up to 1 Mb larger than the genomes of the two previously sequenced *E. adhaerens* strains OV14 (7.709009 Mp) and Casida A (7.267502 Mb). It is also larger than the *E. medicae* WSM419 genome (6.817584 Mb) and *Sinorhizobium meliloti* Rm1021 genome (5.176694 Mb).

Table 1. *E. adhaerens* genome characteristics.

Replicons	Size (bp)	GC%	rRNA	tRNA	ORF
Chr1	5975192	61.62	12	58	5710
Pls1	1003748	59.94	3	3	924
Pls2	799153	58.85	0	1	854
Pls3	295592	58.58	0		333
Pls4	196679	57.99	0		146
Pls5	181460	58.13	0		175
Total	8451824		15	62	8142

Because this strain is able to induce nodule formation on *M. truncatula*, we searched its genome for symbiotic genes. We found one locus on plasmid 3 coding for *Nod* genes but *Nif* genes are absent. The 15kb sequence containing the *Nod* genes is highly homologous (99%) to the *E. medicae* Nod genes and might have been acquired by horizontal gene transfer. However the homology to *E. medicae* is restricted to this Nod gene locus and is surrounded by unrelated sequences. This *Nod* region contains the *NodD*, *NodA*, *NodB*, *NodC*, NodI, *NodJ*,

NodQ, CysD, HsnC, HsnB, HsnA and *nodH* genes. These 12 genes are probably sufficient for the synthesis of a Nod factor specific for the recognition by Medicago plants (see below).

Ensifer adhaerens T4 phenotypic characterization

E. adhaerens T4 behaves as a Medicago pathogen

To confirm the pathogenic phenotype of *E. adhaerens* T4, we compared it to known pathogens. For this, 1 day post germination seedlings of *M. truncatula* A17 and R108 were inoculated by incubating them for 1 hour in 50mL *E. adhaerens* T4, *Sinorhizobium medicae* WSM419, *Xanthomonas alfalfae* subsp *alfalfae* (*Xaa*) or *Xanthomona campestris* subsp *campestris* (*Xcc*) cultures (OD_{600} = 0,1) and then seedlings were transferred on BNM plates. At 21 dpi, 83% of *M. truncatula* A17 seedlings were killed by *E. adhaerens* T4 and 17% of seedlings were diseased. For *M. truncatula* R108 66% of seedling were killed, 17% show disease symtoms and 17% seedlings were healthy. By contrast, 100% of the seedlings inoculated with *S. medicae* WSM419 staid healthy. Following infection by *Xaa* 85% of *M. truncatula* A17 seedling were dead and 14% show disease symptoms. Following *Xaa* infection *M. truncatula* R108 all seedlings show disease symptoms. Following *Xcc* infection *M. truncatula* A17 cotyledons seem to be diseased. In contrast, *M. truncatula* R108 seems to be resistant to *Xcc* (fig.1).

Figure 1. *E. adhaerens* T4 behaves as a pathogen. The pathogen effect of *E. adhaerens* T4 was evaluated by comparing it with the known legumes pathogens *Xanthomonas alfalfae pv. alfalfae (Xaa)* and *Xanthomonas campestris pv. Campestris (Xcc)*. *Medicago truncatula* A17 and R108 seedlings were inoculated in vitro with *S. medicae* WSM419, *E. adhaerens T4*, *Xaa* and *Xcc*. The plants were observed at 21 dpi.

These results indicate that, *M. truncatula* A17 is more sensitive to the pathogens *E. adhaerens* T4 and *Xanthomonas alfalfa* then *M. truncatula* R108. Moreover, *E. adhaerens* T4 and *Xaa* seem to have a similar pathogenic effect on *M. truncatula* A17, but in *M. truncatula* R108 *E. adhaerens* T4 seems more virulent then *Xaa.* Finally, *Xcc* has a slight pathogen effect in *M. truncatula* A17 but it is unable to induce disease in *M. truncatula* R108.

Symbiotic phenotype

***E. adhaerens* T4 produces Nod factors and induces root-nodules formation**

To confirm Nod factors production and excretion by *E. adhaerens* T4, forty-eight *M. truncatula* A17 (promEnod11::GUS) seedlings were inoculated three days post germination with either *S. medicae* WSM419, *A. rhizogenes* A4TC24, *E. adhaerens* T4 or not inoculated (12 plants per condition). Plantlets were GUS-stained two days post-inoculation and observed using the stereomicroscope Stemi 305 (ZEISS) (fig.2). No nodules primordia or GUS staining were observed in the negative control (no inoculation) or when inoculated with *A. rhizogenes* strain, unable to produce Nod factors. In contrast, seedlings inoculated with *S. medicae* WSM419 or with *E. adhaerens* T4 express strongly patches of GUS activity associated to nodules primordia formation.

These results indicate that the *A. rhizogenes* A4TC24 strain that is unable to produce Nod factors and cannot induce nodule formation on *M. truncatula*, is also unable to activate the Nod factor responsive GUS transgene. *S. medicae* WSM419 strain is able to induce nodules in *M. truncatula* roots because it produces NFs recognized by *M. truncatula* Nod factors receptors (MtNFP) and consequently activate the *Enod11::GUS* fusion. Similarly, *E. adhaerens* T4 is able to induce nodules formation in *M. truncatula* roots and to activate the *Enod11::GUS* fusion. This confirms that *E. adhaerens* T4 produces NFs and that they are recognized by *M. truncatula.*

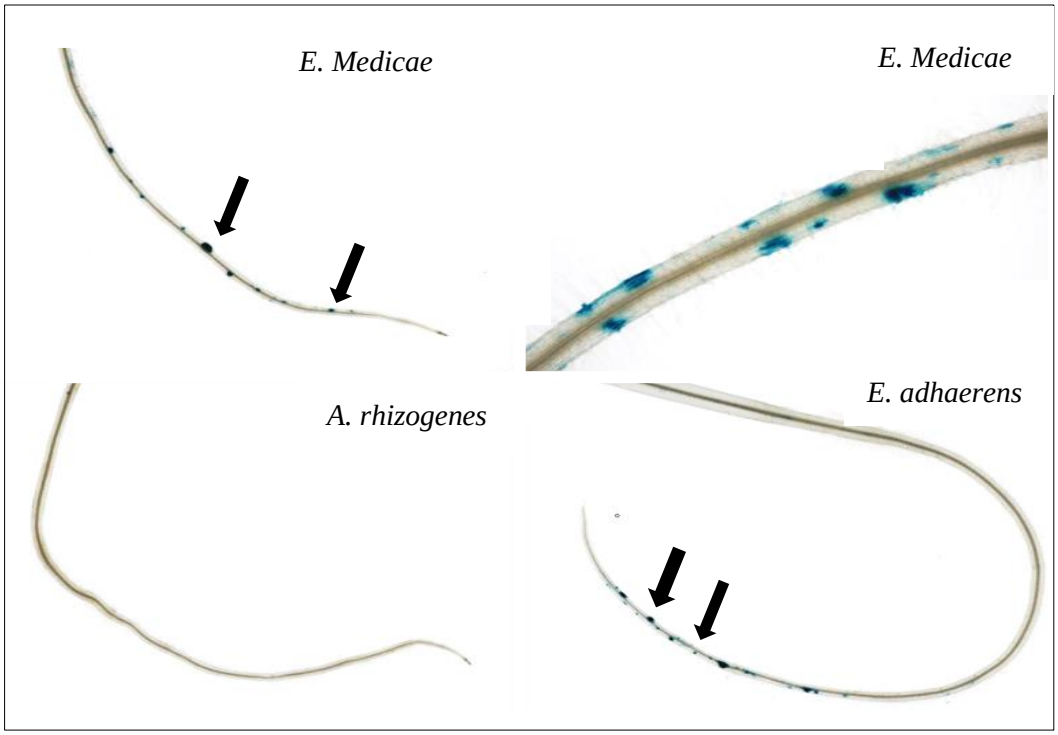

Figure 2. *M. truncatula* seedlings inoculated by *A. rhizogenes* A4TC24, *S. medicae* WSM419 and and *E. adhaerens* T4. The activation of the *promEnod11::GUS* construct reflecting the perception of the Nod factors by *M. truncatula* A17 was evaluated by observing GUS stained 2 dpi in roots inoculated with *S. medicae* WSM419, *Agrobacterium rhizogenes* A4TC24 or *Ensifer adhaerens* T4. The nodule primordia are indicated by black arrows. The pictures were taken using a stereomicroscope Stemi 305 (ZEISS).

Ensifer adhaerens T4 induces nodules formation and colonizes symbiotic cells

To investigate whether *E. adhaerens* T4 not only induces nodules formation but also colonizes symbiotic cells, three days old *M. truncatula* seedlings were inoculated *in vitro* with the labelled stains *S. medicae* WSM419 (pDG71 heamA::RFP), and *E. adhaerens* T4::GFP (P1GFP-A), or co-inoculated with the two strains at the same time. The inoculated plants were observed at 21 dpi. The plants inoculated with *S. medicae* WSM419 present about 10 functional pink nodules per plant (fig.3b). In contrast, plants inoculated with *E. adhaerens* T4 present about twice the number of nodules present on *S. medicae* WSM419 inoculated plants (fig.3a) but all nodules were white (fig.3b) indicating that they were non fuctional. The plants co-inoculated with *S. medicae* WSM419 and *E. adhaerens* T4 present the same number of nodules than *E. adhaerens* T4 inoculated plants and almost all these nodules were white (fig.3a and 3b). The increased number of nodules correlates with the fact that they are nonfunctional and correspond to an auto-regulatory process of nodulation limiting nodule

formation when nodules fix efficiently nitrogen. The results also show that T4 outcompeete *S. medicae* WSM419 for nodule fonction.

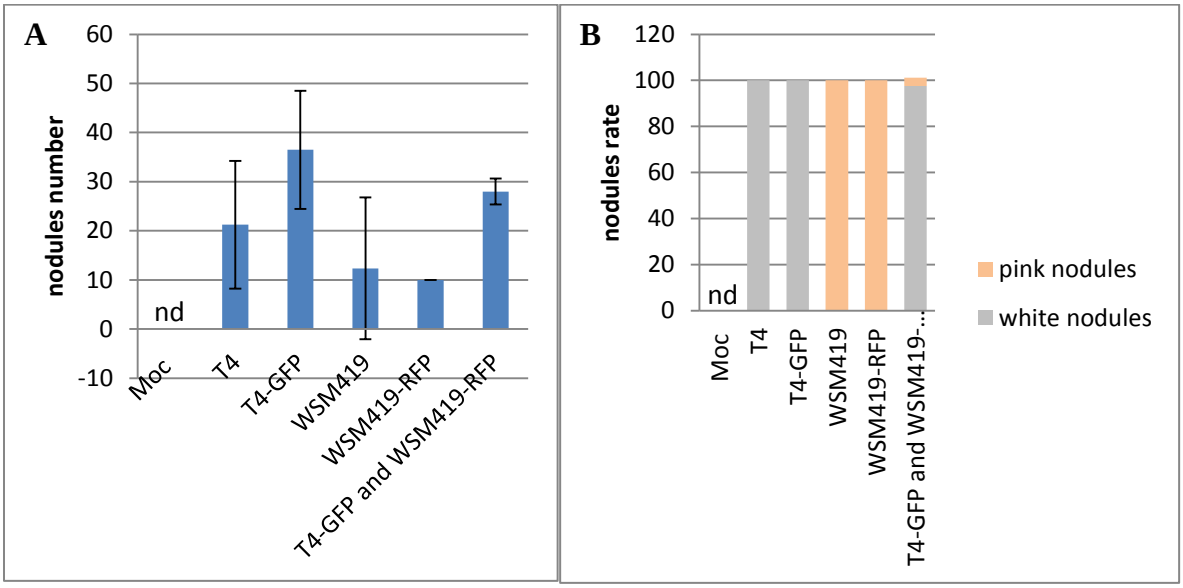

Figure 3. *E. adhaerens* T4 induces the formation of non-functional nodules. *M. truncatula* R108 functional mature nodules induced with *S. medicae* WSM419 and *E. adhaerens* T4 (fluorescent or not) observed at 21 dpi. (a) Number of nodules induced by different strains (fluorescent or not). (b) The nodules were classified according to their color. The rate of pink nodules is represented by pink bars and white nodules (without leghemoglobin) are represented by gray bars. Error bars, ± SE from three independent experiments with one technical replicate for each experiment. nd : not detected.

To check if *E. adhaerens* T4 could coinfect nodules at the same time as rhizobia and be present in functional pink nodules, white and pink nodules from plants coinoculated with *S. medicae* WSM419::RFP and *E. adhaerens* T4::GFP and nodules from plants inoculated with *medicae* WSM419::RFP were subjected to microtome sectioning into semi-thin sections (70µm) and observed under confocal microscope BX53 (OLYMPUS, fig.4). The nodule sections induced with *S. medicae* WSM419::RFP show a normal zonation and the symbiotic cells were filled with differentiated bacteroids (fig.4A). The white nodules from plants co-inoculated with *S. medicae* WSM419::RFP and *E. adhaerens* T4::GFP exhibit abnormal zonation. In these nodules symbiotic cells in inter-zone II-III and zone III seem to be very lowly colonized by *E. adhaerens* T4::GFP compared to zone I, II and zone IV (fig.4B). Moreover, *E. adhaerens* T4::GFP is unable to differentiate in the symbiotic cells (fig.4B). Furthermore, the pink nodules from coinoculated plants with *S. medicae* WSM419::RFP and *E. adhaerens* T4::GFP, show a massive colonization of symbiotic cells of the three first zones by *S. medicae* WSM419::RFP. Interestingly, some symbiotic cells of the fourth zone were

colonized by both strains *S. medicae* WSM419::RFP and *E. adhaerens* T4::GFP (fig.4C). In addition we could also observe adjacent cells infected with either WS419::RFP or *E. adhaerens* T4::GFP. This indicates that *E. adhaerens* T4 can co-colonize nodules with *S. medicae*.

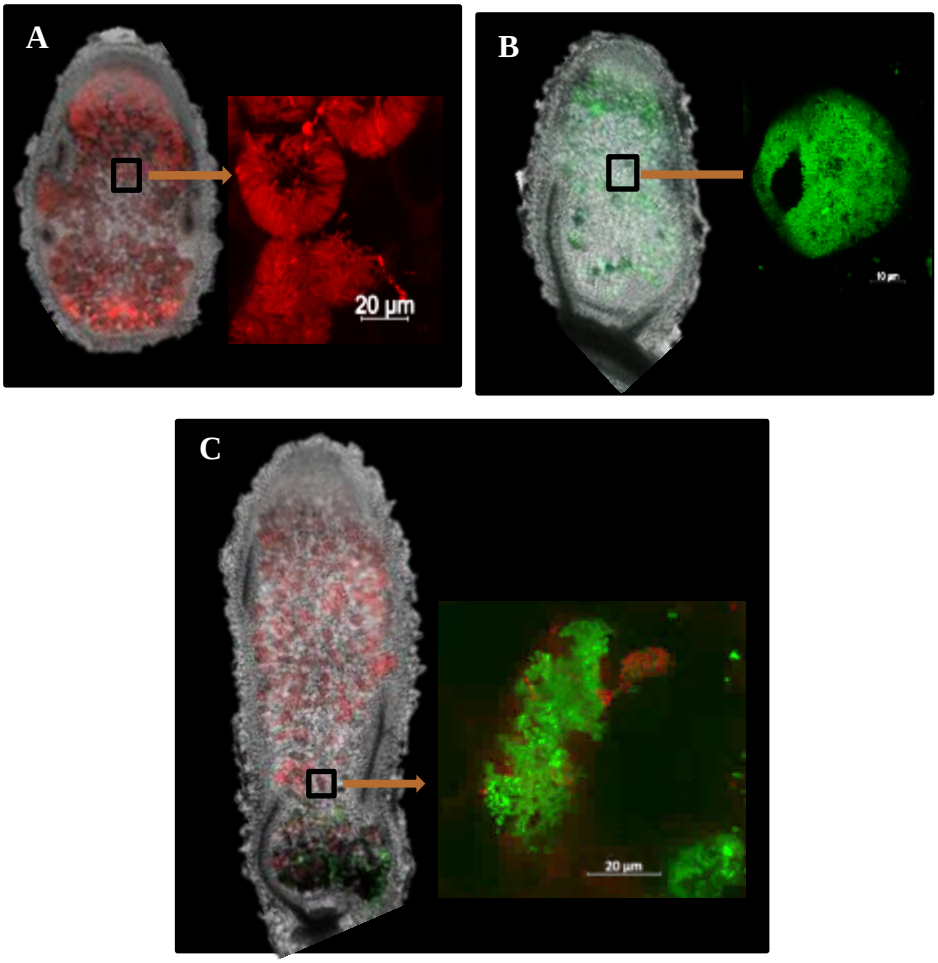

Figure 4. *E. adhaerens* T4 induces mature nodules and colonizes symbiotic cells. (A) *M. truncatula* R108 functional mature nodule induced with *S. medicae* WSM419::RFP, the symbiotic cells are filled with differenciated bacteroides. (B) *M. truncatula* R108 non-functional mature nodules induced with *E. adhaerens* T4::GFP. The symbiotic cells are filled by undifferentiated bacteroids. (c) *M. truncatula* R108 functional mature nodules induced with *S. medicae* WSM419::RFP and *E. adhaerens* T4::GFP. The symbiotic cells of zone I, II and zone III are filled with differenciated *S. medicae* WSM419::RFP bacteroids. ZoneVI is filled by differenciated WSM419::RFP bacteroids and non-differenciated *E. adhaerens* T4::GFP bacteroids.

***Ensifer adhaerens* T4 induces defense and senescence genes in wildtype nodules**

To investigate whether *E. adhaerens* T4 induces defense reactions or senescence in wild-type nonfunctional nodules, the relative expression of seven defense-dependent genes and three senescence-related genes was checked. The defense and senescence markers used in this study were taken from our previous study (*dnf5* characterization part). The relative expression of the gene markers were checked by RT-qPCR using wild-type nodule RNAs from A17 and R108 plants inoculated with either *S. medicae* WSM419 or *E. adhaerens* T4 harvested at 21 dpi.

E. adhaerens T4 in R108 background nodules induces strongly the expression of defense genes *PR10*-like, *FLAVONE SYNTHASE 2* (*FS2)* and *QM* and induces slightly the expression of *PR10* and *FLAVONE SYNTHASE 1 (FS1)* genes (fig.5). By contrast, the genes *Chitinase* and *VSP* were not induced (fig.5). Among the *CYSTEINE PROTEASE* senescence genes tested only the *CP2* gene was induced by *E. adhaerens* T4 (fig.6).

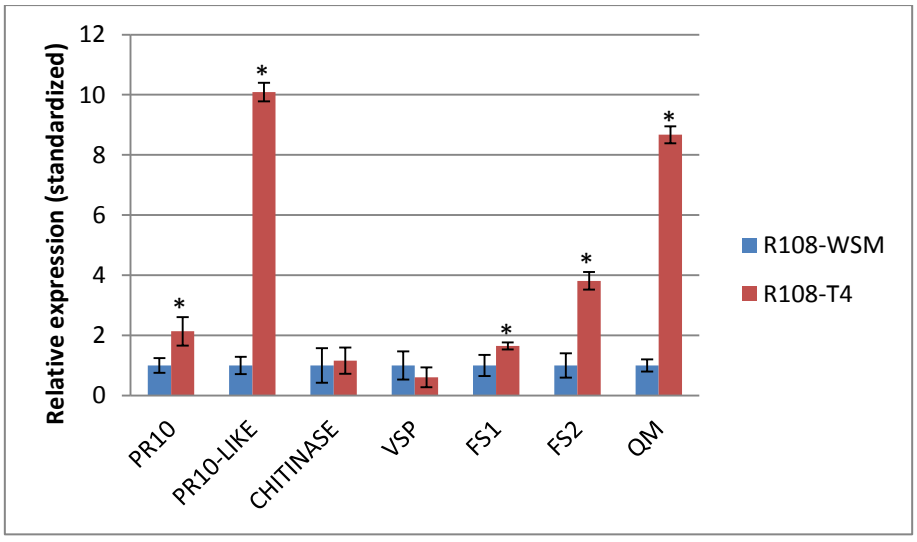

Figure 5. *E. adhaerens* T4 induces defense genes expression in R108 nodules. The expression of defense genes was evaluated by RT-qPCR performed on RNAs extracted from *M. truncatula* R108 wild-type nodules inoculated *in vitro* with *S. medicae* WSM419 or *E. adhaerens* T4 strains at 21 dpi. Fold change versus wild-type is presented after normalization with an *Actin* gene as an internal control. Error bars, ± SE from three independent experiments with one technical replicate for each experiment. Asterisks indicate significant induction ($P<0.05$) compared to the non-treated samples.

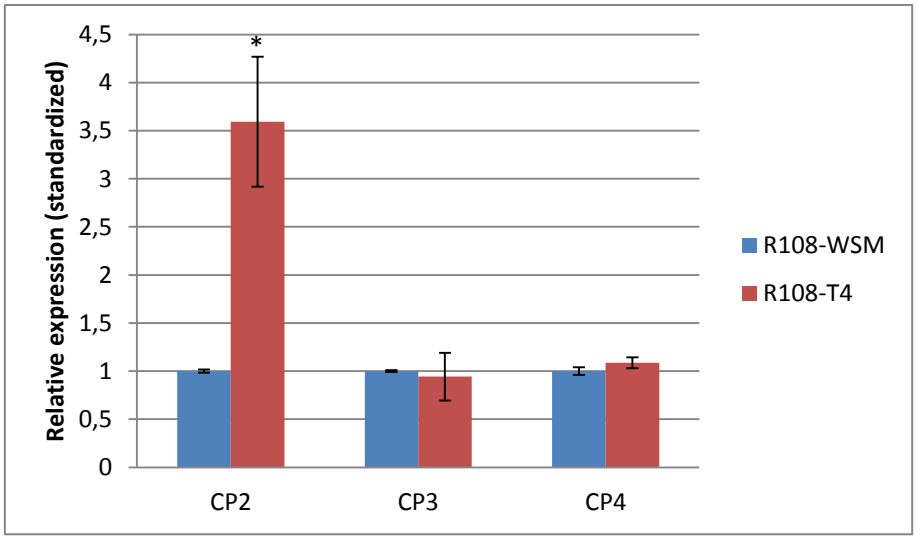

Figure 6. *E. adhaerens* T4 induces senescence gene expression in R108 nodules. The expression of senescence genes was evaluated by RT-qPCR performed on RNAs extracted from *M. truncatula* R108 wild-type nodules inoculated *in vitro* with *S. medicae* WSM419 or *E. adhaerens* T4 strains at 21 dpi. Fold change versus wild-type is presented after normalization with an actin gene as an internal control. Error bars, ± SE from three independent experiments with one technical replicate for each experiment. Asterisks indicate significant induction ($P<0.05$) compared to the non-treated samples.

This result indicates that in R108 background the *E. adhaerens* T4 strain induces the expression of defense genes as compared to nodules colonized by *E. medicae*. In addition the defense genes are more induced in nodules than senescence ones to stop parasitic microorganisms from invading the symbiotic organ and taking nutriment.

Furthermore, in the previous hormones Chapter IV, I suggested that the expression of *VSP* gene is correlated to JA treatment and repressed by SA and ET exogenous treatment. On the other hand, in same Chapter IV, I reported that the genes tested in this study could be induced with SA and ET, however, the *QM* gene is strongly induced with SA which is not the case here. This means that in *M. truncatula* R108 wild-type nodules, the defense system against parasitic bacteria uses ET and SA defense signaling pathways and not JA.

In A17 nodules *E. adhaerens* T4 induces strongly the expression of the *PR10* and *QM* genes and very slightly the expression of the *PR10*-like, *VSP* and *FS2* genes. The genes *Chitinase* and *FS1* were not induced (fig.7). On the other hand, nodules of A17 plants induce very strongly the senescence genes as the three tested genes *CP2*, *CP3* and *CP4* were induce more than 10 times compared to wild-type (fig.8).

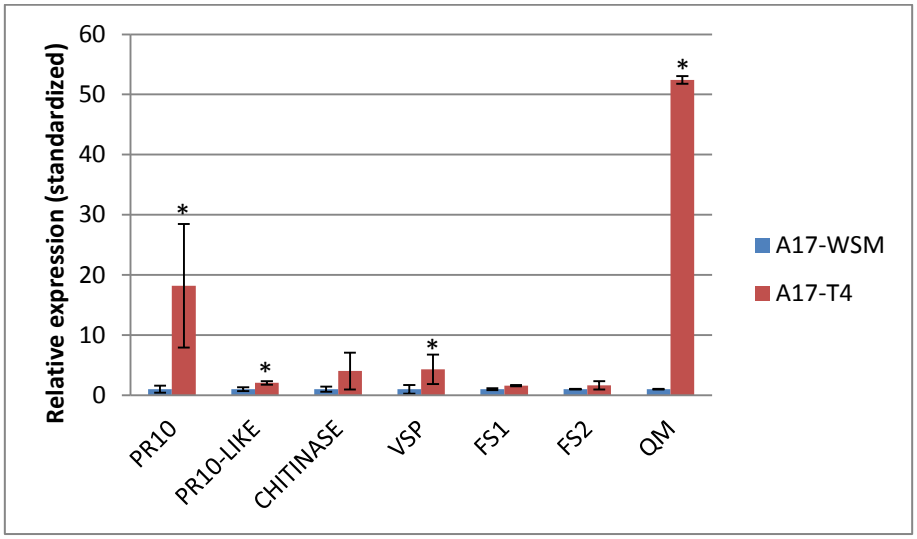

Figure 7. *E. adhaerens* T4 induces defenses gene expression in A17 nodules. The expression of defense genes was evaluated by RT-PCR performed on RNAs extracted from *M. truncatula* A17 wild-type nodules inoculated *in vitro* with *S. medicae* WSM419 or *E. adhaerens* T4 strains at 21 dpi. Fold change versus wild-type is presented after normalization with an *Actin* gene as an internal control. Error bars, ± SE from three independent experiments with one technical replicate for each experiment. Asterisks indicate significant induction ($P<0.05$) compared to the non-treated samples.

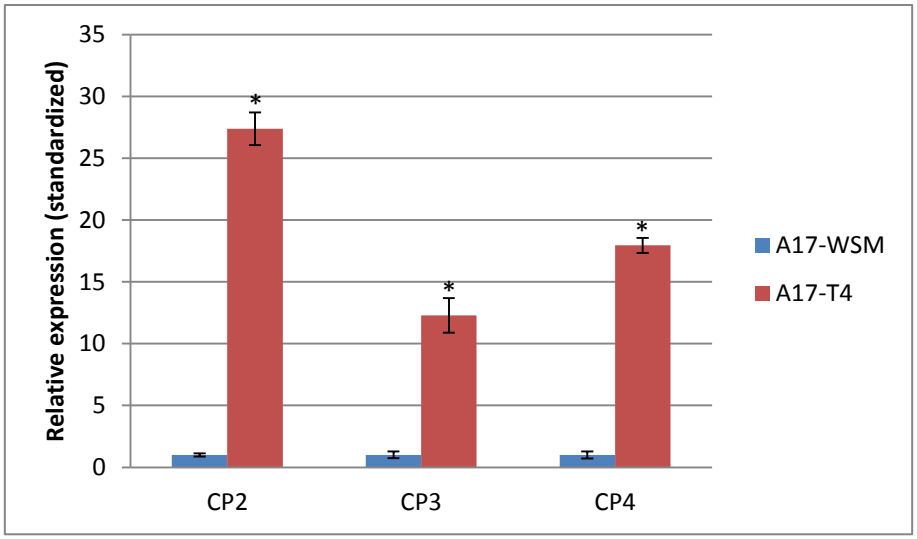

Figure 8. *E. adhaerens* T4 induces senescence gene expression in A17 nodules. The expression of senescence genes was evaluated by RT-qPCR performed on RNAs extracted from *M. truncatula* A17 wild-type nodules inoculated *in vitro* with *S. medicae* WSM419 or *E. adhaerens* T4 strains at 21 dpi. Fold change versus wild-type is presented after normalization with an *Actin* gene as an internal control. Error bars, ± SE from three independent experiments with one technical replicate for each experiment. Asterisks indicate significant induction ($P<0.05$) compared to the non-treated samples.

This result indicates that parasitic microorganisms strongly activate defense and senescence genes in A17 background. On the other hand, the strong induction of the *QM* gene and the induction of *VSP* gene suggest that SA and JA defense hormones are strongly implicated in the defense processes in A17 nodules.

***Ensifer adhaerens* T4 represses the expression of the symbiotic genes in wild-type nodules**

One mechanism that could explain the induction of the defense mechanisms in the nodules induced by the *E. adhaerens* T4 strain is that the symbiotic signaling is not efficient enough to trigger the symbiosis genes like *DNF2* and *SymCRK* that repress immunity. To test this we analyzed the expression of symbiotic genes in nodules induced with *E. adhaerens* T4. The relative expression of the *DNF2, RSD* and *SymCRK* symbiotic gene was analyzed by RT-qPCR using wild-type nodules cDNAs from A17 and R108 plants inoculated with *S. medicae* WSM419 or *E. adhaerens* T4 harvested at 21 dpi. The expression of the three symbiotic genes was reduced in wild-type nodules induced by *E. adhaerens* T4 compared to wild-type nodules induced by *S. medicae* WSM419 (fig.9).

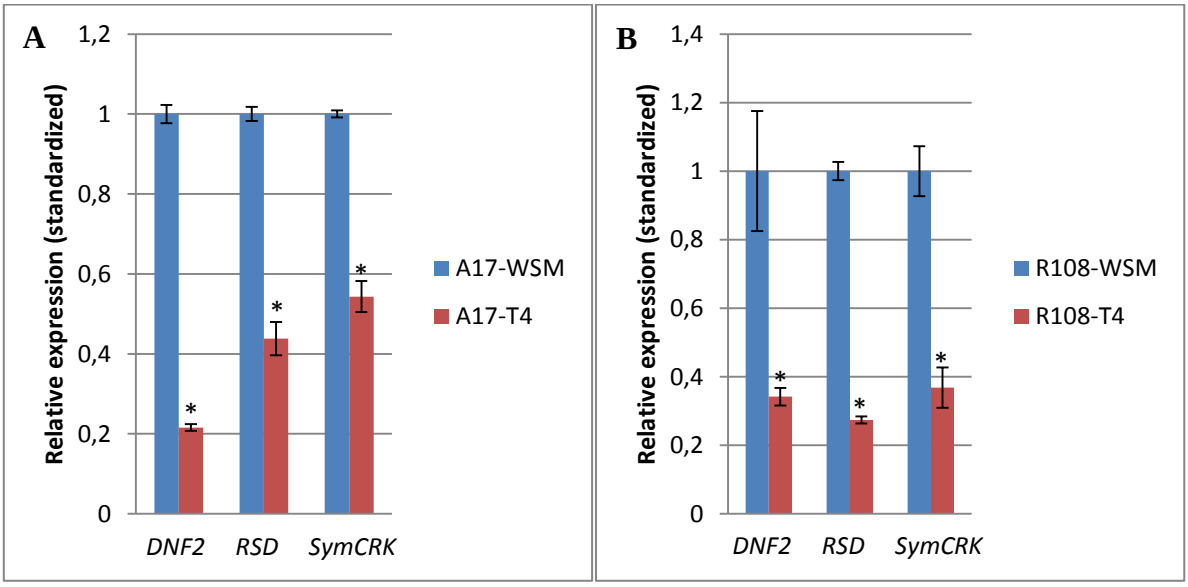

Figure 9. Symbiotic genes expressions repressed by *E. adhaerens* T4. The expression of symbiotic genes was evaluated by RT-qPCR performed on RNAs extracted from *M. truncatula* A17 and R108 nodules inoculated *in vitro* with *S. medicae* WSM419 or *E. adhaerens* T4 strains at 21 dpi. Fold change versus wild-type is presented after normalization with an *Actin* gene as an internal control. Error bars, ± SE from three independent experiments with one technical replicate for each experiment. Asterisks indicate significant induction ($P<0.05$) compared to the non-treated samples.

These results suggest that the symbiotic genes are not expressed correctly in non-functional nodules induced by *E. adhaerens* T4, and this lead to the immune system activation. Or, the activation of the immune systeme in nodules leads to the repression of the symbiotic genes expression. In the other hand, the immune system activation in R108 and

A17 is different, the immune system in R108 nodules is modulated by ET and SA signaling pathway and lead to defense reactions activation. However, in A17 nodules, the activation of the immune systeme is modulated by JA and SA signaling pathway and lead to the activation of the cell death program.

DNF2 gene is the first controller of internalized bacteria

The results described above suggest that *E. adhaerens* T4 triggers defense reactions and lower symbiotic gene expression in WT nodules. We thus hypothesize that if the plant cannot control the defense reactions despite the presence of the *DNF2, RSD* or *SymCRK* genes, than these defense reactions should increase in the corresponding mutant backgrounds. To test this, the relative expression of six defense-related and hormone-related genes (*QM, FS, PR1, EIN3*-2 and *EIN3*-3) were checked by RT-qPCR using nodules cDNAs from wild-type R108 and fix$^-$ mutants nodules [*symCRK* mutant (NF0737), *dnf2* mutant (MS240)] induced with *E. adhaerens* T4 and *S. medicae* WSM419 separately, harvested at 21 dpi. The hormone and defense markers used in this study were described in the previous study (hormone chapters).

The results presented in fig.10 indicate that *E. adhaerens* T4 induces the expression of *QM* gene in wild-type nodules compared to wild-type inoculated with *S. medicae* WSM419. In the *symCRK* mutant the *QM* gene induction does not change in T4 nodules compared to *symCRK* mutant WSM419 nodules. However, the level of *QM* expression were fifteen times more induced in the *dnf2* mutant nodules induced with *E. adhaerens* T4 compared to nodules induced with *S. medicae* WSM419. The *FS* and *PR1* genes were induced in wild-type and mutant nodules inoculated with *E. adhaerens* T4, but this induction was down-regulated in *symCRK* mutant and enhanced in *dnf2* mutant nodules. The *EIN3*-2 is also induced in all nodule conditions but contrary to *FS* and *PR1* genes, the *EIN3*-2 gene expression was stable in the *dnf2* mutant inoculated with *E. adhaerens* T4. In addition the *EIN3*-3 gene was induced in R108 and repressed in the symbiotic mutants.

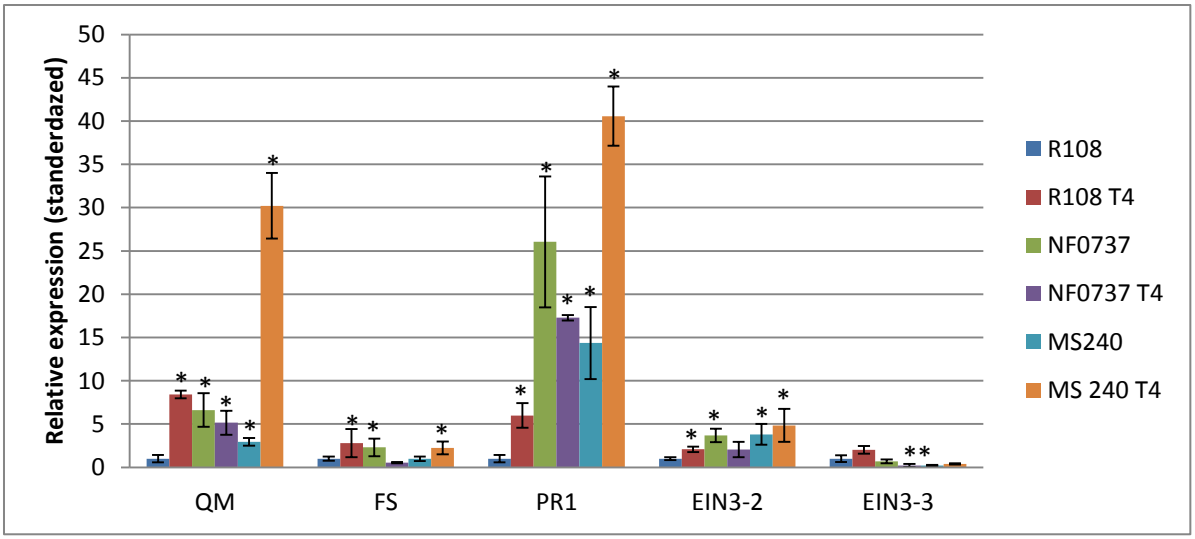

Figure 10. Hormone and defense genes are induced in nodules from symbiotic mutant. The expression of hormone defense genes was evaluated by RT-qPCR performed on RNAs extracted from NF0737 (*symCRK*), MS240 (*dnf2*) and *M. truncatula* R108 wild-type nodules inoculated *in vitro* with *S. medicae* WSM419 or *E. adhaerens* T4 strains at 21 dpi. Fold change versus wild-type is presented after normalization with an *Actin* gene as an internal control. Error bars, ± SE from three independent experiments with one technical replicate for each experiment. Asterisks indicate significant induction ($P<0.05$) compared to the non-treated samples.

These results indicate that *E. adhaerens* T4 induces hormone and defense genes in wild-type and in symbiotic mutant nodules with a stronger induction in the *dnf2* background. This suggests that *DNF2* plays a major role in controlling immunity against invading bacteria in the nodule. In addition, according to results present chapter IV, the *PR1* gene expression is strongly correlated to ET signaling pathway and the *QM* gene expression is strongly induced by SA exogenous treatment. These results confirm the strong implication of ET in the induction of nodule defense reactions in the R108 background and this with the participation of the SA signaling pathway.

Symbiosis and Pathogenic spectrum of *E. adhaerens* T4

To check the symbiotic spectrum of *E. adhaerens*, 1 day post-germination seedlings of five *M. truncatula* ecotypes; five *Medicago sativa* ecotypes, three *Trifolium* species, *Medicago polyforma ciliaris* and *Vicia hirsuta* were inoculated *in vitro* with *E. adhaerens* T4 strain or with sterile water. The inoculated plants were checked at one and two weeks post inoculation.

Inoculation with *E. adhaerens* T4 strain of *M. truncatula* ecotypes

The results presented in Fig 11A show that in the first week post-inoculation, *E. adhaerens* T4 causes the death of all young seedlings of *M. truncatula* R108 ecotype and *M. truncatula* Jemalong A17 and causes the death of more than 80% of *M. truncatula* Parragio, Ghor and F85 ecotypes compared to non-inoculated seedlings. In the second week post-inoculation (fig. 11B), all *M. truncatula* ecotypes seedlings died following *E. adhaerens* T4 infection except 12% of *M. truncatula* Parragio seedlings that survived but show disease symptomes and 6% of *M. truncatula* Ghor seedlings that stay healthy. Moreover, no nodules were formed in all tested *M. truncatula* ecotypes as they died.

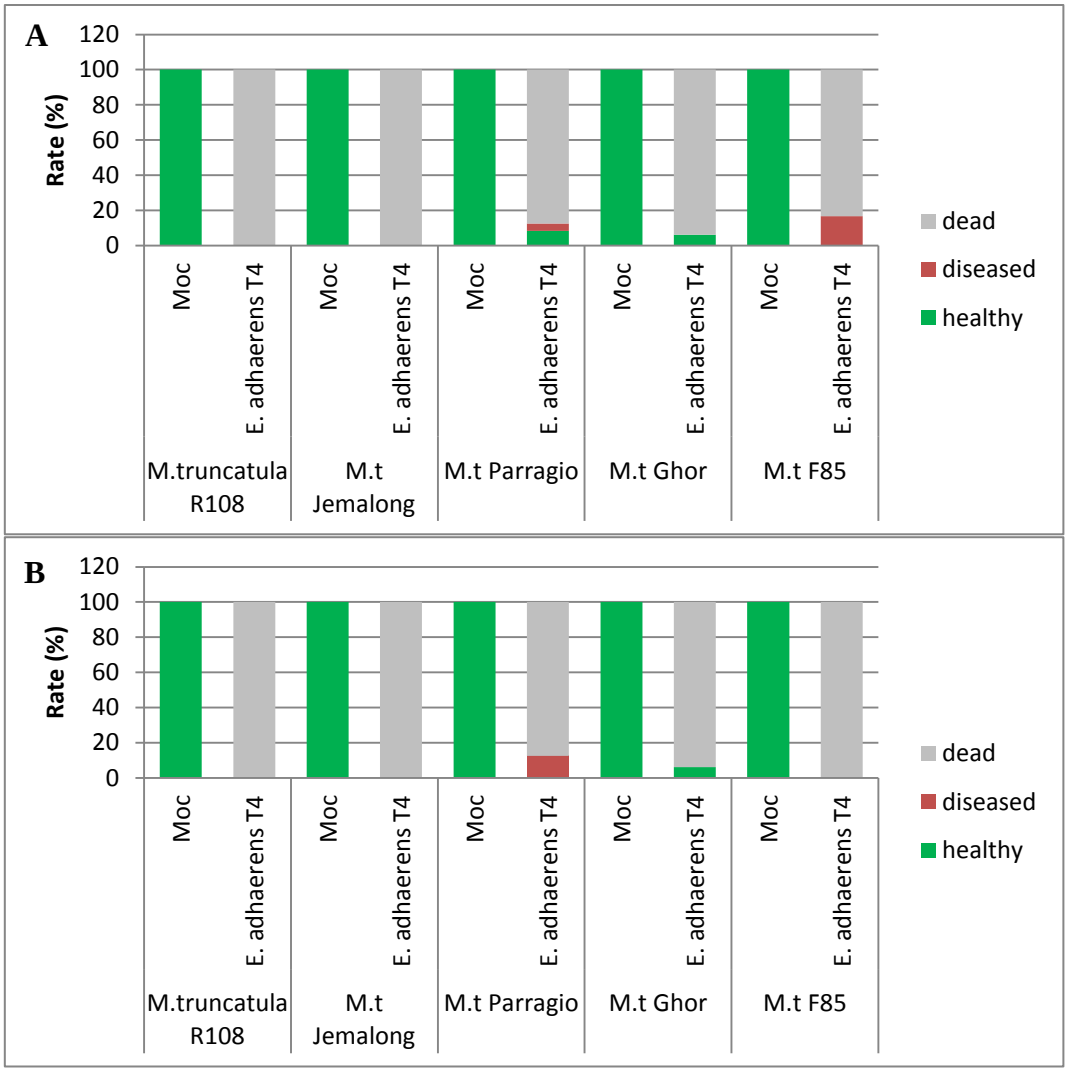

Figure 11. *E. adhaerens* T4 exhibits pathogen phenotype with *M. truncatula* ecotypes. Sixteen young seedlings of each *M. truncatula* ecotypes (R108, A17, Parragio, Ghor and F85) inoculated with sterile water (Moc) or with *E. adhaerens* T4 were cultivated *in vitro* and observed at (A) one week post-inoculation and (B) two weeks post-inoculation.

The results suggest that *E. adhaerens* T4 is lethal for the young seedlings of *M. truncatula* species except for the Ghor ecotype showing low level of resistance.

Inoculation with *E. adhaerens* T4 strain of *M. sativa* ecotypes

The results presented in fig. 12A show that in the first week post-inoculation, all *M. sativa* ecotypes seedling inoculated with *E. adhaerens* T4 were diseased and about 20% of *M. sativa* WL903 and *M. sativa* G968 seedlings and about 5% of *M. sativa* Salina and GR18 seedlings were killed.

Two weeks post-inoculation (fig.12B), *M. sativa* G968 and WL903 were the most sensitive to *E. adhaerens* T4 infection as only 29% of that *M. sativa* G968 and 45% of *M. sativa* WL903 stayed healthy and the rest of the plants were either dead or showed disease symptoms. The *M. sativa* Salina, Oleron and Super ecotypes were more resistant to *E. adhaerens* T4 than *M. sativa* G968 and WL903 ecotypes. Less than 12% of the plants died and almost 16% of plants showed disease symptoms. Furthermore, *E. adhaerens* T4 was able to nodulate all tested *M. sativa* ecotypes, inducing about 20 non-functional nodules per surviving plant per ecotype (fig. 15).

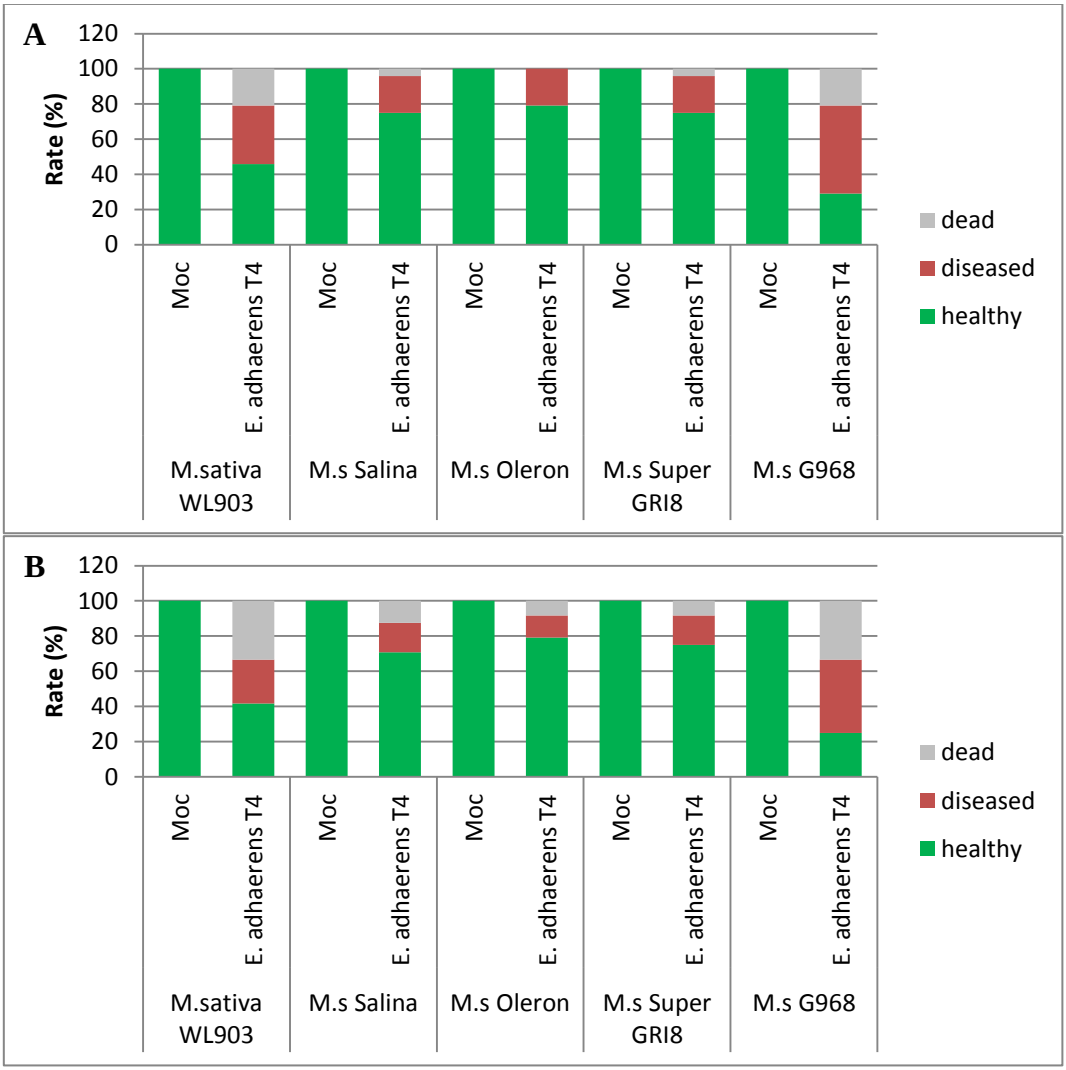

Figure 12. *E. adhaerens* T4 exhibits pathogen phenotype with *M. sativa* ecotypes. Sixteen young seedlings of each *M. sativa* ecotypes (WL903, Salina, Oleron, Super and G968) inoculated with sterile water (Moc) or with *E. adhaerens* T4 were cultivated *in vitro* and observed at (A) one week post-inoculation and (B) two weeks post-inoculation.

These results suggest that *E. adhaerens* T4 behaves as a pathogen for *M. sativa* species and can sometimes kill the infected plants. Furthermore, *E. adhaerens* T4 is able to nodulate *M. sativa* species.

Inoculation with *E. adhaerens* T4 strain of *Trifolium* species

The results presented fig.13 indicate that the three *Trifolium* species were more resistant to *E. adhaerens* T4 when compared to *Medicago*. One week post-inoculation, 4% of *Trifolium pratense* seedlings were killed by *E. adhaerens* T4 and 4% were diseased. At two weeks post-inoculation, the rate of the dead *Trifolium pratense* seedlings did not change, however, the number of diseased plant increased to 8%. *Trifolium subterraneum* shows about 6% of dead seedlings and 12% of diseased seedlings. Furthermore, *E. adhaerens* T4 is unable to induce formation of functional nodules on *Trifolium* species (fig.15). Because of the problems encountered with the moc treated plants that also died, this experiment will be repeated.

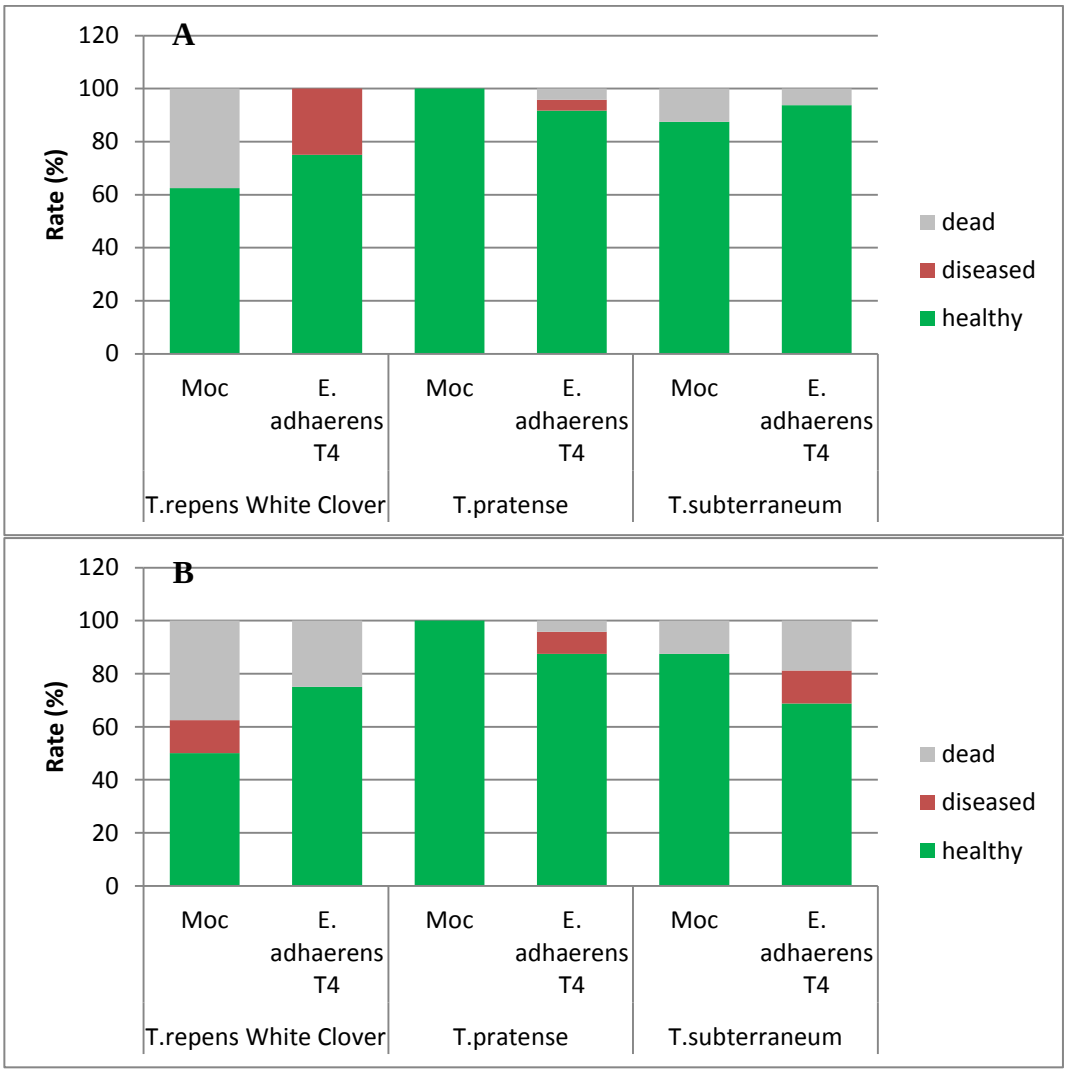

Figure 13. *E. adhaerens* T4 exhibits pathogen phenotype with *Trifolium species*. Sixteen young seedlings of each *Trifolium species* (*T. repens*, *T. pratens* and *T. subterraneum*) inoculated with sterile water (Moc) or with *E. adhaerens* T4 were cultivated *in vitro* and observed at (A) one week post-inoculation and (B) two weeks post-inoculation.

We deduced from these results that *E. adhaerens* T4 does not have a strong pathogenic effect on *Trifolium* species. Moreover, *E. adhaerens* T4 Nod factors are not compatible with *Trifolium* species.

Inoculation with *E. adhaerens* T4 strain of *M. polymorpha and Vicia hirsuta*

The result showed fig. 14 indicate that *E. adhaerens* T4 is not pathogenic on *M. polymorpha* Ciliaris and *Vicia hirsuta* species as no symptoms were observed on these two species. In addition, *E. adhaerens* T4 induces nodule formation on *M. polymorpha* Ciliaris species but not on *Vicia hirsuta* species (fig.15).

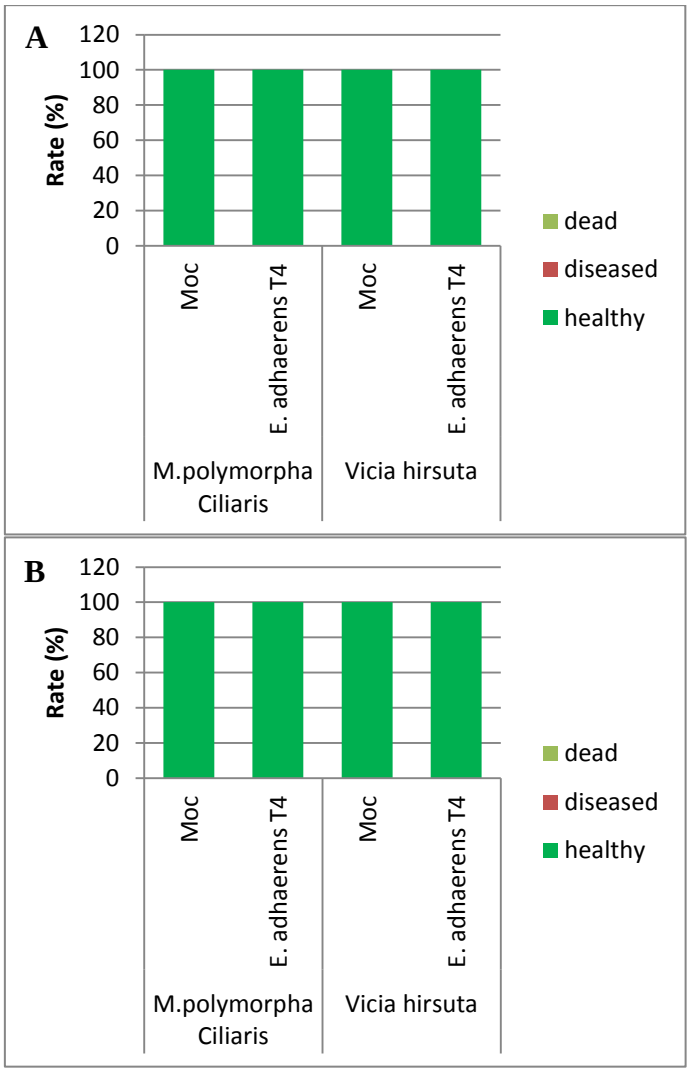

Figure 14. *E. adhaerens* T4 exhibits non-pathogen phenotype with *M. polymorpha and Vicia hirsuta*. Eight young seedlings *M. polymorpha Ciliaris* and two seedling of *Vicia hirsuta* inoculated with sterile water (Moc) or with *E. adhaerens* T4 were cultivated *in vitro* and observed at (A) one week post-inoculation and (B) two weeks post-inoculation.

These results indicate that *E. adhaerens* T4 is able to nodulate *M. polymorpha* Ciliaris without a pathogenic effect. However, *E. adhaerens* T4 is inoffensive and unable to induce nodule formation on *Vicia hirsute.*

E. adhaerens T4 nodulation capacity

Results present fig.15 show *E. adhaerens* T4 is able to induce formation of functional nodules in all tested Medicago species except for *M. truncatula* R108, A17 Parragio, Ghor F83. Moreover, the results show that *E. adhaerens* T4 is unable to induce formation of functional nodules in all tested *Trifolium* species and *Vicia hirsuta* species. Only primordia were observed but we are not able to know if they are nodule or lateral root primordia.

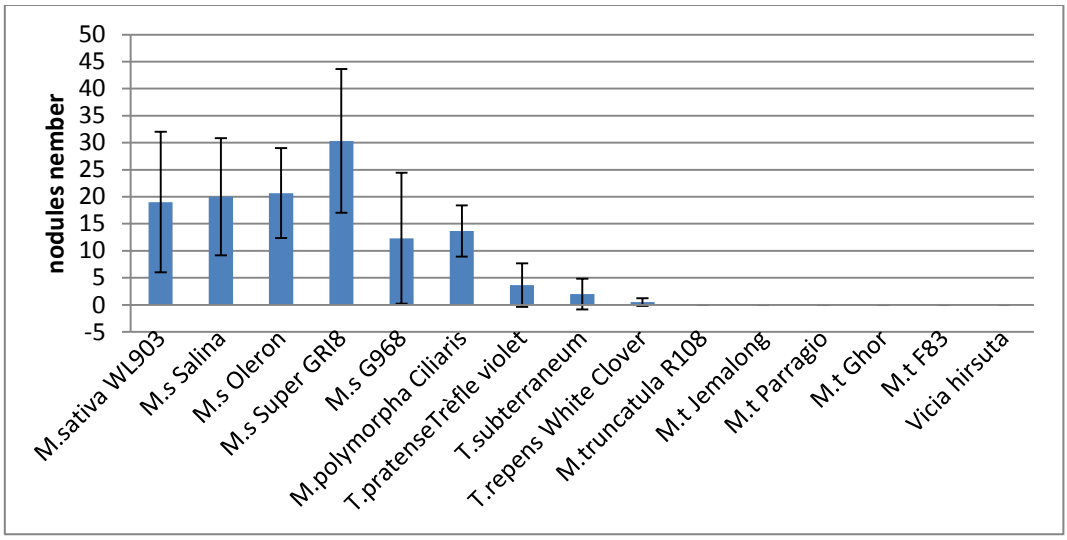

Figure 15. *E. adhaerens* T4 nodulation capacity. Seedlings of different legumes species belonging to different legume genders were inoculated with *E. adhaerens* T4 and cultivated *in vitro*. Nodules were counted 2 weeks post-inoculation.

These results suggest that *E. adhaerens* T4 is compatible with *Medicago sativa* species, and with *Medicago polymorpha* Ciliaris specie. In contrast, *E. adhaerens* T4 is not compatible with *Trifolium* and *Vicia hirsuta* species.

Conclusion

Putting the results of this chapter together, it indicates that *E. adhaerens* T4 has the ability to induce the formation of non-functional nodules in *Medicago truncatula* R108, *M. Jemalong*, *M. sativa* and *M. polyphorma* species. However, it is unable to induce formation of functional nodules in *Trifolium* and *Vicia hirsuta* species. On the other hand, inside the symbtioc cells, *E. adhaerens* T4 is unable to differentiate and to fix atmospheric nitrogen, and this could be explained by the lack of the *nif* and *fix* genes in the *E. adhaerens* T4 genome. The activation of the immune systeme of R108 nodules results the activation of the defense genes expression, induction of ET and SA signaling pathway and the accumulation of phenolic compounds. In contrast, the activation of the immune system of A17 nodules correspond to the activation of cysteine protease genes, induction of SA and JA signaling pathways and activation of the cell death program. This results correlate with the results obtained in chapters III, IV and V, were I correlated JA signaling pathway to the induction of cysteine protease gene expression and activation of the cell death program in A17 background, and ET and SA signaling pathway to the induction of defense genes expression and accumulation of phenolic compounds.

Furthermore, the gene expression patterns observed in *dnf2*^{R108} nodules is similar to the genes expression patterns observed in nodules induced with *E. adhaerens* T4. This suggests that DNF2 participate to regulate negatively the rhizobia recognition steps which control the infection of the symbiotic cells of R108 nodules. This observation is in agreement with Berrabah et al, (2014b) results. This study indicated that the cultivation of *dnf2* mutant in pure medium supplemented with immunogenic molecule as ulvan induce nodules defense reactions. However, on pure medium without the immunogenic molecule, the *dnf2* mutant does not exhibit defense reactions. This indicates that DNF2 act to repress defense reactions induction at the rhizobium recognition steps in the symbiotic cells.

The original behavior of *E. Adhaerens* T4 (pathogen and inducer of nodules) makes it a very valuable tool to study the role of immunity during symbiosis and to understand the control of chronic infection of the symbiotic cells in *Medicago*/*Sinorhizobium* nodules. In addition, the study of this new bacterial strain could improve our understanding of the evolution and the continuum from parasitism to highly beneficial symbiosis.

Chapter VII: MtNBS-LRR role in nodules functioning

Plant NBS-LRR role in *Medicago truncatula* nodules functioning.

Aït-Salem Elhosseyn[1,2] , Berrabah Fathi[3], Ratet Pascal*[1,2].

1. Institute of Plant Sciences Paris-Saclay IPS2, CNRS, INRA, Université Paris-Sud, Université Evry, Université Paris-Saclay, Bâtiment 630, 91405 Orsay, France
2. Institute of Plant Sciences Paris-Saclay IPS2, Paris Diderot, Sorbonne Paris-Cité, Bâtiment 630, 91405, Orsay, France
3. Laboratory of Exploration and Valorization of Steppic Ecosystems, Faculty of Nature and Life Sciences, University of ZianeAchour, 17000 Djelfa, Algeria

Introduction

Plants represent a very important niche of nutrients, which makes them the preferred target of carbon heterotrophic microorganisms. To defend themselves against their invaders and overcome pathogen infection, the plant immune system relies on several defense pathways based on two lines of defenses. The first line of defense is the basal defense; this system is activated by pattern recognition receptors (PRRs) recognizing conserved pathogen-associated molecular patterns (PAMPs) or microbe-associated molecular patterns (MAMPs), which are generic signals for the presence of a pathogen. Theses (M) PAMPS are for example bacterial flagellins, lipopolysaccharides, and fungal chitin and activate PAMP-triggered immunity (PTI) (Jones et Dangl. 2006; Jones et Takemoto, 2004). However, pathogens are able to inhibit the PTI signaling pathways by injecting in the plant cells effectors which are small protein encoded by Avirulence (*Avr*) genes (Jones et Dangl. 2006; Jones et Takemoto, 2004). Here the second line of defense intervenes, based on the action of the adaptive immune system (gene for gene interaction). This system is activated by direct or indirect recognition of the *Avr* gene products by resistance (*R*) genes and activates effector-triggered immunity (ETI). ETI is associated with a strong immune response including apoptosis at the infection site (hypersensitive response) leading to the restriction of pathogen growth (Coll *et al.*, 2011; Dodds et Rathjen, 2010; Jones *et al.*, 2016). Furthermore, *R* genes can be harmful to the plant as their miss-regulation in the absence of pathogen infection, may cause autoimmune reactions and inhibits plants growth (Michael et al. 2006). In addition, in a recent study, it was shown that the *R* genes have a negative effect on nodule formation. This study reported that the suppression of *R* genes activity in legumes could promote the nitrogen-fixing symbiotic interaction and nodule formation of *Medicago truncatula* (Sós-Hegedüs *et al.*, 2019).

The largest proteins class encoded by *R* genes is the nucleotide-binding site and leucine-reach repeats (NBS-LRRs) gene classes. The *R* genes family is composed of around 540 *NBS-LRR* genes (Zhai *et al.* 2011) in *M. truncatula*. NBS-LRRs protein is formed by a NBS domains involved in signaling, an ARC domain implicated in the recruitment of the LRR domain to the N-terminal region and LRRs domains devoted to protein-protein interactions (Dangl et Jones, 2001; Rairdan et Moffett, 2006). Furthermore, the N-terminal domains of NBS-LRR protein classify this R protein family into two subfamilies; the TIR-NBS-LRR (TNL) proteins that contain a Toll-like domain, and the CC-NBS-LRR (CNL) proteins that are characterized by a coiled-coil domain (Pan *et al.*, 2000).

In order to determine how the host plant recognizes its allies from its enemies and how nodules guarantee the intracellular accommodation of rhizobia, the expression of some R proteins was studied using *M. truncatula* symbiotic fix$^-$ mutants exhibiting nodules defense-like reactions, and in wild-type nodules induced with *Ensifer adhaerens* T4 behaving as a pathogen able to induce nodulation and to parasite symbiotic cells.

Materials and methods

Plants materials an growth conditions

Medicago truncatula genotype R108 and Jemalong A17 and symbiotic mutants exhibiting defense-like reactions (NF0737, NF240, *dnf5-2* and *dnf2* lines) were scarified by sulfuric acid for 10 minutes, washed three times in sterile water, then sterilized in sodium hypochlorite for 30 min, washed three times in sterile water and incubated 1 hour in sterile water. The sterilized seeds were transferred onto 50mL water agarose 1% plates and vernalized for at least 48 h at 4° C in the dark. Seeds were germinated by incubating them at 24°C for 36 h.

Seedlings were transferred onto square plates (8 plants per plate) filled with buffered nodulation medium (BNM) solidified with bacto-agar 1.5%. The seedling roots were inoculated with 1mL of bacterial suspension per plate. Plates were then incubated in growth chamber under long day condition (16h light: 8h dark cycle at 24°C). All experiments were conducted on nodules harvested at 21 days post-inoculation dpi.

Bacterial strain and inoculation

The *Sinorhizobium medicae* WSM419 strain (Howieson & Ewing, 1986), and *Ensifer adhaerens* T4 strain were cultivated at 30°C in yeast extract broth (YEB) medium (Krall *et al.*, 2002) supplemented with 12.5 µg.mL^{-1} of chloramphenicol for *S. medicae* WSM419 culture. The bacterial inocula were prepared by washing twice a fresh overnight liquid culture with sterile distilled water and then the culture was suspended and adjusted to optical density 0.15 at OD600 nm in sterile distilled water.

In silico screening

The identification of R genes involved in defense reaction were done by *in silico* screening using public databases ((https://phytozome.jgi.doe.gov/pz/portal.html https://mtgea.noble.org/v3) and personal RNAseq data (not published).

RNA extraction and RT-qPCR

Nodules from different mutants were collected at 21 dpi in 2mL Eppendorf tubes in presence of three metal beads (one 3 mm and two 5 mm of diameter), were frozen in liquid nitrogen and crushed by vortexing at 4° C. The material was re-suspended in 500 µL cold TRIzol reagent (ref# 15596026, AMBION) and incubated for 5 min. 100 µL cold chloroform was added to the mix and incubated for 10 min. The mix was centrifuged 5 min at 16000g and up to 500 µL of the aqueous phase was collected. RNAs were precipitated overnight at -20 °C with 250 µL of isopropanol and 100 µL of sodium acetate 3 M pH5.2 and collected after 60 min centrifugation (16000g). The precipitated pellet was washed with 1 mL of 70 % ethanol and centrifuged two times. The obtained RNAs were re-suspended in RNase-free water.

The reverse transcription of the free-DNA RNAs was performed using SuperScript™ II Reverse Transcriptase kit (Invitrogen, ref. 18064-022). In a 200 µL micro-centrifuge tube, 1 µL of oligo dT primer (500ng/µL; ref. #SO132, Thermoscientific) 1 µl of dNTPs 10 mM, 1µg of DNA-free RNA and sterile RNase-free water were added in a 13µL final volume. The mix was heated 5 min at 65°C, quickly chilled on ice and briefly centrifuged. 4µL of 5X First-Strand Buffer [Tris-HCl pH8.3 250 mM, KCl 375 mM, $MgCl_2$ 15 mM], 2µL of dithiothréitol 0,1 M were added to the previous mix. The mix was gently homogenized and incubated 2 min at 42°C. Then, 1 µL of SuperScript™ II Reverse Transcriptase 200 units was added, the 20µL finale mix was gently homogenized and incubated 50 min at 42°C for the reaction. The reaction was stopped by inactivating the enzyme during 15 min at 70°C. The obtained cDNA was diluted 1/20 with DNAse-free water.

The Relative qPCR were performed on the obtained cDNA using 2X LightCycler 480 SYBR Green I Master (ref. 04 887 352 001, Roche), 2 µL of each primers (2,5 µM each) and 1µL of cDNA, in a final volume of 10 µL. qPCR were launched on a LightCycler (480 II Roche). The SYBR Green fluorescence was detected between 465 and 510 nm. Cycle threshold and primer specificities were performed with the LightCycler 480 software (release 1.5.0 SP4). Primer efficiencies were calculated with LinReg PCR: Analysis of Real-Time PCR Data, version 11.1. The actin gene Medtr2g008050 was used as reference in relative qPCR experiments. The primers used for these experiments are listed in the Table 1.

Table 1. RT-qPCR primers list

Gene ID	Protein	Nam	Primers
Medtr3g018980.1	Disease resistance protein	CC-NBS-LRR-1 (CNL-1)	GGCTTCAATTCCCGAGGCTT
			ATCGATGTCACCAACACGCA
Medtr3g012240.1	disease resistance protein	CC-NBS-LRR-2 (CNL-2)	GGAGGAGCCAATGAAGGAGTC
			TGAGACGCAATCTGGTGGTG
Medtr6g016420.1	disease resistance protein	CC-NBS-LRR-3 (CNL-3)	TTCTTCCCGTCATTGGAGCG
			GCAAGTCAGTCAACTTTGGGC
Medtr1g047800.1	disease resistance protein	CC-NBS-LRR-4 (CNL-4)	AGTGGCACACAAGACACCAA
			TCCTCCCATACCAACAATGGG
Medtr5g018210.1	disease resistance protein	CC-NBS-LRR-5 (CNL-5)	TTAGTCTTGGATGATGTTTGGCCT
			GGCATGTATGAGCTTCTGTGATTC
Medtr4g020590.1	disease resistance protein	TIR-NBS-LRR-1 (TNL-1)	GGTTTCAACATGGAGAACGGG
			GAAGGGAGAGACACCGTGAT
Medtr2g099920.1	disease resistance protein	TIR-NBS-LRR-2 (TNL-2)	GATAATAGCTCTGCTTGATGCC
			CTCGAACAATCTCCCAACCCA
Medtr6g036510.1	disease resistance protein	TIR-NBS-LRR-3 (TNL-3)	GCTGCCCTACAAAGACGAGG
			TCCAATTCTCGCAAACACCAA
Medtr6g008140.2	disease resistance protein	TIR-NBS-LRR-4 (TNL-4)	CTTGTTGAGGTGGAAGGTTTGTAA
			CATATCGAGCCAATGTAGAACTCC

Results

The symbiotic genes used in this study have the same name in the two *M. truncatula* backgrounds (A17 and R108) except for the *SymCRK* gene, which is named *dnf5* in A17 background and *SymCRK* in R108 background. To avoid confusion between the backgrounds, I will refer to *dnf5*/*SymCRK* as *symCRK*^{A17} in the A17 background and as *symCRK*^{R108} in the R108 background. In addition, to differentiate the *DNF2* genes in the two backgrounds, I will refer to *DNF2*^{A17} in A17 background and to *DNF2*^{R108} in R108 background.

To study the role of R proteins in the rhizobia intracellular accommodation in symbiotic cells in R108 and A17 backgrounds, I selected from one *symCRK*^{R108} RNAseq experiments five genes with induced expression in *symCRK*^{R108} nodules and arbitrarily four genes with expression not detected to check if the expression of these genes is similar in the two backgrounds and to confirm the expression observed in *symCRK*^{R108} RNAseq results.

The results present in fig.1 show a two times induction of the expression of *CC-NBS-LRR-2* (*CNL*-2) and *CNL*-5 genes, and a one time induction of the expression of the genes *CNL*-4, *TNL*-1 (*TIR-NBS-LRR-1*) and *TNL*-4 in *symCRK*^{R108} nodules. The expression of *CNL*-1, *CNL*-3, *TNL*-2, *TNL*-3 genes is unchanged between R108 and *symCRK*^{R108} nodules.

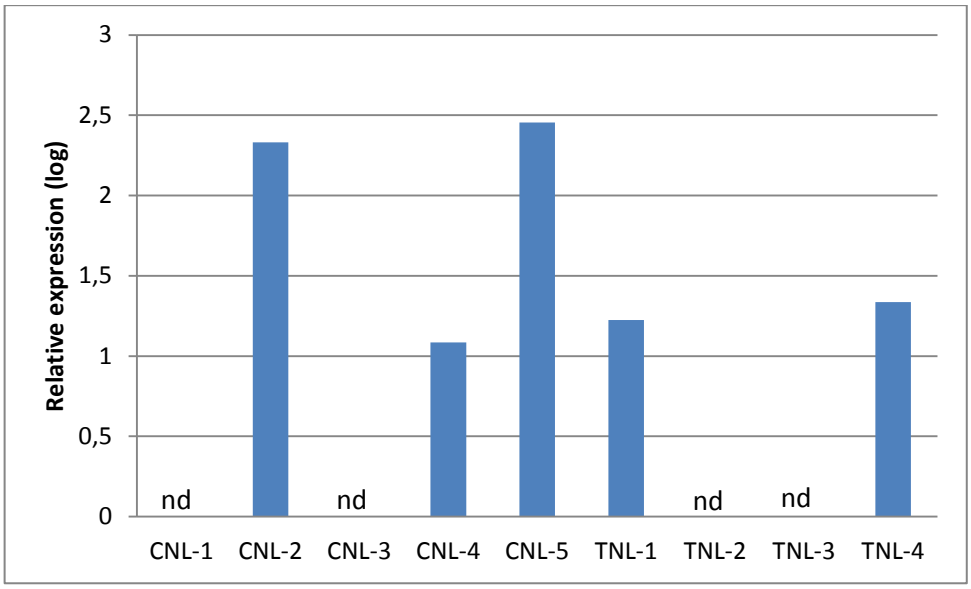

Figure 1. RNAseq results of *CNL* and *TNL* genes expression in *symCRK* mutant (NF0737). The expression of *CNL* (*CC-NBS-LRR*) and *TNL* (*TIR-NBS-LRR*) genes was evaluated by RNAseq using cDNAs prepared from RNAs extracted from wild-type R108 and *symCRK*^{R108} (NF0737) mutant nodules. Nodules were produced *in vitro* after inoculation with *S. medicae* WSM419 strain and harvested at 21 dpi. Fold change versus wild-type is presented after normalization with an *Actin* gene as an internal control and standardized with log (2).

Note that these results correspond to one experiment with one technical replicate. nd; not detected.

This result suggests that *CNL-2*, *CNL-4*, *CNL-5*, *TNL-1* and *TNL-4* genes may participate in defense reactions in *symCRK* nodules mutants, while *CNL-1*, *CNL3*, *TNL-2* and *TNL-3* genes are not participing in nodules defense reactions induction.

To check the implication of R proteins in nodules defense reactions, qPCR were performed on nodules cDNA extracted from fix$^-$ mutants (exhibiting defense-like reactions) inoculated with *S. medicae* WSM419 strain and from R108 and A17 wild-types inoculated with *S. medicae* WSM419 or the *E. adhaerens* T4 strains which is able to induce root-nodule formation and triggers nodule defense like-reactions. The primers used in this study are listed in the Table 1.

The results presented in figure 2, show that in the R108 background, the *CNL*-1 gene is slightly induced in wild-type nodules inoculated with the *E. adhaerens* T4 strain, but it is not induced in fix$^-$ *symCRK* (NF0737) and *dnf2* (MS240) mutant nodules induced with *S. medicae* WSM419. In the A17 background, the *CNL*-1 gene is strongly induced in fix$^-$ mutants *symCRK*^{A17} (dnf5-2) and *dnf2*^{A17} (dnf2) nodules induced with *S. medicae* WSM419, but not in wild-type nodules inoculated with the *E. adhaerens* T4 strain.

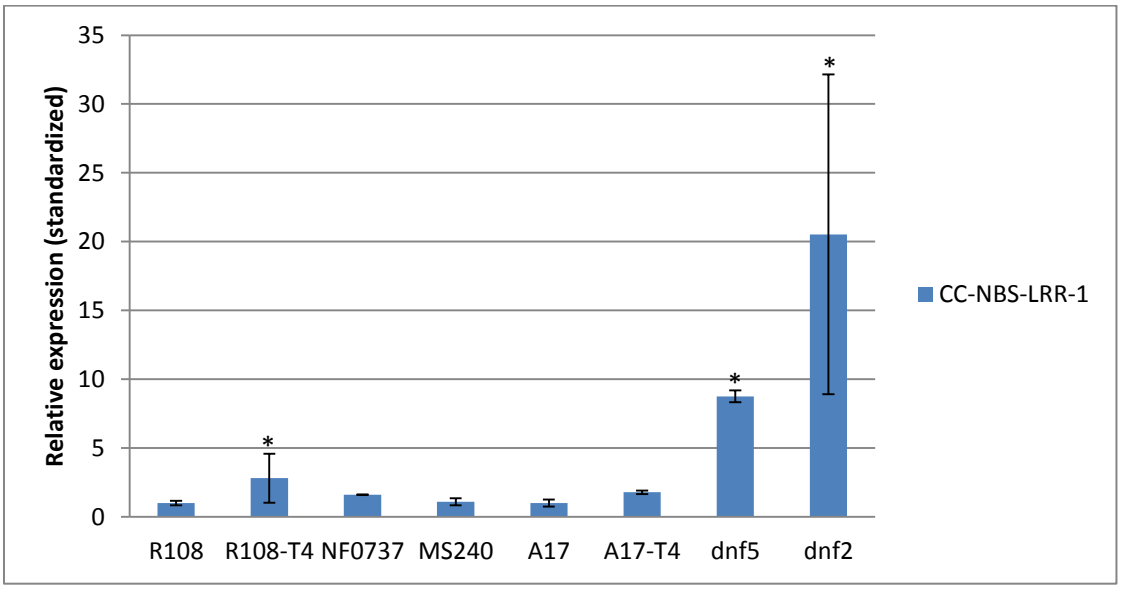

Figure 2. *CNL*-1 gene relative expression in nodules exhibit defense-like reactions. The expression of *CNL*-1 (*CC-NBS-LRR-1*) gene was evaluated by RT-qPCR using cDNAs prepared from RNAs extracted from R108 and A17 wild-types, *symCRK*^{R108} (NF0737), *dnf2*^{R108} (MS240), *symCRK*^{A17} (dnf5-2) and *dnf2*^{A17} (dnf2) mutants. Nodules were produced *in vitro* after inoculation with *S. medicae* WSM419 or with *E. adhaerens* T4 strains separately and harvested at 21 dpi. Fold change versus wild-type is presented after normalization with an *Actin* gene as an internal

control. Error bars, ± SE from three independent experiments with one technical replicate for each experiment. All the plants were inoculated with *S. medicae* unless indicated T4. Asterisks indicate significant induction (P<0.05) compared to the non-treated samples.

These results indicate that in the R108 background, the *CNL*-1 gene seems to play a role in the control of the bacterial internalization in symbiotic cells in R108 nodules. This suggests *CNL*-1 acting before DNF2^{R108}. However, in A17 Jemalong background nodules, the CNL-1 is implicated in the control of the bacterial internalization in symbiotic cells and is strongly controlled by symbiotic genes.

The results presented fig.3, show that in the R108 background, the expression of *CNL*-2 gene is strongly expressed in wild-type nodules induced with *E. adhaerens* T4 strain and slightly induced in fix$^-$ nodules (*symCRK* and *dnf2*). In A17 background the *E. adhaerens* T4 strain does not trigger the *CNL*-2 expression in wild-type nodules and its expression is even reduced in the mutant backgrounds.

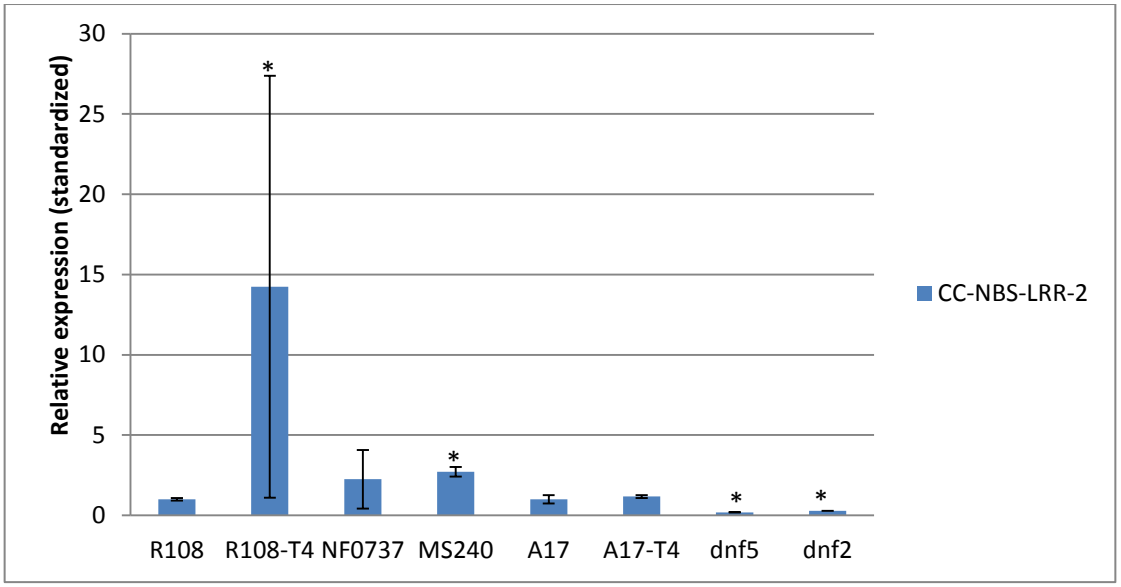

Figure 3. *CNL*-2 gene relative expression in nodules exhibit defense-like reactions. The expression of *CNL*-2 (*CC-NBS-LRR-2*) gene was evaluated by RT-qPCR using cDNAs prepared from RNAs extracted from R108 and A17 wild-types, *symCRK*^{R108} (NF0737), *dnf2*^{R108} (MS240), *symCRK*^{A17} (dnf5-2) and *dnf2*^{A17} (dnf2) mutants. Nodules were produced *in vitro* after inoculation with *S. medicae* WSM419 or with *E. adhaerens* T4 strains separately and harvested at 21 dpi. Fold change versus wild-type is presented after normalization with an *Actin* gene as an internal control. Error bars, ± SE from three independent experiments with one technical replicate for each experiment. All the plants were inoculated with *S. medicae* unless indicated T4. Asterisks indicate significant induction (P<0.05) compared to the non-treated samples.

These results indicate that the *CNL*-2 gene participate in the control of the infection of the symbiotic cells by rhizobia in R108 nodules. In contrast, the expression of this gene is negatively regulated by symbiotic genes in A17 nodules.

The results presented in fig.4 show that the *CNL*-3 gene expression is not affected in wild-type nodules induced by the *E. adhaerens* T4 strain nor in the mutant background. This indicates that the *CNL*-3 gene is not implicated in nodules defense reactions.

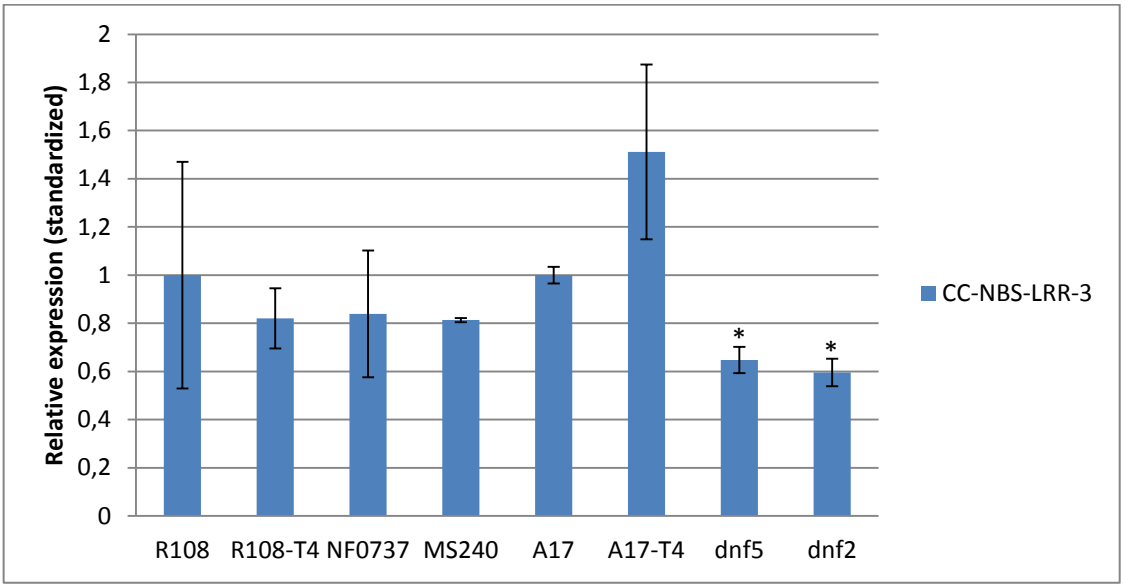

Figure 4. *CNL*-3 gene relative expression in nodule exhibit defense-like reactions. The expression of *CNL*-3 (*CC-NBS-LRR-3*) gene was evaluated by RT-qPCR using cDNAs prepared from RNAs extracted from R108 and A17 wild-types, *symCRK*^{R108} (NF0737), *dnf2*^{R108} (MS240), *symCRK*^{A17} (dnf5-2) and *dnf2*^{A17} (dnf2) mutants. Nodules were produced *in vitro* after inoculation with *S. medicae* WSM419 or with *E. adhaerens* T4 strains separately and harvested at 21 dpi. Fold change versus wild-type is presented after normalization with an *Actin* gene as an internal control. Error bars, ± SE from three independent experiments with one technical replicate for each experiment. All the plants were inoculated with *S. medicae* unless indicated T4. Asterisks indicate significant induction ($P<0.05$) compared to the non-treated samples.

The expression patern of *CNL*-3 gene in A17 is positively regulated by DNF2 and SymCRK. However, it seems this gene is not implicated in nodulation process in R108 background.

The results presented in Fig.5 indicate that the expression of *CNL*-4 gene was repressed in fix$^-$ nodules in both A17 and R108 backgrounds and also in A17 wild-type nodules induced with *E. adhaerens* T4 strain. However, the expression of this gene is not affect in R108 wild-type nodules induced with *E. adhaerens* T4 strain.

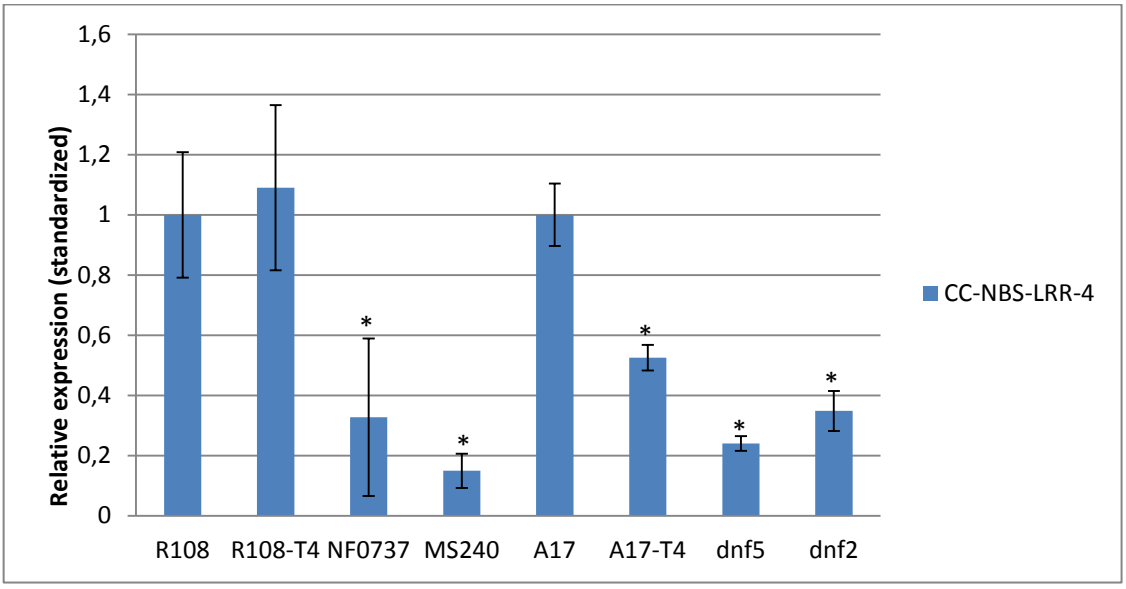

Figure 5. *CNL*-4 gene relative expression in nodules exhibit defense-like reactions. The expression of *CNL*-4 (*CC-NBS-LRR-4*) gene was evaluated by RT-qPCR using cDNAs prepared from RNAs extracted from R108 and A17 wild-types, *symCRK*^{R108} (NF0737), *dnf2*^{R108} (MS240), *symCRK*^{A17} (dnf5-2) and *dnf2*^{A17} (dnf2) mutants. Nodules were produced *in vitro* after inoculation with *S. medicae* WSM419 or with *E. adhaerens* T4 strains separately and harvested at 21 dpi. Fold change versus wild-type is presented after normalization with an *Actin* gene as an internal control. Error bars, ± SE from three independent experiments with one technical replicate for each experiment. All the plants were inoculated with *S. medicae* unless indicated T4. Asterisks indicate significant induction ($P<0.05$) compared to the non-treated samples.

The strong down regulation of CNL-4 gene expression in symbiotic mutants suggests an important role for the CNL-4 in the last steps of symbiotic cells infection by rhizobia.

The results presented in fig.6, show that the expression of *CNL*-5 gene was induced in wild-type R108 and A17 nodules inoculated with *E. adhaerens* T4 strain exhibiting defense-like reactions. Similarly, it is induced in fix$^-$ mutant nodules in both background exhibiting defense-like reactions, except for the line dnf5 (*symCRK*^{A17} mutant) which does not exhibit defense-like reactions and where *CNL*-5 gene expression was not affected.

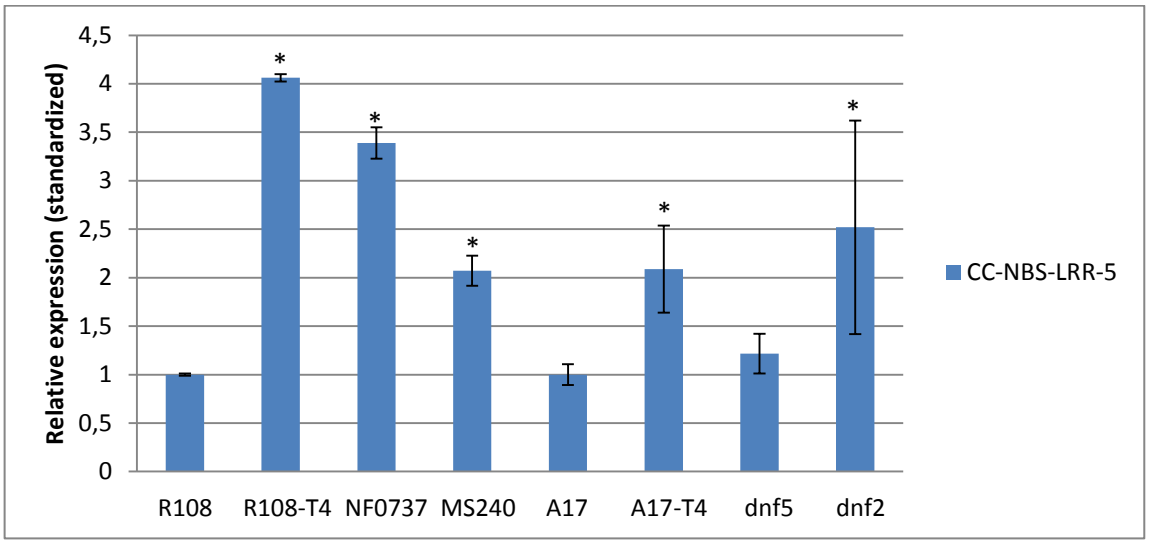

Figure 6. *CNL*-5 gene relative expression in nodules exhibit defense-like reactions. The expression of *CNL*-5 (*CC-NBS-LRR-5*) gene was evaluated by RT-qPCR using cDNAs prepared from RNAs extracted from R108 and A17 wild-types, *symCRK*^{R108} (NF0737), *dnf2*^{R108} (MS240), *symCRK*^{A17} (dnf5-2) and *dnf2*^{A17} (dnf2) mutants. Nodules were produced *in vitro* after inoculation with *S. medicae* WSM419 or with *E. adhaerens* T4 strains separately and harvested at 21 dpi. Fold change versus wild-type is presented after normalization with an *Actin* gene as an internal control. Error bars, ± SE from three independent experiments with one technical replicate for each experiment. All the plants were inoculated with *S. medicae* unless indicated T4**.** Asterisks indicate significant induction (P<0.05) compared to the non-treated samples.

These results indicated that the *CNL*-5 gene expression is induced in nodules mutants (MS240, dnf2 and NF0737) and in wild type nodules induced with *E. adhaerens* T4 exhibiting defense reactions. However, expression of *CNL*-5 gene is not induced in *symCRK*^{A17} mutant (dnf5-2) nodules exhibiting senescence. Moreover, *CNL*-5 gene is negatively controlled by DNF2 in both backgrounds and by SymCRK in R108 background. So CNL-5 seems to play a role in negatively regulating defense reactions in A17 and R108 nodules.

The results presented in fig.7, show that in the R108 background, the *TNL*-1 gene is slightly induced in wild-type nodules inoculated with *E. adhaerens* T4 strain, but it is not induced in fix$^-$ mutants *symCRK* (NF0737) and *dnf2* (MS240) nodules induced with *S. medicae* WSM419. In contrast, in the A17 background, the *TNL*-1 gene is strongly induced in the *symCRK* (dnf5-2) and *dnf2* (dnf2) mutant nodules induced with *S. medicae* WSM419, but not in wild-type nodules inoculated with *E. adhaerens* T4 strain.

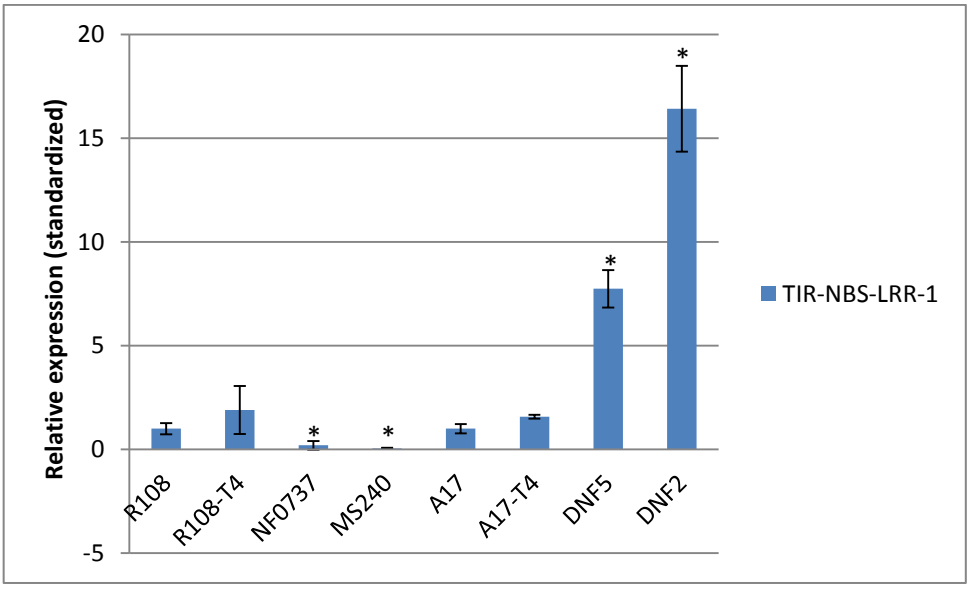

Figure 7. *TNL*-1 gene relative expression in nodules exhibit defense-like reactions. The expression of *TNL*-1 (*TIR-NBS-LRR-1*) gene was evaluated by RT-qPCR using cDNAs prepared from RNAs extracted from R108 and A17 wild-types, *symCRK*^{R108} (NF0737), *dnf2*^{R108} (MS240), *symCRK*^{A17} (dnf5-2) and *dnf2*^{A17} (dnf2) mutants. Nodules were produced *in vitro* after inoculation with *S. medicae* WSM419 or with *E. adhaerens* T4 strains separately and harvested at 21 dpi. Fold change versu wild-type is presented after normalization with an *Actin* gene as an internal control. Error bars, ± SE from three independent experiments with one technical replicate for each experiment. All the plants were inoculated with *S. medicae* unless indicated T4. Asterisks indicate significant induction ($P<0.05$) compared to the non-treated samples.

These results indicate that, the expression of *TNL*-1 gene is positively regulated by DNF2 and SymCRK in R108 nodules. In contrast, in A17 nodules, *TNL*-1 gene is negatively controlled by symbiotic proteins in A17 nodules.

The results presented in fig. 8 indicate that in the R108 background the expression of *TNL*-2 was not affected in wild-type nodules induced with *E. adhaerens* T4 strain. By contrast its expression in the symbiotic *symCRK* and *dnf2* mutant nodules was repressed. Similarly, in A17 background the *TNL*-2 gene expression was downregulated in *symCRK* and *dnf2* fix$^-$ nodules but not affected in wild-type nodules induced with *E. adhaerens* T4 strain despite that they are also fix-.

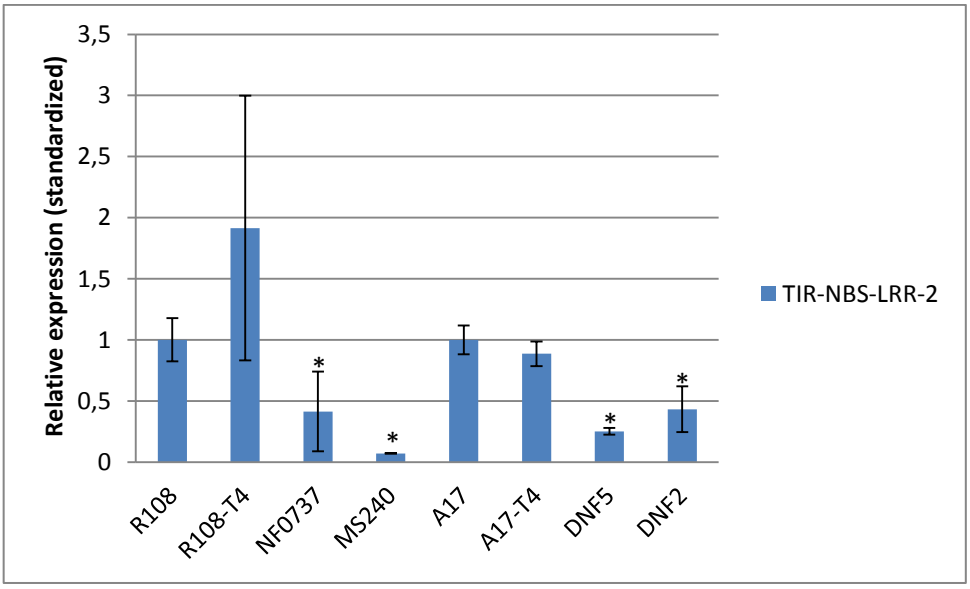

Figure 8. *TNL*-2 gene relative expression in nodules exhibit defense-like reactions. The expression of *TNL*-2 1 (*TIR-NBS-LRR-2*) gene was evaluated by RT-qPCR using cDNAs prepared from RNAs extracted from R108 and A17 wild-types, *symCRK*^{R108} (NF0737), *dnf2*^{R108} (MS240), *symCRK*^{A17} (dnf5-2) and *dnf2*^{A17} (dnf2) mutants. Nodules were produced *in vitro* after inoculation with *S. medicae* WSM419 or with *E. adhaerens* T4 strains separately and harvested at 21 dpi. Fold change versus wild-type is presented after normalization with an *Actin* gene as an internal control. Error bars, ± SE from three independent experiments with one technical replicate for each experiment. All the plants were inoculated with *S. medicae* unless indicated T4**.** Asterisks indicate significant induction (P<0.05) compared to the non-treated samples.

These results suggest that the symbiotic genes *symCRK* and *dnf2* in the two backgrounds control positively the expression of the *TNL*-2 gene. This results is similar to the one obtained for the *CNL*-4 gene. This suggests that the *TNL*-2 and *CNL*-4 are required to establish a functional nodule. On the other hand, these results suggest that these genes are not implicated in defense reaction triggered by *E. adhaerens* T4 strain.

The results presented in fig. 9 indicate that in the R108 background, the expression of the *TNL*-3 gene is induced in the *symCRK* and *dnf2* mutants or by the presence of the parasitic bacteria (*E. adhaerens* T4 strain) in the wild-type nodules. By contrast, in A17 background, the *TNL*-3 gene was induced in the fix$^-$ mutants (*symCRK* and *dnf2*) and not in wild-type nodules induced with the *E. adhaerens* T4 strain.

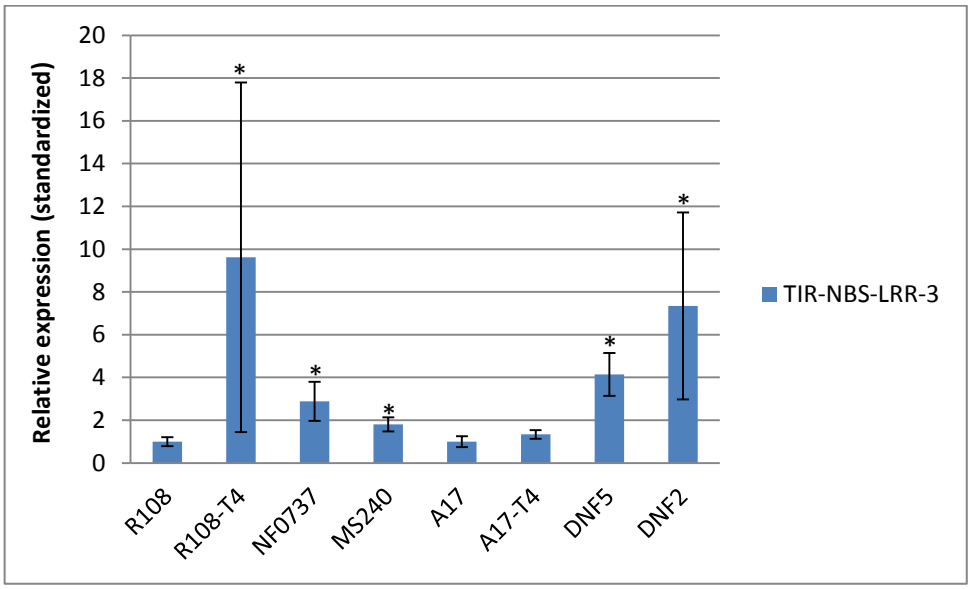

Figure 9. *TNL*-3 gene relative expression in nodules exhibit defense-like reactions. The expression of *TNL*-3 (*TIR-NBS-LRR-3*) gene was evaluated by RT-qPCR using cDNAs prepared from RNAs extracted from R108 and A17 wild-types, *symCRK*^{R108} (NF0737), *dnf2*^{R108} (MS240), *symCRK*^{A17} (dnf5-2) and *dnf2*^{A17} (dnf2) mutants. Nodules were produced *in vitro* after inoculation with *S. medicae* WSM419 or with *E. adhaerens* T4 strains separately and harvested at 21 dpi. Fold change versus wild-type is presented after normalization with an *Actin* gene as an internal control. Error bars, ± SE from three independent experiments with one technical replicate for each experiment. All the plants were inoculated with *S. medicae* unless indicated T4**.** Asterisks indicate significant induction (P<0.05) compared to the non-treated samples.

These results suggest *TNL*-3 gene is implicated in rhizobia internalization in R108 nodules and is controlled negatively by DNF2 and SymCRK in A17 and R108 nodules

The results presented in fig. 10 show that the *TNL*-4 gene was induced in wild-type nodules inoculated with *E. adhaerens* T4 strain and very slightly induced in symbiotic mutant nodules in R108 background. In the A17 background, the expression of the *TNL*-4 gene is induced in the *symCRK* and *dnf2* nodules and not induced in wild-type nodules inoculated with the *E. adhaerens* T4.

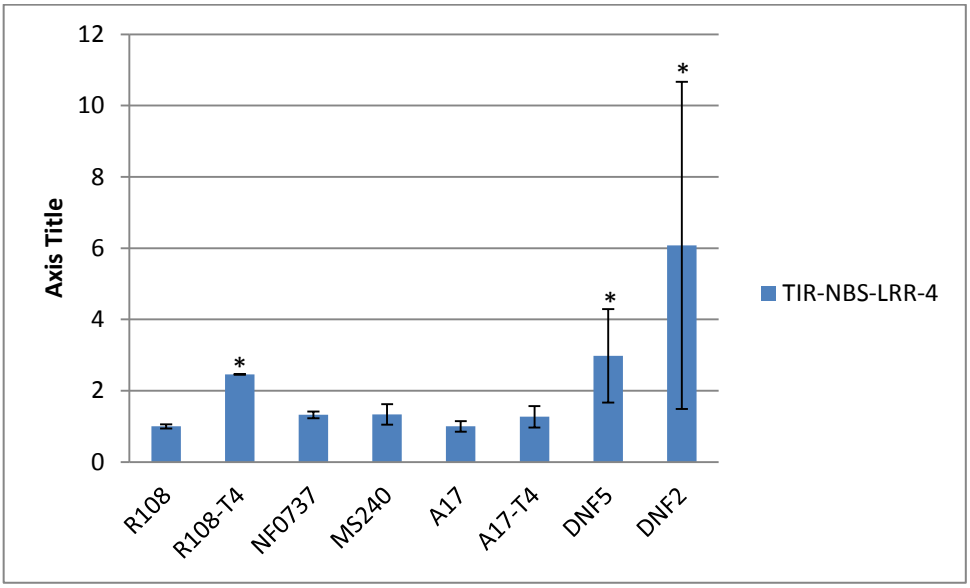

Figure 10. *TNL*-4 gene relative expression in nodules exhibit defense-like reactions. The expression of *TNL*-4 1 (*TIR-NBS-LRR-4*) gene was evaluated by RT-qPCR using cDNAs prepared from RNAs extracted from R108 and A17 wild-types, *symCRK*^{R108} (NF0737), *dnf2*^{R108} (MS240), *symCRK*^{A17} (dnf5-2) and *dnf2*^{A17} (dnf2) mutants. Nodules were produced *in vitro* after inoculation with *S. medicae* WSM419 or with *E. adhaerens* T4 strains separately and harvested at 21 dpi. Fold change versus wild-type is presented after normalization with an *Actin* gene as an internal control. Error bars, ± SE from three independent experiments with one technical replicate for each experiments. All the plants were inoculated with *S. medicae* unless indicated T4. Asterisks indicate significant induction ($P<0.05$) compared to the non-treated samples.

These results suggest that the *TNL*-4 gene expression is negatively regulated by symbiotic genes in the A17 nodules. In R108 nodules, the *TNL*-4 gene is slightly participating in the control of the rhizobia internalization in the symbiotic cells of R108 nodules. In contrast, *TNL*-4 gene expression is independent of symbiotic genes in this background.

Discussion

The implication of the tested *NBS-LRR* genes in defense reactions or in the establishment of successful nodulation varies in function of the plant genotype (fig.11 and 12). Among the tested *NBS-LRR* genes, the genes *CNL*-1, *CNL*-2, *CNL*-5, *TNL*-3, and *TNL*-4 were induced in the symbiotic mutants and/or by the presence of the parasitic bacteria in R108 and A17 nodules. This indicates that these genes participate in nodule defense reactions. In a previous study (see chapter III) I demonstrated that the mutation of the symbiotic genes *SymCRK*^{R108}, *DNF2*^{R108} and *DNF2*^{A17} results in inducing nodule defense reactions. In contrast, the mutation of the symbiotic gene *SymCRK* in the A17 background results in the induction of senescence instead of defense reactions. Moreover, the wild-type nodules induced with the *E. adhaerens* T4 strain exhibit defense reactions (chapter VI). Comparing this information to the expression patterns of the tested R proteins, the expression pattern of the *CNL*-5 gene reflects the defense and the senescence state. In fact, the *CNL*-5 gene expression is induced in *symCRK*^{R108}, *dnf2*^{R108} and *dnf2*^{A17} mutants and in wild-type nodules induced by the parasite *E. adhaerens* T4 which exhibiting nodules defense reactions but in the *symCRK*^{A17} nodule mutant which exhibiting senescence reaction, the *CNL*-5 gene expression is not modified. This interaction between NBS-LRR and pathogenes is often described in many studies. For exemple the *RPS5* gene belongs to the CC-NBS-LRR family and activates the effector triggered immunity (ETI) by recognizing indirectly the *Pseudomonas syringae Avr* gene *AvrPphB* (Ade *et al., 2*007). In nodules, the *TIR-NBS-LRR* genes *Rj2* (*Rhizobium japonicum 2*) and *Rj4* control the rhizobium infection of the symbiotic cells by the recognition of uncompatible rhizobia effectors (Tang *et al.*, 2016; Sugawara *et al.*, 2018). On the other hand, the suppression of *NBS-LRR* genes activity by silencing in legumes promotes the nitrogen-fixing symbiotic interaction and nodule formation for *M. truncatula* (Sós-Hegedüs *et al.*, 2019).

The expression of the genes *CNL*-4 and *TNL*-2 was repressed in the mutants and in nodules induced with the parasitic *E. adhaerens* T4 strain, suggesting that the expression of this gene correlate with a successful nodulation (bacteroid differentiation or nitrogen fixation). This suggests that these two genes participate in the control of the symbiotic cells infection in the late steps of nodulation.

The expression of *CNL*-2 and *TNL*-1 genes varies in function of the nodules background. The expression of *CNL*-2 was induced in R108 background nodules (in fix$^-$ mutants and in wild-type nodules induced with *E. adhaerens* T4). In contrast, in the A17 background, its expression was induced in fix$^-$ mutants and not affect in wild-type nodules induced with *E. adhaerens* T4. Similarly, the expression of *TNL*-1 was repressed in R108 fix$^-$ mutant nodules and not affected in wild-type nodules induced with *E. adhaerens* T4. However, in A17 background, its expression was induced in fix$^-$ mutants and not affect in wild-type nodule induced with *E. adhaerens* T4 strain (fig.11).

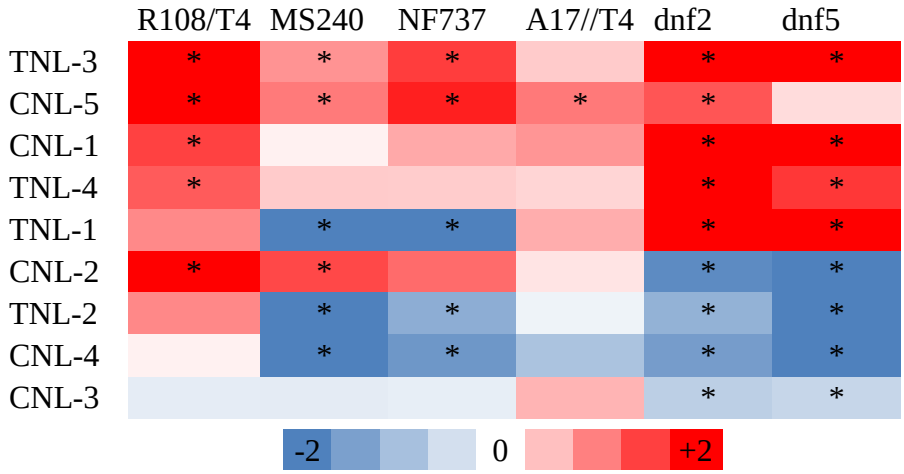

Figure 11. Heatmap showing the expression patterns of *NBS-LRR* genes. The expression of NBS-LRR genes was evaluated by RT-qPCR performed on RNAs extracted from A17 and R108 wild-type nodules induced with *S. medicae* WSM419 or with *E. adhaerens* T4, and from nodules of symbiotic mutants induced with *S. medicae* WSM419, the nodules were harvested at 21 dpi. Asterisks indicate significant induction/down regulation ($P<0.05$) compared to the wild-type nodules.

The expression of *CNL*-1 in R108 background was not affected in the mutant backgrounds but is induced by the presence of the non-fixing bacteria in wild-type nodules. Furthermore, its expression was induced in A17 fix$^-$ nodules and not affected by *E. adhaerens* T4 strain.

These results suggest that NBS-LRR proteins play multiple roles in the first and last steps of nodulation. The *CNL-5* gene seems to control the chronic infection of the symbiotic cells by rizobia. While, the *CNL*-4 and *TNL*-2 genes seem to control the infected symbiotic cells functioning in A17 and R108 backgrounds

In addition these results confirm the difference between the two *Medicago truncatula* ecotypes R108 and A17 observed in previous chapters.

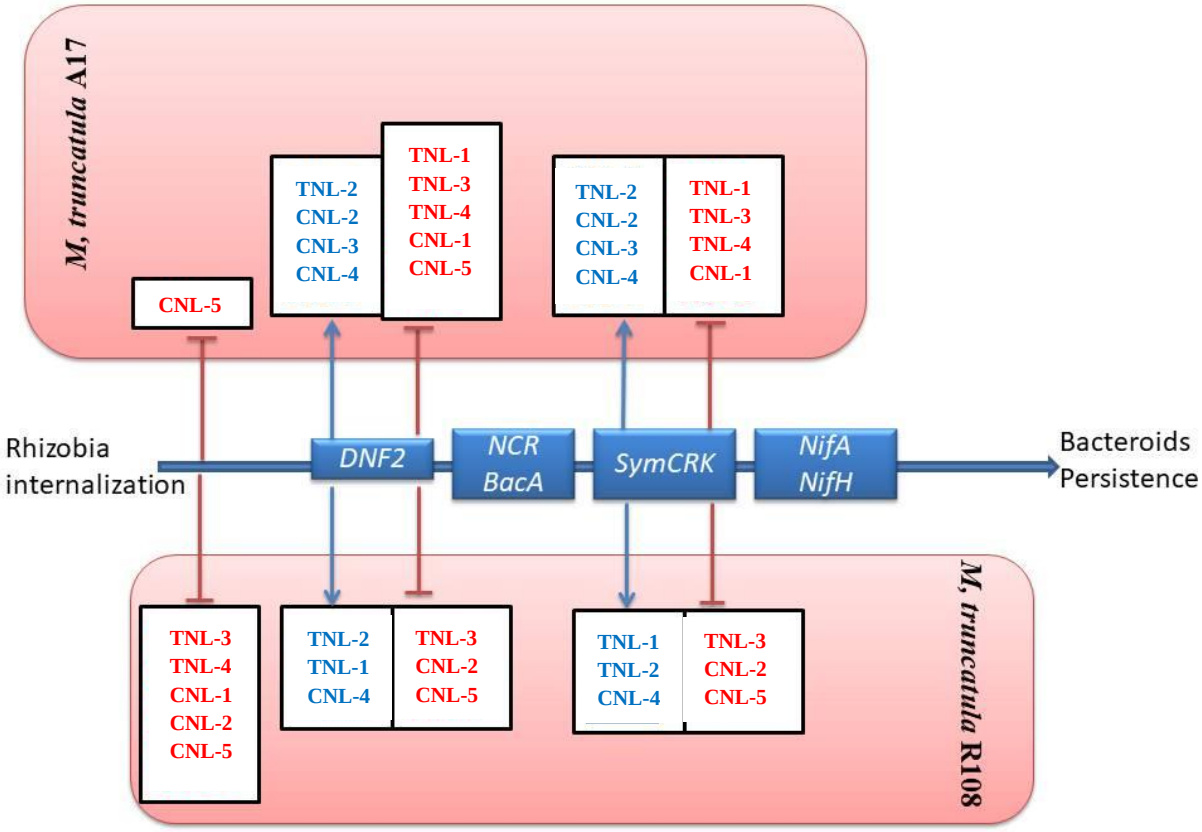

Figure 12. Model showing the expression patterns of *NBS-LRR* genes in the different steps of nodulation. Induced genes are in bleu color and not induced genes are in red color. Lines ending in bars indicate repression; Arrows indicate induction.

Conclusion

General discussion and conclusion

This thesis shows that *M. truncatula* used two different types of defense in *M. truncatula* nodules according to the plant ecotype. The phenotype of *symCRK*^{A17} nodules is caracterised by the formation of white non-fixing nodules that do not accumulate phenolic compounds and do not induce defense genes. In contrast these nodules induce the expression of cysteine protease genes which are senescence markers and jasmonic acid induced genes. . Basso et Veneault-Fourrey (2020) reported that the activation of JA pathway in *Astragalus sinicus* leads to formation of non-fixing white nodules. On the other hand, Guinel (2015) reported that jasmonic acid induce the expression of several lipoxygenase (*LOX*) genes involved in nodules senescence. In addition, Berrabah et al. (2014a) and Bourcy et al. (2013) suggested that the accumulation of the phenolic compound in nodules is linked to the activation of the nodules defense reactions. These data lead us to suggest that SymCRK^{A17} protein controls negatively the jasmonic acid pathway to prevent early senescence activation in mature nodules.

However, the nodules phenotypes of the *dnf2* mutants in the A17 and R108 backgrounds and in the *symCRK*^{R108} mutant exhibit necrotic-white nodules unable to fix atmospheric nitrogen, showing activation of defence gene expression and inducing ethylene and salicylic acid signaling pathways. These results are consistent with those of Berrabah et al. (2018b; 2014a) and Bourcy et al. (2013) which show that *dnf2* and *symCRK* mutant nodules exhibit defence reactions and activation of ethylene signaling pathway. In addition, the results obtained in this thesis suggest that the DNF2 protein controls also the salicylic acid signaling pathway in A17 and R108 nodules. In addition, DNF2 controls jasmonic acid signaling pathway in A17 nodules and also the ethylene signaling pathway in R108 nodules (fig.13). Thus, in both genetic backgrounds DNF2 appears to be directly related to the control of the salicylic acid signalling pathway. Bourcy et al (2013) and Berrabah et al. (2014b) demonstrated that DNF2 protein is required for nitrogen fixation and participates in the control of the nodule microbial environment. On the other hand, salicylic acid is an inhibitor of the formation and the development of undermined nodules (Lian *et al.,* 2000) and the degradation of the salicylic acid in roots cells by salicylic hydroxylase (NahG) leads to an increase in the nodules number (Stacey *et al.*, 2006b). All these results suggest that the DNF2 protein control the salicylic acid pathway to promote nodule formation and ensure effecient nitrogen fixation capacity.

The results also showed that jasmonic and ethylene have an antagonist effect in *M. truncatula* nodules. This antagonist affect is corelated with the results of Song et al. (2014) showing antagonist effect between the jasmonic acid transcription factors *MYC2* with ethylene transcription factors *EIN3* in *A. thaliana*. In addition, as observed in *A. thaliana* (Lawton *et al.*, 1994) salicylic acid and ethylene are acting in synergy to activate *PR1* gene expression in *M. truncatula* R108 nodules. These effects are clealy observed by the respression or the non-effect of ethylene and saliciylic acid on the expression of jasmonic acid related genes *VSP*, *MYC2b* and *MYC2c*. On the other hand, treatment with jasmonate represses the expression of the ethylene and salicylic related gene *PR1*.

In contrast, jasmonic acid and salicylic acid act in synergy in *M. truncatula* A17 nodules. This result aggree with the results obtained by Yang *et al.*, (2011), indicating that salicylic acid and jasmonic acid induce the expression of *PAL*, one of the key gene for phenolic production. In addition, the thesis results demonstrate that the *PR1* gene always considered as marker of the salicylic acid signaling (Pucciariello 2009) is more ethylene dependent in *Medicago*. Moreover, the expression of genes implicated in the ethylene biosynthesis pathway is induced by salicylic acid and jasmonic acid highlighting the crosstalk between the defense hormones.

The double role of NBS-LRR proteins is suggested in this study. The results suggest that some NBS-LRR genes like *CNL*-4 and *TNL*-2 are required for the establishement of succeful colonization of the symbiotic cells and nitrogen fixation by rhizobia, but this result need to be confirmed by genetic approaches. Other NBS-LRR protein like CNL-5, seems to be implicated in the control of the symbiotic cells invasion by rhizobia similarly to as Rj2 and Rj4 proteins (Tang *et al.*, 2016; Sugawara et al.. 2018). This gene need to be more investigated to confirm its role in the detection of uncompatible symbiotes.

On the other hand, this PhD thesis allowed finding a cheater partner of Medicago species: *Ensifer adhaerens* T4. This strain is able to induce the formation of non-functional nodules in *M. truncatula* R108, *M. Jemalong*, *M. sativa* and *M. polyphorma*. However, it is incomptatible with *Trifolium* and *Vicia hirsuta* species. Furthermore, *E. adhaerens* T4 is devoided of *fix* and *nif* genes explaining the non fixing phenotype and induction of nodules senescence and defense reactions. Moreover, *E. adhaerens* T4 strain behaves as a pathogen in contact with young seedlings of *M. truncatula* and *M. sativa*. In fact, *E. adhaerens* T4 is lethal for young seedlings of *M. truncatula* species. Nonetheless, the strain behaves as a pathogen

for *M. sativa* species and can sometimes kill the infected plants. In addition, *Vicia hirsuta, M. polymorpha Ciliaris* and *Trifolium* species seem to be resistant to the *E. adhaerens* T4.

Putting together all the results (Figure 13) suggests that CNL-4 and TNL-2 are positively regulated by DNF2 and SymCRK in both background A17 and R108. CNL-5, ethylene and salicylic acide signaling pathway are repressed by SymCRK and DNF2 proteines in *Medicago truncatula* R108 nodules. While, in *Medicago truncatula* A17 nodules, the DNF2 protein controls CNL-5, jasmonic acid and salicylic acid signaling pathways, and symCRK (dnf5) controls jasmonic acid signaling pathway independently of CNL-5.

This work gives more inside on the control of immunity during the cronic infection of the *M. truncatula* –rhizobium symbiosis.

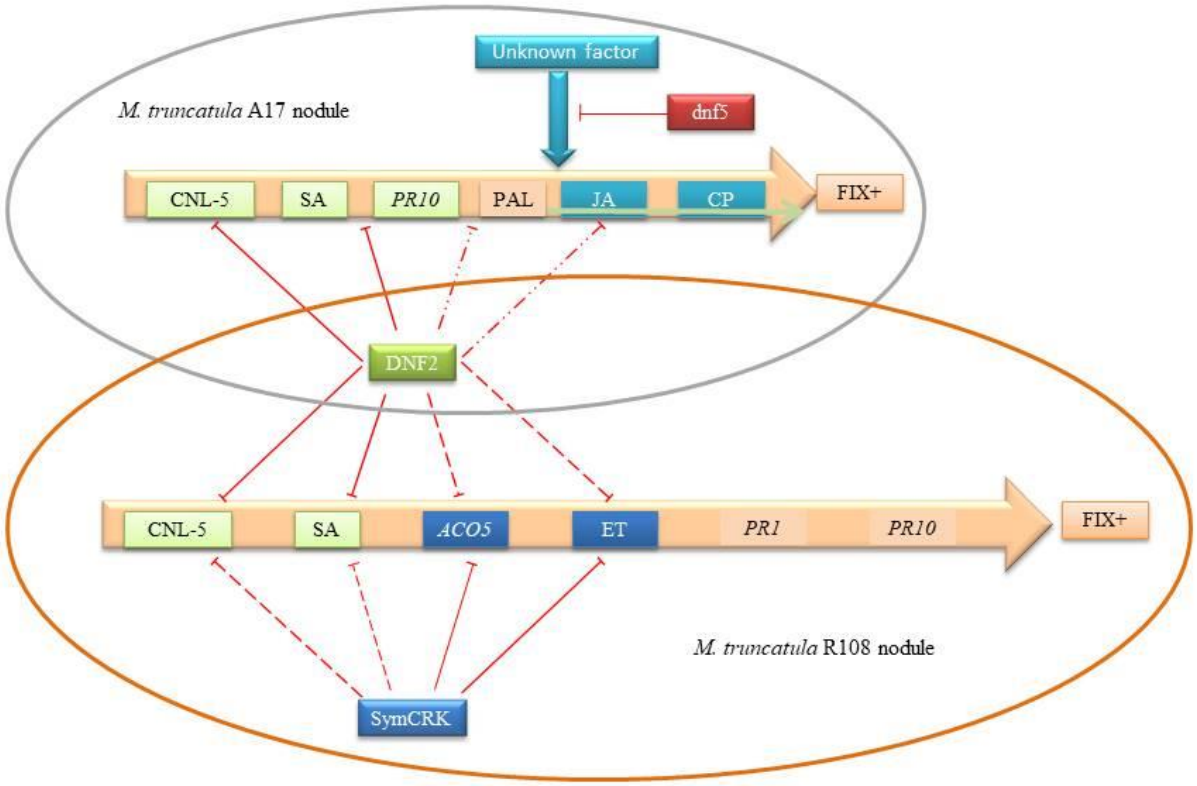

Figure 13. Hormonal signaling pathways regulation by symbiotic proteins DNF2 and SymCRK *in M. truncatula* R108 and A17 nodules

Références

Ade J. de Young BJ. Golstein C. and Innes RW. (2007) Indirect activation of a plant nucleotide binding site-leucine-rich repeat protein by a bacterial protease. Proceeding of Nat Acad SciUSA 104 2531–2536

Abdul M. Nurul A. Ilakiya Sharanee K. and Kalaivani N. (2020) Elicitor and Receptor Molecules: Orchestrators of Plant Defense and Immunity. International Journal of Molecular Sciences 21 (3): 963

Abeles FB. Morgan PW. and Saltveit M. (1992) Ethylene in Plant Biology 2nd edition Academic Press New York NY

Acevedo FE. Rivera-Vega LJ. Chung SH. Ray S. and Felton GW. (2015) Cues from chewing insects—the intersection of DAMPs HAMPs MAMPs and effectors. Curr Op in Plant Biology 26:80–86

Agrios GN (2005) Plant pathology 5th ed New York: Academic 922 p.

Alam I. Antunes A. Kamau AA. alawi W. Kalkatawi M. Stingl U. et al (2013) INDIGO – integrated Data Warehouse of Microbial Genomes with Examples from the Red Sea Extremophiles. PLOS ONE 8 (12) e82210

Alunni B. and Gourion B. (2016) Terminal bacteroid differentiation in the legume-rhizobium symbiosis: nodule-specific cysteine-rich peptides and beyond New Phytol 211:411–417

Anderson LA. Islam MA. and Prather KLJ. (2018) Synthetic biology strategies for improving microbial synthesis of "green" biopolymers. J Biol Chemis. 293:5053–5061

Ané JM. Kiss GB. Riely BK. Penmetsa RV. Oldroyd GED. Ayax C. Levy J. Debelle F. Baek JM. Kalo P. Rosenberg C. Roe BA. Long SR. Denarie J. and Cook DR. (2004) *Medicago truncatula*-DMI1 required for bacterial and fungal symbioses in legumes. Science 303:1364–1367

Arc E. Sechet J. Corbineau F. Rajjou L. and Marion-Poll A. (2013) ABA crosstalk with ethylene and nitric oxide in seed dormancy and germination. Fron Plant Sci. 4: 63

Ariel F Brault-Hernandez M Laffont C Huault E Brault M Plet J et al (2012) Two direct targets of cytokinin signaling regulate symbiotic nodulation in *Medicago truncatula.* Plant Cell 24:3838–3852

Assis SMP. Mariano RLR. Michereff SJ. and Coelho RSB. (1996) Biocontrol of *Xanthomonas campestris pv campestris* on kale with *Bacillus* spp and endophytic bacteria In Advances in Biological control of Plant Diseases Edição no 2; Wenhua T Cook RJ. and Rovira Eds.; China Agricultural University Press: Beijing China 347-353

Atkinson EM Palcic MM Hindsgaul O and Long SR (1994) Biosynthesis of Rhizobium melilotili popolysaccharide Nod factors: NodA isrequired for an N-acyltransferase Proc Nat Acad Sci. USA 91: 8418–8422

Basso V. and Veneault-Fourrey C. (2020) The role of jasmonates in beneficial microbe-root interactions. In Jasmonate in Plant Biology Jasmonate in Plant Biology: Methods and Protocols Methods in Molecular Biology; 2085:43-67 Antony Champion and Laurent Laplaze (eds) Springer

Beckers G and Conrath U (2007) Priming for stress resistance: from the lab to the field. Curr Op in Plant Biol 10:425-431

Beijersbergen JC. and Bergman BHH. (1973) The influence of ethylene on the possible resistance mechanism of the tulip *(Tulipa* spp.) against *Fusarium oxysporum.* Acta Bot Neerl. 22:172

Berrabah F. Ait Salem E. Garmier M. and Ratet P. (2018a) The Multiple Faces of the Medicago-Sinorhizobium Symbiosis In Functional Genomics in *Medicago truncatula* édité par Luis A Cañas et José Pío Beltrán 1822:241-260

Berrabah F. Balliau T. Aït-Salem EH. George J. Zivy M. Ratet P. and Gourion B (2018b) Control of the ethylene signaling pathway prevents plant defenses during intracellularaccommodation of the rhizobia New Phytol 219 (1): 310–323

Berrabah F. Bourcy M. Eschstruth A. Cayrel A. Guefrachi I. Mergaert P. et al (2014a) A nonRD receptor-like kinase prevents nodule early senescence and defense-like reactions during symbiosis New Phytol 203:1305–1314

Berrabah F. Bourcy M. Cayrel A. Eschstruth A. Mondy S. Ratet P. and Gourion B. (2014b) Growth conditions determine the DNF2 requirement for symbiosis PLOS ONE 9:e91866

Berrabah F. Ratet P. and Gourion B. (2015) Multiple steps control immunity during the intracellular accommodation of rhizobia J Ex Bot. 66:1977–1985

Biale JB. (1940) Effect of emanations from several species of fungi on respiration and colour development of citrus fruits. *Science* 91, 458

Bleecker AB.. and Kende H. (2000) Ethylene: A gaseous signalmolecule in plants Annu Rev Cell Dev Biol. 16 1–18

Bleecker AB. Estelle MA. Somerville C. and Kende H. (1988) Insensitivity to ethylene conferred by a dominant mutation in *Arabidopsis thaliana* Science. 241 1088-1089

Blilou I. Ocampo JA. and García-Garrido JM. (1999) Resistance of pea roots to endomycorrhizal fungus or Rhizobium correlates with enhanced levels of endogenous salicylic acid. J Exp Bot. 50: 1663-1668

Böhm H. Albert I. Fan L. Reinhard A. and Nuernberger T. (2014) Immune receptor complexes at the plant cell surface. Curr Opin Plant Biol. 20:47–54

Boller T. and Felix GA. (2009) renaissance of elicitors: perception of microbe-associated molecular patterns and danger signals by pattern-recognition receptors. Annu Rev Plant Biol. 60 379–406

Bolton MD. (2009) Primary metabolism and plant defense – fuel for the fire. Mol Plant Microbe Interac.t 22 487–497

Bourcy M. Brocard L. Pislariu CI. Cosson V. Mergaert P. Tadege M. et al (2013) *Medicago truncatula* DNF2 is a PI-PLC-XD-containing protein required for bacteroid persistence and prevention of nodule early senescence and defense-like reactions New Phytol. 197:1250–1261

Breakspear A. Liu C. Roy S. Stacey N. Rogers C. Trick M. et al. (2014) The root hair "infectome" of *Medicago truncatula* uncovers changes in cell cycle genes and reveals a requirement for Auxin signaling in rhizobial infection. Plant Cell 26:4680–4701

Broekgaarden C. Voorrips RE. Dicke M. and Vosman B. (2011) Transcriptional responses of Brassica nigrato feeding by specialist insects of different feeding guilds Insect. Science. 18:259–272

Burd G. Dixon DG. and Glick BR. (2000) Plant growth promoting bacteriathat decrease heavy metal toxicity in plants. Can J Microbiol. 46:237–245

Burton JC. (1984) Legume Inoculant Production Manual University of Hawaii Department of Agronomy and Soil. Scie Coll Trop Agri Hum Res Hawaii. USA Pp 11-16

Campos-Vargas R. and Saltveit ME. (2002) Involvement of putativewound signals in the induction of phenolic metabolism in wounded lettuce. Physiol Plant. 114:73–84

Capoen W. Den Herder J. Sun .J Verplancke C. De Keyser A. De Rycke R. Goormachtig S. Oldroyd G. and Holsters M. (2009) Calcium spiking patterns and therole of the calcium/calmodulin-dependent kinase CCaMK in lateral root base nodulation of Sesbania rostrate. Plant Cell. 21 1526–1540

Casida LE. (1982) *Ensifer adhaerens* gen nov sp nov: abacterial predator of bacteria in soil. Int J Syst Bacteriol. 32: 339–45

Cerri MR. Frances L. Laloum T. Auriac MC. Niebel A. Oldroyd GE. Barker DG. Fournier J. and de Carvalho-Niebel F. (2012) *Medicago truncatula* ERN transcription factors: regulatory interplay with NSP1/NSP2 GRAS factors and expression dynamics throughout rhizobial infection. Plant Physiol. 160; 2155–2172

Cheng X. Wen J. Tadege M. Ratet P. and Mysore KS. (2011) Reverse genetics in *Medicago truncatula* using *Tnt1* insertion mutants. Meth Mol Biol. 678: 179–190

Chuberre C. Plancot B. Driouich A. Moore JP. Bardor M. Gügi B. and Vicré M. (2018) Plant Immunity Is Compartmentalized and Specialized in Roots. Front Plant Sci. 9:1692

Coll NS. Epple P. and Dangl JL. (2011) Programmed cell death in the plant immune system. Cell Death Differ. 18:1247–56

Combier JP. Frugier F. de Billy F. Boualem A. El-Yahyaoui F. Moreau S. et al (2006) *MtHAP*2-1 is a key transcriptional regulator of symbiotic nodule development regulated by microRNA169 in *Medicago truncatula* Genes. Dev. 20:3084–3088

Cook DE. Mesarich CH. and Thomma BP. (2015) Understanding plant immunity as a surveillance system to detect invasion. Annu Rev Phytopatho. l53 541–563

Couto D. and Zipfel C. (2016) Regulation of pattern recognition receptor signalling in plants. Nature Rev

Immunol. 16 537–552

Couzigou JM. Zhukov V. Mondy S. Abu el Heba G. Cosson V. Ellis TH. et al (2012) NODULE ROOT and COCHLEATA maintain nodule development and are legume orthologs of Arabidopsis BLADE-ON-PETIOLE genes. Plant Cell 24:4498–4510

Cren M. Kondorosi Á.and Kondorosi E. (1994) An insertional pointmutation inactivates *NolR* repressor in *Rhizobium meliloti* 1021. J Bacteriol. 176:518–519

Csukasi F. Merchante C. and Valpuesta V. (2009) Modification of plant hormone levels and signaling as a tool in plant biotechnology. Biotechnol J. 4: 1293–1304

Cui H. Tsuda K. and Parker JE. (2015) Effector-triggered immunity: From pathogen perception to robust defense. Annu Rev Plant Biol. 66 487–511

Czernic P. Gully D. Cartieaux F. Moulin L. Guefrachi I. Patrel D. *et al.* (2015) Convergent evolution of endosymbiont differentiation in dalbergioid and inverted repeat-lacking clade legumes mediated by nodule-specific cysteine-rich peptides. Plant Physiol. 169:1254–1265

D'Erfurth I. Cosson V. Eschstruth A. Lucas H. Kondorosi A. and Ratet P. (2003) Efficient transposition of the *Tnt1* tobacco retrotransposon in the model legume *Medicago truncatula.* Plant J. 34: 95–106

Dakora FD. (2003) Defining new roles for plant and rhizobial molecules in sole and mixed plant cultures involving symbiotic legumes. New Phytol. 58:39–49

Dangl JL. and Jones JD. (2001) Plant pathogens and integrated defence responses to infection. Nature. 411 826–833

De Meyer SE. De Beuf K. and Vekeman B. (2015) A large diversity of non-rhizobial endophytes found in legume root nodules in Flanders (Belgium). Soil Biol Biochem. 83:1-11

De Vleesschauwer D. Xu J. and Höfte M. (2014) Making sense of hormone-mediated defense networking: from rice to Arabidopsis. Front Plant Sci. 51–15

Demont N. Ardourel M. Maillet F. Promé M. Ferro D. Proméand J-C. Dénarié J. (1994) The Rhizobium meliloti regulatory nodD3 and syrM genes control the synthesis of a particular class of nodulation factors N-acylatedby (omega-1)-hydroxylated fatty acids. EMBO J. 13:2139–2149

Denarié J. Debelle F. and Prome JC. (1996) Rhizobiumlipo-chitooligosac-charide nodulation factors: signaling molecules mediating recognition andmorphogenesis. Annu Rev Biochem. 65:503–535

Ding Y. Sun T. Ao K. Peng Y. Zhang Y. Li X. and Zhang Y. (2018) Opposite Roles of Salicylic Acid Receptors NPR1 and NPR3/NPR4 in Transcriptional Regulation of Plant Immunity. Cell 173 1454–1467

Ding Y. and Oldroyd GED. (2009) Positioning the nodule, the hormone dictum. Plant Signal Behav. 4: 89 – 93.

Dixon RA. Achnine L. Kota P. Liu C-J. Reddy MSS. and Wang L. (2002) The phenylpropanoid pathway and plant defence a genomics perspective. Mol Plant Pathol 3 371–390

Doares SH. Narváez-Vásguez J. Conconi A. and Ryan CA. (1995) Salicylic acid inhibits synthesis of proteinase inhibitors in tomato leaves induced by systemin and jasmonic acid. Plant Physiol. 108: 1741-1746

Dodds PN. Rathjen J.P (2010) Plant immunity: towards an integrated view of plant-pathogen interactions. Nat Rev Genet. 11:539–48

Domonkos A. Horvath B. Marsh JF. Halasz G. Ayaydin F. Oldroyd GE. And Kalo P. (2013) The identification of novel loci required for appropriate nodule development in *Medicago truncatula.* BMC PlantBiol. 11(13)157

Ecker JR. (1995) The ethylene signal transduction pathway in plants. Science 268: 667–75

Ehrhardt DW. Atkinson EM. Long SR. (1992) Depolarization of alfalfa root hairmembrane potential by *Rhizobium meliloti* nod factors. Science 256: 998–1000

Endre G. Kereszt A. Kevei Z. Mihacea S. Kalo P. and Kiss GB. (2002) A receptor kinase gene regulating symbiotic nodule development. Nature. 417962–966

Esnault R. Buffard D. Breda C. Sallaud C. El Turk J. and Kondorosi A. (1993) Pathological and molecular characterizations of alfalfa interactions with compatible and incompatible bacteria *Xanthomonas campestris pv alfalfae* and *Pseudomonas syringae pv pisi*. Mol Plant-Microbe Interact. 6:655-664

Fagard M. Alban L. Julia Gilles C. Dellagi A. Courtial M. Farjad A. Krapp MCS. and Céline MD. (2014) Nitrogen metabolism meets phytopathology. J Exp Bot. 5643–5656

Fait A. Hanhineva K. Beleggia R. Dai N. Rogachev I. Nikiforova VJ. Fernie AR. and Aharoni A. (2008) Reconfiguration of the achene and receptacle metabolic networks during strawberry fruit development. Plant Physiol. 148 730–750

Farkas A. Maróti G. Durgő H. Györgypál Z. Lima RM. Medzihradszky KF. et al (2014) *Medicago truncatula* symbiotic peptide NCR247 contributes to bacteroid differentiation through multiple mechanisms. Proc Natl Acad Sci USA. 111:5183–5188

Fernandez-Lopez M. Goormachtig S. Gao M. D'Haeze W. Van Montagu M. Holsters M. (1998) Ethylene-mediated phenotypic plasticity in root nodule development on Sesbania rostrate. Proc Natl Acad Sci USA. 95:12724–12728

Ferrari S. Savatin DV. Sicilia F. Gramegna G. Cervone F. De Lorenzo G. (2013) Oligogalacturonides: plant damage-associated molecularpatterns and regulators of growth and development. Front in Plant Sci. 4 49

Feys BJ. Benedetti CE. Penfold CN. and Turner JG. (1994) Arabidopsis mutants selected for resistance to the phytotoxin coronatine are male sterile insensitive to methyl jasmonate and resistant to a bacterial pathogen. Plant Cell 6:751-759

Fliegmann J. Canova S. Lachaud C. Uhlenbroich S. Gasciolli V. Pichereaux C. Rossignol M. Rosenberg C. Cumener M. Pitorre D. et al (2013) Lipo-chitooligosaccharidic symbiotic signals are recognized by LysM receptor-like kinase LYR3 in the legume *Medicago truncatula.* ACS Chemic Biol. 8: 1900–1906

Flor HH. (1971) Current status of the gene-for-gene concept. Annu Rev Phytopathol. 9:275–296

Fondevilla S. Kuster H. Krajinski F. Cubero JI. and Rubiales D. (2011) Identification of genes differentially expressed in a resistant reaction to *Mycosphaerella pinodes* in pea using microarray technology. BMC Genomics. 12 28

Freebairn HT. and Buddenhagen IW (1964) Ethylene production by Pseudomonas solanacearum. Nature 202:313–314

Freiberg C. Fellay .R Bairoch A. Broughton WJ. Rosenthal A. and Perret X. (1997) Molecular basis between rhizobium and legumes. Nature 387 394-401

Fritig B. Heitz T. Legrand M. (1998) Antimicrobial proteins ininduced plant defense .Curr Opin Immunol. 10:16–22

Fukuda H. and Ogawa T (1989). Microbial ethylene production. in Mattoo A. et Jeffrey CS (1991) The Plant Hormone Ethylene Boca Raton FL: CRC Press (Reissued 2018 by CRC Press)

Gamas P. Brault M. Jardinaud M. Frugier F. (2017) Cytokinins in symbiotic nodulation: when where what for? Trends Plant Sci. 22:792–802

Garcia-Brugger A. Lamotte O. Vandelle C. Bourque S. Lecourieux D. Poinsot B. Wendehenne D. and Pugin A. (2006) Early signaling events induced by elicitors of plant defenses. Mol Plant-Microbe-Inter-act. 19:711-724

Gavrin A. Kulikova O. Bisseling T. Fedorova EE. (2017) Interface symbiotic membrane formation in root nodules of *Medicago truncatula*: the role of synaptotagmins *MtSyt1 MtSyt2* and *MtSyt3.* Front Plant Sci. 8:1–10

Geremia RA. Mergaert P. Geelen D. van Montagu M. and Holsters M. (1994) The NodC protein of *Azorhizobium caulinodans* is an N-acetylglu-cosaminyl transferase. Proc Natl Acad Sci. 91:2669–2673

Glick BR. and Pasternak JJ. (2003) Molecular biotechnology: principles and applications of recombinant DNA. 3 d edition 538-593. ASM Press American Society for Microbiology Washington USA

Godiard L. Lepage A. Moreau S. Laporte D. Verdenaud M. Timmers T. Gamas P. (2011) MtbHLH1 a bHLH transcription factor involved in *Medicago truncatula* nodule vascular patterning and nodule to plant metabolic exchanges. New Phytol. 191:391–40

Gonzalez-Rizzo S. Crespi M. and Frugier F. (2006) The *Medicago truncatula* CRE1 cytokinin receptor regulates lateral root development and early symbiotic interaction with *Sinorhizobium meliloti.* Plant Cell. 18:2680–2693

Goto M. Ishida Y. Takikawa Y. and Hyodo H. (1985) Ethylene production by the Kudzu strains of *Pseudomonas syringae* pv. *phaseolicola* causing halo blight in *Pueraria lobara* (Willd) Ohwi. Plant Cell Plzysiol. 26:141

Göttfert M. Grob P. and Hennecke H. (1990) Proposed regulatory pathway encoded by the *nodV* and *nodW* genes determinants of host specificity in *Bradyrhizobium japonicum.* Proc Natl Acad Sci. 87:2680–2684

Gough C. Cottret L. Lefebvre B. and Bono JJ. (2018) Evolutionary History of Plant LysM Receptor Proteins Related to Root Endosymbiosis. Front Plant Sci. 9:923

Gourion B. Berrabah F. Ratet P. Stacey G. (2015) Rhizobium – legume symbioses: the crucial role of plant immunity. Trends Plant Sci. 20:186–194

Grichko VP. Glick BR. (2001) Amelioration of flooding stress by ACC deaminase-containing plant growth-promoting bacteria. Plant Physiol Bioch 39:11–17

Grobbelaar N. Clarke B. and Hough MC. (1971) The nodulation and nitrogen fixation of isolated roots of *Phaseolus vulgaris* LIII. The effect of carbon dioxide and ethylene. Plant Soil 35 215–223

Gu YQ. Yang C. Thara VK. Zhou J. and Martin GB. (2000) *Pti4* is induced by ethylene and salicylic acid and its product is phosphorylated by the *Pto* kinase. The Plant Cell 12: 771-785

Guan D. Stacey N. Liu C. Wen J. Mysore KS. Torres-Jerez I. et al (2013) Rhizobial infection is associated with the development of peripheral vasculature in nodules of *Medicago truncatula.* Plant Physiol. 162:107–115

Gubry-Rangin C. Garcia M. and Béna G. (2010) Partner choice in *Medicago truncatula*-Sinorhizobium symbiosis. Proc Biol Sci. 277(1690):1947–1951

Guinel FC. (2015) Ethylene a hormone at the center-stage of nodulation. Front Plant Sci. 6:1121

Gupta V. Willits MG. and Glazebrook J. (2000) *Arabidopsis thaliana EDS4* contributes to salicylic acid (SA)–dependent expression of defense responses: Evidence for inhibition of jasmonic acid signaling by SA. Mol Plant-Microbe Interact. 13 503–511

Gupta S. and Pandey S. (2019) Unravelling the biochemistry and genetics of ACC deaminase- An enzyme alleviating the biotic and abiotic stress in plant.s Plant Gene 18:100175

Guzman P. and Ecker JR. (1990) Exploiting the triple response of Arabidopsis to identify ethylene-related mutants. Plant Cell 2 513- 523

Gyaneshwar P. Hirsch AM. Moulin .I Chen WM. Elliott GN. Bontemps C. Estrada de Los Santos P. Gross E. Dos Reis Junior FB. Sprent JI. Young JP. And James EK. (2011) Legume-nodulating betaproteobacteria: diversity host range and future prospects. Mol Plant Microbe Interact. 24: 1276–1288

Haag AF. Baloban M. Sani M. Kerscher B. Pierre O. Farkas A. et al (2011) Protection of Sinorhizobium against host cysteine-rich antimicrobial peptides is critical for symbiosis. PLOS Biol 9:e1001169

Hall AE. Findell JL. Schaller GE. Sisler EC. and Bleecker AB. (2000) Ethylene perception by the ERS1 protein in Arabidopsis. Plant Physiol. 123 1449–1458

Haney CH. and Long SR. (2010) Plant flotillins are required for infection by nitrogen- fixing bacteria. Proc Natl Acad Sci USA. 107:478–483

Hassan S. and Mathesius U. (2012) The role of flavonoids in root-rhizosphere signalling: opportunities and challenges for improving plant-microbe interactions. J Exp Bo.t 63 3429–3444

He XZ. and Dixon RA. (2000) Genetic manipulation of isoflavones 7-O- methyltransferase enhances biosynthesis of 42-O-methylated isoflavonoid phytoalexins and disease resistance in alfalfa Plant. Cell 12 1689–1702

He Y. Fukushige H. Hildebrand DF. and Gan S. (2002) Evidence supporting a role of jasmonic acid in Arabidopsis leaf senescence. Plant Physiol. 128:876–84

Heath MC. (2000) Nonhost resistance and non-specific plant defenses.Curr Opin Plant Biol. 3:315–319

Heidstra R. and Bisseling T. (1996) Nod factor-induced host responses and mechanisms of Nod factor perception. New Phytol. 133 25–43

Hirsch S. Kim J. Munoz A. Heckmann AB. Downie JA. Oldroyd GE. (2009) GRAS proteins form a DNA binding complex to induce gene expressionduring nodulation signaling in *Medicago truncatula.* Plant Cell 21:545–557

Horváth B. Domonkos Á. Kereszt A. Szűcs A. Ábrahám E. Ayaydin F. et al (2015) Loss of the nodule-specific cysteine rich peptide NCR169 abolishes symbiotic nitrogen fixation in the *Medicago truncatula* dnf7 mutant. Proc Natl Acad Sci USA. 112:15232–15237

Horvath B. Bachem CWB. Schell J. Kondorosi A. (1987) Host-specific regulation of nodulation genesin Rhizobium is mediated by a plant-signal interacting with the *nodD* gene product. EMBO J. 6:841-4853

Howieson J. Ewing M. (1986) Acid tolerance in *the Rhizobium meliloti*–Medicago symbiosis. Austra J Agri Res. 37:55–64

Ilag L. and Curtis R. (1968) Production of ethylene by fungi. Science 159:1357

Jia YJ. Ito H. Matsui H. Honma M. (2000) 1-Aminocyclopropane-1-carboxylate (ACC) deaminase induced by ACC synthesized andaccumulated in *Penicillium citrium* intracellular spaces. Bioscience Biotec and Bioch. 64 299–305

Jiang JL. Wu S. Fan W. Li L. Dong and Cheng Q. (2015) Isolation and characterization of a novel pathogenesis-Related protein gene (*GmPRP*) with induced expression in soybean (*Glycine max*) during infection with phytophthora sojae. PLOS One 10 e0129932

John M. Röhrig H. Schmidt J. Wieneke U. and Schell J. (1993) Rhizobium NodB protein involved in nodulation signal synthesis is a chitooligosaccharide deacetylas.e Proc Natl Acad Sci USA. 90:625–629

Johnson PR. and Ecker JR. (1998) The ethylene gas signal transduction pathway: A molecular perspective. Annu RevGenet 32, 227–254

Jones JD. Vance RE. and Dangl JL. (2016) Intracellular innate immune surveillance devices in plants and animals. Science. 354: aaf6395

Jones JD. and Dangl JL. (2006) The plant immune system. Nature 444: 323–329

Jones DA. and Takemoto D. (2004) Plant innate immunity - direct and indirect recognition of general and specific pathogen-associated molecules. Curr Opin Immunol. 16 48-62

Ju C. Chang C. (2015) Mechanistic insights in ethylene perception and signal transduction. Plant Physiol. 169:85–95

Kachroo A. and Robin GP. (2013) Systemic signaling during plant defense. Curr Opin Plant Biol. 16 527–533

Kaló P. Gleason C. Edwards A. Marsh J. Mitra RM. Hirsch S. Jakab J. Sims S. Long SR. Rogers J. Kiss JB. Downie A. and Oldroyd GED. (2005) Nodulation signaling inlegumes requires NSP2 a member of the GRAS family of transcriptional regulators. Science 308:1786-1789

Kankanala P. Nandety RS. and Mysore KS. (2019) Genomics of plant disease resistance in legumes. Front plant sci. 10:1345.

Kaur A. Kumar A. and Reddy MS. (2017) Plant-pathogen interactions a proteomic approach. In Singh R. Kothari R. Koringa PG. and Singh SP. (eds) Understanding host-microbiome interactions- An omics Approach. Springer pp 207-227

Kamoun S. (2001) Nonhost resistance to Phytophthora: novel prospects for a classical problem. Curr Opin Plant Biol. 4:295–300

Kazan K. and Manners JM. (2013) MYC2: The master in action. Mol Plant 6:686–703

Keen NT. (1990) Gene-for-gene complementarity in plant-pathogen interactions. Annu Rev Genet. 24447-463

Kelly S. Sullivan JT. Kawaharada Y. Radutoiu S. Ronson CW. and Stougaard J. (2018) Regulation of nod factor biosynthesis by alternative NodD proteins at distinct stages of symbiosis provides additional compatibility scruting. Enviro Microbiol. 20:97–110

Kereszt A. Mergaert P. Maróti G. and Kondorosi É. (2011) Innate immunity effectors and virulence factors in symbiosis. Curr Opin Microbiol. 14:76–81

Kieber JJ. Rothenberg M. Roman G. Feldmann KA. and Ecker JR. (1993) CTR1 a negative regulator of the ethylene response pathway in Arabidopsis encodes a member of the Raf family of protein kinases. Cell 72 427–441

Kim M. Chen Y. Xi J. Waters C. Chen R. and Wang D. (2015) An antimicrobial peptide essential for bacterial survival in the nitrogen- fixing symbiosis. Proc Natl Acad Sci USA. 112:15238–15243

Kinkema M. and Gresshoff PM. (2008) Investigation of downstream signals of the soybean autoregulation of nodulation receptor kinase *GmNARK.* Mol Plant Microbe Interact. 21:1337-1348

Kiss E. Olah B. Kalo P. Morales M. Heckmann AB. Borbola A. Lozsa A. Kontar K. Middleton P. Downie JA. Oldroyd GED. and Endre G. (2009) LIN a novel type of U-Box/WD40 protein controls early infection by Rhizobia in legumes. Plant Physiol. 151:1239-1249

Kobayashi H. Naciri-Graven Y. Broughton WJ. and Perret X. (2004) Flavonoids induce temporal shifts in gene expression of nod-box controlled loci in *Rhizobium* sp NGR234. Mol Microbiol. 51 335–347

Koch B. and Evans HJ. (1966) Reduction of acetylene to ethylene by soybean roo tnodules .Plant Physiol. 41: 1748–1750

Kondorosi E. Gyuris J. Schmidt J. John M. Duda E. Hoffman B. Schell J. and Kondorosi. A. (1989). Positive and negative control of nod gene expression in *Rhizobium meliloti* is required for optimal nodulation. EMBO J. 5 1331-1340

Kondorosi E. Pierre M. Cren M Haumann U. Buire M. Hoffmann B. Schell J. and Kondorosi A. (1991) Identification of NolR a negative transacting factor controlling the nod regulon in *Rhizobium meliloti*. J Mol Biol. 222:885–896

Koorneef A. and Pieterse C. (2008) Crosstalk in defense signaling. Plant Physiol. 146: 839-844

Krall L. Wiedemann U. Unsin G. Weiss S. Domke N. and Baron C. (2002) Detergent extraction identifies different VirB protein subassemblies of the type IV secretion machinery in the membranes of *Agrobacterium tumefaciens*. Proc Nat Acad of Sci USA. 99: 11405–11410

Kumar D. (2014) Salicylic acid signaling in disease resistance. Plant Science 228127– 134

Kwak JM. Nguyen V. and Schroeder JI. (2006) The role of reactive oxygen species in hormomnal response. Plant Physiol. 141: 323-329

Laloum T. Baudin M. Frances L. Lepage A. Billault-Penneteau B. Cerri MR. Ariel F. Jardinaud MF. Gamas P. de Carvalho-Niebel F. and Nibel A. (2014) Two CCAAT-box-binding transcription factors redundantly regulate early steps of the legume-rhizobia endosymbiosis. Plant J. 79:757–768

Landgraf R. Schaarschmidt S. Hause B. (2012) Repeated leaf wounding alters the colonization of *Medicago truncatula* roots by beneficial and pathogenic microorganisms. Plant Cell Environ. 35:1344–57

Lambertsen L. Sternberg C. and Molin S. (2004) Mini-Tn7 transposons for site specific tagging of bacteria with fluorescent proteins. Environ Microbiol. 6:726–732

Lang C. and Long SR. (2015) Transcriptomic analysis *of sinorhizobium meliloti* and *Medicago truncatula* symbiosis using nitrogen fixation-deficient nodules. Mol Plant Microbe Interac. t28 856–868

Laporte P. Lepage A. Fournier J. Catrice O. Moreau S. Jardinaud MF. et al (2014) The CCAAT box-binding transcription factor NF-YA1 controls rhizobial infection. J Exp Bot. 65:481–494

Larrainzar E. Riely BK. Kim SC. Carrasquilla-Garcia N. Yu HJ. Hwang HJ. Oh M. Kim GB. Surendrarao AK. Chasman D. et al (2015) Deep sequencing of the *Medicago truncatula* root transcriptome reveals amassive and early interaction between nodulation factor and ethylene signals. Plant Physiol. 169:233–265

Lawton KA. Potter SL. Uknes S. and Ryals J. (1994) Acquired resistance signal transduction in Arabidopsis is ethylene independent. Plant Cell 6: 581-588

Lee KH.and LaRue TA. (1992) Exogenous ethylene inhibits nodulation of *Pisum sativum L cv Sparkle.* Plant Physiol. 100:1759–1763

Leite J. Fischer D. Rouws LF. Fernandes-Junior PI. Hofmann A. Kublik S. Schloter M. Xavier GR. and Radl V. (2016) Cowpea Nodules Harbor non-rhizobial bacterial communities that are shaped by soil type rather than plant genotype. Front Plant Sci. 7: 2064

Lévy J. Bres C. Geurts R. Chalhoub B. Kulikova O. Duc G. Journet EP. Ané JM. Lauber E. Besseling T. Dénarié J. Rosenberg C. and Debellé F. (2004) A putative Ca^{2+} and calmodulin-dependentprotein kinase required for bacterial and fungal symbioses. Science 303 1361–1364

Li N. Han X. Feng D. Yuan D. Huang LJ. (2019) Signaling crosstalk between salicylic acid and ethylene/jasmonate in plant defense: Do we understand what they are whispering? Int J Mol Sci. 20 671

Lian B. Zhou X. Miransari M. Smith DL. (2000) Effects of salicylic acid on the development and root nodulation of soybean seedlings. J Agron Crop Sci. 185: 187-192

Lieberman M. (1979) Biosynthesis and action of ethylene, Annu Rev Plant Physiol. 30, 533,

Limpens E. Franken C. Smit P. Willemse J. Bisseling T. Geurts R. (2003) LysM domain receptor kinases regulating rhizobial nod factor- induced infection. Science 302:630–633

Liu Y. and Zhang S. (2004) Phosphorylation of 1-aminocyclopropane-1-carboxylic acid synthase by MPK6 a stress-responsive mitogen-activated protein kinase induces ethylene biosynthesis in Arabidopsis. Plant Cell 16:3386–3399

Loh J. and Stacey G. (2003) Nodulation Gene Regulation in *Bradyrhizobium japonicum*: a unique integration of global regulatory circuits. Appl Environ Microbiol. 69:10–17

Lorenzo O. Chico JM. Sanchez-Serrano JJ. and Solano R. (2004) JASMONATE-INSENSITIVE1 encodes a MYC transcription factor essential to discriminate between different jasmonate-regulated defence responses in Arabidopsis. Plant Cell 161938–1950

Lynch JP. and Brown K. (1997) Ethylene and nutritional stress. Physiol Plant. 100:613-619

Mabood F. and Smith DL. (2005) Pre-inoculation of *Bradyrhizobium japonicum* with jasmonates accelerates nodulation and nitrogen fixation in soybean (*Glycine max*) at optimal and suboptimal root zone temperatures. Physiol Plant. 125:311–323

Macho AP. and Zipfel C. (2014) Plant PRRs and the activation of innate immune signaling. Mol Cell. 54:263–72

Mahajan M. Ahuja PS. and Yadav SK. (2011) Post-transcriptional silencing of flavonol synthase mRNA in tobacco leads to fruits with arrested seed set. PLoS One 6 e28315

Marie C. Barny MA. and Downie JA. (1992) *Rhizobium leguminosarum* has two glucosamine synthases GlmS and NodM required for nodulation and development of nitrogen fixing nodules. Mol Microbial. 6: 843-851

Marsh JF. Rakocevic A. Mitra RM. Brocard L. Sun J. Eschstruth A. Long SR. Ratet P. and Oldroyd ED. (2007) *Medicago truncatula* NIN is essential for rhizobial-independent nodule organogenesis induced by autoactive calcium/calmodulin-dependent protein kinase. Plant Physiol. 144:324–35

Martínez-Abarca F. Herrera-Cervera JA. Bueno P. Sanjuan J. Bisseling T. and Olivares J. (1998) Involvement of salicylic acid in the establishment of the *Rhizobium meliloti*-alfalfa symbiosis. Mol Plant Microbe Interact. 11:153-155

Martinez-Hidalgo P. Hirsch AM. (2017) The nodule microbiome: N2-fixing rhizobia do not live alone. Phytobiomes 1: 70–82

Mattoo A. and Jeffrey CS (1991) The Plant Hormone Ethylene Boca Raton FL: CRC Press (Reissued 2018 by CRC Press)

Maunoury N. Redondo-Nieto M. Bourcy M. Van de Velde W. Alunni B. Laporte P. et al (2010) Differentiation of symbiotic cells and endosymbionts in *Medicago truncatula* nodulation are coupled to two transcriptome switches PLoS One 5:e9519

Mayer KFX. Schoof H. Haecker A. Lenhard M. Jürgens G. Laux T. (1998) Role of WUSCHEL in regulating stem cell fate in the Arabidopsis shoot meristem. Cell 95:805–815

Mergaert P. Uchiumi T. Alunni B. Evanno G. Cheron A. Catrice O. et al (2006) Eukaryotic control on bacterial cell cycle and differentiation in the Rhizobium-legume symbiosis. Proc Natl Acad Sci USA. 103:5230–5235

Mergaert P. van Montagu M. and Holsters M. (1997) Molecular mechanisms of Nod factor diversity. Mol Microbiol. 25:811–817

Messinese E. Mun JH. Yeun LH. Jayaraman D. Rouge P. Barre A. Lougnon G. Schornack S. Bono JJ. Cook DR. and Ané JM. (2007) A novel nuclear protein interacts with the symbiotic DMI3 calcium and calmodulin-dependent protein kinase of *Medicago truncatula.* Mol Plant-Microbe Interact. 20:912-921

Michael WL. Swiderski MR. Li Y. and Jones JD. (2006) The *Arabidopsis thaliana* TIR-NB-LRR R-protein RPP1A; protein localization and constitutive activation of defence by truncated alleles in tobacco and Arabidopsis. Plant J. 47 829–840

Middleton PH. Jakab J. Penmetsa RV. Starker CG. Doll J. Kaló P. et al (2007) An ERF transcription factor in *Medicago truncatula* that is essential for nod factor signal transduction. Plant Cell 19:1221–1234

Miller EV. Winston JR. and Fisher DF. (19940) Production of epinasty by emanations from normal and decaying citrus fruits and from *Penicillium digitatum. J Agric Res.* 60: 269-1940.

Minami R. Uchiyama K. Murakami T. Kawai J. Mikami K. Yamada T. Yokoi D. Ito H. Matsui H. and Honma M. (1998) Properties sequence and synthesis in *Escherichia coli* of 1-aminocyclopropane-1-carboxylate deaminase from *Hansenula saturnus.* J Bioch. 123 1112–1118

Mitra RM. Gleason CA. Edwards A. Hadfield J. Downie JA. Oldroyd GED. and Long SR. (2004) A Ca^{2+}/calmodulin-dependentprotein kinase required for symbiotic nodule development: gene identification by transcript-based cloning. Proc Nat Acad Sci USA. 1014701–4705

Miyahara A. Richens J. Starker C. Morieri G. Smith L. Long S. Downie JA. and Oldroyd GED. (2010) Conservation in function of a SCAR/WAVE component during infection thread and root hair growth in *Medicago truncatula.* Mol Plant-Microbe Interact. 23:1553-1562

Moling S. Pietraszewska-Bogiel A. Postma M. Fedorova E. Hink MA. Limpens E .et al (2014) Nod factor receptors form heteromeric complexes and are essential for intracellular infection in medicago nodules. Plant Cell 26:4188–4199

Montesano M. Brader G. and Palva ET. (2003) Pathogen derived elicitors: searching for receptors in plants. Mol Plant Pathol. 4:73–79

Nakagawa T. and Kawaguchi M. (2006) Shoot-applied MeJA suppresses root nodulation in *Lotus japonicus* Plant Cell Physiol. 47: 176-180

Nascimento FX. Rossi MJ. and Glick BR. (2018) Ethylene and 1-Aminocyclopropane-1-carboxylate (ACC) in plant–bacterial interactions. Front Plant Sci. 9 114

Nemhauser JL. Hong F. and Chory J. (2006) Different plant hormones regulate similar processes through largely nonoverlapping transcriptional responses. Cell 126: 467-475

Nickerson WJ. (1948) Ethylene as a metabolic product of the pathogenic fungus *Blastomyces dermatitidis.* Arch.Biochem. 17:225

Nukui N. Ezura H. Yuhashi K. Yasuta T. and Minamisawa K. (2000) Effects of ethylene precursor and inhibitors for ethylene biosynthesis and perception on nodulation in *Lotus japonicus* and *Macroptilium atropurpureum.* Plant Cell Physiol. 41:893–897

Nürnberger T. Brunner F. Kemmerling B. and Piater L. (2004) Innate immunity in plants and animals: striking similarities and obvious differences. Immunol Rev 198:249–266

O'Neill NR. and Saunders JA. (1994) Compatible and incompatible responses in alfalfa cotyledons to races 1 and 2 of *Colletotrichum trifolii*. Phytopat. 84 283–287

Ogden AJ. Gargouri M. Park J. Gang DR. and Kahn ML. (2017) Integrated analysis of zone-specific protein and metabolite profiles within nitrogen-fixing *Medicago truncatula-Sinorhizobium medicae* nodules. PLoS One12:e0180894

Oldroyd GED. Engstrom EM. and Long SR. (2001) Ethylene inhibitsthe Nod factor signal transduction pathway of *Medicago truncatula.* Plant Cell 13:1835–1849

Oldroyd GED. Murray JD. Poole PS. and Downie JA. (2011) The rules of engagement in the Legume-Rhizobial symbiosis. Annu Rev Genet. 45:119–144

Oldroyd GED (2013) Speak friend and enter: signalling systems that promote beneficial symbiotic associations in plants. Nature Rev Microbiol. 11 252–263

Ott T. van Dongen JT. Günther C. Krusell L. Desbrosses G. Vigeolas H. et al (2005) Symbiotic leghemoglobins are crucial for nitrogen fixation in legume root nodules but not for general plant growth and development. Curr Biol. 15:531–535

Reid DE. Liu H. Kelly S. Kawaharada Y. Mun T. Andersen SU .Des-brosses GJ. and Stougaard J. (2018) Dynamics of *Lotus japonicus* ethylene production in response to compatible Nod factor. Plant Physiol. 1761764–1772

Paink HPCA. Wijffelman E. Pees RJH. Okker and Lugtenberg BJJ. (1987) Rhizobium nodulation gene *nodD* as a determinant of host specificity. Nature 328:337–340

Pan Q. Wendel J. and Fluhr R. (2000) Divergent evolution of plant *NBS-LRR* resistance gene homologues in dicot and cereal genomes. J Mol Evol. 50 203–213

Pandya M. Kumar GN. Rajkumar S. (2013) Invasion of rhizobial infection thread by non-rhizobia for colonization of *Vigna radiata* root nodules. FEMS Microbiol Lett. 348(1):58–65

Park CJ. Kim KJ. Shin R. Park JM. and Shin YC. (2004) Pathogenesis related protein 10 Isolated from hot pepper functions as a ribonuclease in an antiviral pathway. Plant J. 37 186–198

Pathipanawat W. Jones RAC. and Sivasithamparam K. (1994) An improved method for artificial hybridization in annual Medicago species. Aust J Agric Res. 45 1329–1335

Patkar RN. and Chattoo BB. (2006) Transgenic indica rice expressing ns-LTP-like protein shows enhanced resistance to both fungal and bacterial pathogens Mol Breed. 17 159–171

Pel MJC. and Pieterse CMJ. (2013) Microbial recognition and evasion of host immunity. J Exp Bot. 64:1237–1248

Penmetsa RV. and Cook DR. (1997) A legume ethylene-insensitive mutant hyperinfected by its rhizobial symbiont. Science 275:527-530

Penmetsa RV. Frugoli JA. Smith LS. Long SR. and Cook DR. (2003) Dual genetic pathways controlling nodule number in *Medicago truncatula.* Plant Physiol. 131:998–1008

Penrose D. Moffat MBA. and Glick BR. (2001) Determination of 1-aminocyclopropane-1-carboxylic acid (ACC) to assess the effects of ACC deaminase-containing bacteria on roots of canola seedlings. Can J Microbiol. 47:77–80

Pérez Guerra JC. Coussens G. De Keyser A. De Rycke R. De Bodt S. Van de Velde W. Goormachtig S. and Holsters M. (2010) Comparison of developmental and stress-induced nodule senescence in *Medicago truncatula.* Plant Physiology1521574–1584

Peters NK. Frost JW. and Long SR. (1986) A plant flavone luteolin induces expression of *Rhizobium meliloti* nodulation genes. Science (Wash DC) 233:978–980

Pieterse CM. Van der Does D. Zamioudis C. Leon-Reyes A. and Van Wees SCM. (2012) Hormonal modulation of plant immunity. Annu Rev Cell Dev Biol. 28:489–521

Pieterse CM. Leon-Reyes A. Van Der Ent S. and Van Wees SC. (2009) Networking by small-molecule hormones in plant immunity. Nat Chem Biol. 5 308–316

Pieterse CM. and Van Loon LC. (2004) NPR1: the spider in the web of induced resistance signaling pathways. Curr Opin Plant Biol. 7 456-464

Pislariu CI. and Dickstein R. (2007) An *IRE*-like *AGC* kinase gene *MtIRE* has unique expression in the invasion zone of developing root nodules in *Medicago truncatula.* Plant Physiol. 144 682–694

Pontier D. Tronchet M. Rogowsky P. Lam E. and Roby D. (1998) Activation of *hsr203* a plant gene expressed during incompatible plant-pathogen interactions is correlated with programmed cell death. Mol Plant-Microbe Interact. 11:544–554

Poole P. Ramachandran V. and Terpolilli J. (2018) Rhizobia: From saprophytes to endosymbionts. Nat Rev Microbiol. 16291–303

Popp C. and Ott T. (2011) Regulation of signal transduction and bacterial infection during root nodule symbiosis. Curr Opin Plant Biol. 14:458–467

Prayitno J. Imin N. Rolfe BG. and Mathesius U. (2006) Identification of ethylene-mediated protein changes during nodulation in *Medicago truncatula* using proteome analysis. J Proteome Res. 5 3084–3095

Pré M. Atallah M. Champion A. De Vos M. Pieterse CMJ. and Memelink J. (2008) The AP2/ERF domain transcription factor ORA59 integrates jasmonic acid and ethylene signals in plant defense. Plant Physiol. 147:1347–57

Primrose SB. and Dilworth MJ. (1976) Ethylene production by bacteria. J Gen Microbial. 93: 177

Primrose SB. (1977) Evaluation of the role of methional, 2-keto-4-methylthiobutyric acid and peroxidase in ethylene formation by *Escherichia coli.* J Gen Microbial. 98: 519

Pucciariello C. Innocenti G. Van de Velde W. Lambert A. Hopkins J. Clément M. Ponchet M. Pauly N. Goormachtig S. Holsters M.Puppo A. and Frendo P (2009) (Homo)glutathione depletion modulates host gene expressionduring the symbiotic interaction between *Medicago truncatula* and *Sinorhizobium meliloti.* Plant Physiol. 151:1186–1196

Rairdan GJ. and Moffett P. (2006) Distinct domains in the ARC region of the potato resistance protein Rx mediate LRR binding and inhibition of activation. Plant Cell18 2082–2093

Rakocevic A. Mondy S. Tirichine L. Cosson V. Brocard L. Iantcheva A. Cayrel A. Devier B. Abu El-Heba GA. and Ratet P. (2009) MERE1 a low-copy-number copia-type retroelement in *Medicago truncatula* active during tissue culture. Plant Physiol. 151:1250-1263

Redmond JW. Batley M. Djordjevic MA. Innes RW. Kuempel PL. Rolfe BG. (1986) Flavones induce expression of nodulation genes in Rhizobium. Nature 323:632-635

Regus JU. Quides KW. O'Neill MR. Suzuki R. Savory EA. Chang JH. and Sachs JL. (2017) Cell autonomous sanctions in legumes target ineffective rhizobia in nodules with mixed infections. Amer J Bot.104:1299–1312

Remigi P. Zhu J. Young JPW. and Masson-Boivin C. (2016) Symbiosis within symbiosis: Evolving nitrogen-fixing legume symbionts. Trends Microbiol. 24 63–75

Ribeiro B. Erffelinck ML. Colinas M. Williams C. Hamme EV. Lacchini E. Clercq R. Perassolo M. and Goossens A. (2020) ER-Anchored Transcription Factors bZIP17 and bZIP60 Regulate Triterpene Saponin Biosynthesis in *Medicago truncatula* bioRxiv In press

Riker AJ. Jones FR. and Davis MC. (1935) Bacterial leaf spot of alfalfa. J Agric Res. 51177–182

Robert GU. and Martha ER. (2010) Defense-related gene expression in soybean leaves and seeds inoculated with Cercospora kikuchii and *Diaporthe phaseolorum* var *Meridionalis.* Physiol Mol Plant Pathol. 75 64–70

Robert AC. and John EM. (1997) Biosynthesis and action of jasmonates in plants. Annu Rev Plant Physiol Plant Mol Biol. 48:355–81

Rogel MA. Hernández-Lucas I. Kuykendall LD. Balkwill D. and Land Martínez-Romero E. (2001) Nitrogen fixing nodules with *Ensifer adhaerens* harboring *Rhizobium tropici* symbiotic plasmids. Appl Environ Microbiol. 67 3264–3268

Röhrig H. Schmidt J. Walden R. Czaja I. Miklasevics E. Wieneke U. Schell J. and John M. (1995) Growth of tobacco protoplasts stimulated by synthetic mipochitooligosaccharides. Science :269 841-843

Rojas CM. Senthil-Kumar M. Tzin V. and Mysore KS. (2014) Regulation of primary plant metabolism during plant-pathogen interactions and its contribution to plant defense. Front Plant Sci. 5:17

Roux B. Rodde N. Jardinaud MF. Timmers T. Sauviac L. Cottret L. Carrère S. Sallet E. Courcelle E. Moreau S. et al (2014) An integrated analysisof plant and bacterial gene expression in symbiotic root nodules using laser-capture micro dissection coupled to RNA sequencing. Plant J. 77: 817–837

Saeki K. (2011) Rhizobial measures to evade host defense strategies and endogenous threats to persistent symbiotic nitrogen fixation: a focus on two legume-rhizobium model systems. Cell Mol Life Sci. 68: 1327–1339

Santner A. and Estelle M. (2007) The JAZ Proteins Link Jasmonate Perception with Transcriptional Changes. Nature 459 1071–1078

Sato M. Urushizaki S. Nishiyama K. Sakai F. and Ota Y. (1987) Efficientproduction of ethylene byPseudomonas syringaepv.glycineawhich causeshalo blight in soybeans. Agric. Biol. Chem.51:1177–1178

Savatin DV. Gramegna G. Modesti V. and Cervone F. (2014) Wounding in the plant tissue: the defense of a dangerous passage. Front Plant Sci. 5 470

Schell J. Bisseling T. Dülz M. *et al.* (1999) Re-evaluation of phytohormone-independent division of tobacco protoplast-derived. Cells Plant J. 17: 461–466

Schenk PM. Kazan I. Wilson I. and erson JP. Richmond T. Somerville SC. and Manners JM. (2000) Coordinated plant defense responses in Arabidopsis revealed by microarray analysis. Proc Natl Acad Sci USA. 97: 11655-11660

Schmidt JS. Harper JE. Hoffman TK. and Bent AF. (1999) Regulation of soybean nodulation independent of ethylene signaling. Plant Physiol. 119 951–959

Schnabel E. Journet EP. de Carvalho-Niebel F. Duc G. and Frugoli J. (2005) The *Medicago truncatula SUNN* gene encodes a CLV1-like leucine rich repeat receptor kinase that regulates nodule number and root length. Plant Mol Biol. 58:809–822

Schumpp O. and Deakin WJ. (2010) How inefficient rhizobia prolong their existence within nodules. Trends Plant Sci. 15; 189–195

Seo HS. Li J. Lee SY. Yu JW. Kim KH. Lee SH. Lee IJ. and Paek NC. (2006) The hyper nodulating *nts* mutation induces jasmonate synthetic pathway in soybean leaves. Mol Cells. 24: 185-193

Seyfferth C. and Tsuda K. (2014) Salicylic acid signal transduction: the initiation of biosynthesis perception and transcriptional reprogramming. Front Plant Sci. | Plant-Microbe Interac. 5: 697

Shah S. Li J. Moffatt BA. and Glick BR. (1998) Isolation and characterization of ACC deaminase genes from two different plant growth-promoting rhizobacteria. Can J Microbiol. 44:833–843

Singh S. and Parniske M. (2012) Activation of calcium- and calmodulin-dependentprotein kinase (CCaMK) the central regulator of plant root endosymbiosis. Curr Op Plant Biol. 15: 444 – 453

Sinharoy S. Torres-Jerez I. Bandyopadhyay K. Kereszt A. Pislariu CI. Nakashima J. Benedito VA. Kondorosi E. and Udvardia MK. (2013) The C2H2 transcription factor REGULATOR OF SYMBIOSOME DIFFERENTIATION represses transcription of the secretory pathway gene VAMP721a and promotes symbiosome development in *Medicago truncatula.* Plant Cell 25:3584–601

Shipston N. and Bunch AW. (1989) The physiology of L-methionine catabolism to the secondary metabolite ethylene by *Escherichia coli* J Gen Microbial 135 1489

Smit P. Raedts J. Portyanko V. Debelle F. Gough C. Bisseling T. and Geurts R. (2005) NSP1 of the GRAS protein family isessential for rhizobial Nod-factor-induced transcription. Science 308:1789–1791

Snoeijers SS. Pérez-Garcia A. Joosten MHAJ and De Wit PJGM (2000) The effect of nitrogen on disease development and gene expression in bacterial and fungal pathogens. Eur J Plant Pathol. 493506

Solano R. Stepanova A. Chao Q. and Ecker JR. (1998) Nuclear events in ethylene signaling: a transcriptional cascade mediated by ETHYLENE-INSENSITIVE3 and ETHYLENE-RESPONSE-FACTOR1. Genes Develop. 12 3703–3714

Song S. Huang H. Gao H. Wang J. Wu D. Liu X. Yang S. Zhai Q. Li C. Qi T *.et al.* (2014) Interaction between MYC2 and ETHYLENE INSENSITIVE3 modulates antagonism between jasmonate and ethylene signaling in Arabidopsis. Plant Cell. 26: 263–279

Sós-Hegedüs A. Domonkos Á. Tóth T. Gyula P. Kaló P. and Szittya G. (2020) Suppression of *NB-LRR* Genes by miRNAs Promotes Nitrogen-fixing Nodule Development in *Medicago truncatula.* Plant Cell doi:101111/pce13698

Soyano T. Kouchi H. Hirota A. and Hayashi M. (2013) NODULE INCEPTION directly targets NF-Y subunit genes to regulate essential processes of root nodule development in *Lotus japonicas*. PLoS Genet 9:e1003352

Spaink HP. Wijffelman CA. Pees E. Okker RJH. and Lugtenberg BJJ. (1987) Rhizobium nodulation gene nodD as a determinant of host specificity. Nature 328:337-340

Srivastava A. Rahman MH. Shah S. and Kav NNV. (2006) Constitutive expression of the pea ABA-responsive 17 (ABR17) cDNA confers multiple stress tolerance in *Arabidopsis thaliana.* Plant Biotechnol J. 4 529– 549

Stacey G. Libault M. Brechenmacher L. Wan J. May GD. (2006a) Genetics and functional genomics of legume nodulation. Curr Opin Plant Biol. 9:110–121

Stacey G. McAlvin CB. Kim SY. Olivares J. Soto MJ. (2006b) Effects of endogenous salicylic acid on nodulation in the model legumes *Lotus japonicus* and *Medicago truncatula*. Plant physiol. 141: 1473-1481

Starker CG. Parra-Colmenares AL. Smith L. Mitra RM. and Long SR. (2006) Nitrogen fixation mutants of*Medicago truncatula* fail to support plant and bacterial symbiotic gene expression. Plant Physiol. 140:671–80

Sticher L. Mauch-Mani B. and Métraux JP. (1997) Systemic acquired resistance. Annu Rev Phytopat. 35:235-270

Sugawara M. Takahashi S. Umehara Y. Iwano H. Tsurumaru H. Odake H. Suzuki Y. Kondo H. Konno Y. and Yamakawa T. (2018) Variation in bradyrhizobial NopP effector determines symbiotic incompatibility with Rj2-soybeans via effector-triggered immunity. Nat Commun. 9:3139

Sun J. Cardoza V. Mitchell DM. Bright L. Oldroyd G. and Harris JM. (2006) Crosstalk between jasmonic acid ethylene and Nod factor signaling allow integration of diverse inputs for regulation of nodulation. Plant J. 46: 961-970

Suzaki T. Yoro E. and Kawaguchi M. (2015) Leguminous plants: inventors of root nodules to accommodate symbiotic bacteria. Int Rev Cell Mol Biol. 316:111–158

Suzuki A. Suriyagoda L. Shigeyama T. Tominaga A. Sasaki M. Hiratsuka Y. Yoshinaga A. Arima S. Agarie S. Sakai T. Inada S. Jikumaru Y. kamiya Y. Uchiumi T. Abe M. Hashiguchi M. Akashi R. Sato S. Kaneko T. Tabata S. and Hirsch AM. (2011) *Lotus japonicus* nodulation is photomorphogenetically controlled by sensing the red/far red (R/FR) ratio through jasmonic acid (JA) signaling. Proc Natl Acad Sci USA. 108: 16837-16842

Tadege M. Wen J. He J. Tu H. Kwak Y. Eschstruth A. Cayrel A. Endre G. Zhao PX. Chabaud M. *et al.* (2008) Large-scale insertional mutagenesis using the *Tnt1* retrotransposon in the model legume *Medicago truncatula.* Plant J. 54:335–347

Tang F. Yang S. Liu J. and Zh H. (2016) *Rj4* a gene controlling nodulation specificity in soybeans encodes a thaumatin-like protein but not the one previously reported. Plant Physiol 170:26–32

Thomas KC. and Spencer M. (1977) L-Methionine as an ethylene precursor in *Saccharomyces cerevisiae.* Can J Microbial. 23:1669

Tirichine L. Imaizumi-Anraku H. Yoshida S. Murakami Y. Madsen LH. Miwa H. *et al.* (2006) Deregulation of a Ca^{2+}/calmodulin- dependent kinase leads to spontaneous nodule development. Nature 441:1153–1156

Treutter D. (2005) Significance of flavonoids in plant resistance and enhancement of their biosynthesis. Plant Biol. 7 581–591

Trinh TH. Ratet P. Kondorosi E. Durand P. Kamaté K. Bauer P. and Kondorosi A. (1998) Rapid and efficient transformation of diploid *Medicago truncatula* and *Medicago sativa* spp *falcata* lines improved in somatic embryogenesis Plant. Cell Rep. 17:345-355

Udvardi M. and Poole PS. (2013) Transport and metabolism in Legume-Rhizobia symbioses. Annu Rev Plant Biol. 64:781–805

Van de Velde W. Zehirov G. Szatmari A. Debreczeny M. Ishihara H. Kevei Z. *et al.* (2010) Plant peptides govern terminal differentiation of bacteria in symbiosis. Science 327:1122–1126

Van Loon LC. (1997) Induced resistance in plants and therole of pathogenesis-related proteins. Euro J Plant Path.103: 753-765

Van Loon LC. Rep M. and Pieterse CMJ. (2006) Significance of inducible defense-related proteins in infected plants. Annu Rev Phytopathol. 44 135–162

Van Spronsen PC. Tak T. Rood AM. van Brussel AA. Kijne JW. and Boot Kj. (2003) Salicylic acid inhibits indeterminate-type nodulation but not determinate-type nodulation. Mol Plant Microbe Interact. 16: 83-91

Van Zeijl A. Op den Camp RH. Deinum EE. Charnikhova T. Franssen H. Op den Camp HJ. et al. (2015) Rhizobium lipochitooligosaccharide signaling triggers accumulation of cytokinins in *Medicago truncatula* roots. Mol Plant. 8:1213–1226

Vasse J De Billy F. Camut S. Truchet G. (1990) Correlation between ultrastructural differentiation of bacteroids and nitrogen fixation in alfalfa nodules. J Bacteriol. 172:4295–4306

Veereshlingam H. Haynes JG. Penmetsa RV. Cook DR. Sherrier DJ. and Dickstein R. (2004) Nip a symbiotic *Medicago truncatula* mutant that forms root nodules with aberrant infection threads and plant defense-like response. Plant Physiol. 136:3692–3702

Walpole R. and Myers R. (1978) Probability and statistics for engineers and scientists. 2nd edn Macmillan New York

Wang C. Yu H. Luo L. Duan L. Cai L. He X. *et al.* (2016) NODULES WITH ACTIVATED DEFENSE 1 is required for maintenance of rhizobial endosymbiosis in *Medicago truncatula.* New Phytol. 212:176–191

Wang C. Knill BR. Glick and Défago G. (2000) Effect of transferring 1-aminocyclopropane-1-carboxylic acid (ACC) deaminase genes into *Pseudomonas fluorescens* strain CHA0 and its gacA derivative CHA96 on their growth-promoting and disease-suppressive capacities. Can J Micro-biol. 46:898–907

Wang F. Cui X. Sun Y. and Dong CH. (2013) Ethylene signaling andregulation in plant growth and stress responses. Plant Cell Rep. 32:1099–1109

Wang KLC. Li H. and Ecker JR. (2002) Ethylene biosynthesis and signaling networks. Plant Cell. 2002;14:S131–151

Wasternack C. and Strnad M. (2017) Jasmonates are signals in the biosynthesis of secondary metabolites pathways transcription factors and applied aspects - a brief review. N Biotechnol. S1871–6784(17) 30442–30449

Williams L. and Fletcher JC. (2005) Stem cell regulation in the Arabidopsis shoot apical meristem. Curr Opin Plant Biol. 8:582–586

Wilkes J. Dale GT. and Old KM. (1989) Production of ethylene by Endothia gyrosa and *Cytospora eucalypticola* and its possible relationship to kino vein formation in *Eucalyptus maculate.* Physiol Mol. Plant Pathol. 34 171

Wood N. (2001) Nodulation by numbers: The role of ethylene in symbiotic nitrogen fixation. Pl Sci 6 : 501—502

Wu J. and Baldwin IT. (2010) New insights into plant responses to the attack from insect herbivores. Annu Rev Genet. 44:1–24

Xiao TT. Schilderink S. Moling S. Deinum EE. Kondorosi E. Franssen H. Kulikova O. Niebel A. and Bisseling T. (2014) Fate map of *Medicago truncatula* root nodules. Development141:3517–3528

Xie YR. Chen ZY. Brown RL. and Bhatnagar D. (2010) Expression and functional characterization of two pathogenesis-related protein 10 genes from Zea mays. J Plant Physiol. 167 121–130

Xu H. Chang PF. Liu D. Narasimhan ML. Raghothama KG. Hasegawa PM. and Bressan RA. (1994) Plant defense genes are synergistically induced by ethylene and methyl jasmonate. Plant Cell. 6: 1077-1085

Yan S. and Dong X. (2014) Perception of the plant immune signal salicylic acid. Curr Op Plant Biol. 20C:64–68

Yang HR. Tang K. Liu HT. and Huang WD. (2011) Effect of salicylic acid on jasmonic acid-related defense response of pea seedlings to wounding. Scientia Horticulturae128 166–173

Zgadzaj R. James EK. Kelly .S Kawaharada Y. de Jonge N. Jensen DB. Madsen LH. and Radutoiu S. (2015) A legume genetic framework controls infection of nodules by symbiotic and endophytic bacteria. PLOS Genet. 11e1005280

Zhai J. Jeong DH. De Paoli E. Park S. Rosen BD. Li Y. González AJ. Yan Z. Kitto SL. Grusak MA. Jackson SA. Stacey G. Cook DR. Green PJ. Sherrier DJ. and Meyers BC. (2011) MicroRNAs as master regulators of the plant NB-LRR defense gene family via the production of phased transacting siRNAs. Genes Dev. 25 2540–2553

Zhang L. Lu X. Shen Q. Chen Y. Wang T. Zhang F. Wu S. Jiang W. Liu P. Zhang L. Wang Y. and Tang K. (2012) Identification of Putative *Artemisia annua* ABCG transporter unigenes related to artemisinin yield following expression analysis in different plant tissues andin response to methyl jasmonate and abscisic acid treatments. Plant Mol Biol Rep. 30 838–847

Zhang Y. Wang Y. Wei H. Li N. Tian W. Chong K. and Wang L. (2018) Circadian evening complex represses jasmonate-induced leaf senescence in Arabidopsis. Mol Plant 11: 326–337

Zhuo M. Sakuraba Y. and Yanagisawa S. (2019) A jasmonate-activated MYC2-Dof2.1-MYC2 transcriptional loop leaf senescence in Arabidopsis. Plant Cell. 32, 242–262

Zipfel C. (2014) Plant pattern-recognition receptors. Trends Immunol. 35:345–51

Zvereva AS. and Pooggin MM. (2012) Silencing and innate immunity in plant defense against viral and non-viral pathogens. Viruses 4:2578–2597

Annexe

Title: **Control of the ethylene signaling pathway prevents plant defenses during intracellular accommodation of the rhizobia**

Short title: Ethylene affects late stage in endosymbiosis

Fathi Berrabah[1,2], Thierry Balliau[3], El Hosseyn Aït-Salem[1,2], Jeoffrey George[1,2], Michel Zivy[4], Pascal Ratet[1,2], Benjamin Gourion[1,2]

[1]Institute of Plant Sciences Paris Saclay IPS2, CNRS, INRA, Université Paris-Sud, Université Evry, Université Paris-Saclay, Batiment 630, 91405 Orsay, France

[2]Institute of Plant Sciences Paris-Saclay IPS2, Paris Diderot, Sorbonne Paris-Cité, Bâtiment 630, 91405, Orsay, France

[3]INRA, PAPPSO, UMR Génétique Quantitative et Évolution – Le Moulon, INRA/Université Paris-Sud/CNRS/AgroParisTech, Université Paris-Saclay, F-91190 Gif-sur-Yvette, France F-91190 Gif-sur-Yvette, France

[4]CNRS, PAPPSO, UMR Génétique Quantitative et Évolution – Le Moulon, INRA/Université Paris-Sud/CNRS/AgroParisTech, Université Paris-Saclay, F-91190 Gif-sur-Yvette, France F-91190 Gif-sur-Yvette, France

To whom correspondence should be addressed: Benjamin Gourion, Laboratoire des Interactions Plantes Micro-organismes (LIPM) 24 chemin de Borde Rouge - Auzeville CS 52627, 31326 CASTANET TOLOSAN CEDEX, France, Phone : +33 5 61 28 53 20, email : benjamin.gourion@inra.fr and Pascal Ratet, Institut of Plant Sciences Paris-Saclay, Bâtiment 630, 91405 Orsay, France, Phone : +33 1 69 15 33 30, email : pascal.ratet@cnrs.fr

Summary :

- Massive intracellular populations of symbiotic bacteria, referred to as rhizobia, are housed in legume root nodules. Little is known about the mechanisms preventing the development of defense in these organs although genes like *SymCRK* and *DNF2* of the model legume *Medicago truncatula* are required for this control after rhizobial internalization in host nodule cells. Here we investigated the molecular basis of the symbiotic control of immunity.
- Proteomic analysis was performed to compare functional (Wild type) and defending nodules (*symCRK*). Based on the proteomics results, the control of plant immunity during the functional step of the symbiosis was further investigated by biochemical and pharmacological approaches as well as by transcript and histology analysis.
- Ethylene was identified as a potential signal inducing plant defenses in the *symCRK* nodules. Involvement of this phytohormone in the *symCRK* and *dnf2*-developed defenses and in the death of intracellular rhizobia was confirmed. This negative effect of ethylene depended on the *M. truncatula Sickle* gene and was also observed in the legume *Lotus japonicus.*
- Together, these data indicate that prevention of ethylene triggered defenses is crucial for the persistence of endosymbiosis and that the *DNF2* and *SymCRK* genes are required for this process.

Keywords : Nitrogen fixing endosymbiosis, innate immunity, ethylene, *dnf2*, *symCRK*, plant defenses.

Introduction:

Legume plants establish symbiotic associations with rhizobia. These bacteria, which are selected by the plant from the rhizosphere microbiota, trigger the formation of root nodules and colonize plant cells where they fix atmospheric nitrogen for the benefit of the plant (Udvardi & Poole, 2013). As nitrogen content in the soil is a common limiting factor for plant growth, the capacity of legumes to interact with rhizobia often represents an important advantage for the plant. The efficiency of the symbiosis most probably relies largely on the presence in nodules of spectacularly high densities of bacteria, often superior to what is observed during pathogenic interactions. More and more reports indicate that immunity plays a crucial role during the early infection process leading to rhizobia/legume symbiosis (Jones *et al.*, 2008; Yang *et al.*, 2010; Liang *et al.*, 2013; Okazaki *et al.*, 2013; Gourion *et al.*, 2015; Okazaki *et al.*, 2016). In contrast, little is known about the molecular mechanisms that suppress immunity during functional symbiosis, i.e. once rhizobia have been released into symbiotic nodule cells where they fix nitrogen, and the bacterial population reaches its highest density.

symCRK mutants of the model legume *Medicago truncatula* form nodules that develop defense-like reactions manifested by the induction of defense-related genes, the accumulation of phenolic compounds (typically produced during defense) and ultimately the death of bacteria (Berrabah *et al.*, 2014b; Berrabah *et al.*, 2015). As a result, *SymCRK* mutant nodules do not fix nitrogen. The way *SymCRK* prevents defenses is not clear, but interestingly the gene encodes a cysteine rich receptor-like kinase (CR-RLK or CRK), harboring a non-arginine aspartate motif (non-RD) typical of RLKs involved in innate immunity in plants and animals (Dardick & Ronald, 2006; Dardick *et al.*, 2012; Berrabah *et al.*, 2014b). *M. truncatula* mutants altered in the *DNF2* gene (Mitra & Long, 2004; Starker *et al.*, 2006) that encodes a protein similar to phospholipase C proteins (Pislariu *et al.*, 2012; Bourcy *et al.*,

2013), present strong phenotypic similarities with *symCRK* mutants, including the development of defense-like reactions in nodules (Pislariu *et al.*, 2012; Bourcy *et al.*, 2013; Berrabah *et al.*, 2014a). However, the phenotypes of these two types of mutants and the expression patterns of the two genes are not identical, which indicates that *DNF2* and *SymCRK* act in distinct pathways that sequentially repress the plant defenses, *DNF2* acting before *SymCRK* (Berrabah *et al.*, 2014b; Berrabah *et al.*, 2015). Perhaps as a consequence of this chronology, the rhizobial colonization level of *symCRK* mutant nodules is higher than that of *dnf2* nodules (Berrabah *et al.*, 2014b).

With the aim to better understand the mechanisms preventing the development of defenses in infected nodule cells, we analyzed the proteomes of the bacterial and plant partners during functional (Wild type, WT plants) and defense-developing (Wild type, *symCRK*) interactions. The results suggest that the ethylene pathway is activated in defense developing nodules. Pharmacological approaches revealed that ethylene indeed triggered the development of defenses at the site of infected cells and supported a role for the *SymCRK* and *DNF2* genes in the control of ethylene triggered defenses.

Materials and Methods:

Plant, bacterial growth and plant inoculation: *Medicago truncatula* ecotypes R108 (Hoffmann *et al.*, 1997) and its derivative mutant lines NF737 (*symCRK*) (Berrabah *et al.*, 2014b) and MS240 (*dnf2-4*) (Bourcy *et al.*, 2013) seeds were surface sterilized as previously described (Bourcy *et al.*, 2013) and incubated for at least 48h in the darkness at 4°C on agarose water (1 % w/v) plates. Seeds were then transferred for germination to 24°C in the dark for 48h. For the proteomics experiment, seedlings were then transferred on sand/vermiculite substrate (1:3 ratio (v/v)) and plants were cultivated in green house at 24°C, 16/8 dark/light, 60% humidity. *Sinorhizobium medicae* strain WSM419 (Howieson & Ewing, 1986) was cultured in YEB medium (Krall *et al.*, 2002) for 48 hour at 30°C. Cell suspension of *S. medicae* were pelleted and washed in sterile water and $OD600_{nm}$ was adjusted to 0.1 in sterile water. Three days after transfer in the greenhouse, plants were inoculated with 50 mL of *S. medicae* cell suspension per pot (5 seedling/pots). Upon this culture conditions the nodulation kinetics is slower than when the plants are cultivated *in vitro*. Using this methodology, mature nodules were collected for analysis 28 days after inoculation. We never noticed any delay in the *symCRK* nodulation kinetics as compared to the WT. Three independent experiments were performed. For *in vitro* experiments, bacterial and plant culture as well as the plant inoculation were performed as described in (Berrabah *et al.*, 2015).

Ethylene treatment: After cultivation on sand/perlite substrate, root systems of nodulated plants were washed in water and placed individually in 20 ml vials. The vials were sealed with parafilm in order to separate the aerial and underground parts of the plants. Root systems of these plants were then incubated for three days in the presence of the indicated concentration of ethylene.

Expression analysis: For RNAs isolation, nodules were collected from plants using forceps and scalpels and immediately frozen in liquid nitrogen. Material was then ground with steal bead in 2 ml tubes using a Qiagen tissues lyser. cDNA were prepared using 1 µg of RNA, synthesis was performed using oligo dT and SuperScriptII (Life Technology) as recommended by the manufacturer. qPCR was performed as described in (Berrabah *et al.*, 2015), primers used during this study are listed in Supplementary Table 1.

Acetylene reduction assays: Acetylene reduction activity reflecting nitrogenase activity was determined as previously described in (Berrabah *et al.*, 2014a) using a protocol derived from (Koch & Evans, 1966). Briefly, plants displaying similar nodulation were individually placed in 20ml sealed vials containing 0.5 ml water and incubated in 2.5 % acetylene. During the linear phase of ethylene production, between two to six hours, gaseous phases were analyzed by GC-FID. Ethylene peak areas were integrated and results were normalized by the incubation time.

ACC oxidase activity test: Nodules were collected in 100 mM Tris, 10 mM ascorbate pH 7.2 cold buffer on ice. Material was ground to homogenize and suspension were clarified by centrifugation at 16100 g for 30 minutes at 4°C. Protein concentrations in the crude extracts were determined using Bradford assay. 1-Aminocyclopropane-1-carboxylic acid (ACC) oxidase activity test were performed in 200 µl extraction buffer supplemented with 1mM ACC in 10ml sealed vials. Evolved ethylene was measured after two hours by gas chromatography using the ARA method described in (Berrabah *et al.*, 2014a).

Nodule protein fractionation: Protocol inspired from (Valot *et al.*, 2004; Larrainzar *et al.*, 2007) was used to separate the sample into three fractions for proteomics analysis. 26 days post inoculation (dpi) root systems were abundantly washed with water. Nodules were collected using scalpel and forceps (1 to 10 g of fresh weight) and homogenized in a mortar and pestle in a freshly prepared ice-cold extraction buffer (25 mM MES, 450 mM mannitol, 7

mM Na_2EDTA, 7 mM $CaCl_2$, 5 mM $MgCl_2$, 20 mM ascorbic acid, 10 mM dithiothreitol, 1 mM PMSF, pH 7.5). Homogenates were transferred to 2 ml tubes and centrifuged at 100g at 4°C for 5 min to pellet plant debris. Supernatants were collected and centrifuged at 2,000g at 4°C for 15 min. The supernatants (corresponding to nodule plant fractions) were collected and pellets (containing symbiosomes) were washed twice with extraction buffer. Washed pellets were re-suspended in 2 ml of extraction buffer and sonicated for bacteroid disruption. Sonicated fractions were further centrifuged at 16,000g at 4°C for 15 min and supernatants were collected in 1.5 ml tubes (corresponding to nodule symbiosomal fractions; F1 fraction). Nodule plant fractions were centrifuged at 16,000g for 15 min at 4°C. Supernatants were collected and then centrifuged at 100,000g for 1 h at 4 °C to precipitate microsomes, the final supernatants (corresponding to the plant cell cytosolic fractions; F3) were collected, pellets (consisting in the microsomal fractions; F2) were re-suspended into 500 µl of extraction buffer. This procedure is illustrated in Figure 1.

Protein extraction and digestion:

Proteins were extracted in TCA acetone, suspended in Laemmli buffer and heated at 65°C for 5 minutes. Protein concentrations were then determined using Amersham plus one 2D quant kit. Proteins were separated on SDS-PAGE, 7.5µg of proteins were loaded per sample. After a short migration, gels were incubated twice for one hour in phosphoric acid 2%, ethanol 50% and then rinsed in phosphoric acid 2% for one hour. Gels were then stained using G250 Coomassie brilliant blue G 0.1% in phosphoric acid 2%, ethanol 17% and ammonium sulfate 15%. After staining, gels were abundantly rinsed with distilled water. Every lane was separated in 3 gel pieces corresponding to proteins of high, medium and low molecular weights. In gel digestions were performed using trypsin following the protocol described in (Martin *et al.*, 2006) and the three digests from each sample were pooled before being solubilized in 30µL of acetonitrile 2%, formic acid 0.05% and trifluoroacetic acid 0.05%.

Digest analysis and protein identification:

LC-MS/MS analyses were performed on an ultimate 3000 rslc (Thermofinnigan) coupled to a LTQ-Orbitrap Discovery (ThermoFinnigan).

4µl of pooled digests were injected on a PepMap100 C18 pre-column (300µm*5mm 5µm 100Å) with a flux of 15µl.min^{-1} of 0.08% TFA and 2%acetonitrile (ACN) and separated using a gradient on a AcclaimPep map RSLC 75µm*50cm nanoviper, C18 2µm, 100Å at 300nl.min^{-1}. Samples were separated using the following gradient: from 1 to 43 % of buffer B (acetonitrile 80%, formic acid 0.1% in water) in buffer A (2% acetonitrile, 0.1% formic acid in water) for 180 min; from 43 to 98 % of buffer B for 1 min; 98 % of buffer B during 5 min; from 98 % to 1% of buffer B in one min and finally 2% of buffer B for 4 min. Eluted peptides were ionized through a nanoelectrospray with 1.3kV on an uncoated capillary probe (10µm tip inner diameter, New Objective). The orbitrap resolution was set to 15.000 for MS1. MS2 scans were acquired in the linear trap and the 5 most intense peptides were analyzed by fragmentation with data dependent parameters : qz = 0.25, activation time = 30 ms, collision energy = 35%, dynamic exclusion time=60 s. Raw files were converted to mzXML using proteowizard (Kessner *et al.*, 2008). Protein identifications were realized using X!Tandem Sledgehammer (2013.09.01.1) (Craig & Beavis, 2004) and the following parameters: constant modification: carbamidomethylation of the cysteine residues = +57.04 Da; potential modifications: oxidation of the methionines residues: +15.99 Da, N-terminal Acetylation: +42.01Da, N-terminal deamidation on the glutamine residues and carbamidomethylated cystein residues: -17.02Da, loss of N-terminal H_2O on glutamic acid residues : -18.01Da. *M. truncatula* proteome was predicted from the *M. truncatula* genome database that was downloaded from jcvi (v4.01, 62320 entries, http://jcvi.org/medicago/display.php?pageName=General&section=Download) (19, 20). The theoretical proteome of *S. medicae* strain WSM419, predicted by (21), was downloaded

(2015, February the 10th) at http://www.uniprot.org/proteomes/UP000001108 (6213 entries) (21). Data were assembled with X!tandempipeline v3.3.3 (http://pappso/bioinfo/xtandempipeline/) with the following filtering parameters: peptide Evalue < 0.01, two peptides per protein and protein Evalue $<10^{-5}$.

To evaluate the level of contamination resulting from spectrophotometer source memory, blank experiments were performed between each sample injection and proteins were identified during blank. This analysis clearly indicates that contamination level is very low and does not interfere significantly with the analysis.

Proteins were quantified as indicated in Supplemental Figure 1 a method inspired from (Rappsilber *et al.*, 2002).

Statistical analyses were performed using R software. For every proteins identified during the study, spectral counting index (reflecting protein abundance) were compared using the post-hoc Nemenyi test which is a variant of the Kruskal-Wallis test.

Microscopy: Nodules sections were prepared, stained and observed as previously described (Berrabah *et al.*, 2015). Briefly, nodules were embedded in 6% agarose before being processed with a vibratome to generate 70µm thin nodule sections. Live and dead staining was realized as described in (Haag *et al.*, 2011), using propidium iodide and syto 9 that stained dead & living bacteria in red and green respectively. In this case, sections were observed on a confocal microscope. To stain phenolic compounds, a protocol derived from (Vasse *et al.*, 1993) and described in (Bourcy *et al.*, 2013) was applied. Briefly nodule sections were fixed in $KMnO_4$ before being stained with methylene blue 0.01%. ImageJ was used for the determination of the total surface of the sections, the necrotic area, and the surfaces stained by methylene blue.

Results :

Characterization of the fractionated WT and *symCRK* nodules proteomes.

Comparative proteomics analysis was performed on *M. truncatula* wild type and *symCRK* nodules triggered by the efficient rhizobial strain *Sinorhizobium medicae* WSM419. Proteomes were analyzed after separation of three fractions obtained after elimination of cell debris and nuclei. The first fraction corresponds to the soluble proteins of the symbiosomes (F1). The two other fractions derived from the material remaining after symbiosome isolation and are the proteins extracted from microsomes (F2) and the remaining soluble proteins (F3) (Figure 1). In total, 1,011 bacterial and 2,074 plant proteins were identified (Supplementary Table 2). The numbers of bacterial and plant proteins identified in each fraction are summarized in the Table 1. F1 samples on one hand and F2 and F3 samples on the other hand, are enriched in bacterial and plant proteins respectively (Table 1). In addition, the F2 fractions, corresponding to microsomes are clearly enriched in membrane associated proteins as compared to the F3 plant cytoplasmic fraction and, to a lesser extent, to the symbiosomal F1 fractions (Table 1). These results validate the efficiency of the separation protocol for substantial enrichment of the different fractions with the expected type of proteins.

Bacteroid proteomes are enriched in chromosome encoded proteins and poor in strain specific proteins.

Analysis of the proteomes of bacteria rescued from nodules reveals two noticeable features. First, the proteins encoded by bacterial chromosomal genes are over represented in the two plant hosts as compared to those encoded by the three bacterial plasmids. Indeed, whereas proteins were detected for 17 to 20% of the chromosomal genes, the proportions range between two to six percent for the three other replicons (Figure 2A). Secondly, the WSM419 strain specific proteins (encoded by the *S. medicae* WSM419 genome and not by the model strain *Sinorhizobium meliloti* 1021) are underrepresented (Figure 2B). Further analysis

indicates that the overrepresentation of chromosome encoded proteins and of proteins shared with other strain (Sm1021) are not necessary linked as the chromosome and the megaplasmid pSMED01 display similar proportions of shared and specific proteins (Figure 2C) but the proportions of genes for which proteins were detected are drastically different for the two replicons (Figure 2A).

Adaptation to the WT and *symCRK* host is associated with distinct replicon usages.

S. medicae strain WSM419 harbors a mosaic genome constituted by a chromosome, two mega plasmids, pSMED01 and pSMED02 and an accessory plasmid pSMED03 (Reeve *et al.*, 2010). pSMED02 mega plasmid carries the symbiotic genes and pSMED01 display high similarity with the *S. meliloti* strain 1021 pSymB mega plasmid involved in saprophytic lifestyle (Finan *et al.*, 2001) (Supplementary figure 2). More proteins encoded by genes located on pSMED01 were detected in the *symCRK* samples than in the WT one (101 vs 51 in the F1 of the *symCRK* and of the WT respectively). In addition, these pSMED01 encoded proteins were, in general, more abundant in the *symCRK* mutant (Supplementary Table 2, Supplementary figure 3). Remarkably spectral counting indexes (reflecting protein abundances) were higher in the *symCRK* than in the WT for all the seven detected proteins encoded by the WSM419 accessory plasmid pSMED03 (Supplementary Table 2, Supplementary figure 3). Together these data indicate a drastic modification of the replicon usage during the bacterial adaptation to the two hosts.

Ethylene as a candidate mediator eliciting plant defenses in nodules.

Little is known about plant innate immunity in the legume symbiotic organ. In other parts of the plant, ethylene is one of the phytohormones responsible for the induction of plant defenses. This hormone is synthesized through the oxidation of 1-aminocyclopropane-1-carboxylate (ACC), a reaction catalyzed by ACC oxidases. The *M. truncatula* ACC oxidase-like protein (Medtr8g028435.1) was specifically detected in the proteome of *symCRK* mutant

nodules (Supplementary table 2). Also, the specific detection of the *S. medicae* ACC deaminase in *symCRK* nodules (Supplementary table 2), suggests that the ethylene precursor is present in mutant nodules. Furthermore, the expression levels of most of the 11 genes corresponding to defense related proteins (according to their GO terms) that accumulated in *symCRK* nodules, are also induced in *M. truncatula* roots in other studies during a phytopathogen attack and are dependent on the key ethylene perception gene *Sickle* (*Medicago truncatula* Gene Expression Atlas, Figure 3A). Finally, proteins involved in isoflavonoid biosynthesis were accumulated in the *symCRK* nodules (Table 2, Supplementary tables 2 and 3) and the expression of the corresponding genes was also recently shown to be induced in *M. truncatula* by ethylene in a *sickle* dependent manner (Liu *et al.*, 2017). Taken together, these data support a role for the ethylene signaling pathway in the development of defense responses in *symCRK* nodules.

In agreement with the observed protein accumulation in mutant nodules, the transcript coding for the ACC oxidase-like (Medtr8g028435.1) was found to accumulate in *symCRK* nodules (Figure 3B). Finally, data mining also revealed that the transcript of this ACC oxidase-like protein is induced in *M. truncatula* roots during infection by the root pathogens *Aphanomyces euteiches* and *Ralstonia solanacearum*, and that this accumulation is *Sickle* dependent (Figure 3A) indicating a good correlation between *ACC-oxidase-like* gene expression and the development of plant defenses.

ACC oxidases constitute a multigene family of 11 members present in the *M. truncatula* genome (Supplementary Table 1). The expression of 8 ACC oxidase genes were successfully analyzed by RT-qPCR and 4 were found to be clearly upregulated in *symCRK* nodules, the remaining four genes displaying no important difference in their transcript levels between the two genetic backgrounds (Figure 3C), again suggesting that ethylene is produced in *symCRK* nodules.

To further confirm that the ethylene pathway is active in the *symCRK* mutant, ACC oxidase activity was tested and was detected in protein crude extracts of *symCRK* mutant nodules but not in wild type nodule extracts (Figure 3D). Finally, activation of the ethylene pathway in the *symCRK* nodules was confirmed by evaluating the expression of *sickle* dependent genes in WT and in *symCRK* nodules. Those defense-related genes showed a higher expression in the *symCRK* mutant than in the WT (Supplementary figure 4).

Ethylene treatment compromises symbiosis after nodulation establishment through a Sickle dependent pathway.

In order to better understand the effect of ethylene during the later stages of the symbiotic process in *M. truncatula*, nodulated root systems were treated with various concentrations of ethylene. After three days incubation, the capacity to fix nitrogen was evaluated. In the WT ecotype R108 of *M. truncatula*, ethylene treatment was found to drastically reduce nodule nitrogenase activity (Figure 4A). A similar negative effect of ethylene on the nitrogen fixation capacity was observed with another WT ecotype of *M. truncatula*, A17 (Figure 4B) and also on the model legume *Lotus japonicus* (Figure 4C).

The negative effect of ethylene on the nitrogen-fixing stage of the symbiotic process prompted us to investigate whether this inhibition was mediated by the plant. In order to address this question, the expression of the *M. truncatula sickle* gene that is known to be required for ethylene perception, was studied. *Sickle* transcripts were detected by RTqPCR at similar levels in mature WT and *symCRK* nodules (Supplementary Figure 5). Nitrogenase activity was then analyzed after ethylene treatment of nodulated *sickle* and WT plants. The negative effect of ethylene was not observed in the *sickle* mutant (Figure 4B). These results indicate that the negative effect of ethylene on the nitrogen-fixing stage of the symbiotic process is not due to a direct action on nitrogenase activity and is mediated by the plant in a *Sickle* dependent pathway.

Ethylene treatment triggers *symCRK*-like defenses in nodules and these localize to rhizobial infected cells.

In addition to the loss of nitrogen fixation capacity in *M. truncatula* nodules, ethylene treatment also triggered some *symCRK*-like features such as necrosis, accumulation of phenolic compounds, induction of *PR10* and *NDR1* defense-related gene expression, as well as bacteroid death (Figure 5, Supplementary Figure 6). Measurements of necrotic areas and of zones accumulating phenolic compounds in nodule sections suggest a dose dependent response of the nodules (Figure 5, Supplementary Figure 6). Remarkably necrotic area are larger in the *symCRK* mutant samples than in the WT ethylene treated ones (Figure 5A, Figure 6 B and C). In *Medicago truncatula* nodule, the nodule tissue hosting nitrogen fixing bacteroids is composed of both infected and uninfected cells. Examination of randomly chosen field of this zone in the *symCRK* mutant nodule sections indicate that, the development of necrosis were preferentially observed in rhizobial invaded cells, rather than in uninfected cells (Figure 6) in agreement with the expression pattern of *SymCRK* that localized to infected cells (Berrabah et al. 2015). Interestingly, this correlation between infected cells and necrosis development is also observed on nodule sections of WT ethylene treated plants (Figure 6C).

The effects of ethylene treatments were also examined in *L. japonicus* where, in contrast to *M. truncatula*, the treatments did not trigger accumulation of detectable phenolic compounds in the infected tissues and the nodules did not develop necrosis. Despite these differences, bacteroids encountered premature death in ethylene-treated *L. japonicus* nodules as shown by a live and dead staining procedure (Supplementary Figure 7).

In addition to defense reactions and bacteroid viability, other features typical of the *symCRK* mutant were also examined in ethylene treated wild type *M. truncatula* nodules. The

expression of three late nodule specific cysteine rich peptide genes, and of *RSD* (a regulatory plant gene involved in symbiosis (Sinharoy *et al.*, 2013)) was drastically reduced in response to treatment with a high concentration of ethylene (Supplementary Figure 8) similarly to what was observed in the *symCRK* mutant background. Interestingly, two other nodule specific genes (*DNF2* and *NCR121*), whose expression is less dramatically reduced in the *symCRK* mutant, showed an expression level much less altered by an ethylene treatment (Supplementary Figure 8). Finally, at a high concentration, ethylene also strongly impacted the accumulation of the *SymCRK* transcript in *M. truncatula* nodules (Supplementary Figure 8). Together, these data indicate that the development of defenses at the level of cells hosting rhizobia shows strong similarities when triggered by an ethylene treatment or as the result of *symCRK* loss of function.

Ethylene contributes to defense reactions developed in the *symCRK* nodules.

In order to evaluate the potential contribution of ethylene in the phenotype of the *symCRK* mutant, plants were cultivated in the presence of high concentrations of L-α-(2-aminoethoxyvinyl)-glycine (AVG), an inhibitor of ethylene synthesis. Analyses of nodule sections indicated that both the accumulation of phenolic compounds and the development of necrosis were reduced in the *symCRK* mutant upon growth on AVG supplemented medium (Figure 7). RT-qPCR indicated that, in the *symCRK* nodules, the levels of defense-related transcripts decreased upon cultivation in the presence of a high concentration of AVG (Supplementary Figure 4). These data suggest that SymCRK acts directly or indirectly to prevent a negative role for ethylene during the later stage of the symbiotic process in the *Medicago/Sinorhizobium* symbiosis in order to prevent defense reactions in the symbiotic cells.

Ethylene as a candidate mediator of defenses in the *dnf2* nodules

The *dnf2* and *symCRK* mutants of *M. truncatula* develop similar defense-like reactions in their nodules (Berrabah *et al.*, 2014b). However *DNF2* acts earlier than *SymCRK* (Berrabah *et al.*, 2015). It has been previously described that the rhizobial mutant *bacA* triggers inefficient nodules that do not develop defense reactions on both WT and *symCRK* plants (Berrabah *et al.*, 2015). In contrast, nodules induced by *bacA* on the *dnf2* mutant develop defense reactions (Berrabah *et al.*, 2015). Interestingly RT-qPCR results indicate that the *ACC-oxidase-like* gene (Medtr8g028435.1) induction is correlated with the development of defenses in the nodules of both the *symCRK* and the *dnf2* mutants (Figure 3B). Indeed, the induction of *ACC-oxidase-like* was observed in three types of nodule developing defenses: i) those of the *dnf2* mutant induced by WT *S. meliloti* Sm1021, ii) those of the *symCRK* mutant induced by WT *S. meliloti* Sm1021 and iii) in those induced on the *symCRK* mutant by the *bacA* mutant of *S. meliloti*. In contrast, ACC oxidase was not induced in the three type of nodules analyzed that do not develop defenses (WT bacteria-WT plant, *bacA* bacterial mutant-WT plant and *bacA* mutant-*symCRK* mutant).

In order to investigate whether ethylene might contribute to the defense reactions observed in the nodules of the *dnf2* mutant, *dnf2* plants were nodulated by WT rhizobia in the absence or the presence of high concentration of AVG and accumulation of phenolics compounds as well as development of necrosis were evaluated on nodule sections. Similarly to what was observed for the *symCRK* mutant, the presence of AVG in the plant substrate strongly decreases the development of these two features in the nodules of *dnf2* mutant (Figure 7) suggesting that ethylene contributes to the development of defense reactions in the *dnf2* nodules.

Discussion :

Legume tolerance to rhizobial infection is not well understood and essentially all the studies tackling this issue have focalized on the initial step of the symbiotic process. Some bacterial actors, also known to play key roles in pathogen infection, such as components of the bacterial cell surface and protein secretion and translocation machinery are required for optimal infections (Gourion *et al.*, 2015). In addition, Nod Factors (NF), which are lipo-chitooligosaccharides produced by rhizobia and not by phytopathogenic bacteria, are required for infection and nodule development in essentially all rhizobia-legume interactions (Oldroyd *et al.*, 2011). Much less is known about the control of infection once nodules are formed and rhizobia have been released in symbiotic cells. Herein, we present a proteomic analysis that led us to generate data indicating that the *M. truncatula* genes *DNF2* and *SymCRK* contribute to the repression of plant defenses *via* the direct or indirect inhibition of the ethylene signaling pathway in mature legume nodules.

Proteome analysis reflects the symbiotic defect of *symCRK* mutant nodules: amongst the 580 bacterial proteins that are differentially accumulated in the F1 of the two lines are the subunits of the nitrogenase complex (Smed_6223/NifK; Smed_6224/NifD; Smed_6225/NifH) that constitute the key enzymes responsible for nitrogen fixation. Based on the spectral counting indexes, these proteins have been found amongst the 10 most abundant proteins in the WT F1 fraction illustrating the importance of the nitrogen reduction for the bacteroid metabolism. In the same vein, the Leghemoglobin Lb120-1 was strongly accumulated in the cytosolic fraction (F3) of WT plant. This oxygen carrier produced by legumes has been shown, in another legume species, *Lotus japonicus*, to be crucial for nitrogen fixation (Ott *et al.*, 2005). Both nitrogenase and leghemoglobin are often used as markers of nodule functionality. The *symCRK* mutant was previously described as a strict fix minus mutant (Berrabah *et al.*, 2014b). In agreement, NifH, D and K were barely detected in the *symCRK* mutant and Lb120-

1 was much less abundant in the *symCRK* nodules than in the WT (Supplementary Table 2). Together these results validate our proteomics approach and indicate that the bacteroid physiology is drastically modified in the *symCRK* mutant as compared to the WT.

Rhizobia display typical features of starvation in *symCRK* nodules: analysis of the bacterial protein distributions amongst the clusters of orthologous group (COG) functional classes suggest that bacterial transcription and translation are strongly reduced in the *symCRK* mutant (Supplementary Table 2, Supplementary Figure 9). Also, bacterial proteins involved in energy production are less represented in the *symCRK* mutant than in the WT. For instance, all bacterial proteins involved in the citric acid cycle (TCA) are less abundant in the *symCRK* mutant suggesting that bacteroid respiration is reduced in this line. This observation is correlated with the lower amount of leghemoglobin accumulated in the *symCRK* mutant and also with the accumulation of most bacterial transporters in the *symCRK* mutant (Supplementary Table 2). Thus the underrepresentation of TCA enzymes in the *symCRK* bacteroids might reflect the unavailability of oxygen or carbon substrate in the *symCRK* mutant. The accumulation of GloB (Smed_2552) and of PrkA (Smed_1027) in the *symCRK* colonizing bacteria also suggests a metabolic imbalance. Indeed, GloB is involved in detoxification of methylglyoxal, a metabolite that accumulates during metabolic imbalance in bacteria and the *prkA* gene expression is induced upon inorganic phosphate or carbon starvation in *S. meliloti* (Summers *et al.*, 1998). Sulfate metabolism also seems to be modified in the *symCRK* nodules. Indeed, several proteins related to sulfate metabolism such as the three arylsulfatase Smed_5768, Smed_3805 and Smed_3791, as well as the sulfate ABC transporter Smed_5896 were detected specifically in -or strongly accumulated in- the *symCRK* mutant. In contrast, the plant transporter Sat-1 (Medtr6g086170.1) was only detected in the WT microsomal and symbiosomal fractions. The closest *Lotus japonicus* homologue Sst1 is crucial for nitrogen fixation in this species where it was proposed to provide sulfate to

intracellular rhizobia (Krusell *et al.*, 2005). These observations suggest major differences in sulfate metabolism between WT and *symCRK* bacteroids. Together, these data suggest that rhizobia undergo nutrient starvation in the *symCRK* mutant.

Proteome analysis suggest that rhizobia encounter stressful conditions during colonization of *symCRK*: as mentioned above, PrkA is accumulated in *symCRK* colonizing rhizobia. Interestingly, expression of this gene in *Salmonella enterica* is under the control of the general stress response (Ibanez-Ruiz *et al.*, 2000) and the key regulator of the general stress response in alphaproteobacteria, PhyR (encoded by Smed_2347) is specifically detected in the *symCRK* mutant. In various alphaproteobacteria, the PhyR dependent regulatory cascade was shown to be required for adaptation to the bacterial environment and to stress (Francez-Charlot *et al.*, 2015). This PhyR cascade is also required for symbiotic efficiency and for resistance to various stresses in the soybean symbiont, *Bradyrhizobium japonicum* (Gourion *et al.*, 2009). Other proteins typically accumulating during various stressful conditions, such as the Do serine proteinase (Smed_0637), or during osmotic stress such as the ectoine related proteins; EhuB (Smed_3699) and EutD (Smed_3693) and five proteins involved in glycine betaine transport (Smed_0650, Smed_2305, Smed_2583, Smed_4637 and Smed_4885) as well as mscL (Smed_0166) were found in higher amounts in the *symCRK* mutant than in the wild type. Together, accumulation of these proteins suggests that bacteria encounter stressful conditions in the *symCRK* mutant.

Bacterial and plant proteomes of *symCRK* nodules point to the activation of plant defenses: A remarkable feature of the *symCRK* nodule proteome is the accumulation of plant defense related proteins including disease resistance response proteins, pathogenesis related protein and chitinases and subtilisin-like proteins (Supplementary Table 2 and 3, Table 2). Also remarkable was the accumulation of 14 leucine rich repeat receptor-like kinases in the microsomal fraction of the *symCRK* mutant (Supplementary Table 2 and 3, Table 2). This

receptor family is involved in many physiological processes amongst which perception of microorganisms is one of the best characterized. In addition, 10 enzymes representing the entire flavonoid biosynthetic pathway were detected specifically or enriched in *symCRK* nodules. Similarly, 8 and 7 enzymes involved in isoflavonoid and phenylpropanoid biosynthesis, respectively, were enriched in the *symCRK* samples (Supplementary Table 2 and 3, Table 2), suggesting that biosynthesis of antimicrobial phytoalexin compounds is activated in *symCRK* nodules. Together, this proteome analysis confirms the development of plant defense reactions in the nodules of the *symCRK* mutant.

Ethylene is involved in many aspects of plant life (Bleecker & Kende, 2000), and particularly during interactions with pathogenic organisms. This gaseous phytohormone is generally associated with resistance against necrotrophic pathogens (Pieterse *et al.*, 2012; Zipfel, 2013). Ethylene production is also a hallmark of a set of defense reactions triggered by Microbial/Pathogen Associated Molecular Patterns (M/PAMPs) (Boller, 1995; Felix *et al.*, 1999; Felix & Boller, 2003). These reactions, referred to as M/PAMP Triggered Immunity (M/PTI), are developed upon perception of M/PAMPs, such as the active epitopes of flagellin and chitin oligomers, by Pattern Recognition Receptors (PRRs) (Zipfel, 2014). Interestingly, ethylene is required for the correct expression of some PRR genes such as the Leucine Rich Repeat flagellin sensing receptor FLS2 (Boutrot *et al.*, 2010; Mersmann *et al.*, 2010), and is involved in an amplification loop of M/PTI signaling (Liu *et al.*, 2013; Tintor *et al.*, 2013; Zipfel, 2013).

How M/PTI is prevented during rhizobia-legume interactions remains unclear. Modifications of M/PAMPs in rhizobia have been observed (Felix *et al.*, 1999). However, it is now clear that rhizobia induce moderate plant defenses during the earliest stage of the symbiotic process suggesting that not all M/PAMPs are divergent enough to prevent the development of defenses (Gourion *et al.*, 2015).

Ethylene has a negative impact on symbiosis and is antagonistic to NFs during early stages of the symbiotic process (Peters & Crist-Estes, 1989). Thus, ethylene negatively controls the progression of infection structures (the infection threads) (Penmetsa & Cook, 1997) by the inhibition of Nod factor signaling (Oldroyd *et al.*, 2001). Also, additional and more complex roles are attributed to ethylene and its cross talk with NF signaling during rhizobial infection (Goormachtig *et al.*, 2004; Larrainzar *et al.*, 2015). The role of ethylene during the later stages of the symbiotic process is much less documented. In agreement with a potential role of ethylene during the late stage of the symbiotic process, the *acdS* gene of *Mesorhizobium loti*, encoding for an ACC deaminase, was found to be expressed specifically in intracellular rhizobia and the expression of the *acdS* gene depends on a rhizobial symbiotic regulator (Nukui *et al.*, 2006). Also, early work indicates that ethylene reduces nitrogenase activity in pea and clover nodules (Goodlass & Smith, 1979). However, ethylene being a product of nitrogenase under some special conditions, the interpretation of these data remained difficult.

Here, we show that an ethylene treatment stopped nitrogen fixation in WT, but not in the *sickle* plant mutant that is insensitive to ethylene ((Penmetsa & Cook, 1997; Oldroyd *et al.*, 2001; Penmetsa *et al.*, 2008), Figure 4). This observation indicates that the ethylene control of nitrogen fixation is mediated by the plant. In addition, we showed that an ethylene treatment mimics different aspects of a mutation in *SymCRK* including the development of defenses and the death of bacteroids (Figure 4, 5 & 6). Also, using an inhibitor of ethylene biosynthesis, we showed that ethylene contributes to the development of defenses in the *symCRK* and *dnf2* mutants (Figure 7). We report here congruent results about the negative role of ethylene in the accommodation of rhizobia in the symbiotic cells. This includes notably an ACC oxidase activity of nodule protein extracts higher in the *symCRK* mutant than in the WT. However, we were not able to detect directly ethylene production in the nodules of the *symCRK* mutant.

503 This might be due to combined difficulties to produce high quantity of unwounded nodules
504 and to the detection limit of our method (GC-FID).
505 The way SymCRK controls ethylene triggered defenses in mature nodules is not yet perfectly
506 clear. However, in ethylene treated- and in *symCRK* mutant nodules, the necrosis that was
507 induced was associated to infected cells (Figure 6) suggesting either that infected cells are
508 more sensitive to ethylene than uninfected ones or that a bacterial component is required to
509 develop plant defenses in response to ethylene. In this context, it is interesting to highlight the
510 accumulation of receptor-like kinases in the *symCRK* mutant, a feature also known to be
511 triggered by ethylene (Boutrot *et al.*, 2010; Mersmann *et al.*, 2010). It is tempting to speculate
512 that the inability of *symCRK* mutants to modulate the abundance of such receptors confers on
513 this mutant a higher sensitivity to external stimuli including rhizobial M/PAMPs, which could
514 explain the development of localized defenses in this mutant.
515 Based on these results and on our previous study (Berrabah *et al.*, 2015), we propose that
516 *DNF2* and *SymCRK* act consecutively after rhizobial internalization within symbiotic cells to
517 prevent the negative effect of ethylene in nodules of *M. truncatula*.

Acknowlegdements

This work has benefited from the facilities and expertise of the IMAGIF Cell Biology Unit of the Gif campus (www.imagif.cnrs.fr) which is supported by the Conseil Général de l'Essonne. We express our gratitude to Dr. Fabienne Vailleau and to Dr. Marie Françoise Jardinaud (Ecole Nationale Supérieur d'Agronomie de Toulouse, LIPM Toulouse, France) for sharing unpublished transcriptomics data of *M. truncatula* WT and *sickle* mutant upon attack by *R. solanacearum* for fruitful discussions and for help with statistical analysis. This work has benefited from a French State grant (reference ANR-10-LABX-0040-SPS) managed by the French National Research Agency under an Investments for the Future program (reference n°ANR-11-IDEX-0003-02). We are grateful to Clare Gough (LIPM, Castanet Tolosan) for critical reading and correction of the manuscript.

Author Contributions

F.B., M.Z., P.R., B.G. designed the experiments, F.B., B.G., T.B., E.L. A-S, conducted the experiments, F.B., J.G., T.B., P.R. and B.G. analyzed the data and B.G. wrote the paper

References

Berrabah F, Bourcy M, Cayrel A, Eschstruth A, Mondy S, Ratet P, Gourion B. 2014a. Growth conditions determine the DNF2 requirement for symbiosis. *PLoS One* **9**(3): e91866.

Berrabah F, Bourcy M, Eschstruth A, Cayrel A, Guefrachi I, Mergaert P, Wen J, Jean V, Mysore KS, Gourion B, et al. 2014b. A nonRD receptor-like kinase prevents nodule early senescence and defense-like reactions during symbiosis. *New Phytologist* **203**(4):1305-14.

Berrabah F, Ratet P, Gourion B. 2015. Multiple steps control immunity during the intracellular accommodation of rhizobia. *J Exp Bot* **66**(7): 1977-1985.

Bleecker AB, Kende H. 2000. Ethylene: a gaseous signal molecule in plants. *Annu Rev Cell Dev Biol* **16**: 1-18.

Boller T. 1995. CHEMOPERCEPTION OF MICROBIAL SIGNALS IN PLANT-CELLS. *Annual Review of Plant Physiology and Plant Molecular Biology* **46**: 189-214.

Bourcy M, Brocard L, Pislariu CI, Cosson V, Mergaert P, Tadege M, Mysore KS, Udvardi MK, Gourion B, Ratet P. 2013. *Medicago truncatula* DNF2 is a PI-PLC-XD-containing protein required for bacteroid persistence and prevention of nodule early senescence and defense-like reactions. *New Phytologist* **197**(4): 1250-1261.

Boutrot F, Segonzac C, Chang KN, Qiao H, Ecker JR, Zipfel C, Rathjen JP. 2010. Direct transcriptional control of the Arabidopsis immune receptor FLS2 by the ethylene-dependent transcription factors EIN3 and EIL1. *Proc Natl Acad Sci U S A* **107**(32): 14502-14507.

Craig R, Beavis RC. 2004. TANDEM: matching proteins with tandem mass spectra. *Bioinformatics* **20**(9): 1466-1467.

Dardick C, Ronald P. 2006. Plant and animal pathogen recognition receptors signal through non-RD kinases. *PLoS Pathog* **2**(1): e2.

Dardick C, Schwessinger B, Ronald P. 2012. Non-arginine-aspartate (non-RD) kinases are associated with innate immune receptors that recognize conserved microbial signatures. *Curr Opin Plant Biol* **15**(4): 358-366.

Felix G, Boller T. 2003. Molecular sensing of bacteria in plants. The highly conserved RNA-binding motif RNP-1 of bacterial cold shock proteins is recognized as an elicitor signal in tobacco. *J Biol Chem* **278**(8): 6201-6208.

Felix G, Duran JD, Volko S, Boller T. 1999. Plants have a sensitive perception system for the most conserved domain of bacterial flagellin. *Plant J* **18**(3): 265-276.

Finan TM, Weidner S, Wong K, Buhrmester J, Chain P, Vorholter FJ, Hernandez-Lucas I, Becker A, Cowie A, Gouzy J, et al. 2001. The complete sequence of the 1,683-kb pSymB megaplasmid from the N2-fixing endosymbiont *Sinorhizobium meliloti*. *Proc Natl Acad Sci U S A* **98**(17): 9889-9894.

Francez-Charlot A, Kaczmarczyk A, Fischer HM, Vorholt JA. 2015. The general stress response in Alphaproteobacteria. *Trends Microbiol* **23**(3):164-71.

Goodlass G, Smith KA. 1979. Effects of ethylene on root extension and nodulation of pea (*Pisum sativum* L.) and white clover (*Trifolium repens* L.). *Plant and Soil* **51**(3): 387-395.

Goormachtig S, Capoen W, James EK, Holsters M. 2004. Switch from intracellular to intercellular invasion during water stress-tolerant legume nodulation. *Proc Natl Acad Sci U S A* **101**(16): 6303-6308.

Gourion B, Berrabah F, Ratet P, Stacey G. 2015. Rhizobium-legume symbioses: the crucial role of plant immunity. *Trends Plant Sci* **20**(3): 186-194.

Gourion B, Sulser S, Frunzke J, Francez-Charlot A, Stiefel P, Pessi G, Vorholt JA, Fischer HM. 2009. The PhyR-sigma(EcfG) signalling cascade is involved in stress response and symbiotic efficiency in *Bradyrhizobium japonicum*. *Molecular Microbiology* **73**(2): 291-305.

Haag AF, Baloban M, Sani M, Kerscher B, Pierre O, Farkas A, Longhi R, Boncompagni E, Herouart D, Dall'angelo S, et al. 2011. Protection of *Sinorhizobium* against host cysteine-rich antimicrobial peptides is critical for symbiosis. *PLoS Biology* **9**(10): e1001169.

Hoffmann B, Trinh TH, Leung J, Kondorosi A, Kondorosi E. 1997. A new *Medicago truncatula* line with superior *in vitro* regeneration, transformation, and symbiotic properties isolated through cell culture selection. *Mol Plant Microbe Interact* **10**(3): 307-315.

Howieson J, Ewing M. 1986. Acid tolerance in the *Rhizobium meliloti-Medicago* symbiosis. *Australian Journal of Agricultural Research* **37**(1): 55-64.

Ibanez-Ruiz M, Robbe-Saule V, Hermant D, Labrude S, Norel F. 2000. Identification of RpoS (sigma(S))-regulated genes in *Salmonella enterica* serovar typhimurium. *J Bacteriol* **182**(20): 5749-5756.

Jones KM, Sharopova N, Lohar DP, Zhang JQ, VandenBosch KA, Walker GC. 2008. Differential response of the plant *Medicago truncatula* to its symbiont *Sinorhizobium meliloti* or an exopolysaccharide-deficient mutant. *Proceedings of the national academy of sciences* **105**(2): 704-709.

Kessner D, Chambers M, Burke R, Agus D, Mallick P. 2008. ProteoWizard: open source software for rapid proteomics tools development. *Bioinformatics* **24**(21): 2534-2536.

Koch B, Evans HJ. 1966. Reduction of acetylene to ethylene by soybean root nodules. *Plant Physiol* **41**(10): 1748-1750.

Krall L, Wiedemann U, Unsin G, Weiss S, Domke N, Baron C. 2002. Detergent extraction identifies different VirB protein subassemblies of the type IV secretion machinery in the membranes of *Agrobacterium tumefaciens*. *Proc Natl Acad Sci U S A* **99**(17): 11405-11410.

Krusell L, Krause K, Ott T, Desbrosses G, Kramer U, Sato S, Nakamura Y, Tabata S, James EK, Sandal N, et al. 2005. The sulfate transporter SST1 is crucial for symbiotic nitrogen fixation in *Lotus japonicus* root nodules. *Plant Cell* **17**(5): 1625-1636.

Larrainzar E, Riely BK, Kim SC, Carrasquilla-Garcia N, Yu HJ, Hwang HJ, Oh M, Kim GB, Surendrarao AK, Chasman D, et al. 2015. Deep Sequencing of the *Medicago truncatula* Root Transcriptome Reveals a Massive and Early Interaction between Nodulation Factor and Ethylene Signals. *Plant Physiol* **169**(1): 233-265.

Larrainzar E, Wienkoop S, Weckwerth W, Ladrera R, Arrese-Igor C, Gonzalez EM. 2007. *Medicago truncatula* root nodule proteome analysis reveals differential plant and bacteroid responses to drought stress. *Plant Physiol* **144**(3): 1495-1507.

Liang Y, Cao Y, Tanaka K, Thibivilliers S, Wan J, Choi J, Kang C, Qiu J, Stacey G. 2013. Nonlegumes respond to rhizobial Nod factors by suppressing the innate immune response. *Science* **341**(6152): 1384-1387.

Liu Y, Hassan S, Kidd BN, Garg G, Mathesius U, Singh KB, Anderson JP. 2017. Ethylene Signaling Is Important for Isoflavonoid-Mediated Resistance to *Rhizoctonia solani* in Roots of *Medicago truncatula*. *Mol Plant Microbe Interact* **30**(9): 691-700.

Liu Z, Wu Y, Yang F, Zhang Y, Chen S, Xie Q, Tian X, Zhou JM. 2013. BIK1 interacts with PEPRs to mediate ethylene-induced immunity. *Proc Natl Acad Sci U S A* **110**(15): 6205-6210.

Martin A, Lee J, Kichey T, Gerentes D, Zivy M, Tatout C, Dubois F, Balliau T, Valot B, Davanture M, et al. 2006. Two cytosolic glutamine synthetase isoforms of maize are specifically involved in the control of grain production. *Plant Cell* **18**(11): 3252-3274.

Mersmann S, Bourdais G, Rietz S, Robatzek S. 2010. Ethylene signaling regulates accumulation of the FLS2 receptor and is required for the oxidative burst contributing to plant immunity. *Plant Physiol* **154**(1): 391-400.

Mitra RM, Long SR. 2004. Plant and bacterial symbiotic mutants define three transcriptionally distinct stages in the development of the *Medicago truncatula*/*Sinorhizobium meliloti* symbiosis. *Plant Physiol* **134**(2): 595-604.

Nukui N, Minamisawa K, Ayabe S, Aoki T. 2006. Expression of the 1-aminocyclopropane-1-carboxylic acid deaminase gene requires symbiotic nitrogen-fixing regulator gene *nifA2* in *Mesorhizobium loti* MAFF303099. *Appl Environ Microbiol* **72**(7): 4964-4969.

Okazaki S, Kaneko T, Sato S, Saeki K. 2013. Hijacking of leguminous nodulation signaling by the rhizobial type III secretion system. *Proc Natl Acad Sci U S A* **110**(42): 17131-17136.

Okazaki S, Tittabutr P, Teulet A, Thouin J, Fardoux J, Chaintreuil C, Gully D, Arrighi JF, Furuta N, Miwa H, et al. 2016. Rhizobium-legume symbiosis in the absence of Nod factors: two possible scenarios with or without the T3SS. *ISME J* **10**(1): 64-74.

Oldroyd GE, Engstrom EM, Long SR. 2001. Ethylene inhibits the Nod factor signal transduction pathway of *Medicago truncatula*. *Plant Cell* **13**(8): 1835-1849.

Oldroyd GE, Murray JD, Poole PS, Downie JA. 2011. The rules of engagement in the legume-rhizobial symbiosis. *Annu Rev Genet* **45**: 119-144.

Ott T, van Dongen JT, Gunther C, Krusell L, Desbrosses G, Vigeolas H, Bock V, Czechowski T, Geigenberger P, Udvardi MK. 2005. Symbiotic leghemoglobins are crucial for nitrogen fixation in legume root nodules but not for general plant growth and development. *Curr Biol* **15**(6): 531-535.

Penmetsa RV, Cook DR. 1997. A Legume Ethylene-Insensitive Mutant Hyperinfected by Its Rhizobial Symbiont. *Science* **275**(5299): 527-530.

Penmetsa RV, Uribe P, Anderson J, Lichtenzveig J, Gish JC, Nam YW, Engstrom E, Xu K, Sckisel G, Pereira M, et al. 2008. The *Medicago truncatula* ortholog of *Arabidopsis* EIN2, *sickle*, is a negative regulator of symbiotic and pathogenic microbial associations. *Plant J* **55**(4): 580-595.

Peters NK, Crist-Estes DK. 1989. Nodule formation is stimulated by the ethylene inhibitor aminoethoxyvinylglycine. *Plant Physiol* **91**(2): 690-693.

Pieterse CM, Van der Does D, Zamioudis C, Leon-Reyes A, Van Wees SC. 2012. Hormonal modulation of plant immunity. *Annu Rev Cell Dev Biol* **28**: 489-521.

Pislariu CI, Murray JD, Wen J, Cosson V, Muni RR, Wang M, Benedito VA, Andriankaja A, Cheng X, Jerez IT, et al. 2012. A *Medicago truncatula* tobacco retrotransposon insertion mutant collection with defects in nodule development and symbiotic nitrogen fixation. *Plant Physiol* **159**(4): 1686-1699.

Rappsilber J, Ryder U, Lamond AI, Mann M. 2002. Large-scale proteomic analysis of the human spliceosome. *Genome Res* **12**(8): 1231-1245.

Reeve W, Chain P, O'Hara G, Ardley J, Nandesena K, Brau L, Tiwari R, Malfatti S, Kiss H, Lapidus A, et al. 2010. Complete genome sequence of the *Medicago* microsymbiont *Ensifer* (*Sinorhizobium*) *medicae* strain WSM419. *Stand Genomic Sci* **2**(1): 77-86.

Sinharoy S, Torres-Jerez I, Bandyopadhyay K, Kereszt A, Pislariu CI, Nakashima J, Benedito VA, Kondorosi E, Udvardi MK. 2013. The C2H2 transcription factor regulator of symbiosome differentiation represses transcription of the secretory pathway gene *VAMP721a* and promotes symbiosome development in *Medicago truncatula*. *Plant Cell* **25**(9): 3584-3601.

Starker CG, Parra-Colmenares AL, Smith L, Mitra RM, Long SR. 2006. Nitrogen fixation mutants of *Medicago truncatula* fail to support plant and bacterial symbiotic gene expression. *Plant Physiol* **140**(2): 671-680.

Summers ML, Elkins JG, Elliott BA, McDermott TR. 1998. Expression and regulation of phosphate stress inducible genes in *Sinorhizobium meliloti*. *Mol Plant Microbe Interact* **11**(11): 1094-1101.

Tintor N, Ross A, Kanehara K, Yamada K, Fan L, Kemmerling B, Nurnberger T, Tsuda K, Saijo Y. 2013. Layered pattern receptor signaling via ethylene and endogenous elicitor peptides during Arabidopsis immunity to bacterial infection. *Proc Natl Acad Sci U S A* **110**(15): 6211-6216.

Udvardi M, Poole PS. 2013. Transport and metabolism in legume-rhizobia symbioses. *Annu Rev Plant Biol* **64**: 781-805.

Valot B, Gianinazzi S, Eliane DG. 2004. Sub-cellular proteomic analysis of a *Medicago truncatula* root microsomal fraction. *Phytochemistry* **65**(12): 1721-1732.

Vasse J, de Billy F, Truchet G. 1993. Abortion of infection during the *Rhizobium meliloti*—alfalfa symbiotic interaction is accompanied by a hypersensitive reaction. *The Plant Journal* **4**(3): 555-566.

Yang S, Tang F, Gao M, Krishnan HB, Zhu H. 2010. R gene-controlled host specificity in the legume-rhizobia symbiosis. *Proc Natl Acad Sci U S A* **107**(43): 18735-18740.

Zipfel C. 2013. Combined roles of ethylene and endogenous peptides in regulating plant immunity and growth. *Proc Natl Acad Sci U S A* **110**(15): 5748-5749.

Zipfel C. 2014. Plant pattern-recognition receptors. *Trends Immunol* **35**(7): 345-351.

730 **Legends to supplementary figures and tables**

731 Supplementary figure 1: Protein quantification formula

732 Supplementary figure 2: *S. medicae* WSM419-*S. meliloti* 1021 megaplasmids syntheny

733 Supplementary figure 3: *S. medicae* replicon usage in wild type and *symCRK* hosts

734 Supplementary figure 4: AVG reduces defense transcript accumulation in the *symCRK*
735 nodules

736 Supplementary figure 5: *Sickle* is expressed in WT and *symCRK* nodules

737 Supplementary figure 6: Ethylene treatments induce the accumulation of phenolic compounds
738 in nodules

739 Supplementary figure 7: Ethylene effect on *Lotus japonicus* nodules

740 Supplementary figure 8: Ethylene treatment reduces the expression of some nodule specific
741 genes

742 Supplementary figure 9: Distribution amongst COG functional classes of the bacterial
743 proteins differentially accumulated in the F1 fractions of wild type *Medicago truncatula* and
744 of the *symCRK* mutant

745 Supplementary table 1: Primers used during this study

746 Supplementary table 2: Proteins identified during this study

747 Supplementary table 3: Defense-related proteins identified during this study

Legends to figures and table:

	F1		F2		F3	
	WT	*symCRK*	WT	*symCRK*	WT	*symCRK*
Bacterial proteins	879 (22737)	845 (15245)	180 (2162)	122 (830)	316 (4491)	217 (1880)
Plant proteins	374 (3337)	845 (7098)	1280 (19190)	1407 (19474)	1383 (22931)	1448 (23405)
Membrane associated plant proteins (%)	39 (3,1%)	70 (4.1%)	153 (10.5%)	151 (9.9%)	26 (1.5%)	43 (2.6%)

Table 1: Number of detected proteins. Numbers between brackets on bacterial and plant protein lines correspond to the cumulated number of spectra. Are considered as plant membrane associated proteins identified plant proteins associated with one out of the following GO terms: transport, membrane, integral membrane component and transmembrane transport. The proteins without an associated GO term but for which annotation contains the word "membrane" were also included. % s indicated on the membrane associated plant proteins line correspond to the percentages of these proteins amongst the total number of identified proteins.

762

	M. truncatula	*S. medicae*
Wild type	**O_2 transport**	**Nitrogen fixation**
	Leghemoglobin	Nitrogenase reductase
	Transport	Nitrogenase β chain
	Potassium efflux antiporter	Nitrogenase α chain
	Symbiotic sulfate transporter	**Energy production**
	Metabolism	Nucleoside diphosphate kinase
	Malate dehydrogenase	Pyruvate dehydrogenase subunit beta
	Glutamate-1-semialdehyde 2,1-aminomutase	NADH:flavin oxidoreductase
	L-ascorbate oxidase	ATP synthase subunit C
	ATP synthase	
symCRK	**Phenylpropanoid biosynthesis**	**Transporters**
	4-coumarate:CoA ligase-like protein	ABC transporter proteins
	Caffeic acid O-methyltransferase	Polar amino acid ABC transporter
	Cinnamoyl-CoA reductase	Sulfate transporter
	Chorismate synthase	**Stress response**
	Cinnamyl alcohol dehydrogenase-like protein	GroEL
	Phenylalanine ammonia-lyase-like protein	Bacterioferritin
	Flavonoid & isoflavonoid biosynthesis	ACC deaminase
	Chalcone and stilbene synthase family protein	General stress response regulator PhyR
	Chalcone-flavanone isomerase family protein	Ectoine metabolism
	Dihydroflavonol 4-reductase-like protein	GloB
	Isoflavone reductase-like protein	Do serine proteinase
	Isoflavone-7-O-methyltransferase	
	Other pathogen induced proteins	
	Chitinase	
	Subtilisins	
	Patatin-like phospholipase	
	Kunitz type trypsin inhibitor	
	Peroxidase	
	Pathogenesis-like protein	
	Disease resistance response protein	
	Receptor-like kinases	
	Leucine Rich Repeat Receptor-like kinases	

763

764 **Table 2: Summary of proteins accumulated in the WT and *symCRK* nodule proteomes.**

765

Figure 1: Technical workflow allowing the analysis of WT and *symCRK* nodule proteomes. In order to characterize and compared wild type (WT) and *symCRK* proteomes, nodules of the two *Medicago truncatula* lines induced by *Sinorhizobium medicae* strain WSM419 were collected (1) ground (2) and suspended in buffer prior to low speed centrifugation to eliminate debris (3). Supernatant was then centrifuged at higher speed to separate symbiosome and soluble material (4). Successive centrifugations (5-6) were then employed to clean supernatant containing the soluble proteins of the plant cytoplasm and to isolate a microsomal fraction (6). Symbiosome containing pellets were washed (7) and cells were disrupted by sonication (8), debris were eliminated by centrifugation (9). Protein fractions were then extracted using TCA acetone (10) and separated by SDS PAGE (11). Proteins were then digested in gel by trypsin (12) and peptides were analyzed by LC/MS-MS which allowed protein identifications (13).

Figure 2: Rhizobial proteomes of efficient (wild type) and of defense developing (*symCRK*) nodules highlight different replicon exploitation strategy with chromosome-encoded proteins overrepresented and strain specific proteins underrepresented. A, *Sinorhizobium medicae* replicon usage in the *M. truncatula* WT and *symCRK* plants. Identified proteins were mapped on the four replicons of *S. medicae* (the chromosome, the megaplasmids pSMED01 and pSMED02 and the plasmid pSMED03). Chi-square tests indicate significant discrepancies between gene distribution on the different replicons and the location of genes encoding the detected proteins in both WT and *symCRK* proteomes (P values<0.001). Chromosome encoded proteins are overrepresented and the replicon usage is drastically different in the two hosts. Two-ways ANOVA followed by Tukey's multiple comparisons were performed in order to establish the frequency groups (indicated by letters over the histogram bars). Error bars represent the standard errors (n=3). B, The proportion of

strain specific genes of the WSM419 genome is presented as well as the proportion of strain specific protein detected in nodules. C Proportions of common and of strain specific gene of each replicons are presented.

Figure 3: Ethylene as a candidate mediator of defense reactions in nodules. A, Expression of the genes encoding proteins harboring a defense-related GO term and that are accumulated in the *Medicago truncatula symCRK* mutant nodules. The increase in expression of the ACC oxidase-like gene (Mtr.32666.1.S1_at) in the *symCRK* nodule is also shown. The expression levels were determined in root systems upon pathogen attacks (by *Aphanomyces euteiches* and by *Ralstonia solanacearum*) in the wild type *M. truncatula* and in the *sickle* mutant unable to perceive ethylene. Data were extracted from the *Medicago truncula* Gene Expression Atlas. B, The expression of the *ACC oxidase-like* gene (Mtr.32666.1.S1_at) correlates with the development of defense-like reactions. RT-qPCR results indicate that the ACC oxidase-like gene is induced in the *M. truncatula dnf2-4* and *symCRK* nodules triggered by WT rhizobia but not in the non-fixing nodules triggered by the bacterial *bacA* mutant on the WT or on the *symCRK* mutant of *M. truncatula*. In contrast, expression of the ACC oxidase-like gene is induced in the *dnf2-4* mutant nodules triggered by *bacA*. Stars indicate relevant significant difference in gene expression attested by Mann-Whitney test (P value<0.05). This expression pattern correlates with the development of defenses (Berrabah *et al.*, 2015). C, ACC oxidase gene expression in *symCRK* nodules, RT-qPCRs were performed on RNA isolated from WT and *symCRK* nodules. The abundance of transcripts is expressed as a fold change compared to WT after normalization with the internal reference *MtActin*. Error bars represent the standard errors (five biological experiments and two technical replicates per experiments). D, ACC oxidase activity is detected in crude extracts of *symCRK* nodules but not WT ones. Ethylene production was measured by GC FID after a two hour incubation in

816 the presence of 1mM ACC, the x axis represents the retention time (min) and the y axis the
817 signal measured by FID ($pA.s^{-1}$), the ethylene retention time with the used method is 1.65
818 minutes.
819
820 **Figure 4: Ethylene treatment compromises nitrogen fixation in a *Sickle* dependent way.**
821 A, Nodulated root systems of *Medicago truncatula* WT ecotype R108 and of its derivative
822 mutant *symCRK* were treated with the indicated concentration of ethylene during three days
823 before analyzing their capacity to fix nitrogen by acetylene reduction assays (ARA). B, *Sickle*
824 is required for ethylene inactivation of nitrogen fixation. Nodulated root systems of WT and
825 *sickle* plants were treated or not with ethylene during three days before evaluation of
826 nitrogenase activity. C, an ethylene triggered nitrogenase defect is also observed in *Lotus*
827 *japonicus*. Nodulated root systems of WT *L. japonicus* were treated with the indicated
828 concentration of ethylene during three days before analyzing their capacity to fix nitrogen by
829 ARA. Data were normalized by the incubation time in the presence of the substrate
830 (acetylene). Error bars represent the standard errors.
831
832 **Figure 5: Ethylene treatment triggers *symCRK*-like defenses.** A, ethylene treatments
833 induce the development of necrosis in *Medicago truncatula* nodules. Nodule sections
834 prepared from nodulated root systems treated with the indicated ethylene concentrations
835 (ppm) were imaged and for each nodule section, the total surface of the nodule and the
836 necrotic surface were determined, the ratio of necrotic surface over the total surface are
837 plotted. Every nodule section is represented by single dot, whiskers represent minimum to
838 maximum values and horizontal lines represent the medians. Mann and Withney test
839 performed to compare data from the Control and the 25 ppm ethylene treated material
840 indicates significantly different distribution between the two groups (P value<0.0001

841 indicated by the four stars on the box plot). B: RT-qPCRs were performed on RNA isolated
842 from nodules treated or not with ethylene (at the indicated concentration expressed in ppm).
843 The quantity of PR10 and NDR1 transcript is expressed as a fold change compared to
844 untreated WT after normalization with the internal reference *MtActin*. Error bars represent
845 standard errors. C: Ethylene treatments trigger the accumulation of phenolics. Nodule sections
846 were stained with methylene blue that reveals phenolics in blue. Images were analyzed and
847 for each section the total surface of the nodule and the surface responding to methylene blue
848 were determined and plotted, every dot represents one nodule section. D: ethylene treatment
849 triggers bacteroid death. Confocal imaging was performed after a live and dead staining
850 procedure on nodule sections obtained from material treated or not with ethylene, scale bars:
851 20 µm. The procedure reveals dead bacteria in red and living bacteria in green.
852
853 **Figure 6: Ethylene and a *symCRK* mutation triggered necrosis colocalize with rhizobial**
854 **infected cells.** Root systems of nodulated *Medicago truncatula* plants were treated or not for
855 three days with 2500 ppm ethylene. After incubation, nodule sections were prepared from
856 wild type (A) and *symCRK* (B) untreated plants and wild type ethylene treated (C) root
857 systems. Arrows indicate examples of infected cells, and dashed arrows uninfected cells; scale
858 bars represent 50 µm. In the central part of the nodules, randomly chosen microscopic fields
859 were observed and for each observed plant cells infection and development of necrosis were
860 scored (D-F). Ethylene treatment induces nodule necrosis in a pattern similar to the *symCRK*
861 phenotype. The proportions of necrotic and non-necrotic cells amongst infected and
862 uninfected cells are presented for untreated wild type and *symCRK* nodules (D and E
863 respectively) and for ethylene treated wild type (F).
864

Figure 7: The ethylene biosynthesis inhibitor AVG reduces the intensity of the *symCRK* and the *dnf2* mutant phenotypes. *Medicago truncatula dnf2-4* and *symCRK* mutant plants were cultivated *in vitro* in 40 mM AVG supplemented medium. 21 dpi nodule sections were analyzed for the presence of phenolic compounds and for necrotic zones. Whiskers indicate the minimum to maximum values, all points are shown and horizontal lines represent the medians. Mann Whitney tests were performed to compare values obtained with and without AVG, the four asterisks indicate that the values are significantly different with a P value<0.0001.

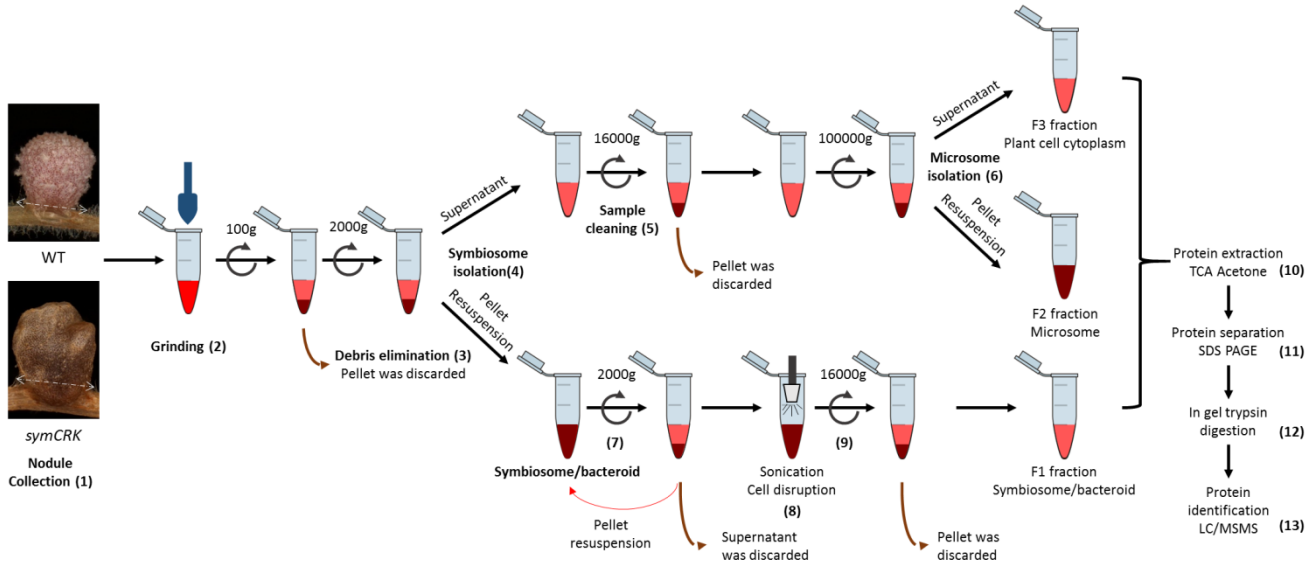
WT
symCRK
Nodule Collection (1)
Grinding (2)
100g
2000g
Debris elimination (3)
Pellet was discarded
Supernatant
Symbiosome isolation(4)
Pellet Resuspension
16000g
Sample cleaning (5)
Pellet was discarded
100000g
Supernatant
Microsome isolation (6)
F3 fraction
Plant cell cytoplasm
Pellet Resuspension
F2 fraction
Microsome
2000g
(7)
Symbiosome/bacteroid
Pellet resuspension
Supernatant was discarded
Sonication
Cell disruption
(8)
16000g
(9)
Pellet was discarded
F1 fraction
Symbiosome/bacteroid
Protein extraction
TCA Acetone (10)
Protein separation
SDS PAGE (11)
In gel trypsin digestion (12)
Protein identification
LC/MSMS (13)

Figure 1

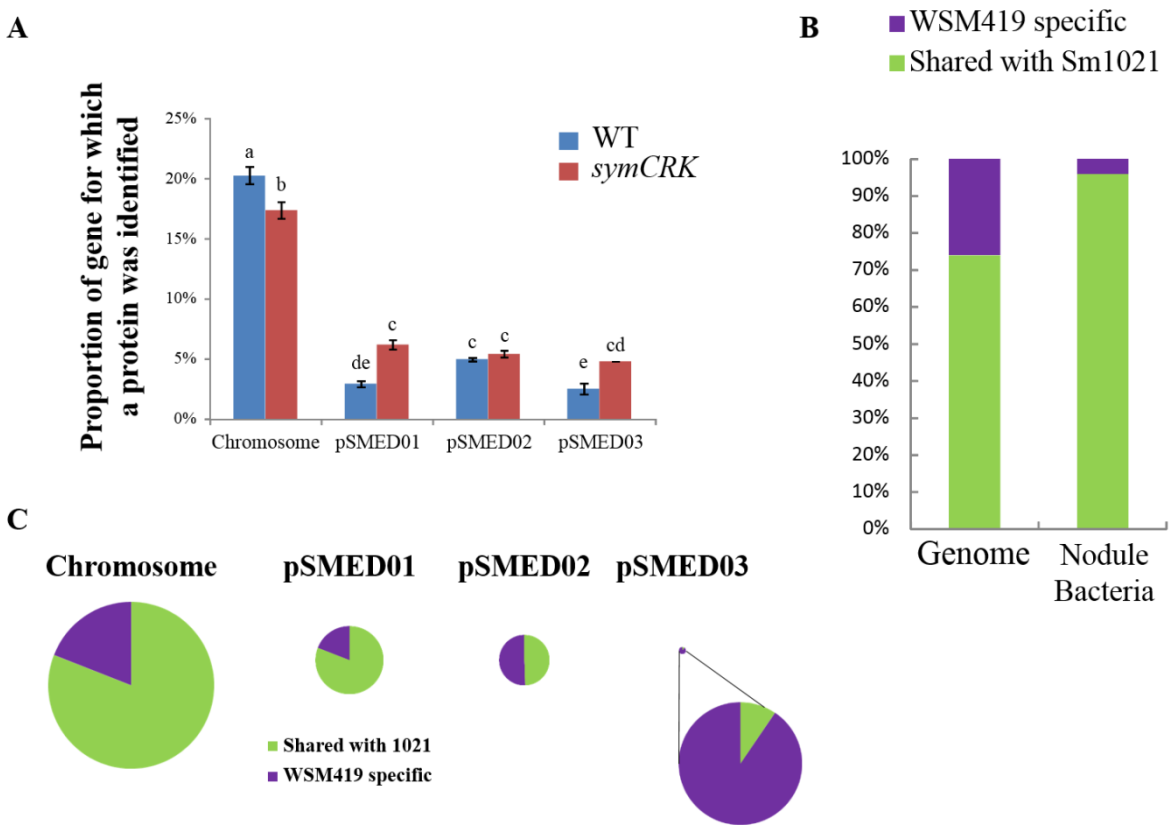

Figure 2 Bacteroid proteomes are enriched chromosome-encoded proteins and poor in strain specific proteins

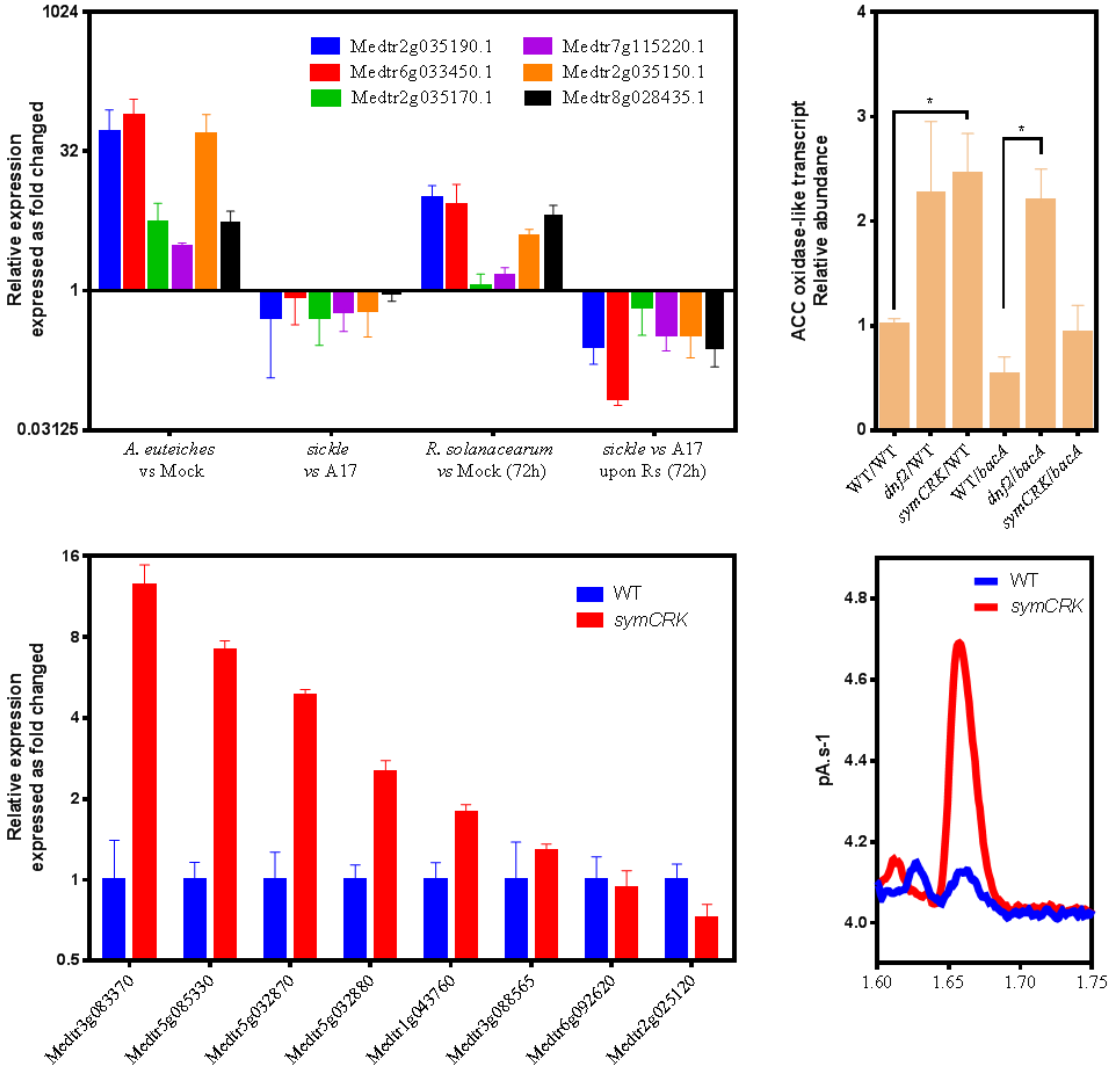

881

882 **Figure 3**

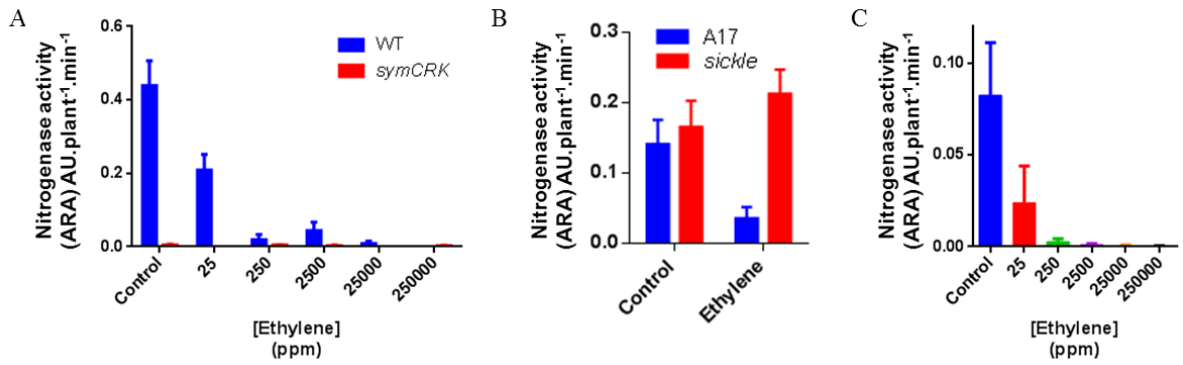

883

884 **Figure 4**

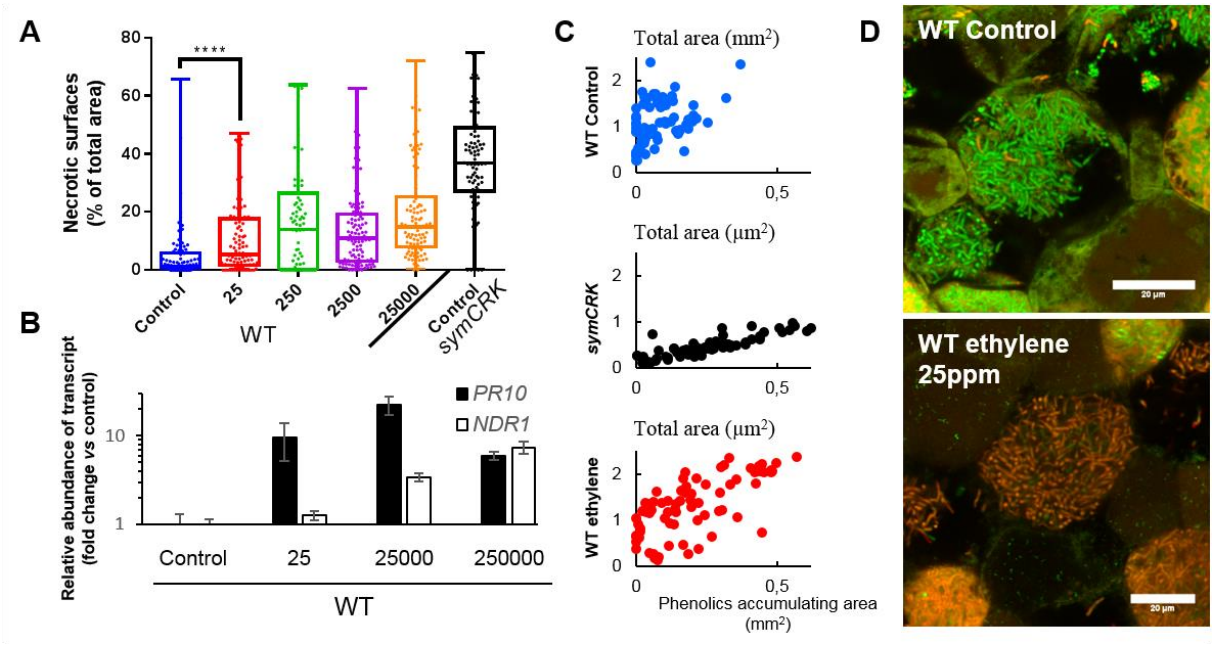

885

886 **Figure 5**

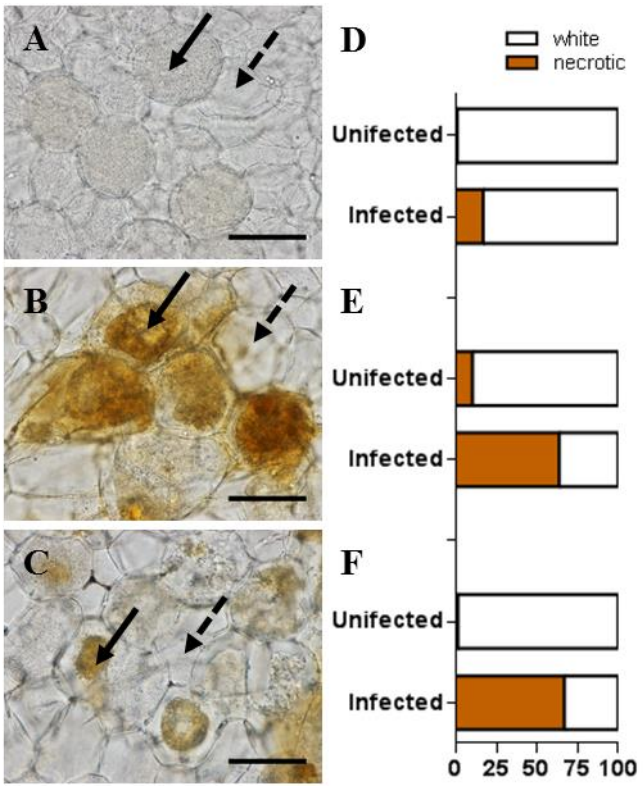

887

888 **Figure 6**

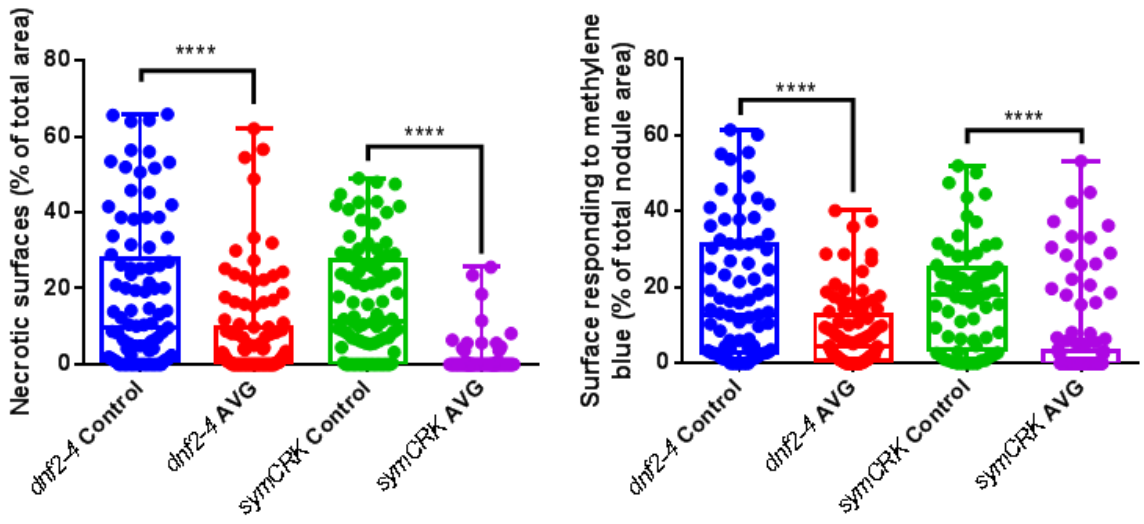

889

890 **Figure 7**

Control of the ethylene signaling pathway prevents plant defenses during intracellular accommodation of the rhizobia

Fathi Berrabah, Thierry Balliau, El Hosseyn Aït-Salem, Jeoffrey George, Michel Zivy, Pascal Ratet, Benjamin Gourion

28 February 2018

Proteins were quantified by a method inspired by (Rappsilber *et al.*, 2002) as follows:

$$A_{ijk} = \frac{\left(\frac{SC_{ijk}}{SC_{jk}} * \overline{SC}_{jk}\right)}{O_i}$$

where A_{ijk} is the abundance estimated for protein i in sample j and in fraction k
SC_{ijk} is the number of MS2 spectra assigned to protein i in sample $j$and fraction k
O_i is the theoretical number of tryptic peptides observable for protein i
$\overline{SC}_{jk}$ is the average number of MS2 spectra assigned in sample j and fraction k
SC_{jk} is the total number of MS2 spectra assigned in sample j and fraction k

Supplementary Information Fig. S1: Protein quantification for proteomics experiment.

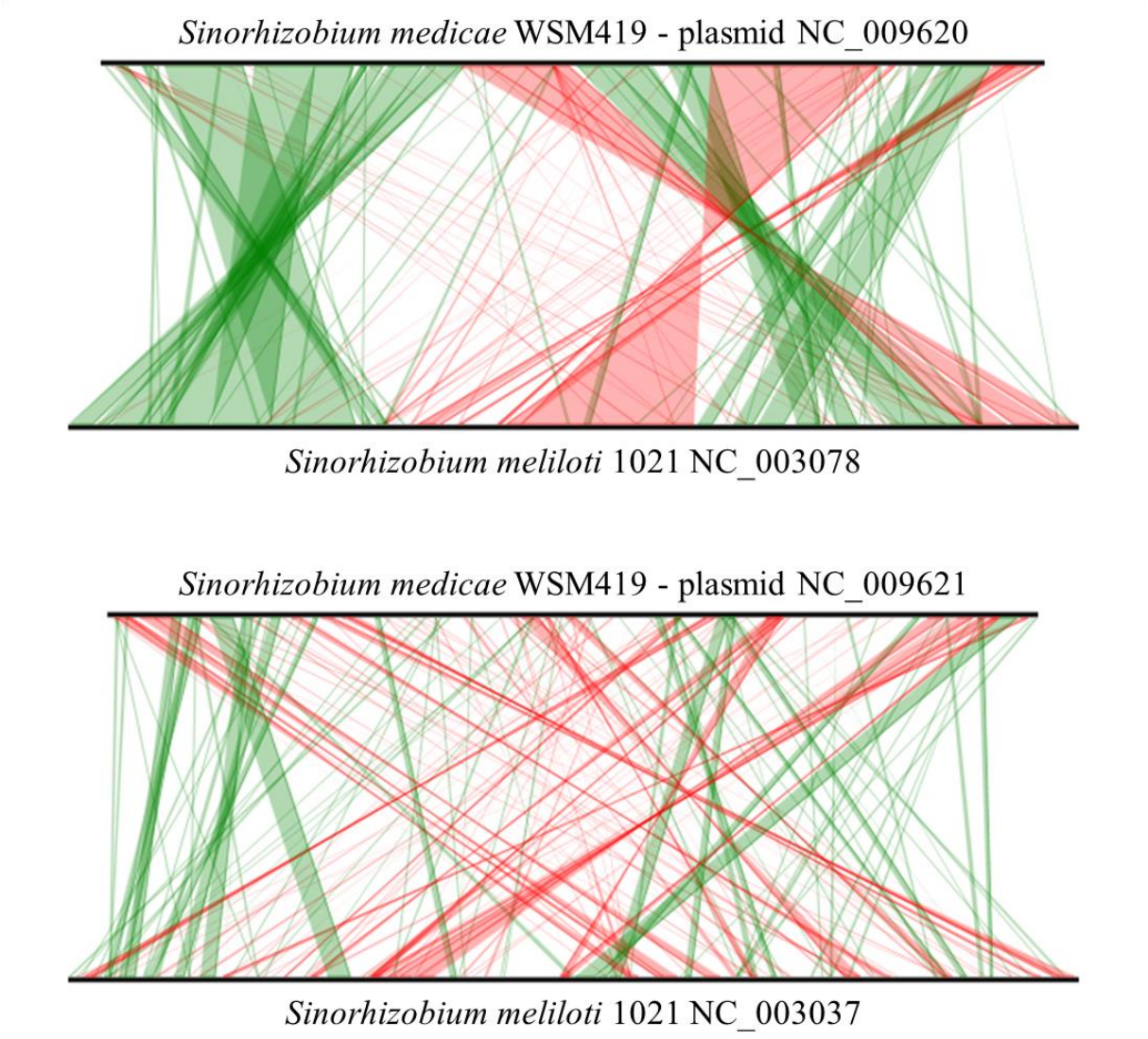

Supplementary Information Fig. S2: *S. medicae* WSM419 and *S. meliloti* Sm1021 megaplasmid synteny. The synteny lineplot was generated using the microscope mage annotation platform (Vallenet *et al.*, 2013). Syntons (≥ 3genes) are represented in green or in red if inverted around the plasmid origin of replication. NC_003037 and NC_009621 are the symbiotic plasmids.

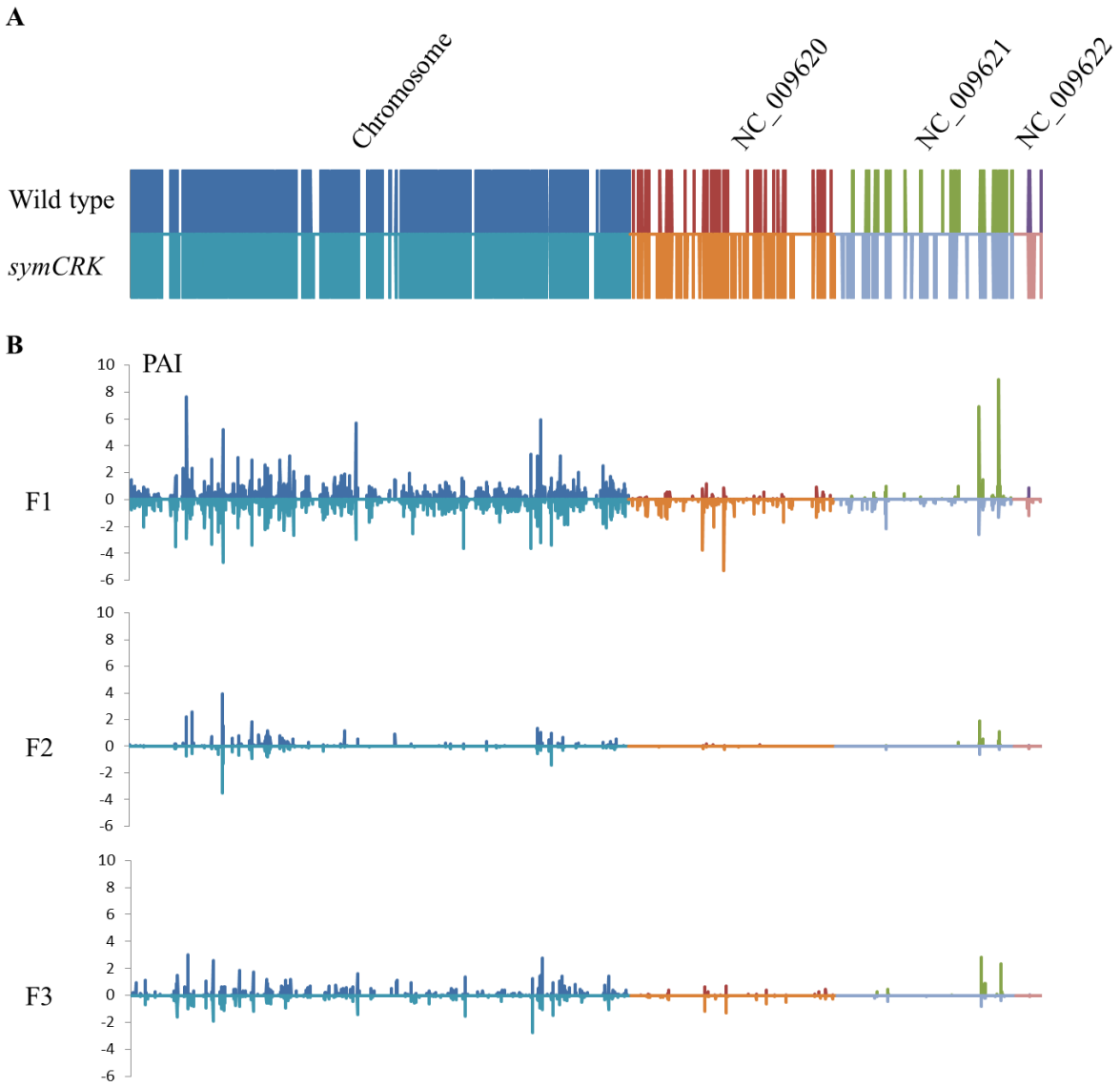

Supplementary Information Fig. S3: *Sinorhizobium medicae* replicon usage in wild type and *symCRK* hosts. A Bacterial proteins detected in the two hosts are represented as colored bars mapped on the *S. medicae* strain WSM419 genome. B The spectral counting index of each protein (noted here protein abundance indexes (PAI)) are represented for every indicated fraction, positive values represent the PAI in the wild type plants, negative values represent the PAI in the *symCRK* mutant.

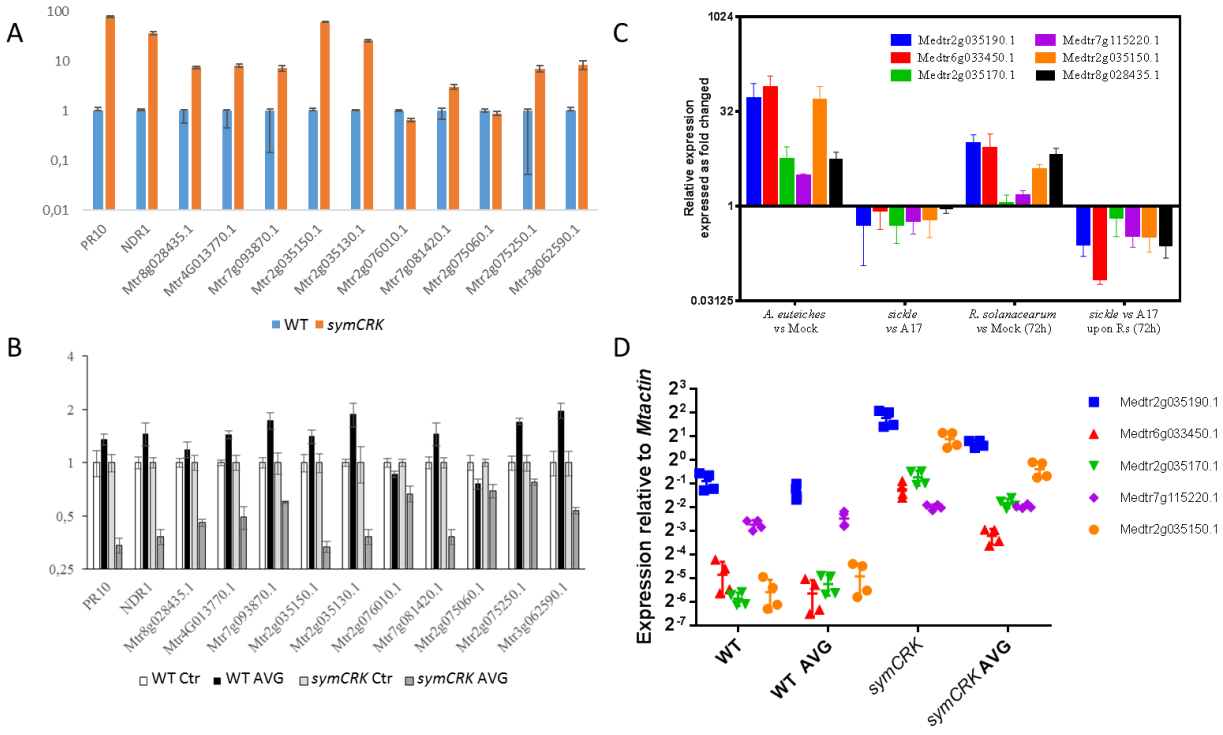

Supplementary Information Fig. S4: AVG reduces defense transcript accumulation in the *symCRK* nodules. RT-qPCRs were performed on RNA isolated from nodules of plants cultivated in the presence or in the absence of the ethylene biosynthesis inhibitor AVG. Panel A represents the data obtained without AVG and are normalized against the expression in the WT nodules (after a first normalization with *MtActin* gene as an internal standard). Panel B: The quantity of transcript is expressed as a fold change compared to the control plants of each line cultivated in the absence of AVG (after normalization with the internal reference *MtActin*; "Crt" stands for control). Error bars represent the standard errors. Panel C represents the expression of a subset of genes presented in figure 3A for which expression was evaluated by RTqPCRs in WT and *symCRK* mutant in absence or in presence of AVG (Panel D).

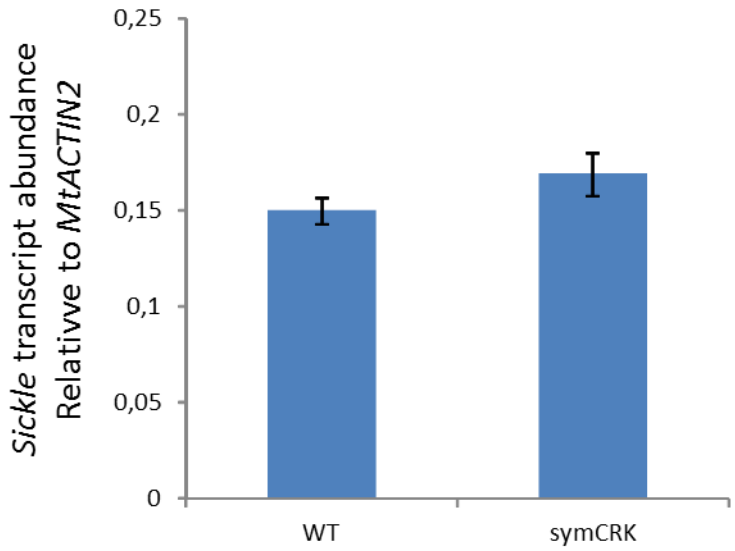

Supplementary Information Fig. S5: *Sickle* is expressed in WT and *symCRK* nodules. Relative *Sickle* transcript levels were determined by quantitative reverse transcription-polymerase chain reaction (qRT-PCR) in WT and *symCRK* nodules. Results were normalized using the constitutive *MtACTIN2* gene transcript level. Error bars represent the standard deviations of results obtain during five independent experiments.

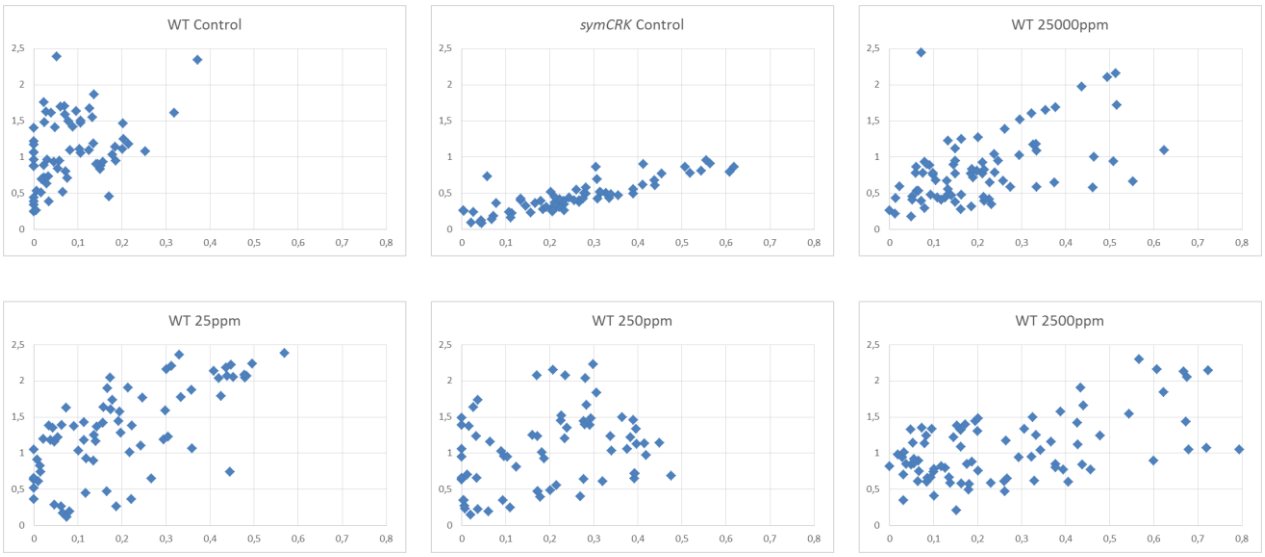

Supplementary Information Fig. S6: Ethylene treatments induce the accumulation of phenolic compounds in nodules. Nodule sections prepared from nodulated root systems treated or not by ethylene, at the indicated concentration, were fixed and stained by $KMnO_4$/Methylene blue before imaging. This procedure reveals phenolics accumulation in the nodule. Each dot on each panel corresponds to the analysis of one nodule section. For each nodule section, the total surface and the surface occupied by the phenol staining were estimated. The total surface of the nodule section and the surface stained with methylene blue are plotted on y and x axes respectively (mm^2). In this representation each dot is positioned at the intersection of its x and y values. Nodule sections with little or no phenolic staining are grouped close to the y axe while those with important surfaces accumulating phenolics are distant to the y axe.

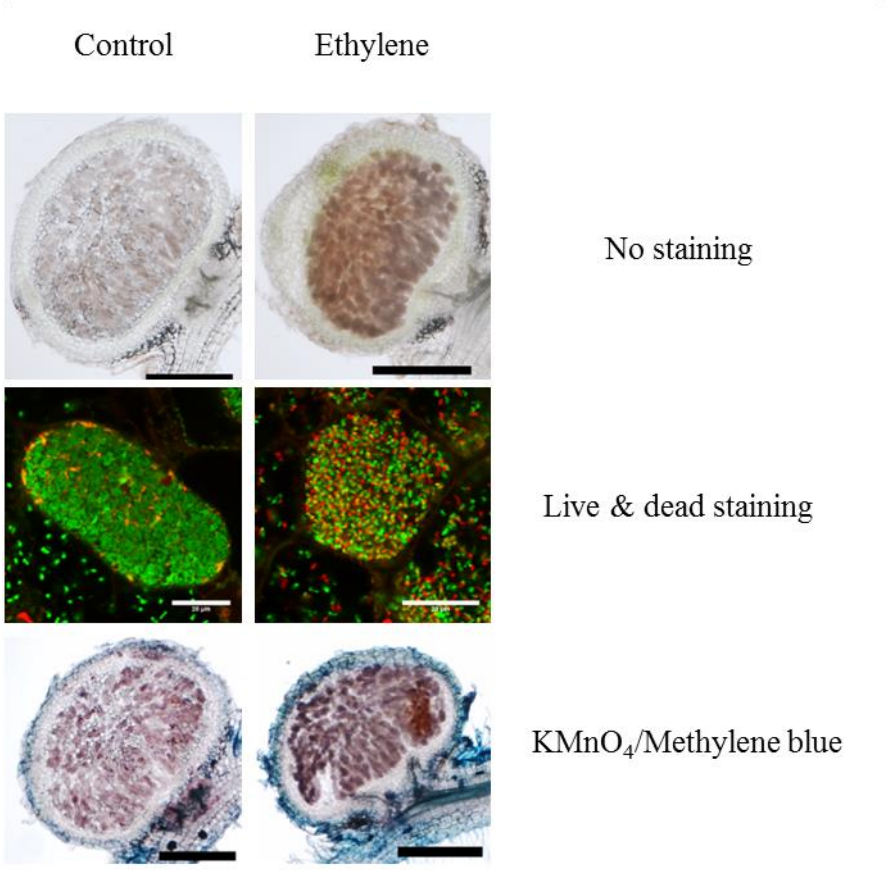

Supplementary Information Fig. S7: Ethylene effect on *Lotus japonicus* nodules. Ethylene treatment triggers modifications in the nodules, necrosis was not observed but bacteroids viability was reduced as showed by the live and dead staining procedure that colors dead bacteria in red and alive bacteria in green. $KMnO_4$/Methylene blue fixation and staining procedure reveals phenolics compounds in blue. Scale bars represent 500µm and 20µm on whole nodule pictures and on live and dead staining pictures respectively.

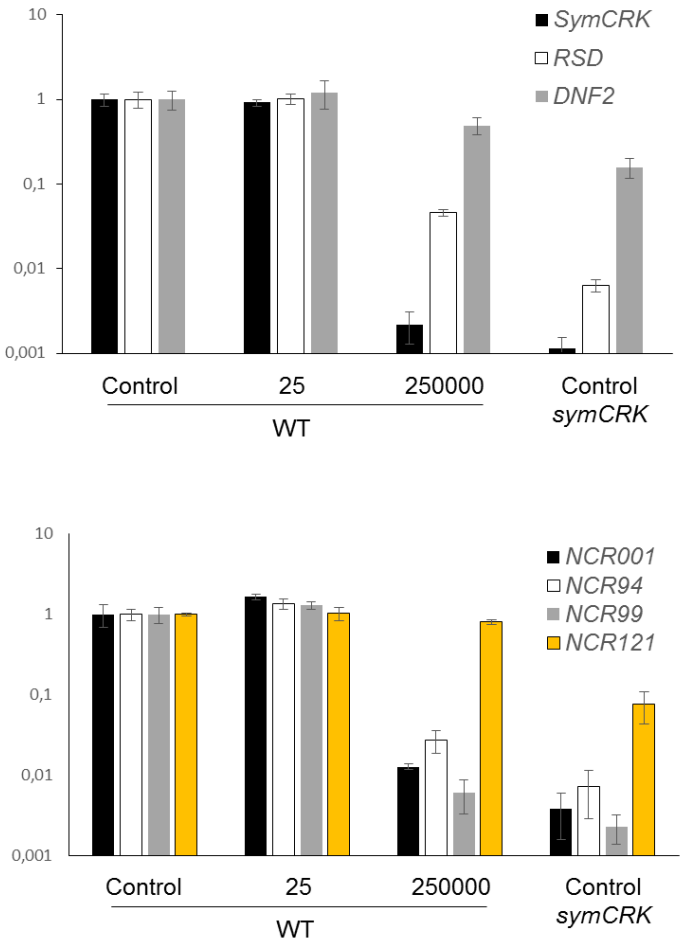

Supplementary Information Fig. S8: Ethylene treatment reduces the expression of some nodule specific genes. RT-qPCRs were performed on RNA isolated from nodules treated or not by ethylene (at the indicated concentration expressed in ppm). The quantity of transcript is expressed as a fold change compared to untreated WT after normalization with the internal reference *MtActin2*. Errors bars represent the standard error (n=4, 2 independent experiments each with two technical replicates).

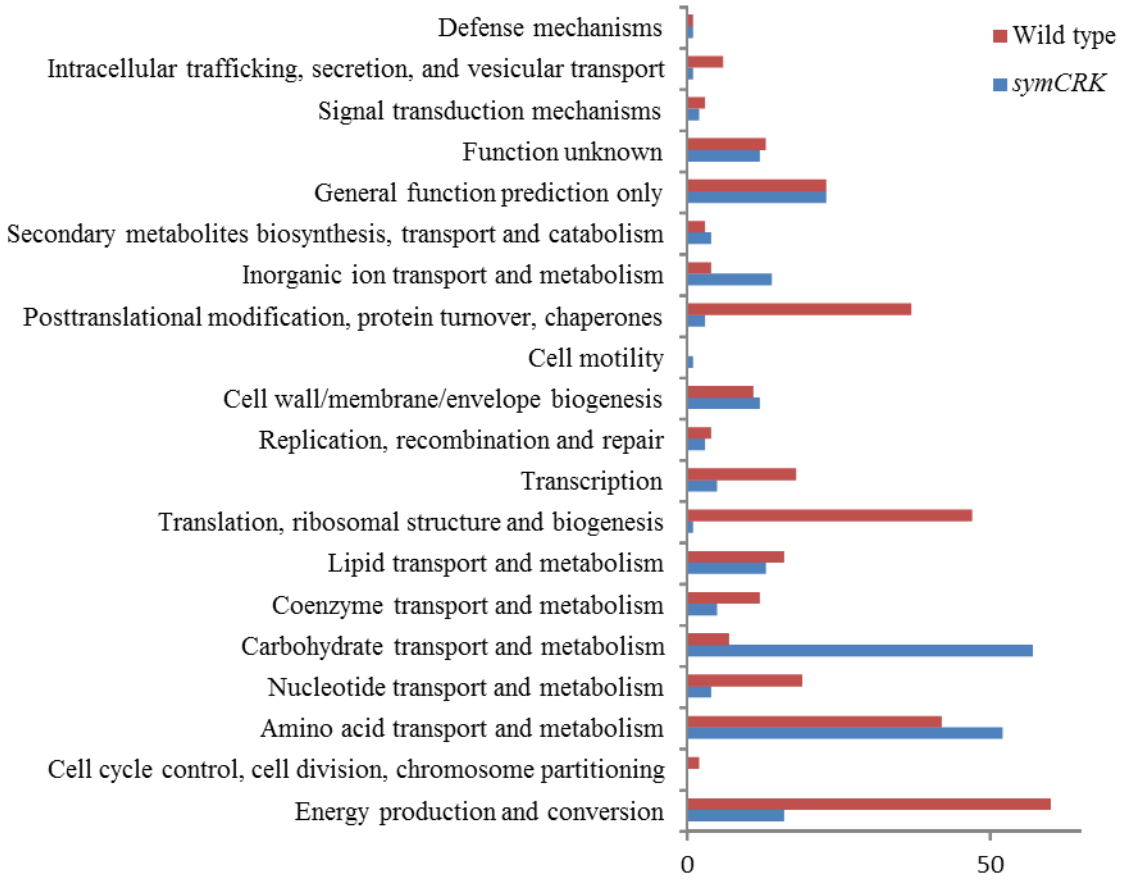

Supplementary Information Fig. S9: Distribution amongst COG functional classes of the bacterial proteins differentially accumulated in the F1 fractions of wild type *Medicago truncatula* and of the *symCRK* mutant.

References:

Rappsilber J, Ryder U, Lamond AI, Mann M. 2002. Large-scale proteomic analysis of the human spliceosome. *Genome Res* **12**(8): 1231-1245.

Vallenet D, Belda E, Calteau A, Cruveiller S, Engelen S, Lajus A, Le Fevre F, Longin C, Mornico D, Roche D, et al. 2013. MicroScope--an integrated microbial resource for the curation and comparative analysis of genomic and metabolic data. *Nucleic Acids Res* **41**(Database issue): D636-647.

The multiple faces of the *Medicago-Sinorhizobium* symbiosis

Fathi Berrabah[1], El Hosseyn Ait Salem[2-3], Marie Garmier[2-3], Pascal Ratet[2-3].

[1]Departement of biology, faculty of nature and life science, University of Ziane Achour, 17000, Djelfa, Algeria.

[2] Institute of Plant Sciences Paris-Saclay IPS2, CNRS, INRA, Université Paris-Sud, Université Evry, Université Paris-Saclay, Bâtiment 630, 91405 Orsay, France

[3] Institute of Plant Sciences Paris-Saclay IPS2, Paris Diderot, Sorbonne Paris-Cité, Bâtiment 630, 91405 Orsay, France

Abstract

***Medicago truncatula* is able to perform a symbiotic association with *Sinorhizobium spp*. This interaction leads to the formation of a new root organ, the nodule, in which bacteria infect the host cells and fix atmospheric nitrogen for the plant benefit. Multiple and complex processes are essential for the success of this interaction from the recognition phase to nodule formation and functioning, and a wide range of plant host genes is required to orchestrate this phenomenon. Thanks to direct and reverse genetic as well as transcriptomic approaches, numerous genes involved in this symbiosis have been described and improve our understanding of this fantastic association. Herein we propose to update the recent molecular knowledge of how *M. truncatula* associates to its symbiotic partner *Sinorhizobium spp*.**

Key words: *Medicago*, *Sinrohizobium*, symbiosis, symbiotic genes, nitrogen fixation

Introduction to legume-rhizobia symbiosis

Leguminous plants growing in poor nitrogen soils are able to establish symbiosis with soil nitrogen-fixing bacteria referred as rhizobia. This interaction leads to the formation of new root organs called nodules, within which rhizobia fix atmospheric nitrogen and deliver the organic nitrogen to their host. In return the plant provides a beneficial environment for the symbiont [1]. Two processes are required for nodule formation; i) infection of the root hair cells by the bacteria via the development of infection threads (ITs), ii) concomitantly an organogenetic process is activated and corresponds to reactivation of cortical cell division. Organogenesis is observed at the site of infection and gives the future nodule primordium [2] (figure 1). In the nodules, bacteria infect massively and chronically the host cells without induction of defense reactions and differentiate in an intracellular form call the bacteroid. This high level of infection is exceptional in nature and a growing number of studies show the complexity of the molecular processes requiring repression of the plant immunity during symbiosis [3]. Inside the host cell, the bacteroid nitrogenase fixes atmospheric nitrogen by converting N_2 into NH_3^+ [4]. As this nitrogenase enzyme is an extremely O_2-sensitive enzyme, the plant host regulates nodule O_2 diffusion via the expression of specific leghemoglobin (Lbs) proteins maintaining low level of free oxygen in the cells [5]. These Lbs confer the pinkish coloration to the nodules that is considered as a marker for healthy and functional symbiotic organs.

Depending of the legume species, two principal types of nodules are found; determinate nodules characterized by spherical shape due to the presence of a diffuse meristem and indeterminate nodules with elongated shape [6]. Different zones are present in these indeterminate nodules (figure 1); the apical meristem or zone I (ZI) is responsible for a constant growth of the organ conferring the elongated shape, ZI is followed by infection zone or zone II (ZII) in which bacteria infect the host cells. Next to the ZII is the fixation zone, or zone III (ZIII), in which the differentiated bacteroids start to express the nitrogenase and to fix N_2. This zone is separated from the ZII by the inter-zone or ZII-III in which undifferentiated bacteroids undergo a terminal differentiation. Finally, when nodules become old, or when the plant is stressed or when organic nitrogen like nitrate is added to the growth media, a senescent zone, or zone IV (ZIV) is observed. In this zone bacteroids as well as host cells are degraded [7] (figure 1). Interestingly, this ZIV can be recolonize by saprophytic rhizobia [8]. Senescence is also observe in determinate nodules, but in this nodule type its starts form the nodule center and spreads to the periphery of the organ [9].

The interaction between the model plant *Medicago truncatula* and its symbiotic partner *Sinorizobium spp* is one of the best-characterized legume-rhizobia associations. This interaction results in the formation of indeterminate nodules. Thanks to mutagenesis approaches such as transposon insertions and fast neutron deletions, reverse genetic approaches using mutant collections and transcriptomic analysis, many genes involved in the *M. truncatula-Sinorhizobium spp* interaction were described. This review summarizes in an integrative model the recent knowledge on the molecular mechanisms underlying this association. In the text, we focus our attention on the best characterized genes, and Table 1 is a more exhaustive list of the genes associated to the symbiosis (see also figure 1 for genes involved in early interaction and nodule organogenesis).

Rhizobial recognition key events to successful interaction

When nitrogen becomes limiting for growth, legumes secrete in the rhizosphere specific secondary metabolites of the flavonoids type that are specifically perceived by rhizobia [10]. Flavonoids bind to and activate the bacterial transcriptional regulators NodD. These activated NodD induce the expression of the *nod* regulon, including the *nodABC* genes responsible for nod factors (NFs) backbone biosynthesis [11]. NFs that are key signaling molecules of the symbiosis are lipo-chitooligosacharides (LCOs) composed by a N-acetylglucosamine (GlcNAc) backbone with fatty acid attached in the non-reducing terminal glucosamine [12]. Different modifications of the NFs structure can occur depending on the rhizobial strain and determine the host-rhizobium compatibility and specificity of recognition [13]. The modifications on the NFs structure can include modifications on the chitin backbone or changes of the length and degree of unsaturation of the fatty acid chain. However, the NFs are not essential for all leguminous-rhizobia interactions as, for example, *Bradyrhizobium spp* can nodulate *Aeschynomene evenia* without production of NFs [14].

NFs are perceived in the roots epidermis by Lysine Motif (LysM) Receptor-Like Kinases (RLKs), but the mechanism of recognition is not yet fully understood. Nod Factor Perception (NFP) and LYsine motif Kinase 3 (LYK3/HCL) are proposed as *M. truncatula* key receptors for the NFs [15], [16], [17]. Furthermore, a new LysM-RLK, LYR3 with high affinity to the NFs has been identified but the corresponding mutant is not affected in its interaction with rhizobium [18]. Does not Make Infection 2 (DMI2) is a leucine-rich repeat (LRR) RLK necessary during the early steps of the interaction and essential for NFs signal transduction [15], [19]. After NFs-RLK interaction, a signaling symbiotic pathway is activated and leads to different signaling events characterized by; i) host cell membrane depolarization, ii) reactive

oxygen spices (ROS) production and iii) intracellular calcium (Ca^{+2}) increase referred as calcium oscillation or calcium spiking [20]. The calcium oscillation requires DMI1, a ligand-gated channel protein localized in the nuclear membrane and responsible for calcium exporting from nucleus to the cytosol [15], [21]. Ca^{2+} is then detected by the calcium-dependent calmodulin kinase DMI3 [15], [22], [23] that phosphorylates Interacting Protein of DMI3 (IPD3) a coiled-coil domain-containing protein [15], [24] required for nodulation [25]. Nodule Signal Pathway 1 and 2 (NSP1 and NSP2) are two GRAS transcription factors (TFs) acting downstream of DMI3 [15], [26], [27]. NSP1 and NSP2 form a complex and activate the expression of two key transcriptional regulators: Nodule INception (NIN) [28], [29] and ERF Required for Nodulation 1 (ERN1) [30]. NIN and ERN1 through the early nodulines (also known as ENOD) genes induction activate the nodule formation [29], [30].

Rhizobia on road: infection of the host tissues by the bacteria

After recognition, the symbiont infects the roots through roots hairs by formation of infection threads (ITs). Bacterial penetration of the roots follows the deformation of the roots hairs and ITs grow toward the roots cortex [15]. Specific RNAi targeting NFs receptor (LYK3, LYK4 and NFP) block ITs penetration [7], [17], suggesting a role for NFs signaling during root infection. Furthermore, the E3 ubiquitin ligase Plant U-Box protein 1 (PUB1) regulates negatively this infection process probably via LYK3 degradation [1], [31]. Several *M. truncatula* mutants with anomalies in the infection process have been identified (See table 1); *rit* shows aborted ITs in the root epidermis. The gene affected in this mutant is member of Suppressor of cAMP Receptor defect/WASP family Verpolin homologous protein (SCAR/WAVE) family [32]. Similarly, the *lumpy infection* (*lin*) mutant shows ITs growth arrest. LIN corresponds to an E3 ubiquitin ligase containing U-box/WD40 domain [33]. The mechanisms of SCAR/WAVE and LIN action are not yet understood. The mutant of the *MtNF-YA* gene also called *HAP2-1* shows disruption of infection threads progression [34]. This gene encodes a CCAAT box-binding transcription factor subunit and its expression is controlled by NIN [35] and the microRNA169 [36]. *NF-YA/HAP2-1* regulates the *ERN1* expression [37] and as the *ern1* mutant is also affected in ITs progression [38], it is proposed that *NF-YA/HAP2-1* controls the infection process at least through *ERN1*. Moreover, suppressing the expression of two *FLOtline* genes, *FLOT2* and *FLOT4*, also arrest ITs progression [39]. These proteins are lipid raft markers and may be implicated in recruiting multiprotein complexes [1]. *MtSICKLE* encodes an orthologue of *AtEIN2*, the *Arabidopsis thaliana* ethylene co-receptor. The *sickle* mutant shows an hyper infection phenotype [40] and

is compromised in immunity, with for example enhance sensitivity to the *Phytophthora medicaginis* pathogen [40]. As ethylene is a defense hormone, it is tempting to speculate that via *MtSICKLE*, ethylene regulates negatively the infection via locale defense activation (figure 1).

When ITs reach the root cortex, bacteria are released into the targeted future symbiotic cell. Silencing of genes encoding the SYnapTogamins MtSyt1/3 or MtSyt2/3, implicated in the membrane trafficking, inhibits releasing of *S. meliloti* into the host cell [41]. NFP, LYK3 and DMI2 are also required for intracellular infection [17], [42] suggesting a role of the NF signaling during the bacterial release. *Numerous Infections and Polyphenolics* (*NIP*) encodes a protein belonging to the nitrate transporter family and shows high affinity to nitrate [43], [44]. Interestingly, the corresponding mutant shows absence of rhizobia release and activation of defense reactions [43].

Nodule organogenesis: building the sweet home

Near to the infection site, the organogenesis is activated and consists of cortical cell dedifferentiation and proliferation to build the nodule primordium, the first hosting tissues for the rhizobia [45]. The NFs signaling is required for activation of the organogenetic program, as treatments of roots with NFs induce formation of nodules-like structure [1], [46]. Moreover, constitutive DMI3 activity causes the formation of spontaneous nodules in absence of rhizobia [47]. It is thus possible to postulate that the organogenetic process is strictly under host control [48]. Application of rhizobial LCO on non-inoculated roots triggers accumulation of active forms of cytokinins (CKs) [49]. This class of hormone is involved in the plant development as well as in nodule organogenesis. It has been suggested that CKs coordinate infection and primordium formation [2], [48]. The cytokinins signaling during nodulation depends on the *Cytokinin REsponse 1* (*MtCRE1*) receptor [50], [51] and mediates induction of *NIN*, *ERN1* and *NSP2* genes [51], [52]. CKs also induce nodule formation through the polar auxin transport disruption over flavonoid accumulation [1], [53]. The CKs signaling is required for successful interaction, for the expression of the ethylene response factor for nodule differentiation (EFD) [54] and for the expression of some members of the KNOX TFs family [55] such as KNOX3 [56] that regulates negatively the CKs pathways. This KNOX3 regulation occurs through the repression of the cytokinins biosynthesis genes like *Lonely Guy* 2 (*LOG2*) [56] or through the activation of negative Response Regulator (RR of type A) like *MtRR4* [54], [55].

The mature nodule is composed by two peripheral vascular bundles (VBs) in which the metabolic exchanges occur. The development of correct vasculature tissues is probably crucial for the functioning of the future nodule. The *lin-4* mutant cannot form infection threads and develops a central vasculature rather than peripheral, indicating that the infection is essential for correct vascular development [57]. Moreover, *MtbHLH1* encodes basic helix-loop-helix TF expressed in nodule primordia and VBs and the loss of the *bHLH1* function leads to abnormal vascular patterning in the nodules [58].

The fix$^-$ mutants: powerful tools to understand nodule physiology

Most of the mutants described above, altered in the early steps of the interaction are not able to produce nodules and are called nod$^-$. In contrast, the fix$^-$ mutants are able to form nodules that are not functional. These fix$^-$ mutants are altered during the late steps of the interaction and the corresponding genes control biological process in the mature nodule. Fix$^-$ mutant represent great opportunity to understand the mechanisms that keep the nodule functional and give access to the genes involved in these steps of the symbiosis. For example Starker and colleagues found seven fix$^-$ complementation groups referred as *does not fix nitrogen* (*dnf*) *1-7* during the screen of a A17 ecotype fast neutron mutant collection [59]. Similarly, Pislariu et al. isolated a set of fix$^-$ mutants during the screening of a insertion mutant collection in the R108 background [60]. The next sections describe genes that act in late steps of the symbiotic interaction, some corresponding to the genes affected in the fix$^-$ mutants, and that are involved in the functioning of the symbiotic organ.

Meristem regulation: expand the activity without forget the identify

M. truncatula forms indeterminate nodules characterized by the presence of a persistent apical meristem. This tissue has an intense mitotic activity and is at the origin of most of the symbiotic tissues of the differentiated nodule. The maintenance of this meristem activity is vital for nodule development. In mature nodules, *MtNF-YA/MtHAP2-1* is expressed in the meristem and in addition to the infection phenotype, the shutdown of *MtNF-YA/MtHAP2-1* expression leads to the formation of abnormal nodules. J-P Combier and colleagues proposed that *MtNF-YA/MtHAP2-1* control the nodulation in the mature nodule through the regulation of the meristem [61]. The CLAVATA3/embryo-surrounding region (CLE) peptides are possibly involved in meristem regulation. The role of the legume *CLE* genes is mostly describe during symbiosis for the autoregulation of the nodulation (AON; see below) and the presence of *CLE12* and *CLE13* transcripts in the nodule meristem suggests a potential role in

meristem regulation [62]. In *A. thaliana* the shoot meristem maintenance requires stem cell precursors expressing the *WUSCHEL* (*WUS*) transcription factors and its repression by the CLV3 peptide through its LRR-RLK receptors CLV1/2 in order to regulate the meristem size and activate cell differentiation [63], [64]. The maintenance of the meristem identity is another important part of the meristem regulation. The Nodule-Root (NOOT1) NBCL gene is an orthologue of *A. thalinana* Blade-On-Petiole (BOP). The *noot1* mutant forms nodules developing roots on their apical region [65]. The description of the mutant phenotype suggests that the VBs are the origin of the emerged roots. Moreover, the *NOOT-1* gene is expressed on apical extremities of VBs suggesting that NOOT represses their root identity to maintain the nodule identity [65].

Terminal differentiation of the bacteroid: keep the symbiont under control

After releasing in the symbiotic cells, the bacteroids are surrounded by the host cell membrane called peri-becteroid membrane (PBM). A peri-bacteroid space (PBS) separates the bacteroids from the PMB. This new organelle is called the symbiosome [4]. In *M. truncatula*, bacteroids undergo a terminal differentiation characterized by endoreduplication of the bacterial genome and an increase of the cell size. This phenomenon is known as the terminal differentiation process [66]. Terminally differentiated bacteroids cannot survive outside their host and this process is considered by certain scientist as a “slavery process” [67], [68]. This differentiation is not generalizable to all leguminous plants but is restricted to the legume Inverted Repeat-Lacking Clade (IRLC) [69]. One hypothesis to explain these differences is that the leguminous plants took different evolution ways to form efficient association. The differentiation process is mediated by small antimicrobial peptides called Nodule Cysteine Reach (NCRs) [67], [70], [71]. *M. truncatula* possesses a very large number of these peptides (around 600 genes) [72], [73] with the majority of them being specifically expressed at different stages of the symbiosis [74], [75]. NCRs are targeted to the symbiosomes and reach the PBS [66], [76]. *DNF1*, an endopeptidase subunit targeted to the symbiosome is required for NCRs penetration because the *dnf1* mutant shows undifferentiated bacteroids and defaults in NCRs folding [77] (figure 2). The bacterial ABC transporter BacA is also essential for the bacteroid intracellular surviving and the *bacA* mutant shows higher *in vitro* sensitivity to the NCRs than the WT [71]. The authors of this work speculated that NCRs are toxic when reaching the PBS and BacA is essential for their internalization into the bacteroid where they are detoxified [66], [71]. In the endosymbiont, NCRs can interfere with various cellular functions to mediate differentiation. For example, NCR247 can interact with

FtsZ, a protein required for septum formation and bacterial division suggesting that NCR247 blocks the bacterial division by FtsZ inhibition [78]. In contrast, the two fix$^-$ mutants *dnf4* and *dnf7* are mutated in the *NCR211* and NCR169 respectively [79], [80] and they show increased intracellular death of the undifferentiated (*dnf7*) and differentiated (*dnf4*) bacteroids. Thus in this example NCR211, NCR169 protect the bacteria from intracellular death [79], [80]. These observations are in contradiction with the speculated function of NCRs, but point to their essential role in symbiosis (figure 2). *Rhizobium meliloti* 41 is incompatible with the *M. truncatula* Jemalong A17 background. A comparative analysis between the incompatible A17 and compatible DZA315 *M. truncatula* backgrounds reveals the role of the NCR Nitrogen Fixation Specificity 2 (NFS2) in the bacterial strain specificity and that this NCR has a bacterial lysis properties against *R. meliloti 41* after bacteroid differentiation [81]. Furthermore, NCR *NFS1* gene also controls the A17 specificity to *R. meliloti 41* [82] (figure 2). These results indicate that NCRs can also play a role in the specificity of the symbiotic host selection.

Repression of immunity is necessary for successful nodulation

During the symbiotic recognition phase, the repression of the defense reactions is required to reduce the roots immune status and to initiate effective rhizobial infection [3]. For example massive repression of defense genes is observed during early steps of *Medicago-Sinorhizobium* interaction [70]. The role of ethylene in this process is well described [40, 97] but the role of other defense hormones in symbiosis is less known. Various mechanisms participate in this repression of the plants defenses and NFP-LYK3 can contribute to the regulation of the immunity during the symbiotic interaction [3]. Moreover, recent studies show the co-localization of NFP and LYK3 in the ZII of the mature nodule [42], suggesting that they may participate in the regulation of the defense reactions in this zone (figure 2). A recent study shows that two LysM RLKs; LYK9 and LYR4 participate in the recognition of the chitin oligomeric Microbe Associated Molecular Pattern (MAMP) and activate defense in response to pathogens. The corresponding mutants do not show alteration in the symbiotic ability suggesting that *M. truncatula*, via certain LysM receptors, is able to distinguish the "good" from the "bad" microbes [83]. Most of the studies concerning the symbiotic regulation of the immunity focused on the early steps of the interaction and few things are known about the repression of defense reactions in the mature nodules. Recently, several genes were describes that regulate negatively the nodule immunity. We will refer to the corresponding genes as *Nodule Deficient in Immune Repression* (*NDIR*). The corresponding class of *ndir*

mutants shows typical feature of defense induction in their nodules like accumulation of phenolic compounds and induction of defense genes expression [43], [84]–[86]. The *DNF2*, *SymCRK* and *RSD* genes encode a putative phospholipase C phosphatidyl-inositol dependent protein, an RLK containing a domain Unknown Function 26 (DUF26) and a C_2H_2 transcription factors respectively. The corresponding mutants belong to the *ndir* class and form fix$^-$ nodules with induction of defense leading to intracellular death of the bacteroid [84], [85], [87], [88] (figure 2). When the *dnf2* mutant is grown in media without potential priming agent, the formation of functional nodules is observed [89] indicating that *DNF2* represses defense reactions in an environment-dependent manner. By contrast, the environmental conditions do not affect the *symCRK* phenotype [85], but *symCRK* and *rsd* inoculation with the bacterial *bacA* mutant produces nodules devoided of defense reactions. This suggests that the correct infection or differentiation of the bacteroids are required to induce defenses in *symCRK* and *rsd* [88]. By analysing the *dnf2-symCRK* double mutant phenotype and comparing *DNF2, SymCRK* and *RSD* expressions in different bacterial and plant mutant backgrounds, we have speculated for successive steps required for defenses suppression after bacterial internalization [88]. *Nodule Activation Defense 1* (*NAD1*) is also involved in prevention of the defense reactions in the nodules. *NAD1* encodes a small transmembrane protein with unknown function [86] and the corresponding mutant displays typical features of the *ndir* class. Furthermore, *DNF2*, *SymCRK* and *RSD* are down regulated in this mutant [86] suggesting that *NAD1* may act before these genes.

Host regulation of the symbiosis: control the nodulation to optimize the benefit

Symbiotic nitrogen fixation by the rhizobia requires large amount of energy provided by the plant [4] suggesting that a tight regulation of this process maximizes the profits for the host. Leguminous plants have developed different mechanisms to prevent inefficient interactions or to establish interactions with rational utilization of energy. Bacterial mutants impaired in *nifA* or *nifH* genes corresponding respectively to a transcriptional activator [90], [91] and a subunit of the nitrogenase [92] are not able to produce functional nitrogenase and do not fix nitrogen [70], [93]. These mutants show intracellular death of the differentiated bacteroid [88] suggesting that the host is able to control bacteroid survival when they are not efficient. One hypothesis is that the absence of nitrogen fixation generates a nitrogen/carbon (N/C) imbalance, that the plant senses this N/C balance perturbation and kills the inefficient bacteroids. In certain cases, the plant can suppress the formation and functioning of the nodules, for example when nitrate is supplied to nodulated plants. In this case, the plant host

stops the nodule functioning, activates a senescence process leading to tissue recycling (see below). Actually, the control of the C/N balance is not understood and need more investigation.

The host adjusts the number of the nodules depending on its ability to provide carbon to the bacteroid and on its nitrogen requirement [94]. This regulation occurs during the infection process and is call the autoregulation of the nodulation (AON). It acts at a systemic level and requires shoot-roots communication [45], [95]. *Super Numerary Nodules* (*SUNN*) gene encodes a LRR-RLK CLV1-like protein [96] and is expressed in root and shoot tissues. The *sunn* mutant shows high density of small poorly efficient nodules [96], [97] and this phenotype is shoot controled [97]. The current hypothesis proposes the presence of a long distance messenger, produced in the roots during the symbiotic interaction that is exported to the shoot, where it is recognized by *MtSUNN*. A second signal is then produced in the shoots and comes back to the roots to regulate negatively the infection process through a local action [98]. In comparison with *A. thaliana* where CLV1 forms heterodimer with CLV2 and recognize the CLV3 peptides [64], it is proposed that CLV3/ Embryo-surrounding region peptides (CLE12 and CLE13) produced in dividing nodule cells play the role of the roots signal [62]. Moreover, SUNN can interact with the homologues of the CLV1-interacting proteins MtCLV2 and MtCORYN (MtCRN). It is thus speculated that MtCLV2 and MtCRN can form a protein complex with SUNN to regulate the AON [99]. The Root Determined Nodulation 1 (RDN1) belongs to a family of uncharacterized peptide specific to plants and algae, expressed in roots and that negatively controls the nodule number. RDN1 is proposed to interact with SUNN in the AON process and to regulate the nodule number in roots [100]. Furthermore, the C-terminally Encoded Peptides (CEPs) were recently shown to play a role in AON regulation and to interact with the Compact Root Architecture 2 (CRA2) LRR-RLK. They regulate negatively the lateral roots emergence and positively the nodule formation at a local level [101]–[103].

Senescence process at the end of the road

The senescence of the nodule occurs when the plant suffers from environmental stresses, when nitrogen is added to the medium or when the nodule are old [9]. The senescence result in the apparition of a senescent zone (or ZIV) where the bacteroids start dying before that the host cell is degraded. This process is progressive and characterized by cellular constituents recycling [9]. Transcriptional analyses revealed differences in genes expression between developmental senescence and dark induced senescence. These results show the presence of

common and different patterns of gene expression suggesting the presence of common and specialized host responses between developmental and induced senescence [104]. In both types of senescence, induction of certain Cysteine Proteases (CPs1-6) is observed and they were proposed as nodule senescence markers [9], [104]. Interestingly, down regulation of *MtCP6* and of the *Vacuolar Processing Enzyme* (*MtVPE*) delay the senescence program. The corresponding proteins accumulate in the vacuole of uninfected cells and in the symbiosome, suggesting that CPs participate to the cell recycling during senescence [105]. Nitric oxide (NO) is produced in the nodules by the nitrite reductase (NRs) activity, also responsible for nitrite to NO conversion [106]. Nitric oxide is proposed to stimulate the senescence in the nodule because symbiosis with a *S. meliloti* strain over-expressing a flavohaemoglobin encoded by the *hmp* gene (*hmp*$^+$) responsible for NO detoxification, shows a delay of nodule senescence [107]. The mechanism of NO action is actually unknown but we can speculate that it acts via cell signaling activation [108]. It should be noted that the *ndir* mutants show also typical early senescent phenotypes. As other fix$^-$ mutants show early senescence without defense induction as *dnf7*, *bacA* or *nifH & nifA* [80], [88], [89] this suggests that the immune deficiency in these *ndir* mutants is the origin of the senescence and not the reverse.

Concluding remarks

The *Medicago-Sinorhizobium* symbiosis is a complex interaction with multiple aspects that involves various process and numerous genes. Since the discovery of the NFs, our understanding of the symbiosis has been largely improved using transcriptomic, genetic and reverse genetic approaches. However, despite these recent advances, certain aspects of the interaction remain unclear. These include the role of immunity and signaling defense pathways. The role of the specificity of recognition towards specific rhizobial strains is also an emerging field that will allow understanding how plants specifically select their symbiont. This specific selection may allow developing cultivars that would select the most efficient N_2 fixing partners. Thus further investigations are still required to better describe this symbiosis and better use it in sustainable agriculture.

Bibliography

1. Oldroyd GED, Murray JD, Poole PS, Downie JA (2011) The rules of engagement in the Legume-Rhizobial symbiosis. Annu Rev Genet 45:119–144

2. Oldroyd GED, Downie JA (2008) Coordinating nodule morphogenesis with Rhizobial infection in Legumes. Annu Rev Plant Biol 59:519–546

3. Gourion B, Berrabah F, Ratet P, Stacey G (2015) Rhizobium – legume symbioses : the crucial role of plant immunity. Trends Plant Sci 20:186–194

4. Udvardi M, Poole PS (2013) Transport and metabolism in Legume-Rhizobia symbioses. Annu Rev Plant Biol 64:781–805

5. Ott T, van Dongen JT, Günther C, Krusell L, Desbrosses G, Vigeolas H et al (2005) Symbiotic leghemoglobins are crucial for nitrogen fixation in legume root nodules but not for general plant growth and development. Curr Biol. 15:531-535.

6. Vasse J, De Billy F, Camut S, Truchet G (1990) Correlation between ultrastructural differentiation of bacteriods and nitrogen fixation in alfalfa nodules. J Bacteriol 172:4295–4306

7. Popp C, Ott T (2011) Regulation of signal transduction and bacterial infection during root nodule symbiosis. Curr Opin Plant Biol 14:458–467

8. Timmers AC, Soupène E, Auriac MC, de Billy F, Vasse J, Boistard P, Truchet G (2000) Saprophytic intracellular rhizobia in alfalfa nodules. Mol Plant Microbe Interact 13:1204-1213.

9. Van de Velde W, Guerra JC, De Keyser A, De Rycke R, Rombauts S, Maunoury N et al (2006) Aging in legume symbiosis. A molecular view on nodule senescence in Medicago truncatula. Plant Physiol. 141:711-720.

10. Liu C-W, Murray J (2016) The role of flavonoids in nodulation host-range specificity: An update. Plants (Basel) 5:33

11. Jones KM, Kobayashi H, Davies BW, Taga ME, Walker GC (2007) How rhizobial symbionts invade plants: the Sinorhizobium-Medicago model. Nat Rev Microbiol 5: 619–633

12. Fliegmann J, Bono JJ (2015) Lipo-chitooligosaccharidic nodulation factors and their perception by plant receptors. Glycoconj J 32:455-464

13. Dénarié J, Debellé F, Promé J-CC (1996) Rhizobium lipo-chitooligosaccharide nodulation factors: signaling molecules mediating recognition and morphogenesis. Annu Rev Biochem 65:503–535

14. Arrighi JF, Cartieaux F, Brown SC, Rodier-Goud M, Boursot M, Fardoux J et al (2012) Aeschynomene evenia, a model plant for studying the molecular genetics of the nod-independent rhizobium-legume symbiosis. Mol Plant Microbe Interact 25:851-861

15. Oldroyd GE (2013) Speak , friend , and enter : signalling systems that promote beneficial symbiotic associations in plants. Nat Rev Microbiol 11:252–263

16. Madsen EB, Madsen LH, Radutoiu S, Olbryt M, Rakwalska M, Szczyglowski K et al (2003) A receptor kinase gene of the LysM type is involved in legume perception of rhizobial signals. Nature 425:637-640

17. Limpens E, Franken C, Smit P, Willemse J, Bisseling T, Geurts R (2003) LysM domain receptor kinases regulating rhizobial Nod factor-induced infection. Science 302:630–633

18. Fliegmann J, Canova S, Lachaud C, Uhlenbroich S, Gasciolli V, Pichereaux C (2013) Lipo-chitooligosaccharidic symbiotic signals are recognized by LysM receptor-like kinase LYR3 in the legume Medicago truncatula. ACS Chem Biol 8:1900-1906

19. Endre G, Kereszt A, Kevei Z, Mihacea S, Kalo P, Kiss GB (2002) A receptor kinase gene regulating symbiotic nodule development. Nature 417:962–966

20. Oldroyd GED, Downie JA (2006) Nuclear calcium changes at the core of symbiosis signaling. Curr Opin Plant Biol 4:351–357

21. Ané JM, Kiss GB, Riely BK, Penmetsa RV, Oldroyd GE, Ayax C et al (2004) Medicago truncatula DMI1 required for bacterial and fungal symbioses in legumes. Science 303: 1364-1367

22. Mitra RM, Gleason CA, Edwards A, Hadfield J, Downie JA, Oldroyd GE, Long SR (2004) A Ca^{2+}/calmodulin-dependent protein kinase required for symbiotic nodule development: Gene identification by transcript-based cloning. Proc Natl Acad Sci U S A 101:4701-4705

23. Lévy J, Bres C, Geurts R, Chalhoub B, Kulikova O, Duc G et al (2004) A putative Ca^{2+} and calmodulin-dependent protein kinase required for bacterial and fungal symbioses. Science 303:1361-1364

24. Messinese E, Mun JH, Yeun LH, Jayaraman D, Rougé P, Barre A et al (2007) A novel nuclear protein interacts with the symbiotic DMI3 calcium- and calmodulin-dependent protein kinase of Medicago truncatula. Mol Plant Microbe Interact 20:912-921

25. Horváth B, Yeun LH, Domonkos A, Halász G, Gobbato E, Ayaydin F et al (2011) Medicago truncatula IPD3 is a member of the common symbiotic signaling pathway required for rhizobial and mycorrhizal symbioses. Mol Plant Microbe Interact 24:1345-1358

26. Kaló P, Gleason C, Edwards A, Marsh J, Mitra RM, Hirsch S et al (2005) Nodulation signaling in legumes requires NSP2, a member of the GRAS family of transcriptional regulators. Science 308:1786-1789.

27. Smit P, Raedts J, Portyanko V, Debellé F, Gough C, Bisseling T, Geurts R (2005) NSP1 of the GRAS protein family is essential for rhizobial Nod factor-induced transcription. Science 308:1789-1791.

28. Hirsch S, Kim J, Muñoz A, Heckmann AB, Downie JA, Oldroyd GED (2009) GRAS proteins form a DNA binding complex to induce gene expression during nodulation signaling in Medicago truncatula. Plant Cell 21:545–557

29. Marsh JF, Rakocevic A, Mitra RM, Brocard L, Sun J, Eschstruth A et al (2007) Medicago truncatula NIN is essential for rhizobial-independent nodule organogenesis induced by autoactive calcium/calmodulin-dependent protein kinase. Plant Physiol 144:324-335

30. Cerri MR, Frances L, Laloum T, Auriac MC, Niebel A, Oldroyd GE et al (2012) Medicago truncatula ERN transcription factors: regulatory interplay with NSP1/NSP2 GRAS factors and expression dynamics throughout rhizobial infection. Plant Physiol 160:2155-2172

31. Mbengue M, Camut S, de Carvalho-Niebel F, Deslandes L, Froidure S, Klaus-Heisen D et al (2010) The Medicago truncatula E3 ubiquitin ligase PUB1 interacts with the LYK3 symbiotic receptor and negatively regulates infection and nodulation. Plant Cell 22:3474-3488

32. Miyahara A, Richens J, Starker C, Morieri G, Smith L, Long S et al (2010) Conservation in function of a SCAR/WAVE component during infection thread and root hair growth in Medicago truncatula. Mol Plant Microbe Interact 23:1553-1562

33. Kiss E, Oláh B, Kaló P, Morales M, Heckmann AB, Borbola A et al (2009) LIN, a novel type of U-box/WD40 protein, controls early infection by rhizobia in legumes. Plant Physiol 151:1239-1249

34. Laporte P, Lepage A, Fournier J, Catrice O, Moreau S, Jardinaud MF et al (2014) The CCAAT box-binding transcription factor NF-YA1 controls rhizobial infection. J Exp Bot 65:481-494

35. Soyano T, Kouchi H, Hirota A, Hayashi M (2013) NODULE INCEPTION directly targets NF-Y subunit genes to regulate essential processes of root nodule development in Lotus japonicus. PLoS Genet 9: e1003352

36. Combier JP, De Billy F, Gamas P, Niebel A, Rivas S (2008) Trans-regulation of the expression of the transcription factor MtHAP2-1 by a uORF controls root nodule development. Genes Dev 22:1549–1559

37. Laloum T, Baudin M, Frances L, Lepage A, Billault-Penneteau B, Cerri MR et al (2014) Two CCAAT-box-binding transcription factors redundantly regulate early steps of the legume-rhizobia endosymbiosis. Plant J. 79:757-768

38. Middleton PH, Jakab J, Penmetsa RV, Starker CG, Doll J, Kaló P et al (2007) An ERF transcription factor in Medicago truncatula that is essential for Nod factor signal transduction. Plant Cell 19:1221-1234

39. Haney CH, Long SR (2010) Plant flotillins are required for infection by nitrogen-fixing bacteria. Proc Natl Acad Sci U S A 107:478–483

40. Penmetsa RV, Uribe P, Anderson J, Lichtenzveig J, Gish JC, Nam YW et al (2008) The Medicago truncatula ortholog of Arabidopsis EIN2, sickle, is a negative regulator of symbiotic and pathogenic microbial associations. Plant J 55:580-595

41. Gavrin A, Kulikova O, Bisseling T, Fedorova EE (2017) Interface symbiotic membrane formation in root nodules of Medicago truncatula : the role of synaptotagmins MtSyt1, MtSyt2 and MtSyt3. Frontier in plant science 8:1–10

42. Moling S, Pietraszewska-Bogiel A, Postma M, Fedorova E, Hink MA, Limpens E et al (2014) Nod factor receptors form heteromeric complexes and are essential for intracellular infection in medicago nodules. Plant Cell 26:4188-4199.

43. Veereshlingam H, Haynes JG, Penmetsa RV, Cook DR, Sherrier DJ, Dickstein R (2004) nip, a symbiotic Medicago truncatula mutant that forms root nodules with aberrant infection threads and plant defense-like response. Plant Physiol 136:3692-3702

44. Bagchi R, Salehin M, Adeyemo OS, Salazar C, Shulaev V, Sherrier DJ, Dickstein R. (2012) Functional assessment of the Medicago truncatula NIP/LATD protein demonstrates that it is a high-affinity nitrate transporter. Plant Physiol 160:906-916

464 45. Suzaki T, Yoro E, Kawaguchi M (2015) Leguminous plants: inventors of root nodules to
465 accommodate symbiotic bacteria. Int Rev Cell Mol Biol 316:111-158

466 46. Stacey G, Libault M, Brechenmacher L, Wan J, May GD (2006) Genetics and functional
467 genomics of legume nodulation. Curr Opin Plant Biol 9:110–121

468 47. Tirichine L, Imaizumi-Anraku H, Yoshida S, Murakami Y, Madsen LH, Miwa H et al (2006)
469 Deregulation of a Ca^{2+}/calmodulin-dependent kinase leads to spontaneous nodule
470 development. Nature 441:1153-1156

471 48. Crespi M, Frugier F (2009) De novo organ formation from differentiated cells: root nodule
472 organogenesis. Sci Signal 2:er1.

473 49. van Zeijl A, Op den Camp RH, Deinum EE, Charnikhova T, Franssen H, Op den Camp HJ et al
474 (2015) Rhizobium lipo-chitooligosaccharide signaling triggers accumulation of cytokinins in
475 Medicago truncatula roots. Mol Plant 8:1213-1226

476 50. Gonzalez-rizzo S, Crespi M, Frugier F (2006) The Medicago truncatula cre1 cytokinin receptor
477 regulates lateral root development and early symbiotic interaction with Sinorhizobium
478 meliloti. Plant Cell 18:2680–2693

479 51. Gamas P, Brault M, Jardinaud M, Frugier F (2017) Cytokinins in symbiotic nodulation : When,
480 where, what for ? Trends Plant Sci, 22:792-802

481 52. Ariel F, Brault-Hernandez M, Laffont C, Huault E, Brault M, Plet J et al (2012) Two direct targets
482 of cytokinin signaling regulate symbiotic nodulation in Medicago truncatula. Plant Cell
483 24:3838-3852

484 53. Ng JL, Hassan S, Truong TT, Hocart CH, Laffont C, Frugier F, Mathesius U (2015) Flavonoids and
485 auxin transport inhibitors rescue symbiotic nodulation in the medicago truncatula cytokinin
486 perception mutant cre1. Plant Cell 27:2210-2226

487 54. Vernie T, Billy D, Plet J, Combier J, Rogers C (2008) EFD is an ERF transcription factor involved
488 in the control of nodule number and differentiation in Medicago truncatula. Plant cell
489 20:2696–2713

490 55. Di Giacomo E, Laffont C, Sciarra F, Iannelli MA, Frugier F, Frugis G (2017) KNAT3/4/5-like class 2
491 KNOX transcription factors are involved in Medicago truncatula symbiotic nodule organ
492 development. New Phytol 213:822-837

493 56. Azarakhsh M, Kirienko AN, Zhukov VA, Lebedeva MA, Dolgikh EA, Lutova LA (2015) KNOTTED1-
494 LIKE HOMEOBOX 3 : a new regulator of symbiotic nodule development. J Exp Bot 66:7181–
495 7195

496 57. Guan D, Stacey N, Liu C, Wen J, Mysore KS, Torres-Jerez I et al (2013) Rhizobial infection is
497 associated with the development of peripheral vasculature in nodules of Medicago truncatula.
498 Plant Physiol 162:107-115

499 58. Godiard L, Lepage A, Moreau S, Laporte D, Verdenaud M, Timmers T, Gamas P (2011)
500 MtbHLH1, a bHLH transcription factor involved in Medicago truncatula nodule vascular
501 patterning and nodule to plant metabolic exchanges. New Phytol 191:391-404

59. Starker CG, Parra-Colmenares AL, Smith L, Mitra RM, Long SR (2006) Nitrogen fixation mutants of Medicago truncatula fail to support plant and bacterial symbiotic gene expression. Plant Physiol 140:671–680

60. Pislariu CI, Murray JD, Wen J, Cosson V, Muni RR, Wang M et al (2012) A Medicago truncatula tobacco retrotransposon insertion mutant collection with defects in nodule development and symbiotic nitrogen fixation. Plant Physiol 159:1686-1699

61. Combier JP, Frugier F, de Billy F, Boualem A, El-Yahyaoui F, Moreau S et al (2006) MtHAP2-1 is a key transcriptional regulator of symbiotic nodule development regulated by microRNA169 in Medicago truncatula. Genes Dev. 20:3084-3088

62. Mortier V, Den Herder G, Whitford R, Van de Velde W, Rombauts S, D'Haeseleer et al (2010) CLE peptides control Medicago truncatula nodulation locally and systemically. Plant Physiol 153:222-237

63 Mayer KFX, Schoof H, Haecker A, Lenhard M, Jürgens G, Laux T (1998) Role of WUSCHEL in regulating stem cell fate in the Arabidopsis shoot meristem. Cell 95:805–815

64. Williams L, Fletcher JC (2005) Stem cell regulation in the Arabidopsis shoot apical meristem. Curr Opin Plant Biol 8:582–586

65. Couzigou JM, Zhukov V, Mondy S, Abu el Heba G, Cosson V, Ellis TH et al (2012) NODULE ROOT and COCHLEATA maintain nodule development and are legume orthologs of Arabidopsis BLADE-ON-PETIOLE genes. Plant Cell 24:4498-4510

66. Kereszt A, Mergaert P, Maróti G, Kondorosi É (2011) Innate immunity effectors and virulence factors in symbiosis. Curr Opin Microbiol 14:76–81

67. Mergaert P, Uchiumi T, Alunni B, Evanno G, Cheron A, Catrice O et al (2006) Eukaryotic control on bacterial cell cycle and differentiation in the Rhizobium-legume symbiosis. Proc Natl Acad Sci U S A 103:5230-5235

68. Alunni B, Gourion B (2016) Terminal bacteroid differentiation in the legume-rhizobium symbiosis: nodule-specific cysteine-rich peptides and beyond. New Phytol 211:411-417

69. Czernic P, Gully D, Cartieaux F, Moulin L, Guefrachi I, Patrel D et al (2015) Convergent evolution of endosymbiont differentiation in dalbergioid and inverted repeat-lacking clade legumes mediated by nodule-specific cysteine-rich peptides. Plant Physiol 169:1254-1265

70. Maunoury N, Redondo-Nieto M, Bourcy M, Van de Velde W, Alunni B, Laporte P et al (2010) Differentiation of symbiotic cells and endosymbionts in Medicago truncatula nodulation are coupled to two transcriptome-switches. PLoS One 5:e9519

71. Haag AF, Baloban M, Sani M, Kerscher B, Pierre O, Farkas A et al (2011) Protection of Sinorhizobium against host cysteine-rich antimicrobial peptides is critical for symbiosis. PLoS Biol 9:e1001169

72. Mergaert P, Nikovics K, Kelemen Z, Maunoury N, Kondorosi A, Kondorosi E (2003) A novel family in Medicago truncatula consisting of more than 300 nodule-specific genes coding for small , secreted polypeptides with conserved cysteine motifs. Plant Physiol 132:161–173

73. Alunni B, Kevei Z, Redondo-Nieto M, Kondorosi A, Mergaert P, Kondorosi E (2007) Genomic organization and evolutionary insights on GRP and NCR genes, two large nodule-specific gene families in Medicago truncatula. Mol Plant Microbe Interact 20:1138–1148

74. Guefrachi I, Nagymihaly M, Pislariu CI, Van de Velde W, Ratet P, Mars M et al (2014) Extreme specificity of NCR gene expression in Medicago truncatula. BMC Genomics 15:712

75. Nallu S, Silverstein KAT, Samac DA, Bucciarelli B, Vance CP, Vandenbosch KA (2013) Regulatory patterns of a large family of defensin-like genes expressed in nodules of Medicago truncatula. Plos One 8:e60355

76. Van de Velde W, Zehirov G, Szatmari A, Debreczeny M, Ishihara H, Kevei Z et al (2010) Plant peptides govern terminal differentiation of bacteria in symbiosis. Science 327:1122-1126

77. Wang D, Griffitts J, Starker C, Fedorova E, Limpens E, Ivanov S et al (2010) A nodule-specific protein secretory pathway required for nitrogen-fixing symbiosis. Science 327:1126-1129

78. Farkas A, Maróti G, Durgő H, Györgypál Z, Lima RM, Medzihradszky KF et al (2014) Medicago truncatula symbiotic peptide NCR247 contributes to bacteroid differentiation through multiple mechanisms. Proc Natl Acad Sci U S A 111:5183-5188

79. Kim M, Chen Y, Xi J, Waters C, Chen R, Wang D (2015) An antimicrobial peptide essential for bacterial survival in the nitrogen-fixing symbiosis. Proc Natl Acad Sci U S A 112: 15238-15243

80. Horváth B, Domonkos Á, Kereszt A, Szűcs A, Ábrahám E, Ayaydin F et al (2015) Loss of the nodule-specific cysteine rich peptide, NCR169, abolishes symbiotic nitrogen fixation in the Medicago truncatula dnf7 mutant. Proc Natl Acad Sci U S A 112:15232-15237

81. Wang Q, Yang S, Liu J, Terecskei K, Ábrahám E, Gombár A et al (2017) Host-secreted antimicrobial peptide enforces symbiotic selectivity in Medicago truncatula. Proc Natl Acad Sci U S A 114:6854-6859

82. Yang S, Wang Q, Fedorova E, Liu J, Qin Q, Zheng Q et al (2017) Microsymbiont discrimination mediated by a host-secreted peptide in Medicago truncatula. Proc Natl Acad Sci U S A 114:6848-6853

83. Bozsoki Z, Cheng J, Feng F, Gysel K, Vinther M, Andersen KR et al (20174) Receptor-mediated chitin perception in legume roots is functionally separable from Nod factor perception. Proc Natl Acad Sci U S A 114:E8118-E8127

84. Bourcy M, Brocard L, Pislariu CI, Cosson V, Mergaert P, Tadege M et al (2013) Medicago truncatula DNF2 is a PI-PLC-XD-containing protein required for bacteroid persistence and prevention of nodule early senescence and defense-like reactions. New Phytol 197:1250-1261

85. Berrabah F, Bourcy M, Eschstruth A, Cayrel A, Guefrachi I, Mergaert P et al (2014) A nonRD receptor-like kinase prevents nodule early senescence and defense-like reactions during symbiosis. New Phytol 203:1305-1314

86. Wang C, Yu H, Luo L, Duan L, Cai L, He X et al (2016) NODULES WITH ACTIVATED DEFENSE 1 is required for maintenance of rhizobial endosymbiosis in Medicago truncatula. New Phytol 212:176-191

87. Sinharoy S, Torres-Jerez I, Bandyopadhyay K, Kereszt A, Pislariu CI, Nakashima J et al (2013) The C2H2 transcription factor regulator of symbiosome differentiation represses transcription of

580 the secretory pathway gene VAMP721a and promotes symbiosome development in Medicago
581 truncatula. Plant Cell 25:3584-3601

582 88. Berrabah F, Ratet P, Gourion B (2015) Multiple steps control immunity during the intracellular
583 accommodation of rhizobia. J Exp Bot 66:1977–1985

584 89. Berrabah F, Bourcy M, Cayrel A, Eschstruth A, Mondy S, Ratet P, Gourion B (2014) Growth
585 conditions determine the DNF2 requirement for symbiosis. PLoS One 9:e91866

586 90. Fischer HM (1994) Genetic regulation of nitrogen fixation in rhizobia. Microbiol Rev 58:352–
587 386

588 91. Dixon R, Kahn D (2004) Genetic regulation of biological nitrogen fixation. Nat Rev Microbiol
589 2:621–631

590 92. Rubio LM, Ludden PW (2008) Biosynthesis of the Cofactor of Nitrogenase. Annu Rev Microbiol
591 62:93–111

592 93. Hirsch M, Bang M, Ausubel FM (1983) Ultrastructural Analysis of Ineffective Alfalfa Nodules
593 Formed By Nif-Tn5 Mutants of Rhizobium Meliloti. J Bacteriol 155:367–380

594 94. Kosslak RM, Bohlool BB (1984) Suppression of nodule development of one side of a split-root
595 system of soybeans caused by prior inoculation of the other side. Plant Physiol 75:125–130

596 95. Mortier V, Holsters M, Goormachtig S (2012) Never too many ? How legumes control nodule
597 numbers. Plant, Cell Environ 35:245–258

598 96. Schnabel E, Journet EP, De Carvalho-Niebel F, Duc G, Frugoli J (2005) The Medicago truncatula
599 SUNN gene encodes a CLV1-like leucine-rich repeat receptor kinase that regulates nodule
600 number and root length. Plant Mol Biol 58:809–822

601 97. Penmetsa RV, Frugoli JA, Smith LS, Long SR, Cook DR (2003) Dual genetic pathways controlling
602 nodule number in Medicago truncatula. Plant Physiol 131:998–1008

603 98. Oka-Kira E, Kawaguchi M (2006) Long-distance signaling to control root nodule number. Curr
604 Opin Plant Biol 9:496–502

605 99. Crook AD, Schnabel EL, Frugoli JA (2016) The systemic nodule number regulation kinase SUNN
606 in Medicago truncatula interacts with MtCLV2 and MtCRN. Plant J 88:108–119

607 100. Schnabel EL, Kassaw TK, Smith LS, Marsh JF, Oldroyd GE, Long SR, Frugoli JA (2011) The ROOT
608 DETERMINED NODULATION1 gene regulates nodule number in roots of Medicago truncatula
609 and defines a highly conserved, uncharacterized plant gene family. Plant Physiol 157:328-340

610 101. Huault E, Laffont C, Wen J, Mysore K S, Ratet P, Frugier F (2014) Local and systemic regulation
611 of plant root system architecture and symbiotic nodulation by a receptor- like kinase. Plos
612 Genetics 10:e1004891

613 102 Imin N, Mohd-Radzman NA, Ogilvie HA, Djordjevic MA (2013) The peptide-encoding CEP1 gene
614 modulates lateral root and nodule numbers in Medicago truncatula. J Exp Bot 64:5395–5409

615 103. Mohd-Radzman NA, Laffont C, Ivanovici A, Patel N, Reid D, Stougaard J et al (2016) Different
616 pathways act downstream of the cep peptide receptor cra2 to regulate lateral root and nodule
617 development. Plant Physiol 171:2536-2548

104. Pérez Guerra JC, Coussens G, De Keyser A, De Rycke R, De Bodt S, Van De Velde W et al (2010) Comparison of developmental and stress-induced nodule senescence in Medicago truncatula. Plant Physiol 152:1574-1584

105. Pierre O, Hopkins J, Combier M, Baldacci F, Engler G, Brouquisse R et al (2014) Involvement of papain and legumain proteinase in the senescence process of Medicago truncatula nodules. New Phytol 202:849-863

106. Horchani F, Prévot M, Boscari A, Evangelisti E, Meilhoc E, Bruand C et al (2011) Both plant and bacterial nitrate reductases contribute to nitric oxide production in Medicago truncatula nitrogen-fixing nodules. Plant Physiol 155:1023-1036

107. Cam Y, Pierre O, Boncompagni E, Hérouart D, Meilhoc E, Bruand C (2012) Nitric oxide (NO): A key player in the senescence of Medicago truncatula root nodules. New Phytol 196:548–560

108. Moreau M, Lindermayr C, Durner J, Klessig DF (2010) NO synthesis and signaling in plants - where do we stand ? Physiol Plant 138:372–383

109. Cerri MR, Frances L, Kelner A, Fournier J, Middleton PH, Auriac MC et al (2016) The symbiosis-related ERN transcription factors act in concert to coordinate rhizobial host root infection. Plant Physiol 171:1037-1054

110. Rey T, Laporte P, Bonhomme M, Jardinaud MF, Huguet S, Balzergue S et al (2016) MtNF-YA1, a central transcriptional regulator of symbiotic nodule development, is also a determinant of Medicago truncatula susceptibility toward a root pathogen. Front Plant Sci 7:1837

111. Harris JM, Dickstein R (2010) Control of root architecture and nodulation by the LATD / NIP transporter. Plant Signal Behav 5:1365-1369

112. Lefebvre B, Timmers T, Mbengue M, Moreau S, Hervé C, Tóth K et al (2010) A remorin protein interacts with symbiotic receptors and regulates bacterial infection. Proc Natl Acad Sci U S A 107:2343-2348

113. Murray JD, Muni RR, Torres-Jerez I, Tang Y, Allen S, Andriankaja M et al (2011) Vapyrin, a gene essential for intracellular progression of arbuscular mycorrhizal symbiosis, is also essential for infection by rhizobia in the nodule symbiosis of Medicago truncatula. Plant J 65:244-252

114. Sinharoy S, Liu C, Breakspear A, Guan D, Shailes S, Nakashima J et al (2016) A Medicago truncatula cystathionine-β-synthase-like domain-containing protein is required for rhizobial infection and symbiotic nitrogen fixation. Plant Physiol 170:2204-2217

115. Arrighi J-F, Godfroy O, de Billy F, Saurat O, Jauneau A, Gough C (105) The RPG gene of Medicago truncatula controls Rhizobium-directed polar growth during infection. Proc Natl Acad Sci U S A 105:9817–9822

116. Op den Camp RH, De Mita S, Lillo A, Cao Q, Limpens E, Bisseling T, Geurts R (2011) A phylogenetic strategy based on a legume-specific whole genome duplication yields symbiotic cytokinin type-A response regulators. Plant Physiol 157:2013-2022

117. Mortier V, Wasson A, Jaworek P, De Keyser A, Decroos M, Holsters M et al (2014) Role of LONELY GUY genes in indeterminate nodulation on Medicago truncatula. New Phytol 202:582-593

118. Lohar DP, Schaff JE, Laskey JG, Kieber JJ, Bilyeu KD, Bird DM (2004) Cytokinins play opposite roles in lateral root formation, and nematode and Rhizobial symbioses. Plant J 38: 203–214

119. Hopkins J, Pierre O, Kazmierczak T, Gruber V, Frugier F, Clement M (2014) Mt ZR1 , a PRAF protein, is involved in the development of roots and symbiotic root nodules in Medicago truncatula. Plant, Cell Env 37:658–669

Figure 1: Nodule formation and structure in the *Medicago-Sinorhizobium* symbiosis. Under nitrogen deficiency, *M. truncatula* interacts with *Sinorhizobium spp*. The recognition phase (Rec) is followed by roots infection (Inf). During this Inf phase the rhizobia penetrate the roots hairs by formation of infection threads. In parallel to the infection, the organogenesis (Org) takes place. For Org, cortical cell divisions are reactivated, produce the nodule primordium and the bacteria are released into the primordium cells (EndoCy). The box indicates the genes associated to the different steps of the early symbiotic association. This interaction leads to the formation of the nodule, composed by a meristem or ZI, an infection zone or ZII, a fixation zone or ZIII separated from ZII by an inter-zone or ZII-III. Finally a senescent zone or ZIV is observed in old nodules or stressed plants or when organic nitrogen is added to the growth media after nodulation. Two peripheral vascular bundles (VBs) are present in the root organ and connect the nodule to the root vasculature. These VB tissues are responsible for host-symbiont metabolic exchange. 1: nodules epidermis, 2: meristem, 3: nodule cortex and endodermis, 4: xylem, 5: phloem, 6: empty cells, 7: roots epidermis, 8: roots cortex, 9: roots endodermis, 10: xylem, 11: phloem.

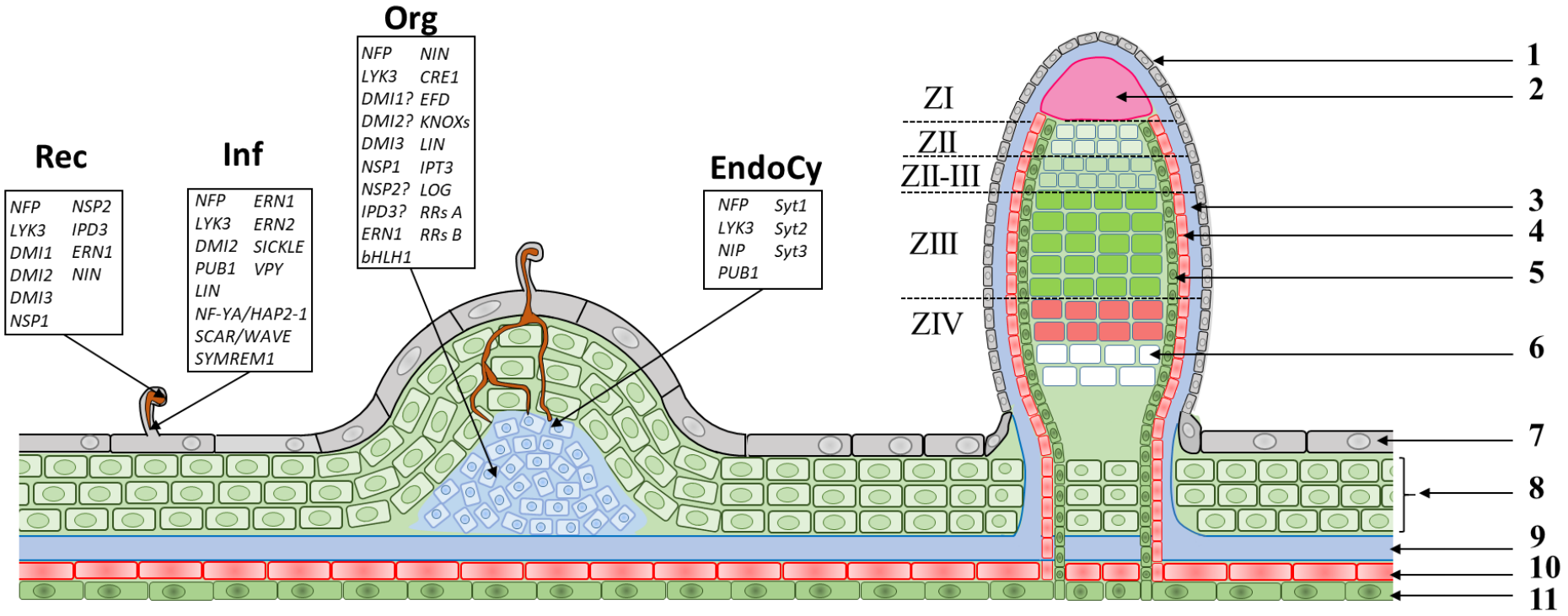
Org
NFP NIN
LYK3 CRE1
DMI1? EFD
DMI2? KNOXs
DMI3 LIN
NSP1 IPT3
NSP2? LOG
IPD3? RRs A
ERN1 RRs B
bHLH1
Rec
NFP NSP2
LYK3 IPD3
DMI1 ERN1
DMI2 NIN
DMI3
NSP1
Inf
NFP ERN1
LYK3 ERN2
DMI2 SICKLE
PUB1 VPY
LIN
NF-YA/HAP2-1
SCAR/WAVE
SYMREM1
EndoCy
NFP Syt1
LYK3 Syt2
NIP Syt3
PUB1
ZI
ZII
ZII-III
ZIII
ZIV
1
2
3
4
5
6
7
8
9
10
11

Figure 2. Endosymbiotic process from infection to senescence. In the ZII, the bacteria infect the cell; NFP/LYK3 and DMI2 are required for the infection via symbiotic signaling and potentially through defense repression. PUB1 negatively regulates the infection by LYK3 degradation. Moreover NIP is also required for bacteria endocytosis and prevents defense reactions. In the host cells, the symbiosome is composed by the bacteroid (intra cellular form of the rhizobia) surrounded by the peri-bacteroid membrane (PBM) and separated from it by the peri-bacteroid space (EPS). In the ZII-III, the bacteroid undergoes a terminal differentiation mediated by NCRs peptides. DNF1, situated in the peri-bacteroid membrane, is required for NCR folding into the symbiosome. NCRs located in the peri-bacteroid space are internalized into bacteroid via BacA. The bacA mutant is unable to resist to NCR toxicity and in this mutant intracellular death of bacteroid is observed. In the bacteria, NCRs can act in different pathways to mediate differentiation. NCR247 can for example block the division by FtsZ inhibition; moreover NCRs can protect the bacteria from intracellular lysis. The NCR NFS1 & 2 lead to bacterial lysis of the incompatible rhizobia under host-dependent genotype. During the infection, the repression of the defense reactions is essential and requires symbiotic genes: *SymCRK*/*RSD* and *DNF2* prevent defense reactions elicited by bacterial infection or differentiation and by the environment respectively. Furthermore *NAD1* also represses defense reactions. In ZIII, bacteroid fix N_2 for the plant benefit. The absence of N_2 fixation observed in fix^- mutant such as *nifA* or *nifH* leads to the killing of the bacteria by the host. The absence of N_2 fixation probably induces nitrogen/carbon (N/C) imbalance and activates early senescence or other unknown processes to kill the bacteroids. Finally, in the zone IV, a destruction of the bacteroids is observed following a developmental program.

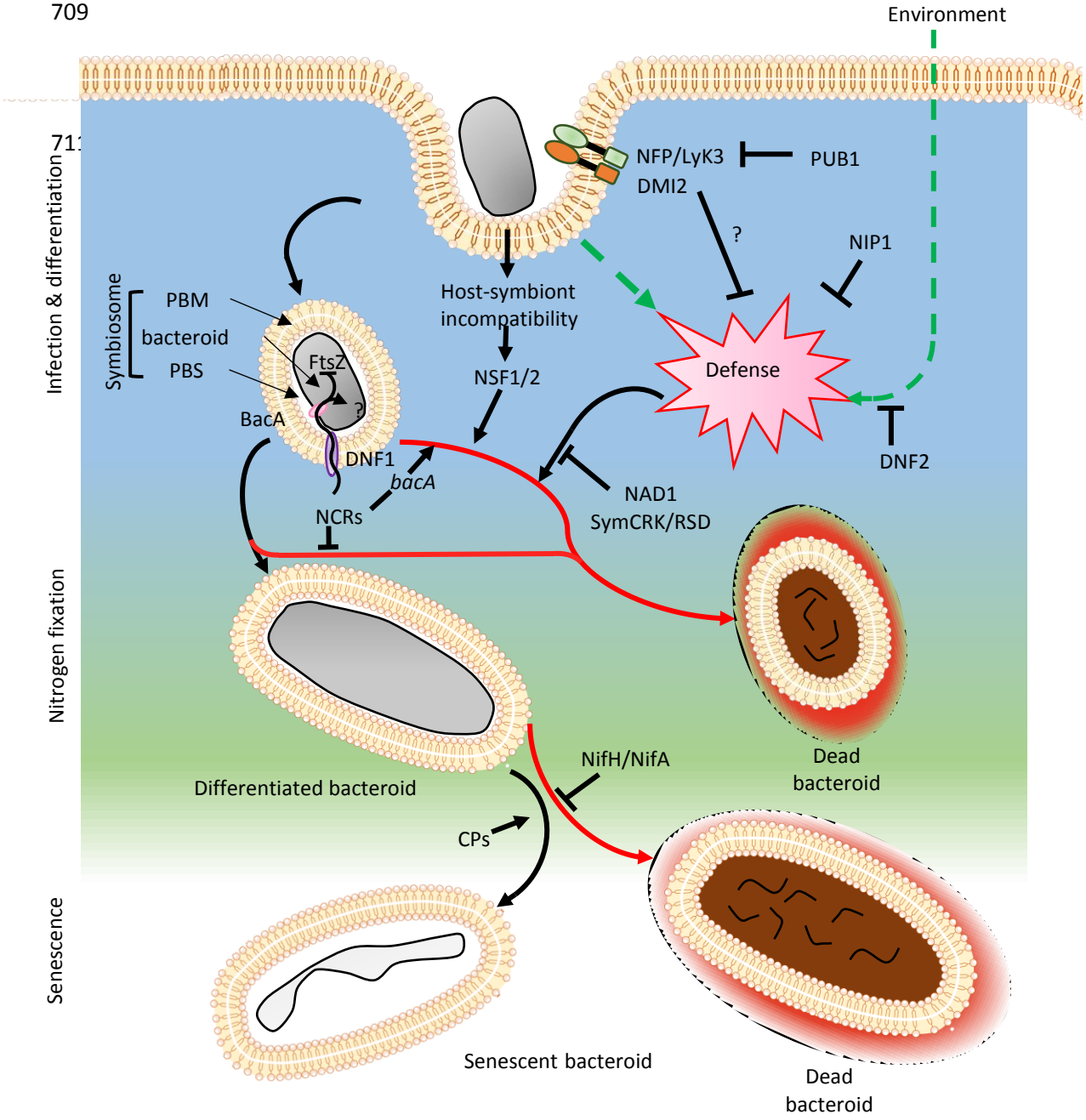
Environment
Infection & differentiation
Nitrogen fixation
Senescence
NFP/LyK3
DMI2
PUB1
?
NIP1
Host-symbiont
incompatibility
Symbiosome
PBM
bacteroid
PBS
FtsZ
?
BacA
DNF1
bacA
NCRs
NSF1/2
Defense
DNF2
NAD1
SymCRK/RSD
Dead
bacteroid
Differentiated bacteroid
NifH/NifA
CPs
Senescent bacteroid
Dead
bacteroid

712

713 **Table 1: mutants and corresponding genes involved in the control of *Medicago-***
714 ***Sinorhizobium* symbiosis.** Certain genes can act at different symbiotic steps. Please refer to
715 the text and figure 1 for a more detailed information.

Symbiotic steps	Mutant	Gene product	Biological function	Publication reference
Recognition and symbiotic signaling	*nfp*	NFP	NFs perception	[16]
	lyk3	LYK3	NFs perception	[17]
	dmi2	DMI2	NFs signaling	[19]
	lyr3	LYR3	NFs perception	[18]
	lyk4	LYK4	NFs perception	[17]
	dmi1	DMI1	Calcium speaking	[21]
	dmi3	DMI3	Calcium speaking	[23]
	ipd3	IPD3	Symbiotic signaling	[25]
	nsp1	NSP1	Symbiotic TF	[27]
	nsp2	NSP2	Symbiotic TF	[26]
	nin	NIN	Symbiotic TF	[29]
	ern1	ERN1	Symbiotic TF	[38]
	ern2	ERN2	Symbiotic TF	[109]
Infection	*RNAi*	PUB1	E3 ligase	[31]
	rit	SCAR/WAV	SCAR/WAV	[32]
	lin	LIN	E3 ligase	[33]
	nf-ya/RNAi	NF-YA/HAP2	CCAAT box-binding FT	[36], [110]
	nip	NIP/LATD	Nitrate transporter	[43], [44], [111]
	sickle	SICKLE	Ethylene receptor	[40]
	RNAi	Syt1/2/3	Synaptogamin, membrane fusion	[41]
	RNAi/*Tnt1*	SYMREM1	SYMBIOTIC REMORIN 1; lipid micro domain formation	[112]
	RNAi	FLOT2	Membrane shaping	[39]
	RNAi	FLOT4	Membrane shaping	[39]

	RNAi/*Tnt1*	VPY	VAPYRIN; IT formation	[113]
	cbs	CBS1	Cystathionine-β-Synthase: IF formation	[114]
	rpg	RPG	Coil-coil protein, unknown function	[115]
Organogenesis	*cre1*	CRE1	Cytokinins receptor	[50]
	RNAi	RR4	RR type A	[54]
	RNAi	RR9	RR type B	[116]
	RNAi	LOG	Lonely guy: cytokinine biosynthesis	[117]
	RNAi	CKX1	Cytokinin oxidase; cytokinin degradation	[118]
	RNAi/*bhlh476*	bHLH476	TF	[52]
	RNAi	bHLH1	TF	[58]
	RNAi	KNAT3/4/5	TF	[55]
	RNAi	KNOX3	TF	[56]
	RNAi	ZR1	TF	[119]
Meristem regulation	*noot*	NOOT	TF	[65]
Terminal differentiation	*dnf1*	DNF1	Endopeptidase	[76]
		NCR247	Antimicrobial peptide	[78]
	dnf4	NCR211	Antimicrobial peptide	[79]
	dnf7	NCR169	Antimicrobial peptide	[80]
	rsd	RSD	C_2H_2 TF	[87]
Host selection	Genotype	NFS1	Antimicrobial peptide	[82]
	Genotype	NFS2	Antimicrobial peptide	[81]
Defense repression	*dnf2*	DNF2	PI-PLC like protein	[84]
	nad1	NAD1	Unknown function	[86]

	symCRK	SYMCRK	DUF26-RLK	[85]
Autoregulation of the nodulation (AON)	*sunn*	SUNN	LRR-RLK	[96]
	RNAi	CLE12	CLV3/ embryo-surrounding region	[62]
	RNAi	CLE13	CLV3/ embryo-surrounding region	[62]
		CLV2	LRR-RLK	[99]
	crn	CRN	LRR-RLK	[99]
	rdn1	RDN1	Small uncharacterized peptide	[100]
	RNAi	CEP1	Small signaling peptide	[102]
	cra2	CRA2	LRR-RLK	[101], [103]
Senescence	RNAi	CP6	Cysteine protease	[105]
	RNAi	VPE	vacuolar processing enzyme	[105]

716

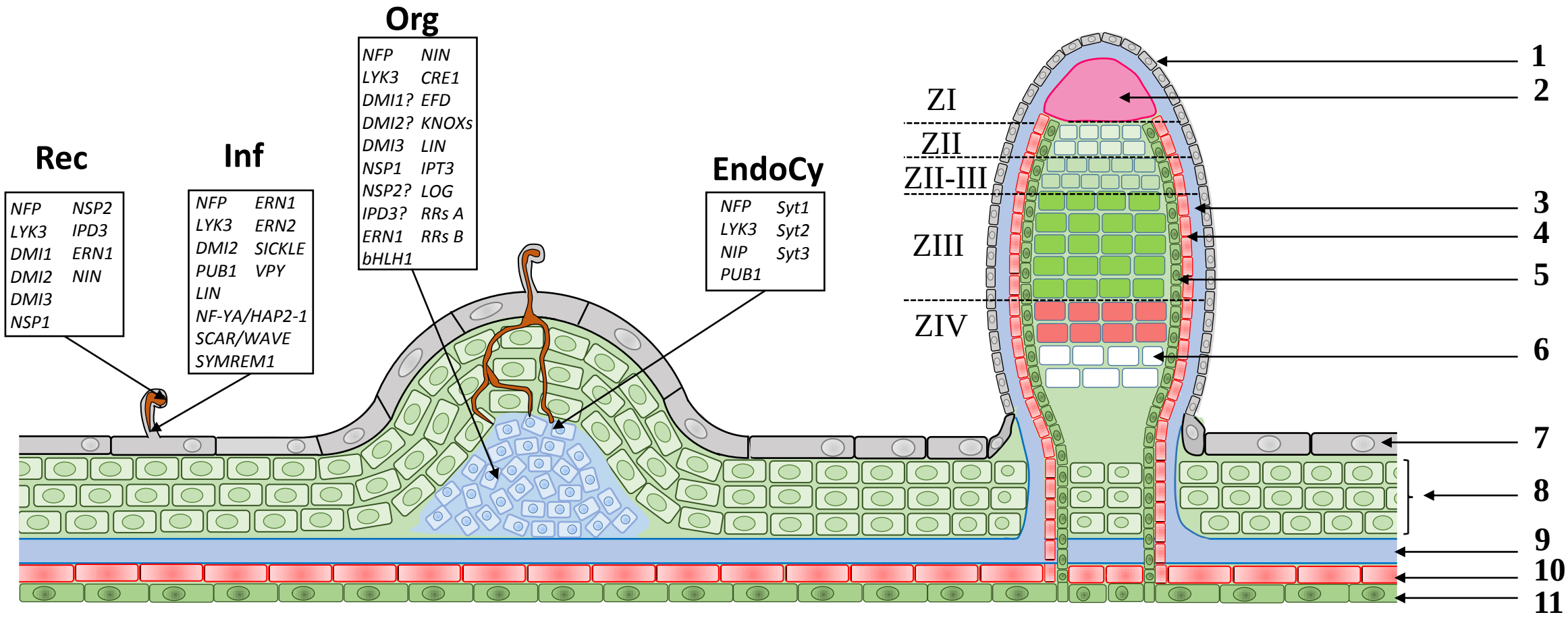
Rec
NFP NSP2
LYK3 IPD3
DMI1 ERN1
DMI2 NIN
DMI3
NSP1
Inf
NFP ERN1
LYK3 ERN2
DMI2 SICKLE
PUB1 VPY
LIN
NF-YA/HAP2-1
SCAR/WAVE
SYMREM1
Org
NFP NIN
LYK3 CRE1
DMI1? EFD
DMI2? KNOXs
DMI3 LIN
NSP1 IPT3
NSP2? LOG
IPD3? RRs A
ERN1 RRs B
bHLH1
EndoCy
NFP Syt1
LYK3 Syt2
NIP Syt3
PUB1
ZI
ZII
ZII-III
ZIII
ZIV
1
2
3
4
5
6
7
8
9
10
11

Figure 1: Nodule formation and structure in The *Medicago-Sinorhizobium* symbiosis. Under nitrogen deficiency, *Medicago* interact with *Sinorhizobium spp*, a recognition phase occur (Rec); followed by roots infection (Inf); the rhizobia penetrate trough the roots hairs by formation of infection threads. In parallel to the infection, the organogenesis occur (Org); cortical cells are reactivate and produce the nodule primordium, the bacteria are release into the primordium cells (EndoCy). The box indicates the genes associated to the different steps of the early symbiotic association. The interaction led to formation of the nodule, composed by meristem or ZI, infection zone or ZII, fixation zone or ZIII separate from ZII by inter-zone or ZII-III, finally a senescent zone or ZIV is observe old nodules or stressed plant. Two peripheral vascular bundles (VBs) connected to root vasculature is formed and responsible for host-symbiont metabolic exchange. 1: nodules epidermis, 2: meristem, 3: nodule cortex and endodermis, 4: xylem, 5: phloem, 6: empty cells, 7: roots epidermis, 8: roots cortex, 9: roots endodermis and pericycl, 10: xylem, 11: phloem.

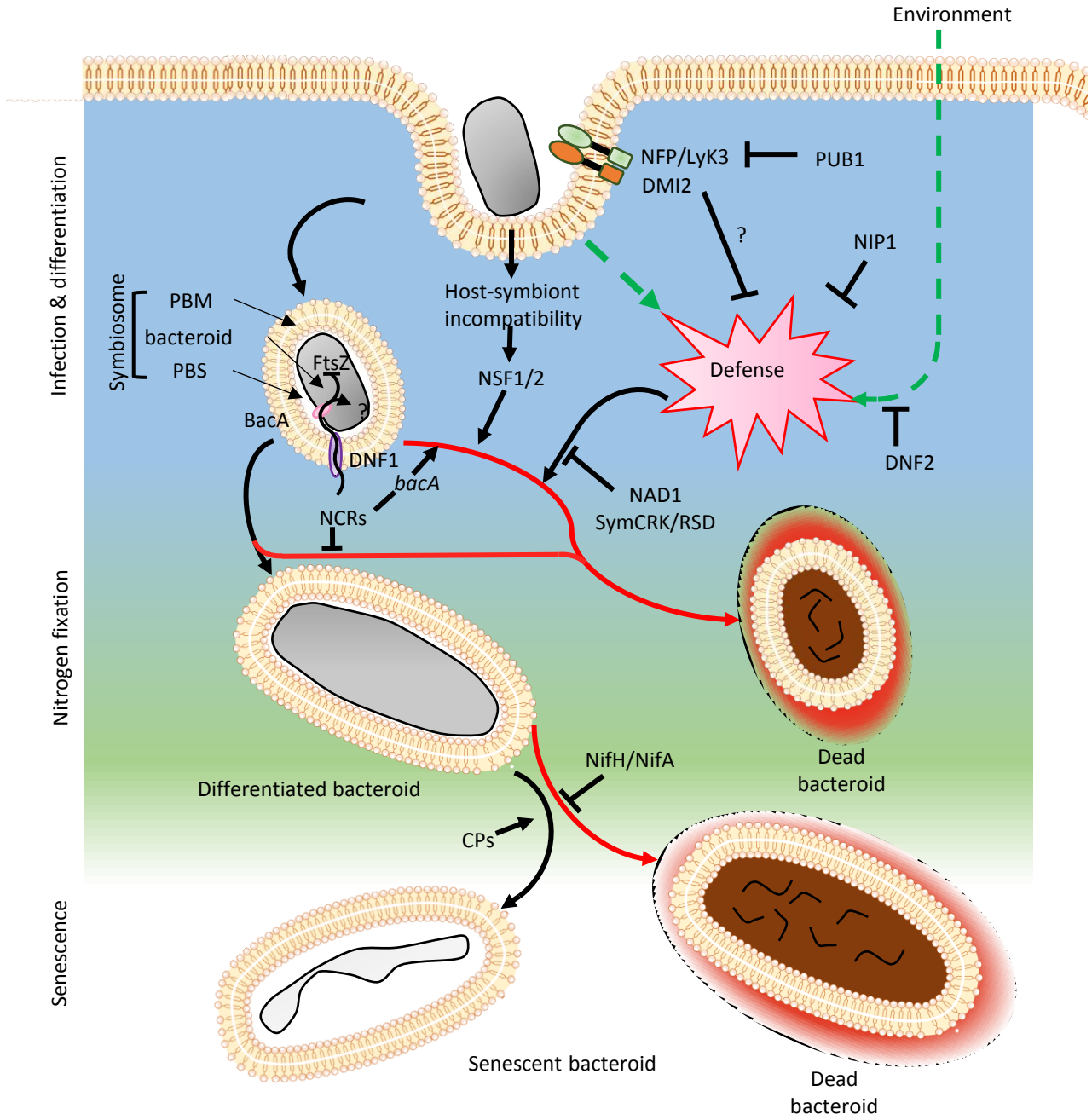
Environment
Infection & differentiation
Nitrogen fixation
Senescence
NFP/LyK3
DMI2
PUB1
?
NIP1
Host-symbiont
incompatibility
Symbiosome
PBM
bacteroid
PBS
FtsZ
?
BacA
DNF1
NSF1/2
Defense
DNF2
bacA
NCRs
NAD1
SymCRK/RSD
Dead
bacteroid
Differentiated bacteroid
NifH/NifA
CPs
Senescent bacteroid
Dead
bacteroid

Figure 2. Endosymbiotic process from infection to senescence: In the ZII, the bacteria infect the cell; NFP/LYK3 and DMI2 are required for the infection maybe via symbiotic signaling and defense repression, PUB1 regulate negatively the infection by LYK3 degradation, moreover NIP is also required to prevent defense reactions. In the ZII-III, the bacteroid undergo a terminal differentiation mediated by NCRs peptides, DNF1 situated in the peri-bacteroid membrane is required for NCR folding into the symbiosome, NCRs located in the peri-bacteroid space are internalized into bacteroid via BacA, moreover *bacA* mutant is unable to resist to NCR toxicity and intracellular death of bacteroid is observed. Into the bacteria, NCRs can act in different pathways to mediate the differentiation for example; NCR247 can block the division by FtsZ inhibition, moreover NCRs can protect the bacteria from intracellular lysis. The NCR NFS led to bacterial lysis of the incompatible rhizobia under host-dependent genotype. During the infection, the repression of the defense is essential and involve the symbiotic genes: *SymCRK/RSD and DNF2* prevent defense elicited by bacterial infection or differentiation and by the environment respectively, furthermore *NAD1* also repress defense reactions. In ZIII, bacteroid fix N_2 for the plant benefit, incapacity of fixation observed in mutant as *nifA* or *nifH* led to suppression of the bacteria by the host, absence of fixation probably induce azote/carbon (N/C) imbalance and activate early senescence or unknown process to kill the bacteroid. Finally, in the zone IV, a destruction of bacteroid are observed resulting of developmental.

Université Paris-Saclay
Espace Technologique / Immeuble Discovery
Route de l'Orme aux Merisiers RD 128 / 91190 Saint-Aubin, France

université PARIS-SACLAY | ÉCOLE DOCTORALE Sciences du végétal : du gène à l'écosystème

Titre : Etude de la signalisation contrôlant l'accommodation intracellulaire au cours de la symbiose *Medicago/Sinorhizobium*

Mots clés : Rhizobium, Medicago, Symbiose fixatrice d'azote, Immunité, Hormones de défense, *E. adhaerens.*

Résumé : Les légumineuses en milieu carencé en azote, établissent une relation symbiotique avec les bactéries du sol appelées rhizobia. Cette interaction conduit à la formation d'un nouvel organe racinaire, la nodosité. Au sein de celle-ci, les rhizobia se différencient en bactéroïdes fixant l'azote atmosphérique au profit de la plante. La colonisation massive et chronique des cellules symbiotiques de nodosités par les rhizobia ne déclenche aucune réaction de défense visible. Au laboratoire nous avons isolé deux mutants symbiotiques développant des réactions de défense dans les nodosités de *Medicago truncatula* indiquant qu'il existe un contrôle strict de l'immunité dans cet organe.

L'objectif de cette thèse est de comprendre comment l'immunité symbiotique contrôle les voies de signalisation hormonales de défense afin d'héberger le partenaire symbiotique et de trouver de nouveaux outils pour mieux comprendre les mécanismes de défense. Pour cela, des approches moléculaires, pharmacologiques et génétiques sont utilisées.

Les résultats obtenus dans cette thèse suggèrent que les mécanismes de défense adoptés par *M. truncatula* varient en fonction de l'écotype de la plante. L'écotype A17 exploite deux voies de résistance : la voie de la sénescence et la voie des réactions de défense. Cependant, l'écotype R108 n'exploite que la voie des réactions de défense.

Ce travail suggère également que chez *M. truncatula* A17, la protéine SymCRK réprime la voie de signalisation de l'acide jasmonique qui conduit au déclenchement de la sénescence, tandis que la protéine DNF2 réprime principalement la voie de signalisation de l'acide salicylique qui conduit au déclenchement des réactions de défense et aussi réprime secondairement la voie acide jasmonique. Chez *M. truncatula* R108, les deux protéines SymCRK et DNF2 contrôlent les voies de signalisation de l'acide salicylique et de l'éthylène, avec DNF2 contrôlant préférentiellement la voie acide salicylique et SymCRK contrôlant préférentiellement la voie éthylène.

Cette thèse suggère aussi l'implication des protéines R dans le contrôle de l'accommodation intracellulaire des rhizobia. Un gène *CNL*-5 semble être impliqué dans le contrôle de l'infection des cellules symbiotiques, et deux autres gènes *CNL*-4 et *TNL*-2 semblent être impliqués dans le contrôle de l'efficacité de l'infection.

Finalement, cette thèse a permis d'isoler une souche bactérienne *E. adhaerens*, capable se comporter comme un symbiote ou comme un pathogène pour plusieurs espèces de Medicago.

Title: Understanding the signaling pathway controlling the intracellular recognition steps of *Medicago/Sinorhizobium* symbiosis.

Keywords: Rhizobium, Medicago, Nitrogen-fixing Symbiosis, Immunity, Edefense hormones, E. *adhaerens.*

Abstract: _When grown under limited nitrogen resources, legumes establish a symbiotic relationship with soil bacteria called rhizobia. This interaction leads to the formation of a new root organ, the nodules. Within nodules, rhizobia differentiate into bacteroids and fix atmospheric nitrogen for the plant. The massive and chronic colonization of nodule symbiotic cells by the rhizobia does not trigger any visible defense reactions. In the laboratory, we previously isolated two symbiotic mutants developing defense reactions in *Medicago truncatula* nodules, indicating a strict control of the nodule immunity.

The thesis project aimed first to understand the relationship between symbiotic genes and immunity mediated by defense hormones and second to find new tools to help to better understand nodules defense mechanisms. For this, molecular, pharmacological and genetic approaches were used.

The results obtained in this thesis suggest that the defense mechanisms adopted by *M. truncatula* vary depending on the plant ecotypes. The A17 ecotype uses two resistance pathways; senescence and defense reactions. While, the R108 ecotype uses defense reactions pathway to fight against rhizobia.

This work also suggests that in *M. truncatula* A17, the SymCRK protein represses jasmonic acid signaling

This work also suggests that in *M. truncatula* A17, the SymCRK protein represses the jasmonic acid signaling pathway involved in senescence triggering. In contrast, the DNF2 protein mainly represses the salicylic acid signaling pathway involved in defense reactions and also represses the JA pathway. In *M. truncatula* R108, the two proteins SymCRK and DNF2 control salicylic acid and ethylene signaling pathways involved in triggering defense reactions. DNF2 controls the salicylic acid pathway more than the ethylene signaling pathway, while, SymCRK controls more the ethylene pathway than the salicylic acid signaling pathway in nodules.

This thesis also suggests the involvement of R proteins in the control of intracellular accommodation of rhizobia. The intracellular receptor CNL-5 appears to be involved in controlling the infection of symbiotic cells and the receptors *CNL-4* and *TNL-2* genes appear to be involved in controlling the infection efficacy of the symbiotic cells.

Finally, this thesis allowed the identification of a new bacterial strain *E. adhaerens*, capable of behaving as a symbiont or as a pathogen for several Medicago species. This can be used as a tool to study the nodules defense induction and to understand the rhizobia intracellular accommodation in symbiotic cells.

Université Paris-Saclay
Espace Technologique / Immeuble Discovery
Route de l'Orme aux Merisiers RD 128 / 91190 Saint-Aubin, France